TESLA - COLLABORATION

TESLA Input Coupler Workshop
DESY, May 29 and 30, 1996

Editors: D. Proch, P. Schmüser

DESY

August 1996, TESLA 96-09

Table of Contents
Input Coupler Workshop
DESY, May 29 and 30, 1996 in Bldg. 30B, room 459

Input Coupler Production

FNAL Coupler

The FNAL coupler consists of a coaxial cold window, a room-temperature doorknob transition from coax to rectangular wave guides without window, and a commercial disc window in the wave guide. So far two complete couplers were fabricated and tested with the coupler processing stand. Both couplers showed problems with the bellow copper coating, the coating of warm bellows was stripped off before testing. One coupler had a small leak at the cold bellow to coax weld. After assembly of the leak-tight coupler to C19 in CHECHIA, another leak developed at the cold bellow (as in the other coupler). Therefore the cold part with the window was replaced by a new production piece and conditioning was carried out with C19.

The leak problem at the bellow weld is probably due to insufficient cleaning before resistive welding. This has been improved for the next coupler. Furthermore a new welding scheme without resistive welding is worked out.

The first coupler coatings with Cu showed blisters and peal-off regions during ultrasonic cleaning. The ultrasonic cleaning of a good coating should not destroy the coated film. Improvements have been made at the company by intermediate electropolish.

The "cold" ceramic (+ the annealed coax parts) were baked at 300 °C for 22 hours at DESY. The dominant residual gas content during the baking is H_2 and CO_x (x: 1, 2, 3). The origin of the CO_x contamination is unknown. There is the suspicion that lubricants are the reason of the contamination. They are used during milling the ceramic surface to be metallised.

The following points were discussed:

- Stress annealing of stainless steel parts is necessary for those parts which will be chemically treated for coating afterwards. Otherwise stress corrosion will lead to leaks.
- The Al_2O_3 ceramic of windows has micro stress in the bulk material. These defects will grow under thermal stress ("ageing of ceramics"). Therefore fast cool down of the window should be avoided. More information can be gained from the Frauenhofer Institute of Ceramic Materials in Dresden.
- Leaks through the ceramic of a RF window have been observed at the DALINAC (D. Graef) after some years of operation. The reason is not known, but it could be due to the above mentioned ageing process.
- The well known rule was stressed again, that excessive braze material at the window has to be avoided or has to be carefully shielded.

DESY Coupler Design

The DESY input coupler consists of a cold window with a cylindrical ceramic and another cylindrical ceramic of the same diameter at room temperature, located at the coax to wave guide transition. Four couplers have been produced. RF tests started with two couplers, the other two need some cleaning of the window area (insufficient shielding of ceramic during brazing?). No problems with the Cu plating and the bellow welding were encountered. Several minor handling mistakes during brazing and welding delayed the fabrication because of some repair steps. The fabrication sequence foresees brazing at different temperatures to prevent a reduction of the RRR of the Cu plating. In spite of good results with samples, the fabrication brazing at low temperatures (Ag-Ge-Cu braze; T ≤ 550 °C) was not leak-tight. It was decided to use high temperature braze (Cu-Ag, 820 °C) at the cost of reduced RRR of the plated copper.

POINTS OF DISCUSSION:

- The fabrication of the cold window part foresees several brazing cycles at different temperatures with the need of shipping the parts forth and back between brazing and plating company. This sequence should be revised and simplified.
- The consequence of reduced RRR of the Cu plating after high temperature brazing should be reconsidered for a minimum heat load design.
- The origin of the dark window coating should be investigated (braze material?) (by BAM, Berlin).

Multipacting Calculations

Multipacting has been simulated in detail by the Helsinki group: coaxial lines are analysed and scaling laws are given for frequency, size and impedance of the coaxial line. So far pure travelling and standing waves are analysed. There is clear evidence that the breakdown phenomenon in the LEP-2 coupler is driven by one-point multipacting (outer coax line) of order four. New results were presented for a mixed configuration of standing and travelling waves. These conditions happen during the filling time the TESLA cavities.

The FNAL and DESY configuration of the window area have been analysed by the Helsinki group and by A. Mosnier, Saclay:

Conical Window (FNAL): Both calculations show a multiplication of electrons over a large range of field strength. This is caused by the tilt of the ceramic surface so that a large range of "gap distance" between the ceramic surface and the outer coax line is present. The Saclay calculations indicate some sharp multipacting resonances which are not present in the Helsinki simulation. One difference in the calculation is the assumption of a high secondary yield of 7 in the Saclay case whereas in the Helsinki simulation a yield of 1.5 is assumed everywhere. The later case seems to describe the condition of a coated ceramic more realistically.

Cylindrical Window (DESY): In the Helsinki calculations no multipacting resonance is observed whereas in the Saclay case resonances are detected at the end region of the ceramic. It was pointed out that the assumed field configuration is not very precise here and that it depends on simplified geometric assumptions.

RESULT OF DISCUSSION:

- The latest results of the Helsinki simulations for the mixed standing- and travelling case need to be analysed and should be applied to the transient filling process of the cold cavity.
- More active exchange of information between Saclay and Helsinki is recommended to explore the difference in the calculations.
- The impact energy of electrons should be displayed together with the multiplication factor in order to indicate the severeness of a multipacting resonance.

Experience with the LEP-2 Couplers

The LEP-2 coupler suffers from one-point multipacting of order 4 (impact energy is 400 eV). Several modifications have been carried out to suppress this phenomenon:

a DC-bias of the coaxial line. This method is in use since many years at Novosibirsk and was proposed as a cure against multipacting for the CERN coupler, too. Simulations by Tückmantel (CERN) and the Helsinki group confirmed the mechanism of suppressing of multipacting: the DC voltage of correct polarity and magnitude repels electrons from the inner conductor and thus destroys the resonant condition.
b The outer coax tube (with the heat exchanger) is made from one piece of forged tube. This avoids the risk of stress corrosion (as mentioned above) because there is no tube to flange weld.
c The collar at the cylindrical ceramic has been changed: some surfaces were Cu plated to reduce RF heating; the outer contact surface is rectified to get a defined contact surface; the Ti coating of the ceramic extends to the metallic collar.
d The assembled coupler line (including window) is baked for one day at 200 °C to remove water.

In a test- and processing set up (two couplers are connected through a coaxial line) the multipacting phenomenon and especially the role of condensed gases for multipacting was investigated. This set up was processed and worked fine at room temperature. Afterwards the coupler vacuum was opened to air for 2 hours. In a second test the couplers were operated after cooling the intermediate coax line to the temperature of LN_2 (by a heat exchanger at the outer coax line). Heavy multipacting was encountered now. Several electron probes located the place of multipacting at the cold coax part. This experiment as well as the operating experience with the HERA couplers prove that condensed gases on cold surfaces play a dominant role in initiating multipacting. Therefore effort has to be put into improvement of the vacuum conditions, e.g. by in situ bake out of coupler parts, especially of the ceramic of the window.

Glow discharge cleaning has been applied to coupler parts, but no convincing progress has been reported. A recent experiment at CERN concluded that only a few seconds of glow discharge are sufficient to clean surfaces. Under those conditions the risk of sputter coating is reduced. It was recommended to try out the short discharge cleaning for RF parts.

Saclay Coupler Test Facility

At Saclay a coupler test area is under construction. Start of operation is scheduled for September 96. Several windows will be tested: FNAL window (conical type), DESY window with 60 mm Ø coax, TW disc window. The test set up has a nice option to shift the standing wave pattern without moving contact plates: some metres of wave guide are placed between the test window and the final short. Therefore slight changes in operating frequencies transform into a shift of standing wave pattern.

LAL Coupler Ideas

At LAL a design of a "telescope type" of input coupler was worked out. It has the advantage that the radial extension of the coupler is small during module assembly. After some discussion it was concluded that the risk of sliding contact and of difficulties in cleaning are so severe not to proceed further with this design.

Novosibirsk

At Novosibirsk cylindrical windows are used in coaxial coupler lines. The connection of the collar is done by diffusion bonding, thus avoiding braze material and its risk for multipacting. DC-bias is used in all coaxial coupling lines to suppress multipacting.

Jefferson Lab

At TJNAF (former CEBAF) 351 couplers are operated with superconducting cavities for the two linacs. The window in the rectangular wave guide is placed near to the cavity. Two major problems are encountered:

- losses at the window frame load the 1.8 K level,
- field emitted electrons from the cavity charge the ceramic: hereby sparks are initiated or the ceramic is punctured (vacuum problems). This experience underlines the rule to shield the window ceramic against "direct sight" to the beam area.

Main Conclusions of Discussion

a) Adjustable coupling
The adjustable coupling of the input coupler should not be given up. Field unflatness in the cavity and subsequent scatter in coupling strength cannot be compensated otherwise.

b) DC-bias
DC-bias should be foreseen to eliminate any risk of multipacting. Although a large coax diameter reduces the probability of multipacting, DC-bias is the only remedy against unforeseen multipacting resonances in coax- or window areas.

c) Warm window

- The first operating experience with the Thomson window is positive. Furthermore this window is commercially available. A drawback is the need of a heavy doorknob and a separate window.
- The CERN type of cylindrical window in the wave guide to coax transition operates without problems at 150 cavities in LEP. This design is more compact, but operating experience with the 1.3 GHz scaled version (Dwersteg design) is needed.

d) Coax diameter
A large diameter of the coaxial line (outer Ø 60 mm, not Ø 40 mm) is recommended to suppress multipacting.

e) Coax line impedance

An increase of the impedance of the coaxial line is recommended for a new design (scaling of multipacting level). The increase of the antenna tip field has to be considered.

f) Cold window

- The conical window (FNAL) works up to 1 MW. But it shows "non-resonant" multipacting, as predicted by simulation. This could be improved by an optimum tilt angle (experience at Novosibirsk). Simulations at Helsinki will investigate this subject as well as the benefit of DC bias.
- The cylindrical window worked up to 1 MW in a resonant test set up. Operating experience with a complete coupler is still ahead. Multipacting is not expected according to simulations. The fabrication sequence is too complicated as compared to a conical window and needs a re-design.
- So called "travelling wave" windows (no $E_\perp$ on the ceramic surface) seem attractive but operating experience is needed (will be done at the Saclay test set up).

g) Brazing

Standard Ag-Cu braze works but needs careful shielding of excessive braze material. Diffusion bonding is an attractive alternative but has been demonstrated on cylindrical ceramic windows only (Novosibirsk). Fabrication of such windows for TTF is planned at Novosibirsk.

h) Fix point at coupler location

At the present design the coupler has to compensate longitudinal (coupler itself) and transverse (cavity shrinkage) thermal expansion. This results in the present coupler and costly design. For an improved coupler lay out the idea of a "fix point" coupler should be considered.

D. Proch, DESY, MHF-SL

Agenda
Input coupler workshop
DESY, May 29 and 30, 1996 in Bldg. 30B, room 459

REPORTS WEDNESDAY, MAY 29

10:00 - 10:15	Introduction, B. Aune, D. Proch
10:15 - 10:35	Report on TTF input coupler (FNAL): Experience with fabrication: Welding, brazing, Cu-plating, Ti coating, quality control, leak checking, cleaning, M. Champion.
10:35 - 10:55	Report on TTF input coupler (DESY): Experience with fabrication: Welding, brazing, Cu-plating, Ti coating, quality control, leak checking, cleaning, B. Dwersteg
10:55 - 11:35	Final cleaning of TTF couplers (ultrasonic rinse, bake out) and dust free assembly, A. Matheisen, M. Kuchnir, K. Zapfe-Düren
11:35 - 11:50 Coffee	
11:50 - 12:10	Experience with coupler processing (TTF couplers), W.-D. Möller
12:10 - 12:40	Multipacting simulations in input coupler line, Helsinki, A. Mosnier
12:40 - 13:00	Analysis of TTF coupler processing behaviour, J. Sekutowicz
13:00 - 14:00 Lunch	
14:00 - 14:20	Experience with input couplers at CERN, E. Haebel
14:20 - 14:40	Experience with input couplers at Novosibirsk, V. Veshcherevich
14:40 - 14:50	Coupler Activities at LAL Orsay, N. Solyak
14:50 - 15:00	Coupler Activites at Saclay, S. Chel
15:00 - 15:20	Experience with input couplers at CEBAF, D. Proch
15:20 Coffee	

WORKING GROUP ON COUPLERS:

Items to be discussed:

- Understanding of multipacting and means to avoid it (multipacting on cold surfaces?)
- Choice of ceramics and connecting technique (braze, weld, diffusion weld), coating
- Cu plating: adhesion, RRR, cleaning
- Diagnostics for R & D and operation
- Importance of in situ bake out? How to make it?
- Do we need adjustable coupling by bellows?
- **Design ideas for an improved TTF coupler**

List of Participants

Fermi Nat. Acc. Lab (FNAL), P.O. Box 500, Batavia, IL 60510, USA
M. Champion (champion@adcalc.fnal.gov)
M. Kuchnir (kuchnir@fnalv.fnal.gov)

Rolf Nevanlinna Institute, Helsinki University, Yliopistokatu 5, P.O. Box, 00014 University of Helsinki, Finland
P. Ylä-Oijala
J. Sarvas (jos@rolf.helsinki.fi)

INFN Milano, L.A.S.A., Via Fratelli Cervi 201, I-20090 Segrate (Milano)
C. Pagani (pagani@mvlasa.mi.infn.it)

CERN. CH-1211 Geneva 23
D. Bloess (dbloess@cernvm.cern.ch)
E. Haebel (Tel; +41-22-767 6614)
H.P. Kindermann (Tel: +41-22-767 4787)
V. Vechtcherevich, Budker INP

TH Darmstadt, Inst. für Kernphysik, Schlossgartenstr. 9, D-64289 Darmstadt
H.D. Graef (graef@linac.ikp.physik.th-darmstadt.de)

LAL Orsay, Centre Orsay, Bat. 200, F-91405 Orsay Cedex
(T. Garvey, garvey@lalcls.in2p3.fr)
R. Panvier
N. Soliak

CEA Saclay, DAPNIA/SEA - Bat. 701, F-91191 Gif-sur-Yvette Cedex:
St. Chel (chel@hep.saclay.cea.fr)
A. Mosnier (mosnier@hep.saclay.cea.fr)

DESY, Notkestraße 85, D-22603 Hamburg
B. Aune (aune@aune.desy.de)
B. Dwersteg (dwersteg@desy.de)
H. Edwards (hedwards@desy.de)
M. Ferrario (ferrario@vaxlnf.lnf.infn.it)
A. Gamp (gamp@gamp.desy.de)
D. Hubert(f52pv2@dsyibm.desy.de)
A. Matheisen (math@vxdesy.desy.de)
W.- D. Möller (wolf-dietrich.moeller@desy.de)
D. Proch (proch@proch.desy.de)
K. Rehlich (rehlich@sun52a.desy.de)
P. Schmüser (f35psc@dsyibm.desy.de)
J. Sekutowicz (jacek@teslahe.desy.de)
W. Singer (singer@singer.desy.de)
J. Wojtkiewicz (woj@sun52a.desy.de)
S. Wolff (swolff@desy.de)
K. Zapfe-Düren (zapfe@vxdesy.desy.de)

SLAC, P.O. Box 4349, Stanford, CA 94309, USA
H.D. Schwarz (hds@slac.stanford.edu)

Fabrication of the Fermilab TTF Input Coupler

Mark Champion

29 May 96

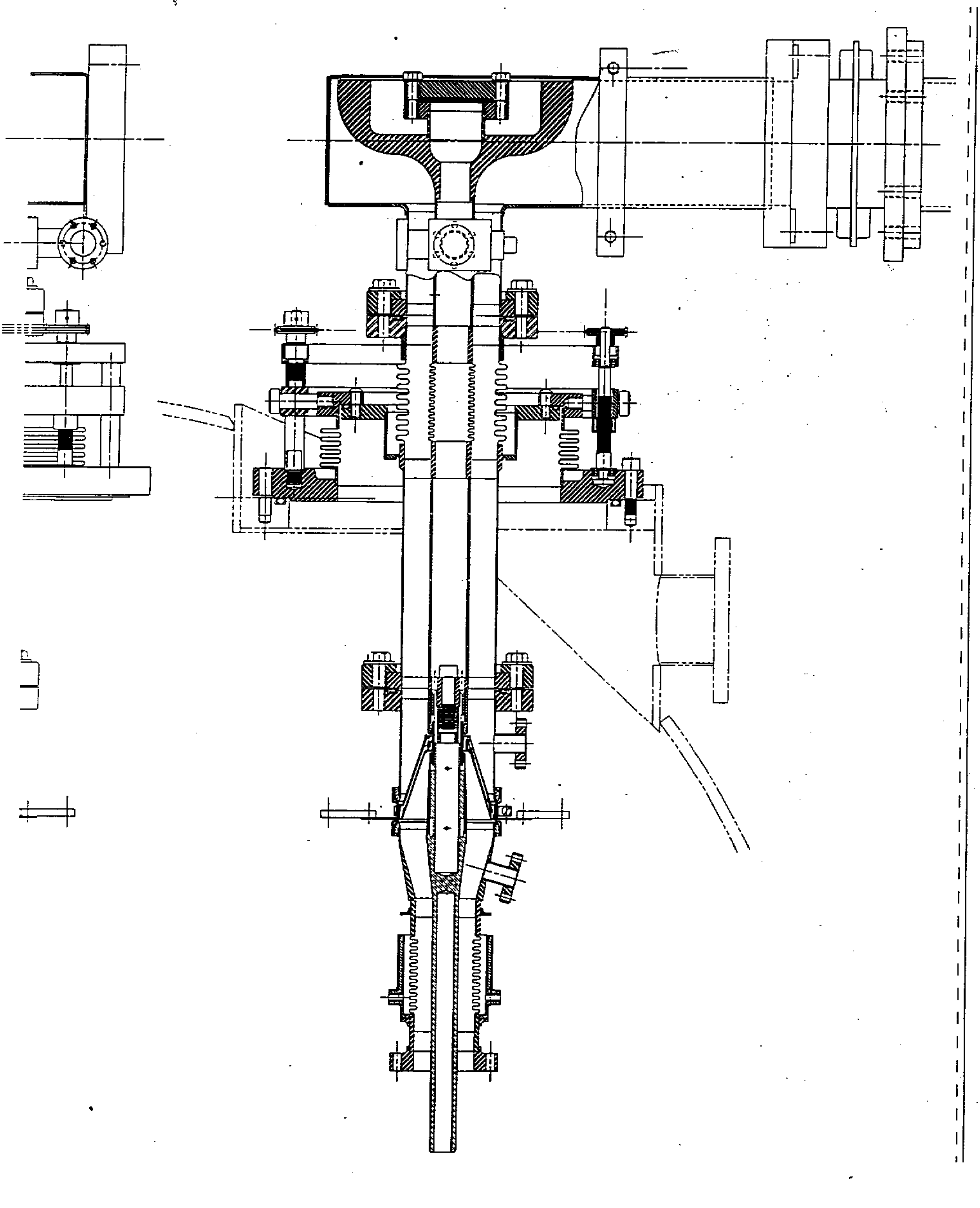

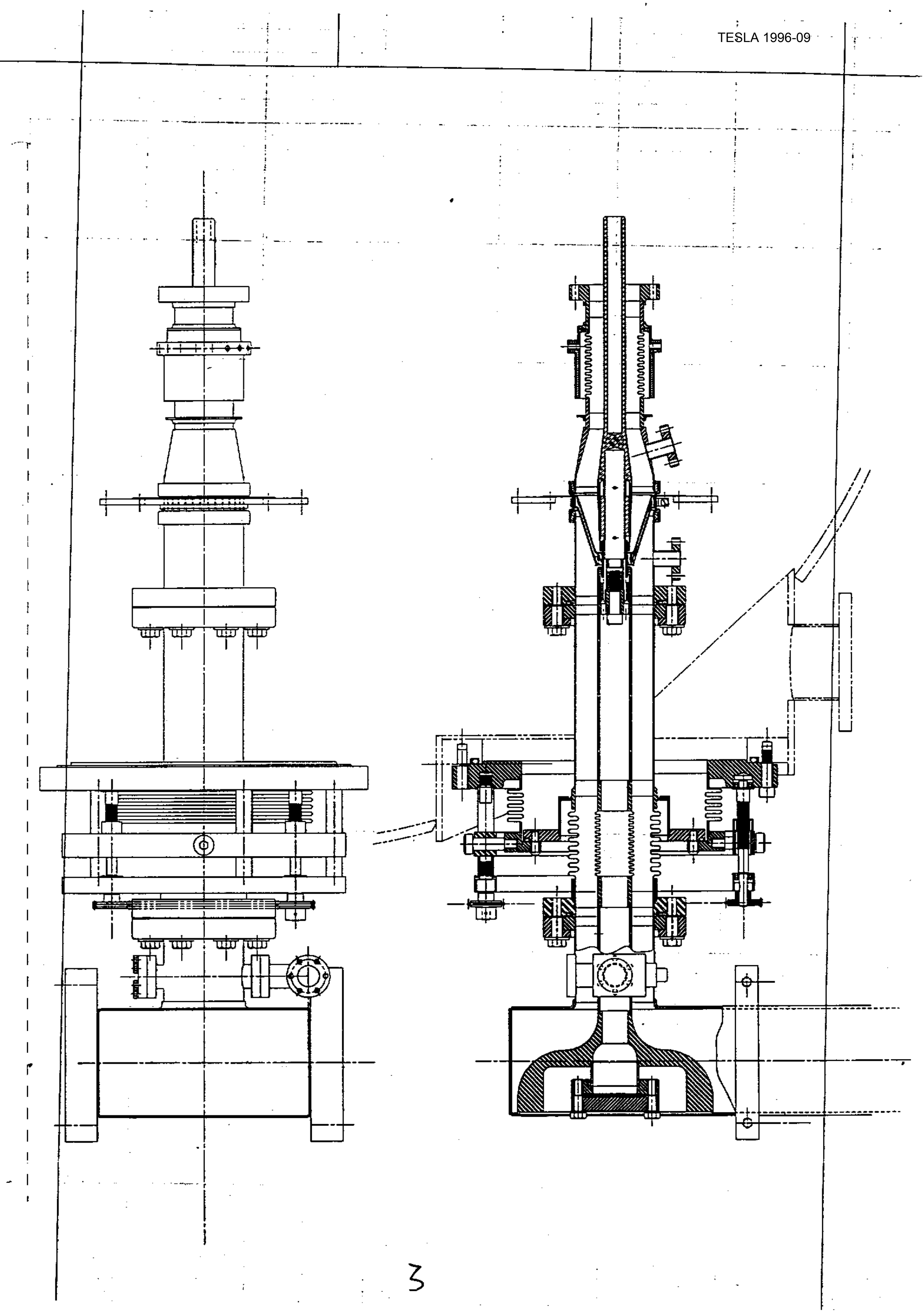

MATERIALS

- 316L stainless steel (DIN 1.4404)
- OFHC copper
- 35 % gold / 65 % copper braze alloy
- molybdenum manganese metallization on conical ceramic
- 99.5% Aluminum Oxide conical ceramic
- Helicoflex seals: silver, aluminum, inconel, nimonic

WELDING NOTES

Stainless Steel

- All welding of stainless steel components is done via the TIG method with a shielding gas of Helium and/or Argon.
- Preparation for welding may include abrasive cleaning with scotch-brite and always includes wiping with ethyl or isopropyl alcohol.
- A wire brush is normally used to clean the welds for inspection by the weldor.
- Welds are specified to be fusion welds, using filler of the same material only if absolutely necessary.
- Machining of welds is not allowed.

Copper

- All welding of copper components is performed either by electron beam welding in a vacuum chamber or by TIG welding in a glove-box filled with Helium and Argon.
- To prevent oxidation it is important during the glove-box welding to apply a continuous interior purge to the assembly being welded.
- The general cleaning procedure is applied prior to welding. Sometimes a final cleaning of the weld area is performed at the time of welding using scotch-brite and alcohol.
- During electron beam welding it is important to shield certain areas, such as the ceramic, from vapor deposition.

BRAZING NOTES

- 35% Gold / 65% Copper braze alloy is used for stainless steel to copper and copper to ceramic connections. (brazing temperature is ~1050 C)
- The gold/copper braze alloy is used for the ceramic to copper braze joint because silver migration has been observed on windows brazed with silver/copper braze alloy.
- Tight tolerances are needed for successful brazing.

CLEANING PROCEDURE

Ingredients:

- distilled water
- Micro soap
- ethyl alcohol
- (citric acid)
- (copper brite)
- ultrasonic cleaner with power density as in TTF chemistry room.
- compressed dry nitrogen gas

(Effective Date: 3/30/90)

~~TESLA 1996-09~~

SECTION I — MATERIAL IDENTIFICATION AND USE

MATERIAL NAME / IDENTIFIER

MICRO® LIQUID LABORATORY CLEANER

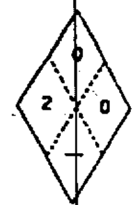

N.F.P.A.
H.M.I.S.

TO COMPLY WITH OSHA'S HAZARD COMMUNICATION STANDARD 29 CFR 1910.1200

MANUFACTURER'S NAME: International Products Corporation	SUPPLIER'S NAME: Not Applicable
STREET ADDRESS: P.O. Box 70,	STREET ADDRESS: Not Applicable
CITY: Burlington, NJ 08016 — COUNTRY: U.S.A.	CITY: Not Applicable — COUNTRY: Not Applicable
POSTAL CODE: — EMERGENCY PHONE NO.: 609-386-8770	TELEPHONE NO. FOR INFORMATION: 609-386-8770

CHEMICAL NAME: a mixture	CHEMICAL FAMILY: a mixture	CHEMICAL FORMULA: Not Applicable
TRADE NAMES AND SYNONYMS: MICRO®	MOLECULAR WEIGHT: Not Applicable	MATERIAL USE: Cleaner

SECTION II — HAZARDOUS INGREDIENTS OF MATERIAL

HAZARDOUS INGREDIENTS	APPROXIMATE CONCENTRATION %	C.A.S., N.A. OR U.N. NUMBERS	LD_{50} (SPECIFY SPECIES AND ROUTE)	LC_{50} (SPECIFY SPECIES AND ROUTE)

No MICRO ingredient, present at 1% or more, is contained in the SARA Title III, 313 list. However, the following composition information is provided for medical reference purposes.

MAJOR INGREDIENTS

Water	7732-18-5
Glycine, N,N'-1,2-ethanediylbis-(N-(carboxymethyl)-, tetra-sodium salt	64-02-8
Benzenesulfonic acid, dimethyl-, ammonium salt	26447-10-9
Benzenesulfonic acid, dodecyl-, cpd. with 2,2',2"-nitrilotris-(ethanol)	27323-41-7
Poly(oxy-1,2-ethanediyl),alpha-(nonylphenyl)-omega-hydroxy	9016-45-9

SECTION III — PHYSICAL DATA FOR MATERIAL

PHYSICAL STATE: ☐ GAS ☒ LIQUID ☐ SOLID	VISCOSITY: 8.2 cp	ODOR AND APPEARANCE: Pale yellow liquid with slight ammonia odor	
ODOR THRESHOLD (P.P.M.): Not Determined	SPECIFIC GRAVITY: 1.14	VAPOR PRESSURE (MM): about same as water	VAPOR DENSITY (AIR = 1): about same as water
EVAPORATION RATE: about same as water	BOILING POINT (°C): ca. 212°F (100°C)	FREEZING POINT (°C): ca. —8°C	SOLUBILITY IN WATER (20°C): miscible
% VOLATILE (BY VOLUME): Not Determined	pH: 9.7 (concentrate)	MELTING POINT: —	COEFFICIENT OF WATER/OIL DISTRIBUTION

TOTAL P.02

Procedure:

- If copper is heavily oxidized, first clean with citric acid or copper brite followed by rinsing with distilled water.
- Clean in ultrasonic bath for 10 minutes. A heated bath is preferred, but a room temperature bath is sometimes used.
- Rinse with distilled water.
- Rinse with clean ethyl alcohol.
- Blow dry with nitrogen gas.
- Wrap in Kimwipes, place in plastic bag or box.

STRESS ANNEALING

- Until now no stress annealing has been performed after welding.
- One 300 K outer conductor assembly has been sent for annealing at 950 C. It will undergo visual inspection, dimensional inspection, and vacuum leak testing upon its return to FNAL.
- We plan to stress anneal all welded stainless steel components in the future.
- Some components include brazed connections between copper and stainless steel. Because the brazing was done at 1050 C with 35% Gold / 65% Copper alloy, it is expected that the 950 C bake will not damage the integrity of the braze joints.

Fermi National Accelerator Laboratory
Energy Saver Division
Specification No. 0428-ES-157007 Rev.A

Technical Specification for Vacuum Degassing 304 and 316 L Stainless Steel

Prepared by G. Lee

November 16, 1983

General Description

Stainless steel is baked at high temperature in a vacuum of 1×10^{-4} Torr or better to reduce the desorbtion of absorbed gases and as a final cleaning step for ultra-high vacuum components.

To reduce grain boundry precipitations, the time in the temperature range of 600 to 900°C is kept to a minimum

1. <u>Initial Heating</u>

   Normal furnace heating characteristics are used to heat the parts to 550 or 600°C and held at that temperature for one-half (1/2) hour to equalize temperatures.

2. <u>Rapid Heating</u>

   Rapid heating is attempted after the above to raise parts to 950°C in one half (1/2) hour or less.

3. <u>Bakeout</u>

   Parts should be baked at 950°C for two hours and at a pressure of 1×10^{-4} Torr or better.

4. <u>Cooldown</u>

   Parts should be cooled from 950°C to 600°C as rapidly as possible, preferably in less than one half (1/2) hour.

5. <u>Cleanliness</u>

   Degassed parts should be kept as clean as possible. Small parts should be wrapped in clean white paper or clean aluminum foil; all handling should be done with clean white nylon gloves. Tubing should be capped with aluminum foil or clean plastic caps and wrapped in paper or polyethylene tubing. Adhesive tape shall not be used in contact with any parts.

COPPER PLATING

- SILVEX, Inc., Westbrook, Maine, USA. They plated beam tubes for Brookhaven and the SSC, and the waveguide extensions (between cold and warm windows) on the CEBAF input coupler.
- A cyanide process is used with reagent grade ingredients.
- No brighteners or other additives are allowed.
- At this time a special line is being set up exclusively for the input coupler plating. Once the part to be plated is mounted in its fixture, the plating process can be completed by operating valves to the appropriate baths.
- The process includes an electropolishing step to improve adhesion.
- The pulsed plating method is going to be developed upon completion of the new plating line.

CERAMICS

Coaxial Window

- 99.5% Aluminum Oxide from WESGO, Inc.
- Metallization and brazing by Alberox, Inc.
- Upon delivery to FNAL: Inspection, vacuum leak test, liquid Nitrogen thermal shock, vacuum leak test.
- In the past, the ceramics have been ultrasonically cleaned in ethyl alcohol prior to being coated with Titanium Nitride.
- The coated ceramics are now being baked at 300 C in a vacuum oven prior to being welded into an assembly. (This was not done for the first two production couplers, F01 & F02)
- In the future, it is planned to bake the ceramics before applying the TiN coating.

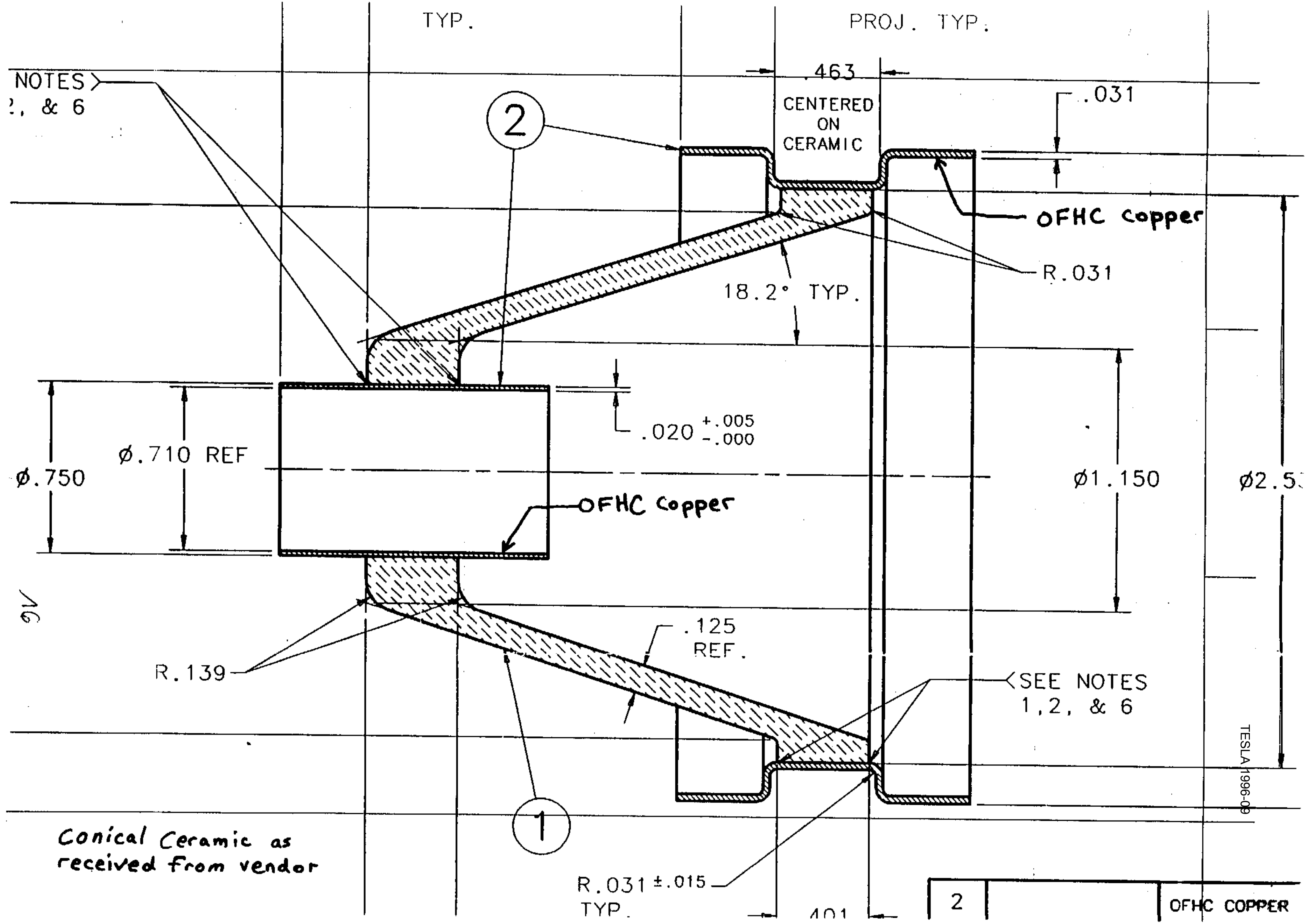
TYP.
PROJ. TYP.
NOTES
2, & 6
.463
CENTERED ON CERAMIC
.031
2
OFHC copper
R.031
18.2° TYP.
.020 +.005 -.000
ø.750
ø.710 REF
ø1.150
ø2.5
OFHC copper
R.139
.125 REF.
SEE NOTES 1,2, & 6
1
R.031 ±.015 TYP.
.401
2
OFHC COPPER
Conical Ceramic as received from vendor

Waveguide Window

- This is a Philips window that is normally used as the output window on a klystron.
- We add a waveguide vacuum flange and an impedance matching section on the air side of the window.
- The first windows were coated with TiN at FNAL, but were not baked.
- The program now is to apply the standard cleaning procedure followed by a 300 C vacuum oven bake and TiN coating.

BELLOWS

- Vacuum leaks have been a problem with both sizes of outer conductor bellows.
- The first design required two welds:
  1. A resistance weld was used to attach a reinforcing collar to the bellows neck.
  2. A TIG weld was used to attach the end pieces to the bellows assembly.
- The company did not perform the TIG welding as specified. The bellows were returned to the company where the welding was repeated. It was a terrible mistake to use these bellows in the first couplers!
- Two solutions are in progress:
  1. Use the first design, but perform the TIG welding at FNAL.
  2. Use a new design that eliminates the resistance weld.
- Assemblies now under production will undergo 950 C stress annealing to reduce the likelihood of stress corrosion cracking.

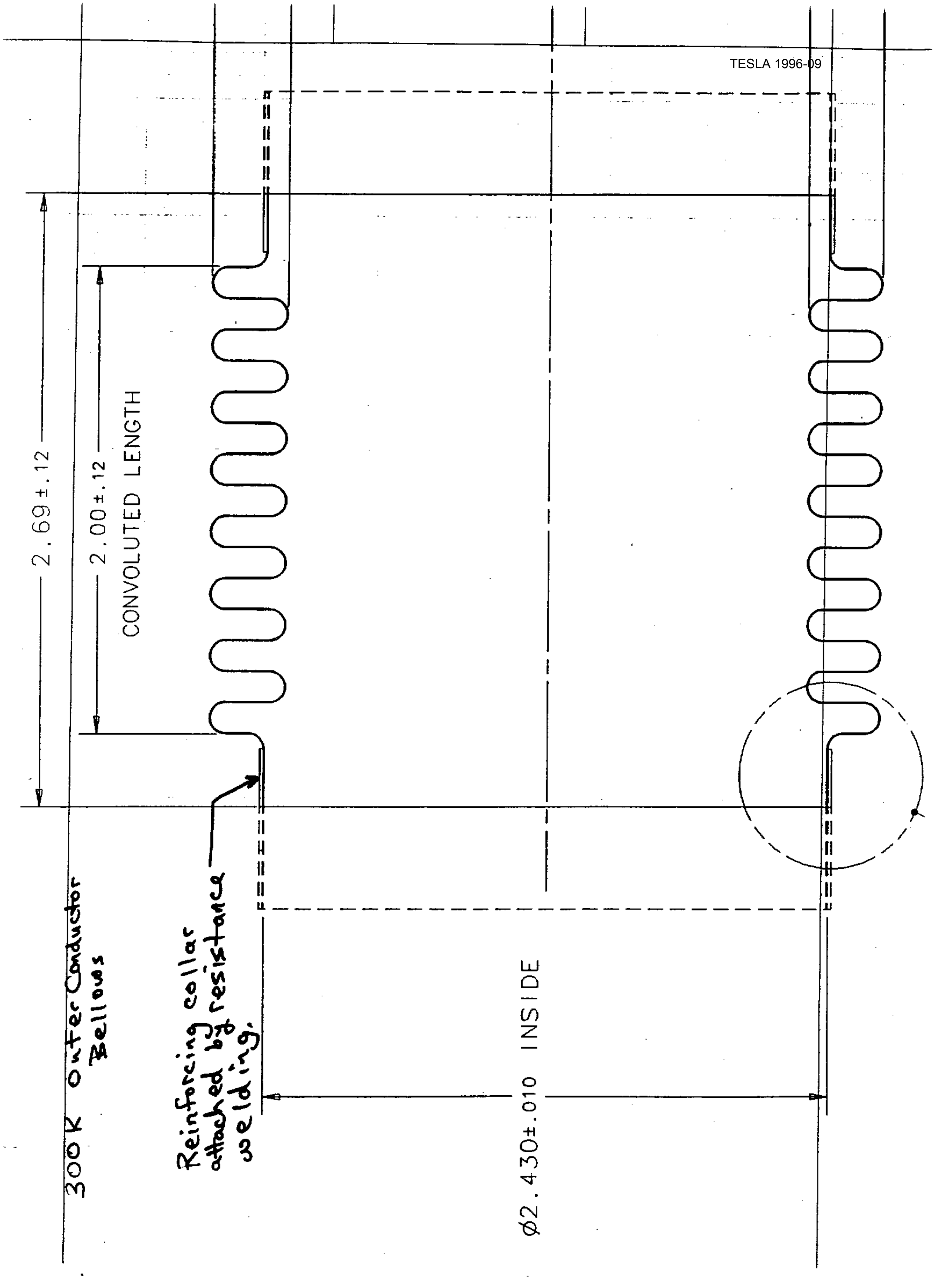
2.69±.12
2.00±.12
CONVOLUTED LENGTH
Ø2.430±.010 INSIDE
300K Outer Conductor Bellows
Reinforcing collar attached by resistance welding.

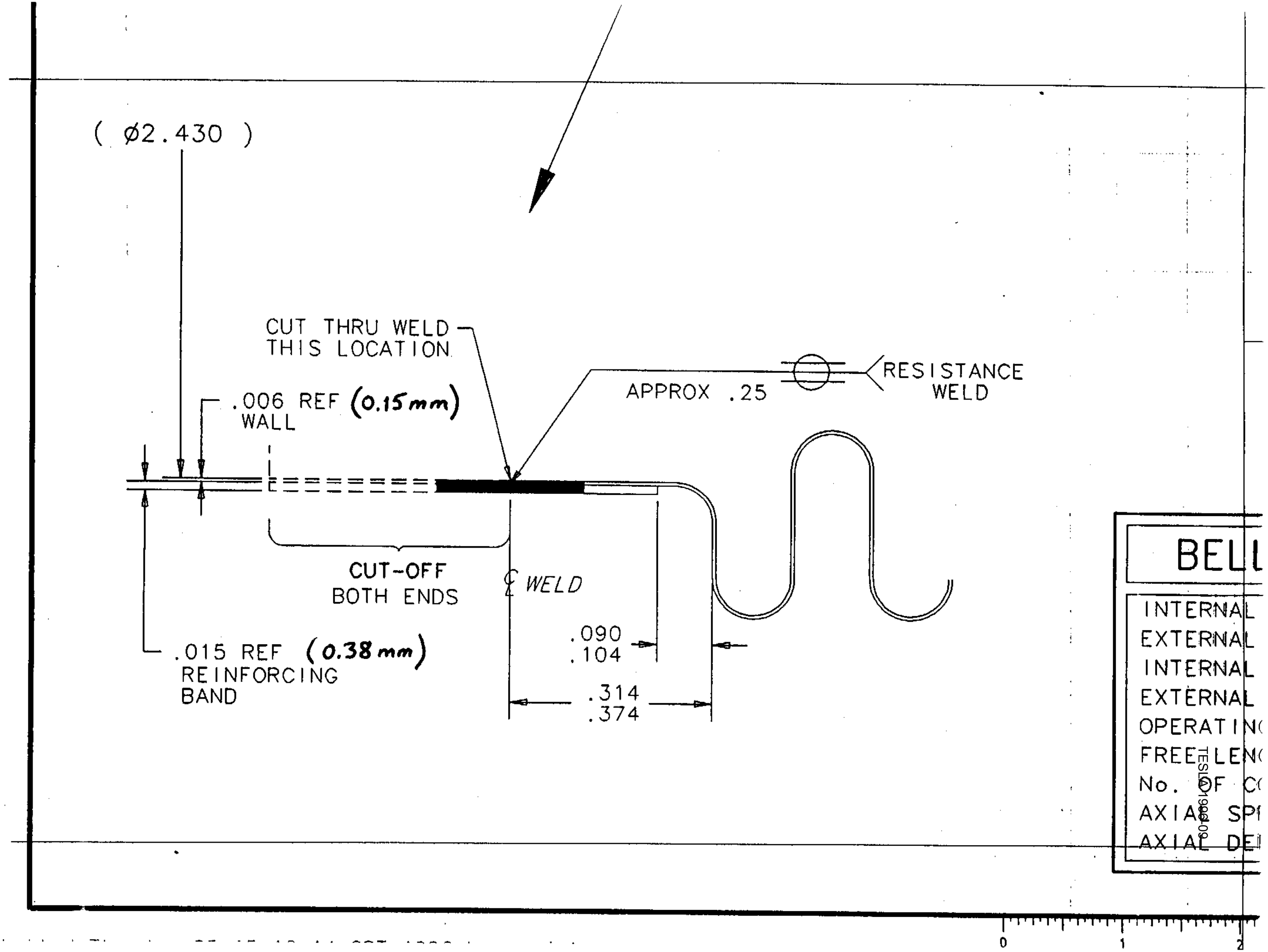
(Ø2.430)
CUT THRU WELD
THIS LOCATION
.006 REF (0.15mm)
WALL
APPROX .25
RESISTANCE
WELD
CUT-OFF
BOTH ENDS
℄ WELD
.015 REF (0.38mm)
REINFORCING
BAND
.090
.104
.314
.374
BELL
INTERNAL
EXTERNAL
INTERNAL
EXTERNAL
OPERATIN
FREE LEN
No. OF C
AXIAL SP
AXIAL DE
0
1
2

300 K Outer Conductor Bellows

No resistance weld or intermediate collar.

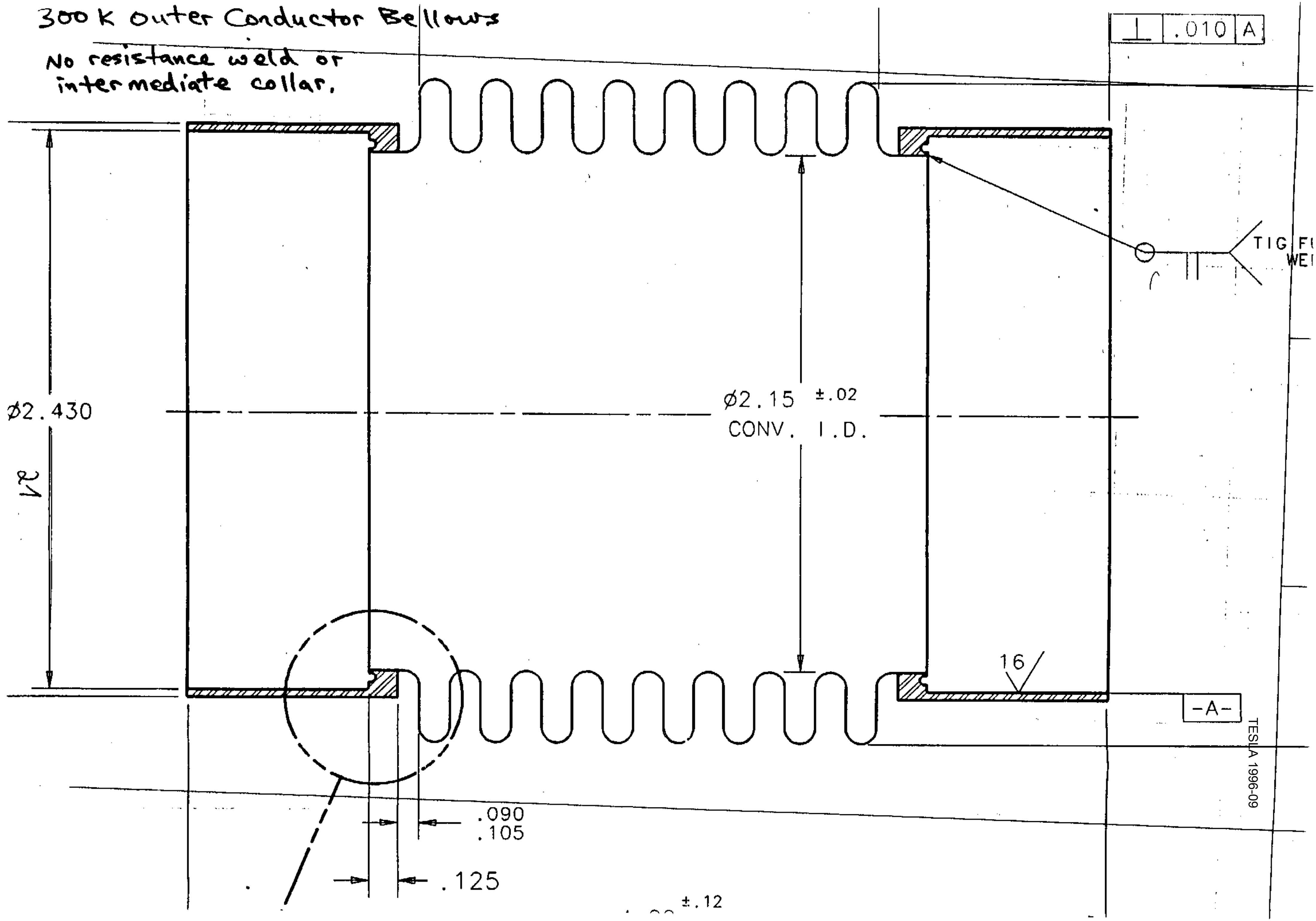

Report : DW280596

DESY-Type TESLA-Coupler
Technology , Fabrication

Coupler specifications

Primary design goals

Construction / Design parameters / choices

Manufacturing the coupler

problems during fabrication

first experiences with the prototype couplers

22

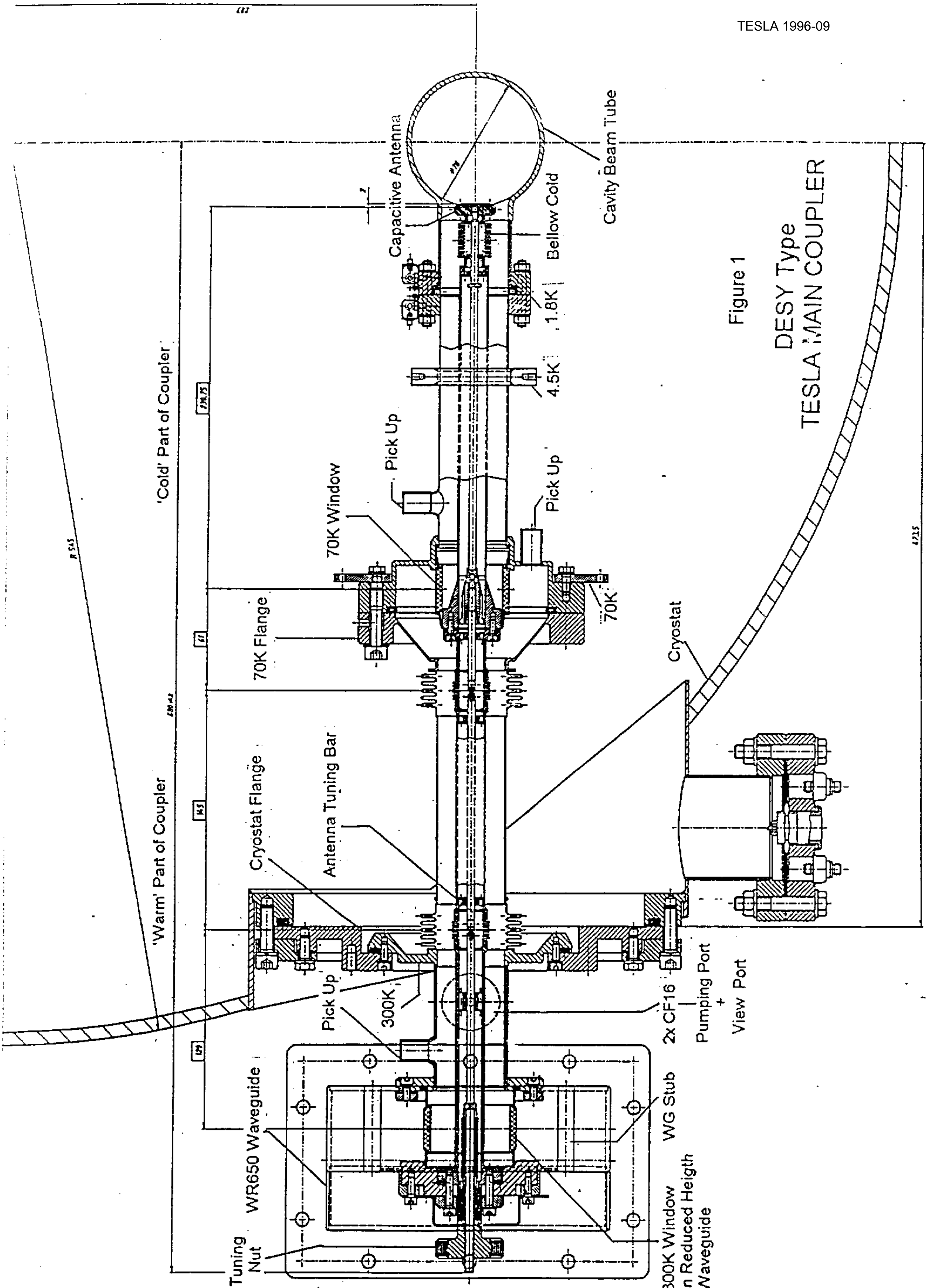

Figure 1
DESY Type
TESLA MAIN COUPLER

Coupler specifications :

rf technique :

center / operation frequency	1.3 Ghz
operation power	10 pulses/sec of 208 kW 1.33msec length (average 2.9 kW)
peak power capability at reduced pulse rate and length	up to 1MW
operation modes	transmission and full reflection at any phase

mechanics :

cavity coupling	coaxial to antenna
rf input at room temperature 300K	outside cryostat
rf output at 1.8K inside cryostat	cavity flange
one ceramic window at	(room temperature) 300K
one ceramic window at	70 K level
length inside cryostat	≈ 400mm
dimensions matched to cryostat construction	
transverse flexibility of	±15 mm
length flexibility	>3‰ + mechanical tolerances
coupler at 70K window	separable
Qext variation of≥10 times	in situ variable antenna length ≈10mm

cryogenics :

minimized static and dynamic cryogenic losses at	1.8K, 4.2K, 70K
at full rf load of about	0.06W , 0.6W , 6W
thermal intercept (cryostat) connections at	4.2K , 70K

vacuum :

two independent vacua of very high quality 10^{-8} mbar
cold part vacuum must correspond to cavity cleanliness requirements

Primary design goals :

transverse+length flexibility	by 4 bellow arrangement , (advantage rigid outside construction)
Q-tuning	inside inner conductor by deformation of bellow near antenna tip (no center displacement by tuning , simple tuning mechanics)
cold window	special geometry (avoids direct impact of particles or radiation from cavity port)
warm window	integrated cylindrical ceramic (small , lightweight)
ceramic to metall connection areas	hidden by ceramic or corners towards rf fields
corners at cold ceramic	have been designed in a way not to exceed 132V across a gap of 0.2mm at 1MW transmission , not enough for multipacting
detectors	for measurement of coupler behaviour and monitoring dangerous operation situations

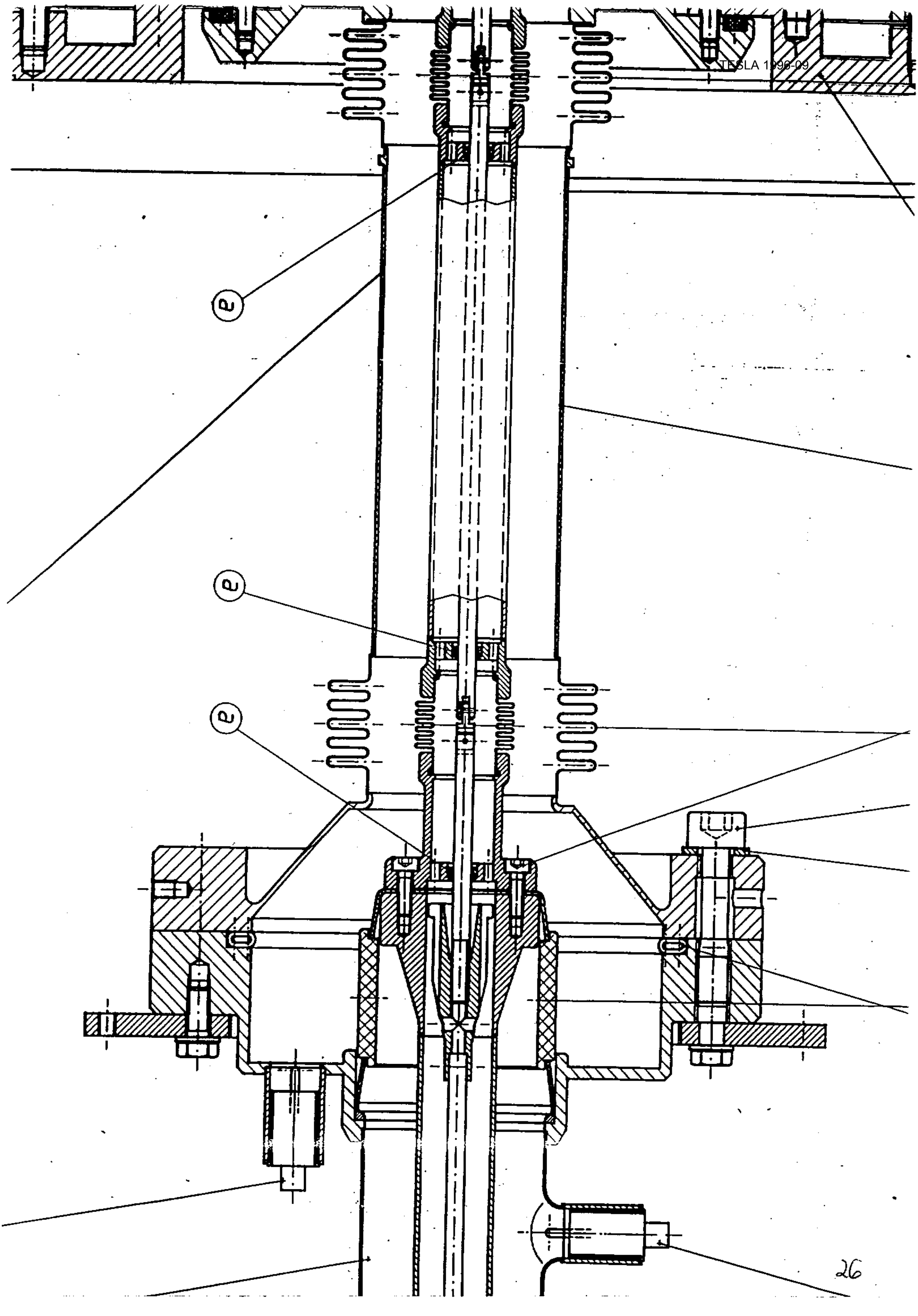

Construction / Design parameters / choices

waveguide types / coupling :

coax inside cryostat	50Ω
inner conductor / outer conductor	17.39mm⌀ / 40mm ⌀
outside cryostat transition	coax to WR650 waveguide
cavity coupling	capacitive antenna

fields and voltages :

50Ω line , max peak voltage at 1MW and full reflection	20kV (≤1MV/m)
50Ω line , max peak current at 1MW and full reflection	400A
waveguide near window , maximum voltage across (HFSS)	17kV (0.3MV/m)
corresponding (local) waveguide impedance	≈150Ω
'warm' window , total maximum voltage inside at 1MW	
in travelling wave mode (HFSS)	25kV/2.5cm (1.0MV/m)
with local peak field (at collars) inside ceramic	(1.6MV/m)
(in worst case standing wave position : values*2)	
connected to cavity , at pulse beginning (HFSS)	≈30kV/2.5cm (1.2MV/m)
with local peak field (at collars) inside ceramic	(1.7MV/m)
'cold' window , total maximum voltage inside at 1MW	
in travelling wave mode (HFSS)	≤14kV/2.5cm (0.6MV/m)
with local peak field (at collars) inside ceramic	(1.6MV/m)
(in worst case standing wave position : values*2)	
connected to cavity , at pulse beginning (HFSS)	≈27kV/2.6cm (1.1MV/m)
with local peak field (at collars) inside ceramic	(2.5MV/m)
antenna , connected to cavity , local peak field at 1MW	4.2MV/m
(maximum electric field strength in air	30kV/cm)

rf losses / heat flow :

cold ceramic window loss at average transmission of 3kW rf 0.14W
total expected ΔT (heat transfer including inner conductor losses) ≈ 2°C

temperatures and heat flow on inner and outer conductors at coating qualities of RRR ≈ 10
and average rf power load corresponding to transmission of 3KW

	Temp. level / K at		Power Flow / W			Temp. max.
	cold end	warm end	to cold end	from warm to cold end	rf losses / W	between cold and warm
inner conductor cold 70K - 107K	**70**	**107**	**0.85**	**0**	**0.85**	**-**
outer conductor cold 1.4K - 4.2K	**1.8**	**4.2**	**0.06**	**-0.04**	**0.1**	**5.3**
outer conductor cold 4.2K - 70K	**4.2**	**70**	**0.61**	**0.35**	**0.26**	**-**
inner conductor warm 70K - 300K	**70**	**300**	**2.8**	**0.04**	**2.8**	**-**
outer conductor warm 70K - 300K	**70**	**300**	**1.9**	**-0.2**	**2.1**	**-**

tuning mechanics :

external Q tuning by a rod with 2 cardanic links inside inner conductor
rod material stainless steel , silver coated 1μ
special bearing rings for low abrasion of rod are made of Nimonic

materials / coatings :

inner conductor cold and warm consist of copper
flexible parts of inner conductor
3 standard stainless steel bellows of 0.1 mm wall thickness
+15μ copper inside +15μ copper outside
additional cooling of antenne tip by 4mm² copper braid

outer conductor cold 0.5mm stainless steel, 10μ copper coated
outer conductor warm 0.7mm stainless steel, 20μ copper coated

flexible parts of outer conductor
2 standard stainless steel bellows of 0.2 mm wall thickness
+20μ copper

window material (both) 97% Al_2O_3 (WESGO Al300)
windows (vacuum side) coated against multipacting ≈100Å Ti, ≈100MΩ/square
window to coupler connection brazed copper rings

vacuum :

(additional) vacuum ports 3 CF16
'warm' vacuum pumping, view port for multiplier,
port for demountable pick up
sealings of coupler helicoflex
towards cryostat rubber ring
cF16 ports sealing copper rings

coupler diagnostics :

3 e^- detectors	with SMA connectors at window vacuum sides (2 welded feed throughs, 1 mounted on CF16 flange)
1 photo-multiplier	looking into the coax from outside the cryostat
1 foto-diode	looking into the rectangular waveguide
1 infrared detector	for monitoring the warm window temperature
differential temperature	(heatflow) measurement at 70K flange
temperature measurement at	1.8K flange

Manufacturing the coupler :

detailed manufacturing procedures have been developed for the complete fabrication , which are tried to concentrate to the following rules :

assembly techniques :

stainless steel to stainless parts are preferably	welded to subgroups
bellows and stainless steel subgroups	copper coating before next step
copper to copper (inner conductors cold and warm)	EB welded
copper to stainless steel (inner conductor bellows ..)	UHV brazed after Cu coating
ceramic windows (metallized)	UHV brazed within final step
final step of assembling the whole coupler	brazing inUHV furnace

brazing + welding statistics		
welds		≈22
braze connections	high vac. proof	11
	only connection	9
furnace cycles of those 20 braze connections		7

(every braze geometry was tested before finalizing the construction)

copper coating :

copper coating of stainless steel parts necessary	after welding and before brazing
copper surfaces of cold parts of the coupler	defined RRR and defined heat conductivity important
heat treatment after coating for detection of blisters	400°C

coating of windows :

vacuum side surfaces of the ceramic Al_2O_3 windows were sputter coated with Ti

(also vapor coating with TiN was applied)

brazing :

for the cold coupler parts
main goal : brazing temperature ≤ 550°C
(2 of those brazes were necessary) using Au-Ge-Cu braze

(at 550°C temperature highest RRR of copper coating : ≥250 ,
RRR≤10 after 820°C treatment at thickness of 20μ , RRR after this heat treatment decreases with thickness)

renewal of critical copper plating where 820°C were unavoidable

during brazing the surfaces of the windows were protected by Al_2O_3 cylinders against additional deposition of metal vapor

(tests have shown, that after 820°C treatment the Ti coating has still a low secondary emission coefficient)

problems during fabrication :

In spite of successful EB welding of test parts the EB welding of the copper inner conductor parts was not satisfying (more shrinkage than at test , one weld was leaky , no inner conductor was straight)

Tube pull-outs for e-pick ups turned out to be a problem in spite of succesful test longtime before ; reason : some variation of diameter and wall thickness ; pull-outs of the old diameter were made ;
This lead to a chain of consequences :

a) additional rings had to be welded to the pick up tube connection for length and diameter correction .
b) the weld at the pick up position nearest to the cavity was so big as to bend the outer conductor. This was not early enough detected .
c) the final consequence was the impossibility to braze the 'cold' inner conductor vacuum proof and concentric into the cold coupler part :
Due to application of a centering tool for the 'cold' inner conductor the braze gap between the copper cup and the warm conical end of the 'cold' inner conductor was always to big on one side. (Also the inner conductor of the cold coupler part was not straight originally.)
This lead to a sequence of unsuccessful braze cycles and leaks and to damage of some ceramic windows and to loss of much time by repairs.
Only heavy excentricity of the antenna tip lead to a vacuum proof braze.
d) This was corrected later by mechanical bending the outer conductor of the cold coupler part corresponding to the position of the inner conductor.

No tool was prepared to test the bellow welds just after welding ; this led to nonelastic compression and later nonelastic readjustment of the bellows (but no damage)

During welding of the outer conductor bellows it turned out , that due to not enough space one bellow got holes by welding through. This caused a change of construction at that position.
Direct welding at the bellows turned out to be critical because of the thin walls. It is preferable to provide enough space and thicker collars at the bellow ends for welding connection.

At 2 copper coated parts were small blisters detected after heat treatment at 400°C . (coating repeated)

It seems still to be a certain difficulty to prevent the eutectic braze completely from expansion on the surfaces in spite of careful definition of the braze quantity.

Copper silver braze on vacuum side surfaces of high power rf components is assumed to be harmful .

An additional braze problem was the low temperature Au-Ge-Cu braze. It failed to braze the outer conductor bellow at the generator side to the neighboring flange . This braze was successful with test pieces.

One sealing problem is still open. During construction it was assumed that the aluminum helicoflex seals could be copper coated. This was not successful. Copper is preferable in presence of rf fields and vacuum.

For proper cleaning of the cold part of the coupler there was a requirement to replace the welded feed through next to the cavity by an exchangeable feedthroug (CF16 flange connection)

2 CF16 flanges have been made out of 1.4435 instead of 1.4429 (necessary because of 820°C brazing : highly temperature resistant quality)

Tests showed , that a titanized ceramic surface is very sensitive towards additional metal vapor deposition. This causes surface conductivity . Hence there were Al_2O_3 shieldings provided in order to prevent this effect . In spite of this the window surfaces looked dirty after brazing and some of them showed electrical conductivities of down to several hundred kΩ , in one case 17 kΩ.
The reasons and the deposited material leading to these surface effects are not clear.
This situation was improvable by treatment with nitric acid which will not attack the Ti coating.

Ti coating of the ceramic window surfaces by sputtering turned out to be uneconomic and difficult.
The reason is that the small size of those cylinders was not allowing radial sputtering. Hence homogeneous thickness of coating was difficult.
Coating by evaporation seems much easier.

Due to more brazes than planned and finally using eutectic or Ag-Cu-In braze instead of low temperature braze it was not possible at the prototypes to guarantee the design RRR of the copper coatings in the critical cold areas.

A lot of experiences with fabrication and ideas exist now which allow to make improvements and to avoid the above described mistakes.

first experiences with the prototype couplers :

vacuum check of the coupler parts was successful , no leak occured

cleaning in the clean room to dust free quality of class 10 was no problem
the copper coatings showed no problem at ultrasonic treatment

after that cleanroom procedure all parts were heated in a vacuum furnace at 300°C ; it was no problem to come down to low evaporation rates in that furnace

mounting of the couplers to the test cryostat was relatively easy and needed only a few hours

main problems here were still some missing parts and tools
one sealing surface had to be grinded because it was damaged

after mounting the vacuum came to values of 10^{-8} mbar after short time

testing of the first 2 prototype couplers was actually possible up to only 300kW in travelling wave , 200kW in standing wave operation mode
the reason is sparking across the ceramic window in the waveguide to coax transition area ; the sparking occurs at the air side of both couplers
due to field enhancement at the edge of metallization / braze
this effect was not visible on HFSS computations because the critical area seemed to have higher fields only inside the ceramic where they are uncritical

remedies are thinkable :
a) removing the edges by sand blusting and adding an anticorona ring device (will be tried in the next future)
b) as a final solution : imbedding the metal to ceramic transition into the ceramic as done on the vacuum side of this window ;
this is possible even with the prototype couplers by exchange of the ceramic ;
the critical area has to be studied very detailed and carefully with field computation programs ;

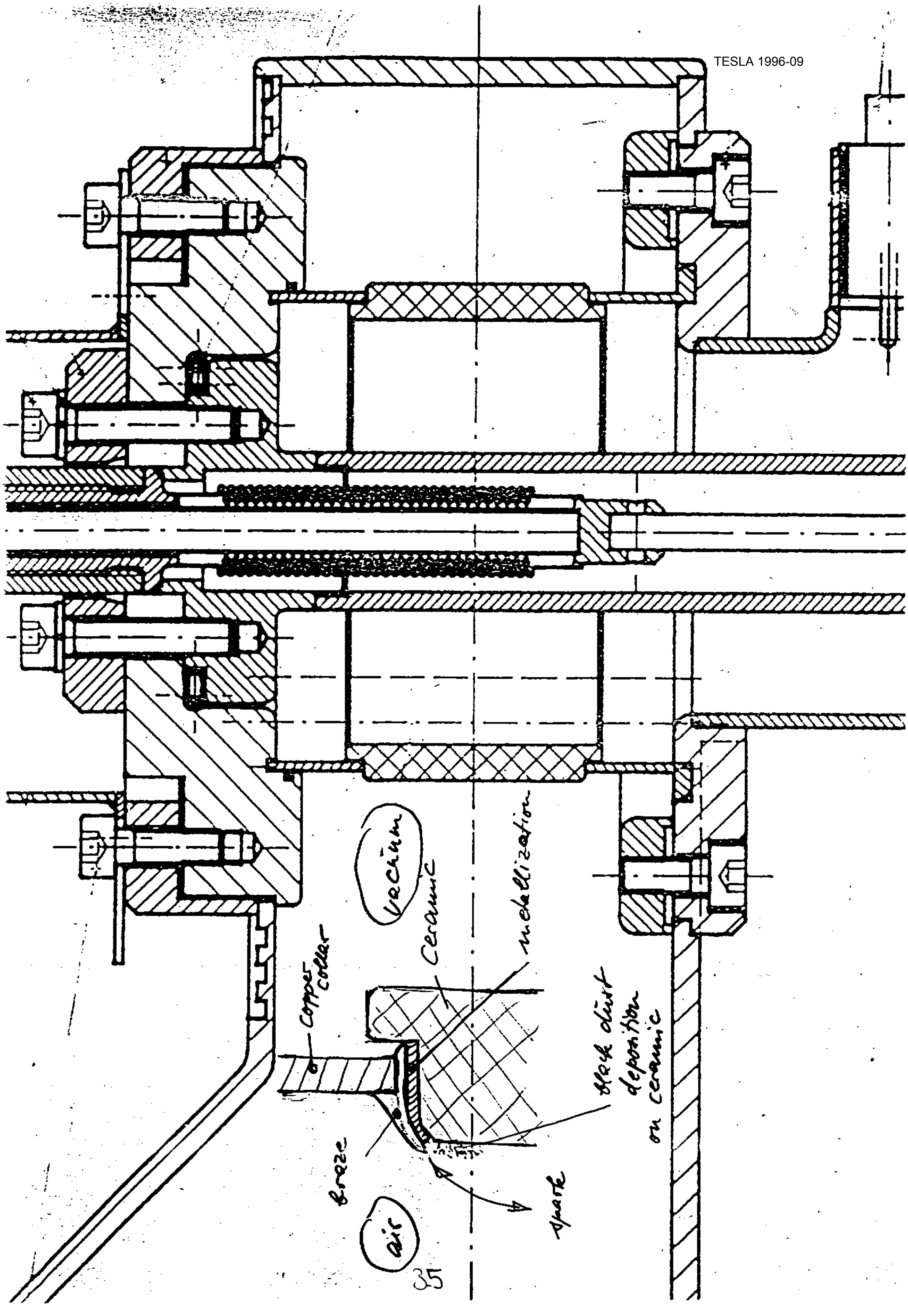
vacuum
ceramic
metallization
copper collar
black dust deposition on ceramic
braze
air
spark

AM29596

Cleanroom Preparation and Assembly of FERMI Coupler 2 +(3)

- 1. Experiences with coupler No 1
- 2 Change in procedures
- 3 sequence for FERMI 2+3
- 4 Assembly to cavity C 19

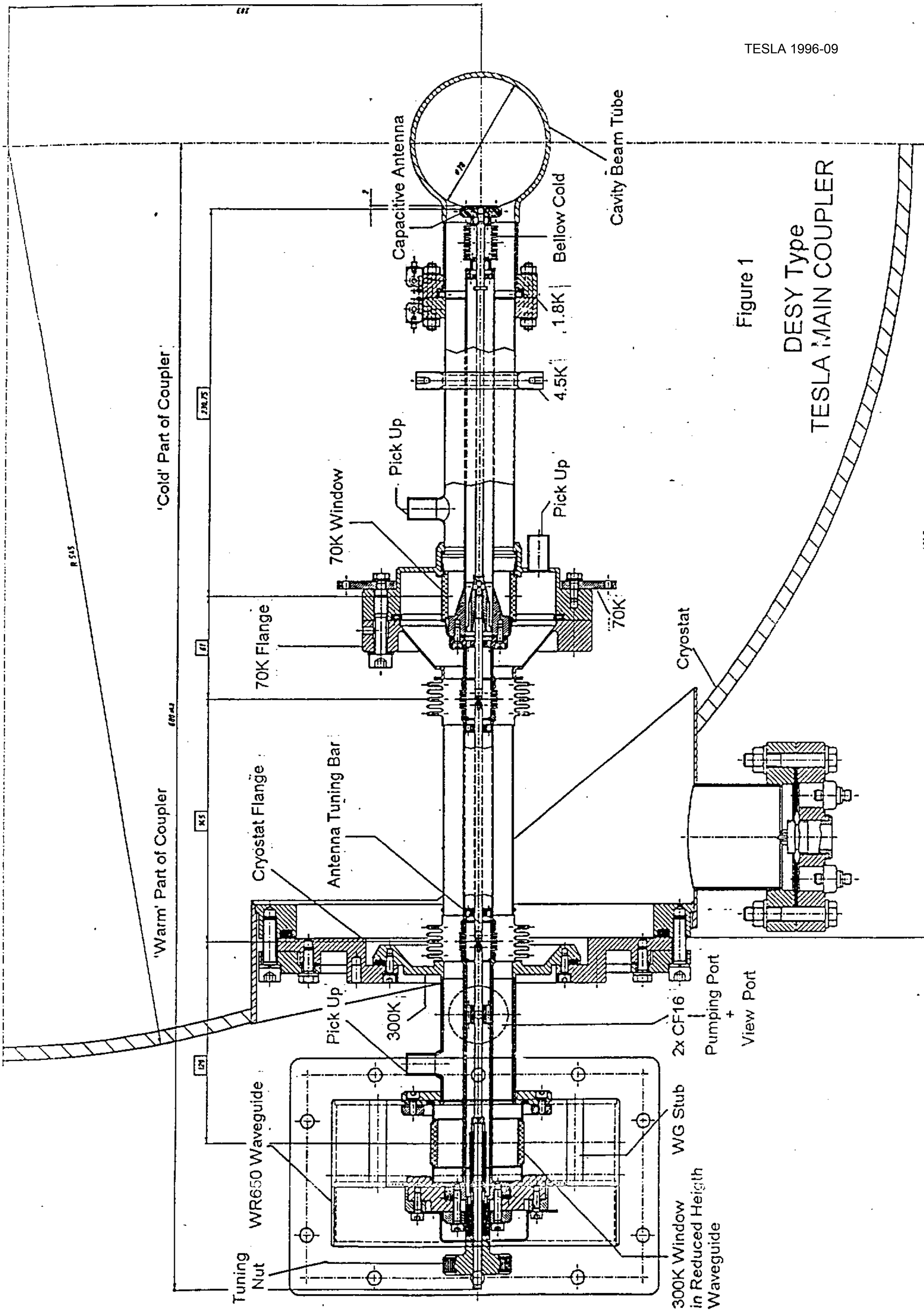

Figure 1

DESY Type TESLA MAIN COUPLER

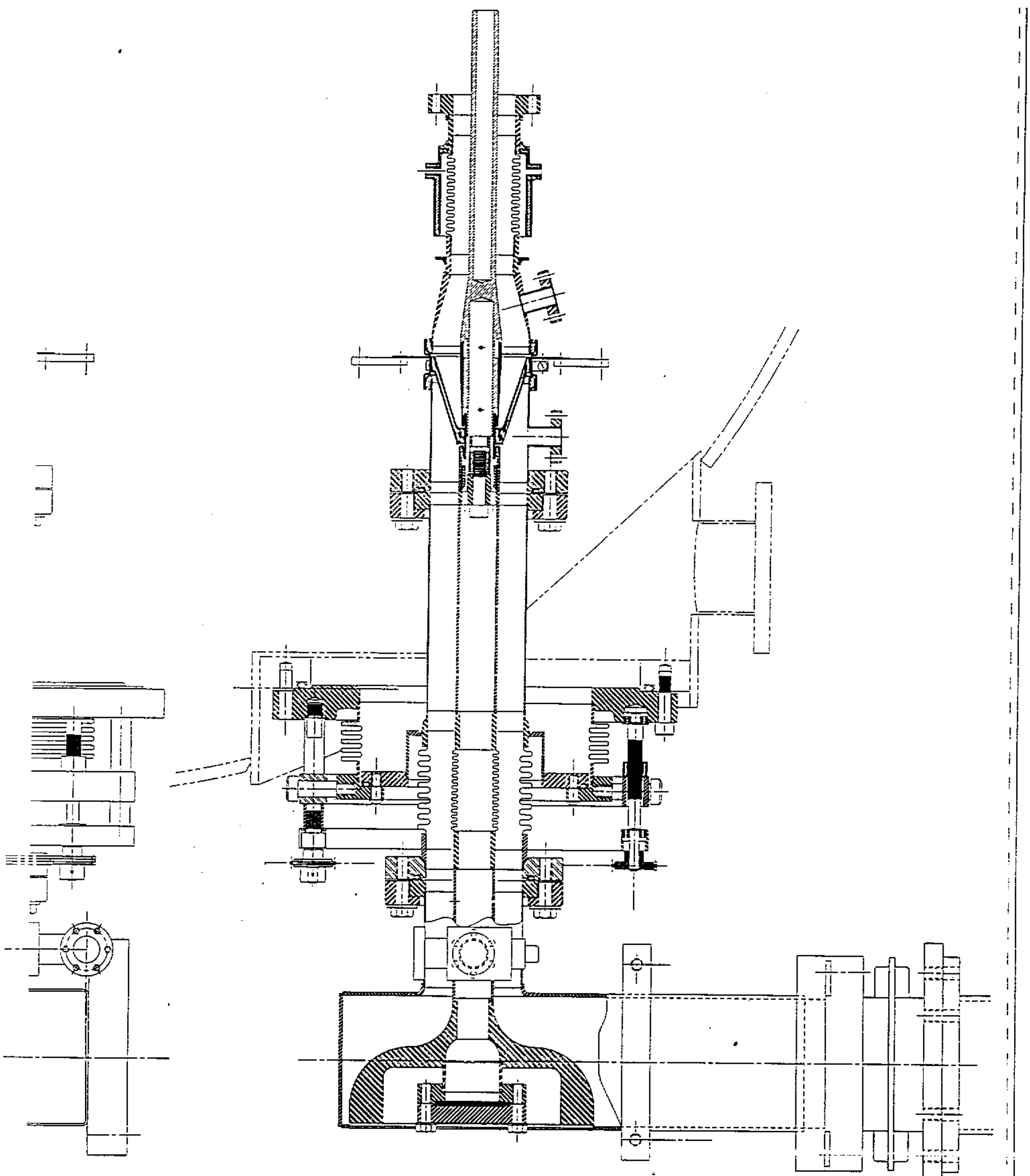

AM 29396

Experiences with FERMI one (Prototyp coupler)

Ultrasonic cleaning -	Peal off of plating
	burned in "durt " on the outside penetrated to the inside
Dust free rinse-	No excess to the bellow region. Bellow with lot´s of nesty areas
	Best value reached 4.2 MΩ cm resistivity
Transportation/ Handling	No dust free protection available
	No handling tools available

consequence -> clean parts during fabrication as good as possible and ceep them clean

change tooling and procedure for cleanroom preparation

AM29596

Change in procedure

Fabrication procedure-> see M.Kuchnir

Handling	design changed for fixtures to have good access to bellow region
Transportation	transport box for clean parts
oven	local cleanroom at the oven
	oven supplied with clean gas venting system
fixture	modified for insertion of coupler to cavity

Cleaning Sequence on Coupler Fermi 2 + 3

o unpacking after delivery	< class 10000>
o blowing with air gun	< class 10000>
o spraying with DI water (4 bar water pressure)	
roomtemperature part	
cold part	<class 10/10000>
o rinsing in water tank up to 12 MΩ cm	< class 10000>
o spraying with DI water	< class 100>
o Drying in class 10 area 24 h	< class 10>
o blowing with clean gas (particle filtered)	< class 10>
o transport in clean box to oven	< class 10>
o open box under class 100 laminar flow	< class 100>
o insertion to „oven „ under class 100 conditions	< class 100>

Assembly to cavity C19

- venting of oven by clean gas <10>
- insertion to transport box <100>
- cleaning of transport box outside <100>
- drying of box in class 10 <10>
- removal of coupler from box <10>
- blow with air gun <10>
- control of residual particles in clean Argon gas stream ((result better than 10 without flexing)) <10>
- venting of cavity with clean Argon <10>
- remove coupler # 1 under argon over pressure inside resonator <10>
- insertion of coupler # 2 under argon over pressure inside resonator <10>
- pump down and leak test <10>

ULTRA HIGH VACUUM BAKING SYSTEM

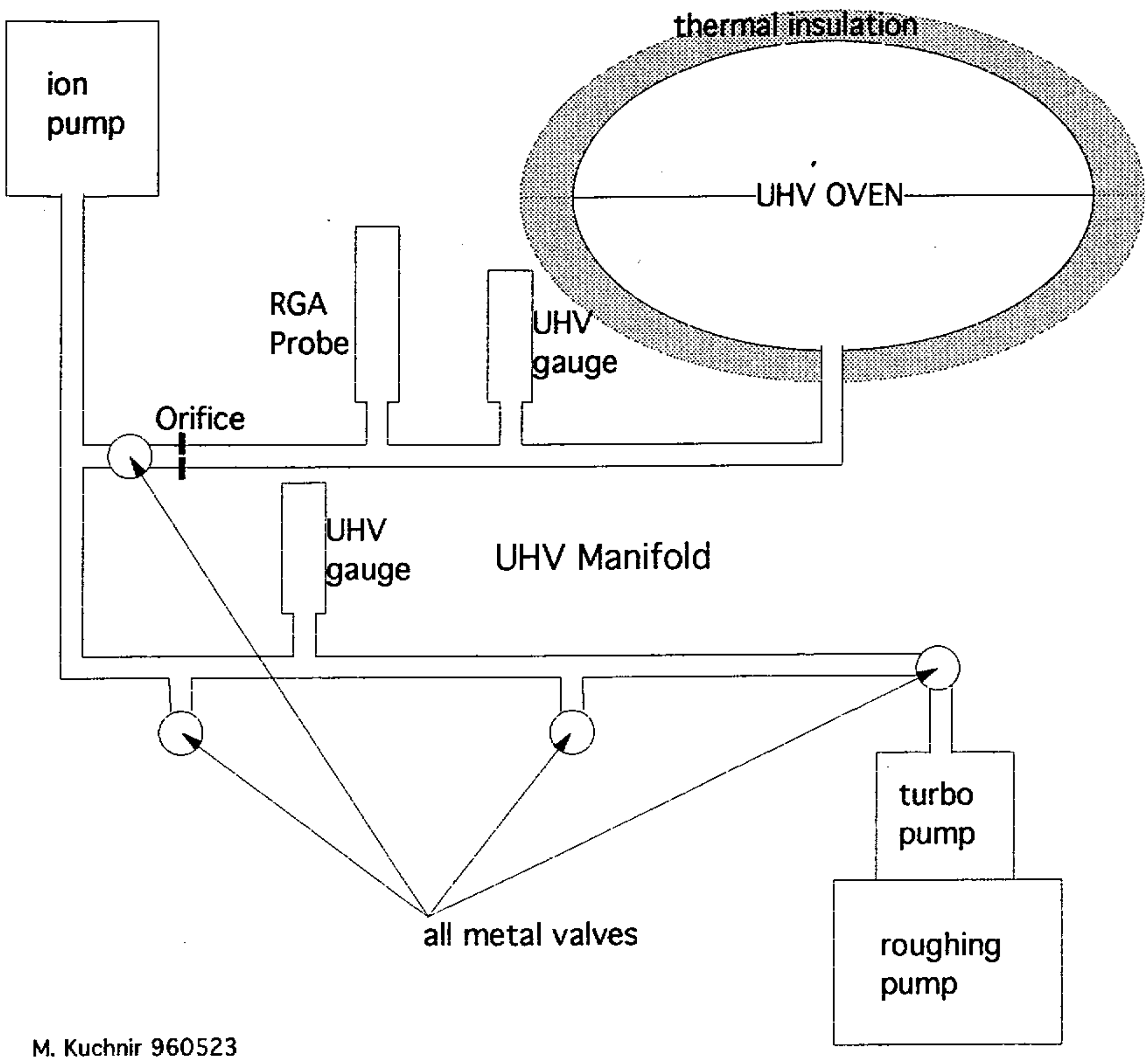

M. Kuchnir 960523

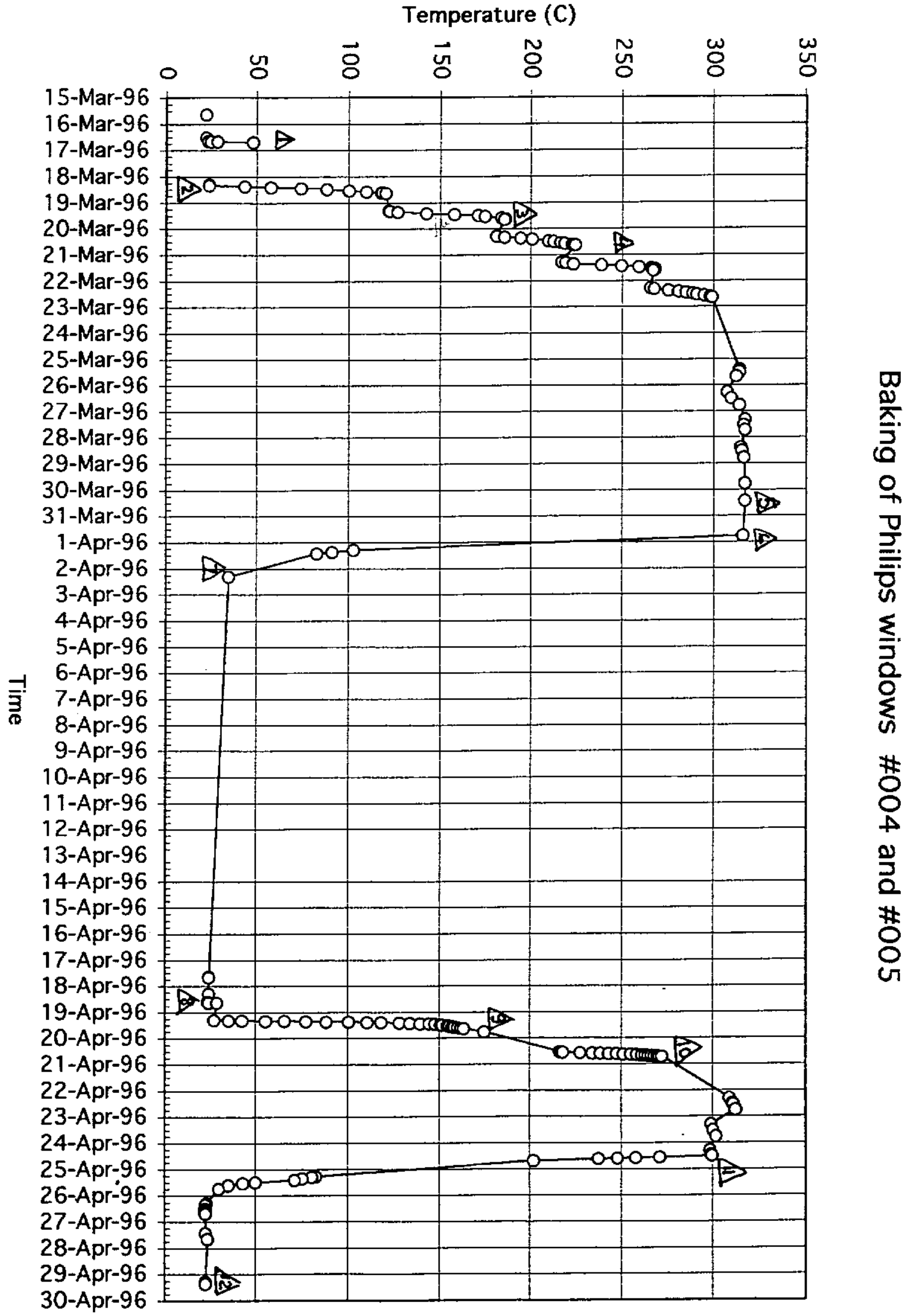
Baking of Philips windows #004 and #005
Temperature (C)
0
50
100
150
200
250
300
350
Time
15-Mar-96
16-Mar-96
17-Mar-96
18-Mar-96
19-Mar-96
20-Mar-96
21-Mar-96
22-Mar-96
23-Mar-96
24-Mar-96
25-Mar-96
26-Mar-96
27-Mar-96
28-Mar-96
29-Mar-96
30-Mar-96
31-Mar-96
1-Apr-96
2-Apr-96
3-Apr-96
4-Apr-96
5-Apr-96
6-Apr-96
7-Apr-96
8-Apr-96
9-Apr-96
10-Apr-96
11-Apr-96
12-Apr-96
13-Apr-96
14-Apr-96
15-Apr-96
16-Apr-96
17-Apr-96
18-Apr-96
19-Apr-96
20-Apr-96
21-Apr-96
22-Apr-96
23-Apr-96
24-Apr-96
25-Apr-96
26-Apr-96
27-Apr-96
28-Apr-96
29-Apr-96
30-Apr-96

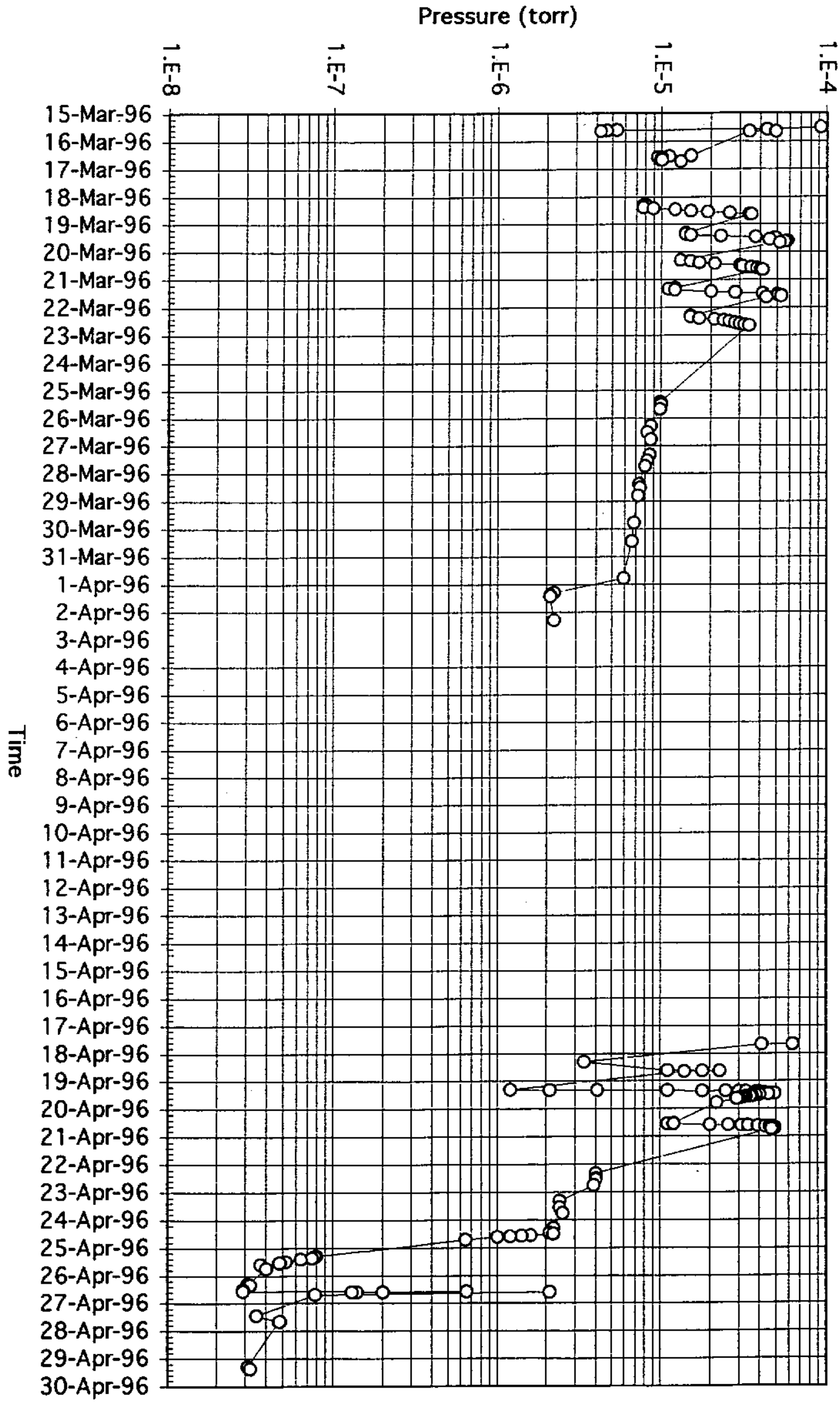

Baking of Philips windows #004 and #005

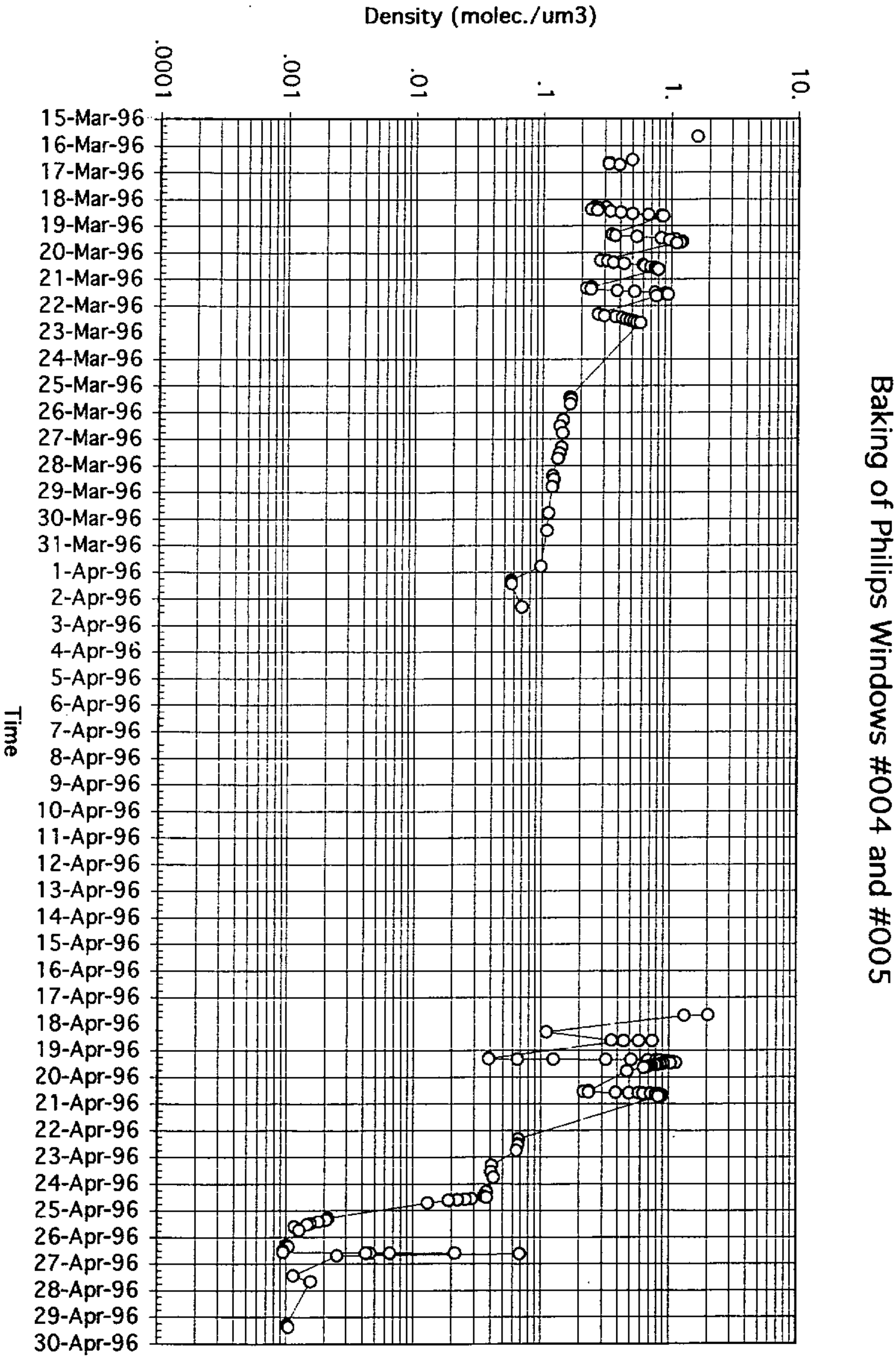
Baking of Philips Windows #004 and #005
Density (molec./um3)
.0001
.001
.01
.1
1.
10.
Time
15-Mar-96
16-Mar-96
17-Mar-96
18-Mar-96
19-Mar-96
20-Mar-96
21-Mar-96
22-Mar-96
23-Mar-96
24-Mar-96
25-Mar-96
26-Mar-96
27-Mar-96
28-Mar-96
29-Mar-96
30-Mar-96
31-Mar-96
1-Apr-96
2-Apr-96
3-Apr-96
4-Apr-96
5-Apr-96
6-Apr-96
7-Apr-96
8-Apr-96
9-Apr-96
10-Apr-96
11-Apr-96
12-Apr-96
13-Apr-96
14-Apr-96
15-Apr-96
16-Apr-96
17-Apr-96
18-Apr-96
19-Apr-96
20-Apr-96
21-Apr-96
22-Apr-96
23-Apr-96
24-Apr-96
25-Apr-96
26-Apr-96
27-Apr-96
28-Apr-96
29-Apr-96
30-Apr-96

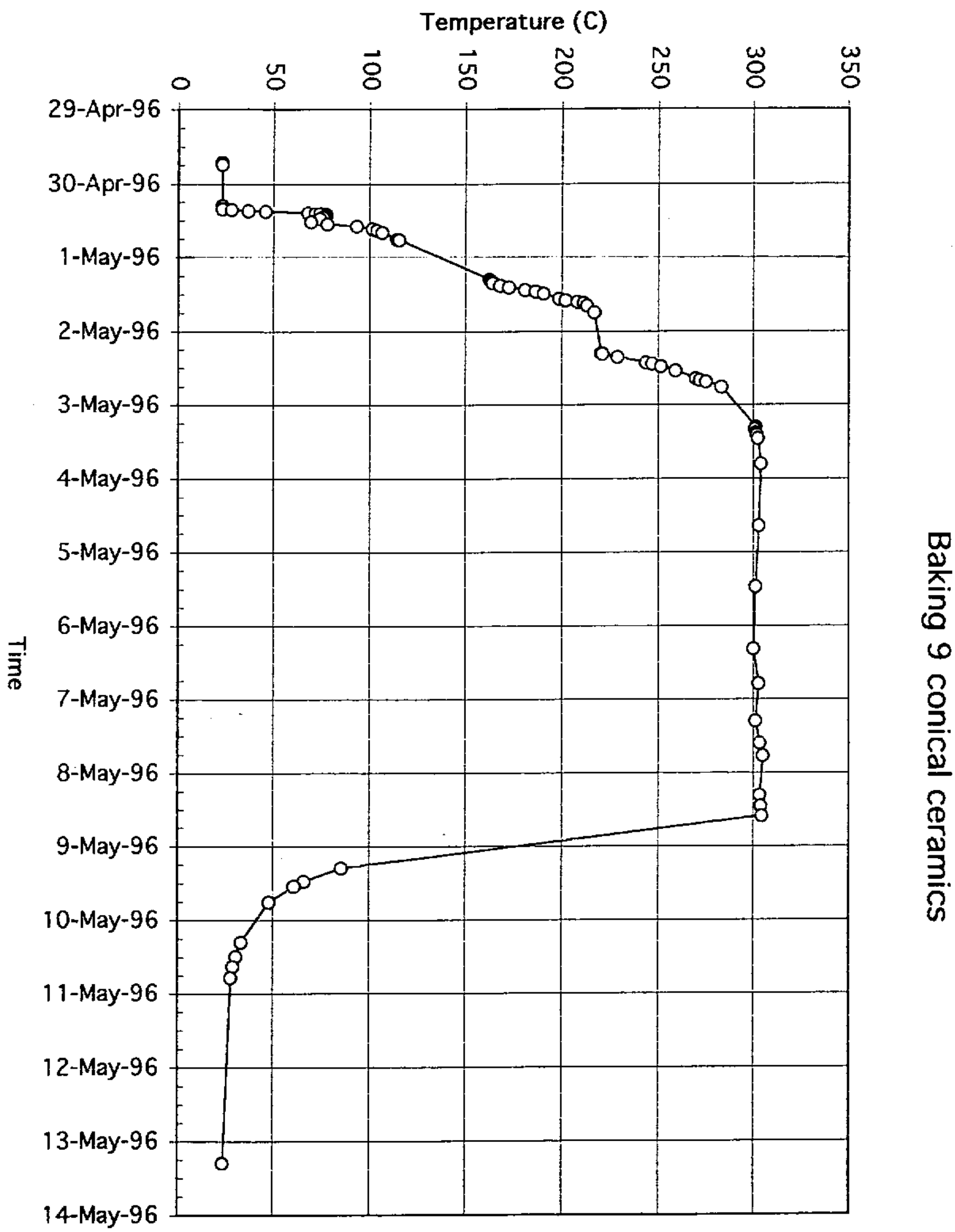
Baking 9 conical ceramics
Temperature (C)
0
50
100
150
200
250
300
350
Time
29-Apr-96
30-Apr-96
1-May-96
2-May-96
3-May-96
4-May-96
5-May-96
6-May-96
7-May-96
8-May-96
9-May-96
10-May-96
11-May-96
12-May-96
13-May-96
14-May-96

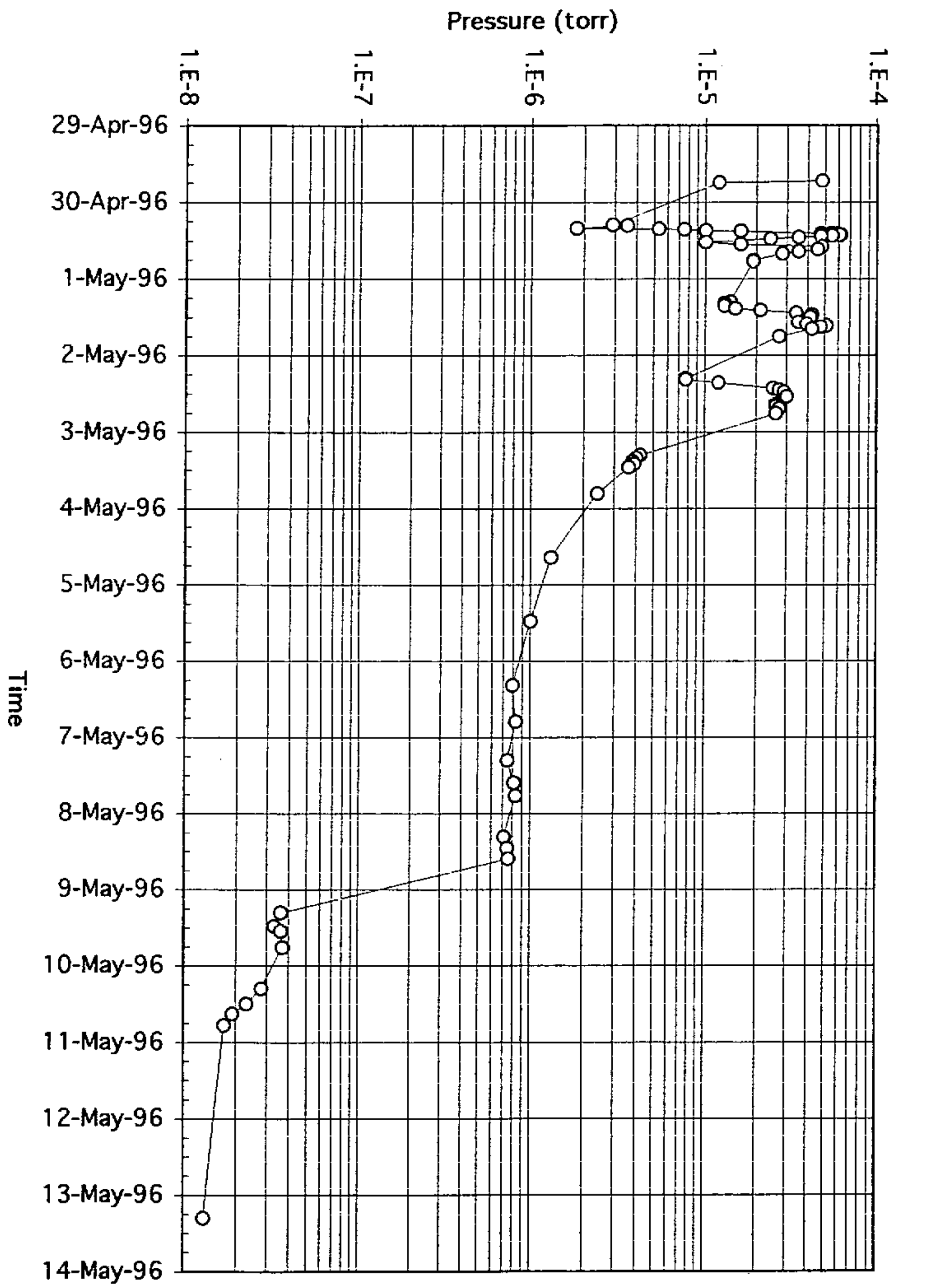

Baking 9 conical ceramics

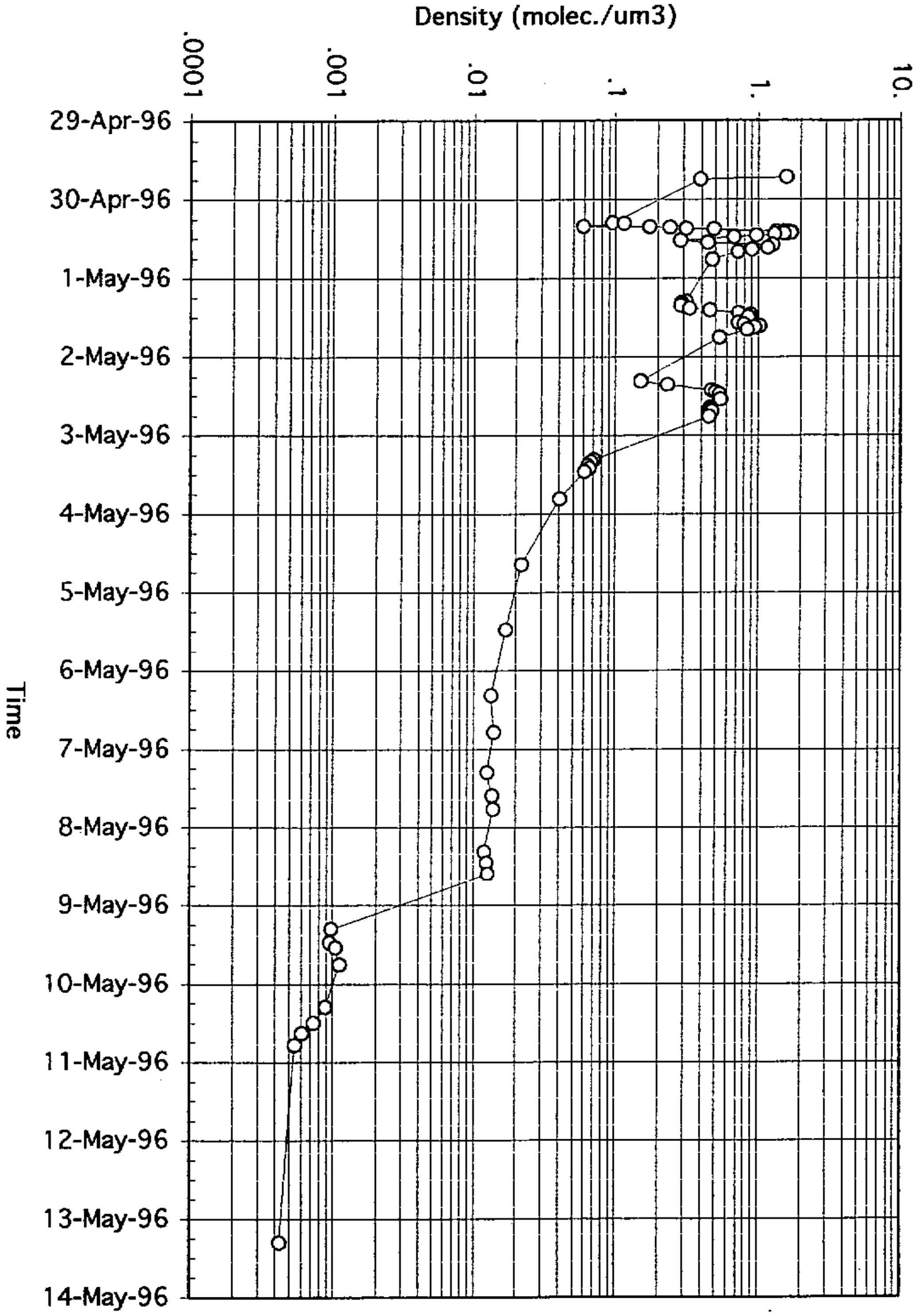

Baking 9 conical ceramics

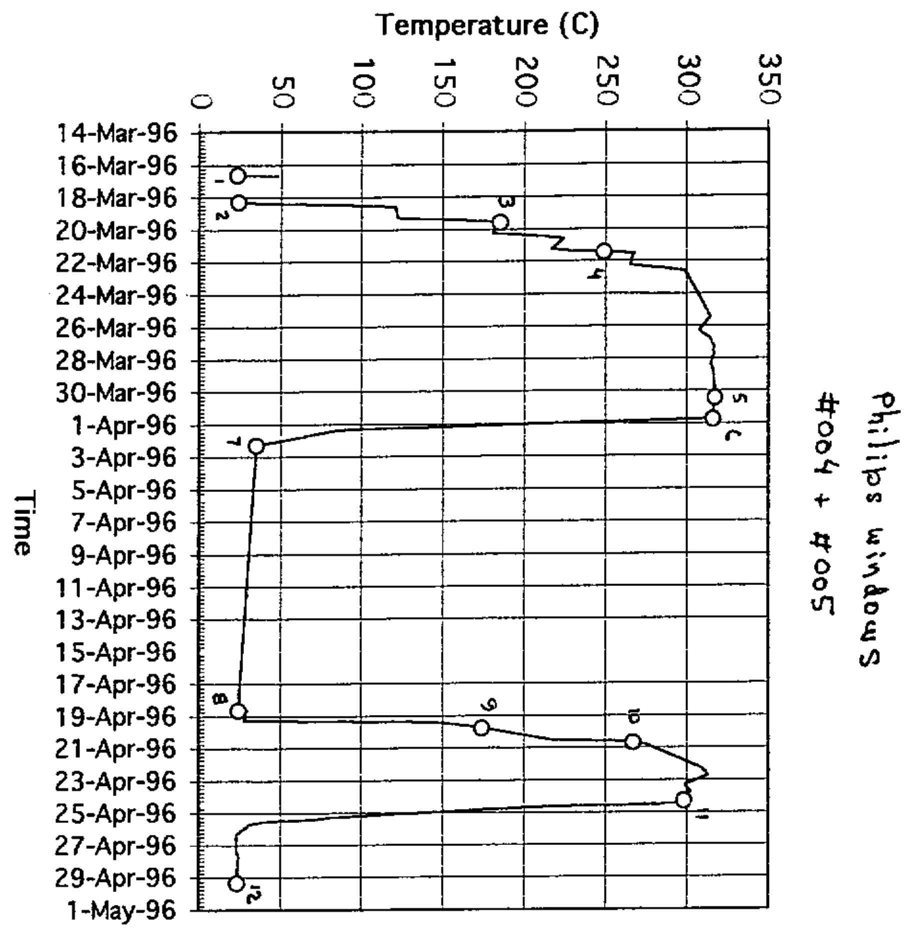
Temperature (C)
0
50
100
150
200
250
300
350
14-Mar-96
16-Mar-96
18-Mar-96
20-Mar-96
22-Mar-96
24-Mar-96
26-Mar-96
28-Mar-96
30-Mar-96
1-Apr-96
3-Apr-96
5-Apr-96
7-Apr-96
9-Apr-96
11-Apr-96
13-Apr-96
15-Apr-96
17-Apr-96
19-Apr-96
21-Apr-96
23-Apr-96
25-Apr-96
27-Apr-96
29-Apr-96
1-May-96
Time
Philips windows
#004 + #005

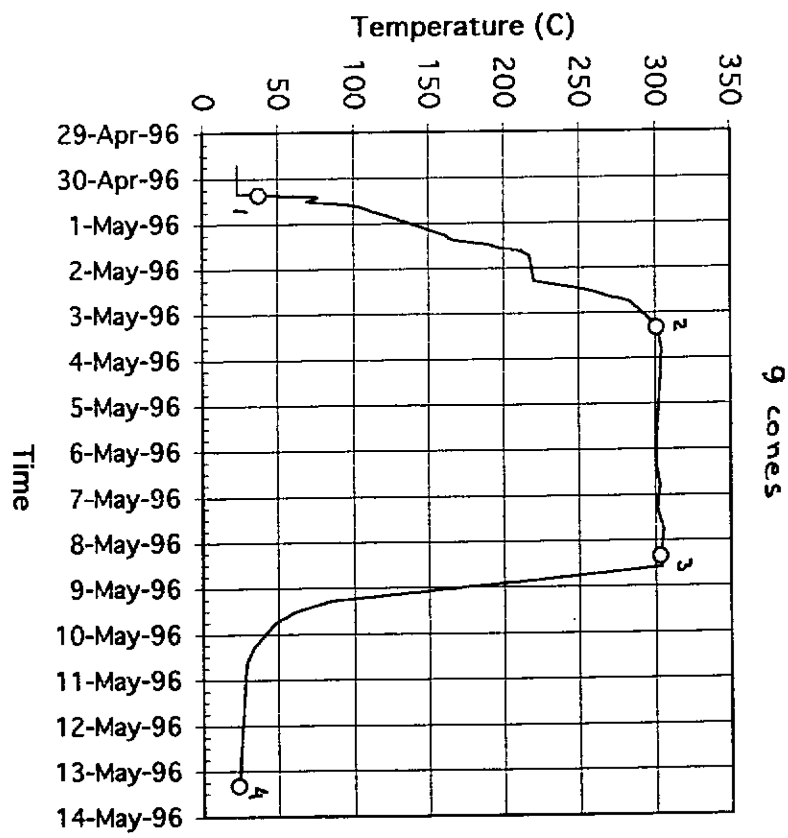
Temperature (C)
0
50
100
150
200
250
300
350
29-Apr-96
30-Apr-96
1-May-96
2-May-96
3-May-96
4-May-96
5-May-96
6-May-96
7-May-96
8-May-96
9-May-96
10-May-96
11-May-96
12-May-96
13-May-96
14-May-96
Time
9 cones

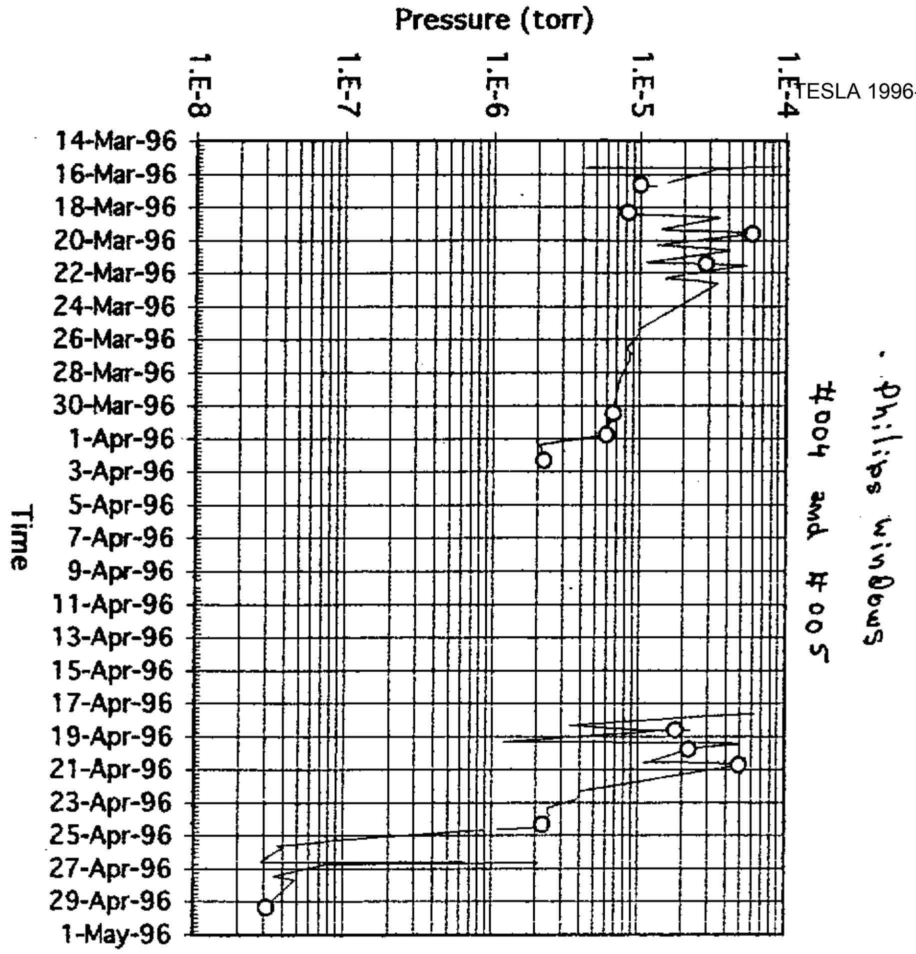
Pressure (torr)
1.E-8
1.E-7
1.E-6
1.E-5
1.E-4
Time
14-Mar-96
16-Mar-96
18-Mar-96
20-Mar-96
22-Mar-96
24-Mar-96
26-Mar-96
28-Mar-96
30-Mar-96
1-Apr-96
3-Apr-96
5-Apr-96
7-Apr-96
9-Apr-96
11-Apr-96
13-Apr-96
15-Apr-96
17-Apr-96
19-Apr-96
21-Apr-96
23-Apr-96
25-Apr-96
27-Apr-96
29-Apr-96
1-May-96
· Philips windows
#004 and #005

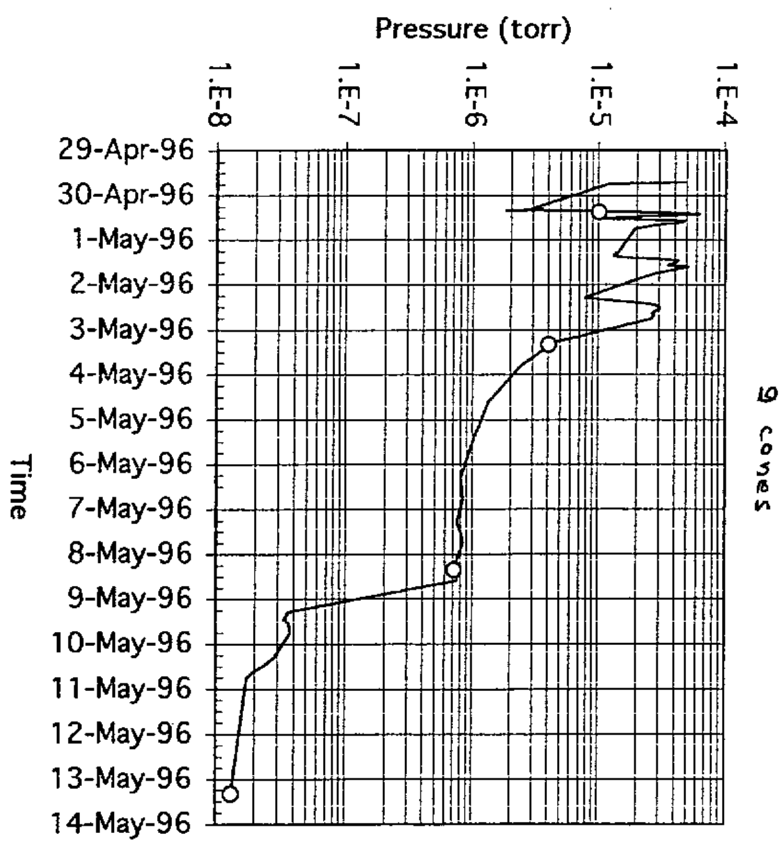
Pressure (torr)
1.E-8
1.E-7
1.E-6
1.E-5
1.E-4
Time
29-Apr-96
30-Apr-96
1-May-96
2-May-96
3-May-96
4-May-96
5-May-96
6-May-96
7-May-96
8-May-96
9-May-96
10-May-96
11-May-96
12-May-96
13-May-96
14-May-96
9 cones

Philips windows #4 and #5

TESLA 1996-09

end time MASS	1	2	12	14	15	16	17	18	20	28	29	30	32	40	44	Pt. #
96/3/16 15:43	170	60	21	100	3	61	107	510	2	2100	23	46	50	27	87	1
96/3/18 07:23	150	59	12	145	6.4	62	64	235	3	3000	24	76	210	33	240	2
96/3/19 14:39	390	280	90	39	55	220	140	2800	1.7	1100	10	6.3	4.9	2.8	1500	3
96/3/21 11:11	610	980	69	61	59	150	370	1300	1	1700	20	8	1	6	1000	4
96/3/30 10:44	490	3200	3.6	60	9	61	70	66	3	1100	15	0.001	0.001	20	29	5
96/3/31 18:40	470	3100	2.9	61	8	56	65	48	3	1100	13	0.001	0.001	20	23	6
96/4/2 07:36	25	6.5	1	49	0.3	3.2	1.5	2.6	2	900	6.6	3	8.9	7	7.2	7
96/4/18 15:21	350	525	100	85	70	750	1600	4600	6	3700	80	87	7	5	1400	8
96/4/19 19:00	210	70	130	42	78	270	590	2300	6	2200	27	9	1	2	1400	9
96/4/20 16:56	390	250	300	110	38	590	820	3100	1.6	5500	47	12	2	2.2	100	10
96/4/24 07:31	120	500	3	1.8	6.7	11	11	38	0.001	70	0.5	0.001	0.001	0.001	20	11
96/4/29 08:07	1	4.7	0.21	0.06	0.042	0.35	0.22	0.9	0.001	6.1	0.02	0.001	0.001	0.002	1.4	12

Baking 9 conical ceramics

time MASS=	1	2	12	14	15	16	17	18	20	28	29	30	40	44	pt. #	obs.
96/4/30 08:50	210	350	50	12	66	200	680	2600	5.9	1400	22	7	1	53	1	
96/5/3 08:09	98	120	9.1	7.5	2.9	45	47	160	0.1	440	1.4	0.5	0.1	150	2	
96/5/8 08:27	47	101	1	0.3	0.74	6	4.2	14	0.12	62	0.25	0.05	0.02	15	3	
96/5/13 07:57	0.86	3.4	0.095	0.014	0.09	0.18	0.022	0.26	0.008	0.72	0.021	0.01	0.008	0.038	4	

Residual Gas in the bakeout of Philips windows #004 and #005

GAS	PARTIAL PRESSURE (ntorr)											
Point #	1	2	3	4	5	6	7	8	9	10	11	12
Water	510	227	520	1300	66	48	2.6	4600	2300	3100	38	1
Amonia	0.01	0.01	31	100	56	55	1	634	107	170	3	0.01
Methane	6	7.5	61	60	6	4	0.3	70	78	38	6.7	0.01
Carbon Dioxide	87	240	1500	1000	29	23	7.2	1400	1400	100	20	1.4
Carbon Monoxide	400	100	440	750	60	20	10	2520	1680	3500	50	4
Nitrogen	2000	2880	560	950	1040	1180	980	1180	1180	2000	20	2
Oxygen	50	210	5	1	0.01	0.01	8.9	7	1	2	0.01	0.01
Argon	27	33	2.8	6	20	20	7	5	2	2.2	2.2	0.01

Residual Gas in the bakeout of 9 conical ceramics

GAS	PARTIAL PRESSURE (ntorr)			
Point #	1	2	3	4
Water	2600	160	14	0.26
Amonia	134	30	1	0.01
Methane	66	2.9	0.7	0.01
Carbon Dioxide	53	150	15	0.01
Carbon Monoxide	920	100	35	0.01
Nitrogen	480	140	20	0.01
Oxygen	6.3	6.3	0.2	0.01
Argon	1.2	0.1	0.01	0.01

Residual Gas in the bakeout of Philips windows #004 and #005

GAS	PARTIAL PRESSURE (ntorr)											
Point #	1	2	3	4	5	6	7	8	9	10	11	12
Water	510	227	520	1300	66	48	2.6	4600	2300	3100	38	1
Amonia	0.01	0.01	31	100	56	55	1	634	107	170	3	0.01
Methane	6	7.5	61	60	6	4	0.3	70	78	38	6.7	0.01
Carbon Dioxide	87	240	1500	1000	29	23	7.2	1400	1400	100	20	1.4
Carbon Monoxide	400	100	440	750	60	20	10	2520	1680	3500	50	4
Nitrogen	2000	2880	560	950	1040	1180	980	1180	1180	2000	20	2
Oxygen	50	210	5	1	0.01	0.01	8.9	7	1	2	0.01	0.01
Argon	27	33	2.8	6	20	20	7	5	2	2.2	2.2	0.01

Residual Gas in the bakeout of 9 conical ceramics

GAS	PARTIAL PRESSURE (ntorr)			
Point #	1	2	3	4
Water	2600	160	14	0.26
Amonia	134	30	1	0.01
Methane	66	2.9	0.7	0.01
Carbon Dioxide	53	150	15	0.01
Carbon Monoxide	920	100	35	0.01
Nitrogen	480	140	20	0.01
Oxygen	6.3	6.3	0.2	0.01
Argon	1.2	0.1	0.01	0.01

Bake out of coupler parts

Input Coupler Workshop, DESY May 29/96

K. Zapfe-Düren
D. Hubert
G. Wojtkiewicz

- vacuum pipe + 400 l/s Getter pump } no furnace
  heating tapes → 300°C 'bake out'
- p ≤ 10^{-5} mbar during heating cycle
- bake out after cleanroom procedure → A. Matheisen

	FERMILAB 1/2	FERMILAB 3/4	DESY 1/2
pre treatment	optically dirty	bake out of ceramics (300°C) bake out of cold part before shipping (300°C) clean vacuum handling	clean vacuum handling
installation		lokal cleanroom	lokal cleanroom
bake out	300°C / 22 h Long time needed (~ several days)	300°C / 19 h	300°C / 24 h

- all couplers are similiar in mass sprectra
- bake out improves spectra (e.g. FERMILAB 3/4)
- clean vacuum handling important !
- improvement of material recommended (e.g. SS 316 LN)
- bake out of ceramics at T > 1000°C in clean vacuum
  vacuum firing (950°C) of SS parts (no 'C's)

⇒ fabrication process should be optimized to minimize necessary steps

Empty vacuum tank used for bake out of Fermilab couplers

DESY pVAK Massenspektrometer 16:48.20 30.Oct.95
Bereich: 3.12E-8 mbar (A) I emission: .19 mA SEV: 0 V Offset 5
P total: 2.32E-8 mbar Speed: 400 msec/Masse (A) Filter 20 (-)

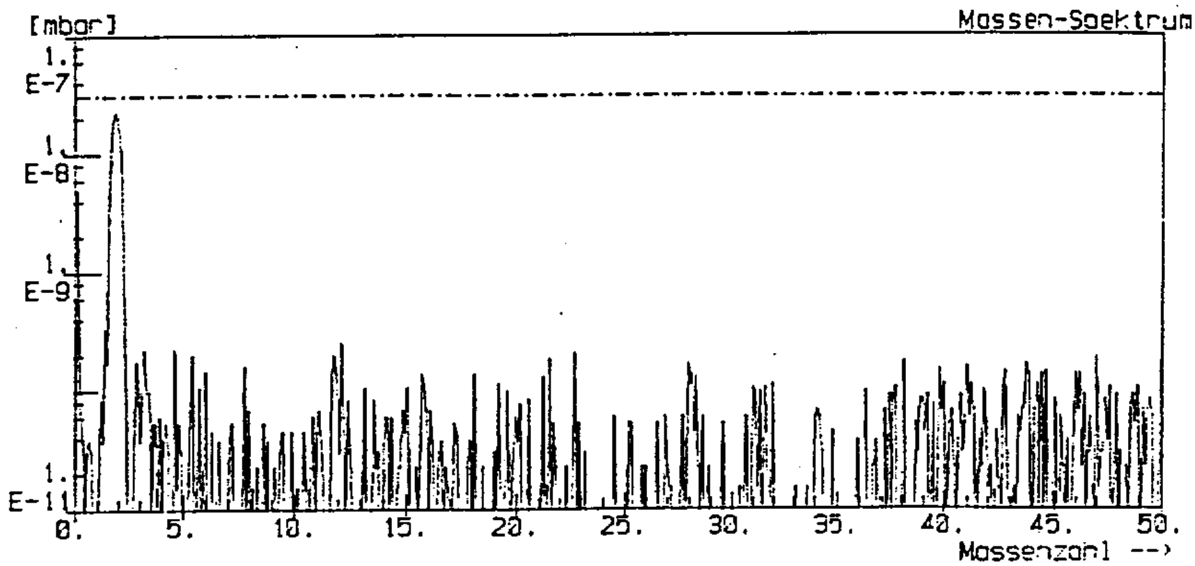

before coupler bake out

FIGURE 1. Massenspektrum der leeren Vakuumkammer bei ca. 70 °C vor dem Ausheizen der Kopplerkomponenten (Empfindlichkeit p = 10^{-8} mbar).

DESY pVAK Massenspektrometer 21:13.17 30.Nov.95
Bereich: 3.90E-9 mbar (A) I emission: .19 mA SEV: 0 V Offset 574
P total: 2.03E-9 mbar Speed: 1200 msec/Masse (A) Filter 60 (-)

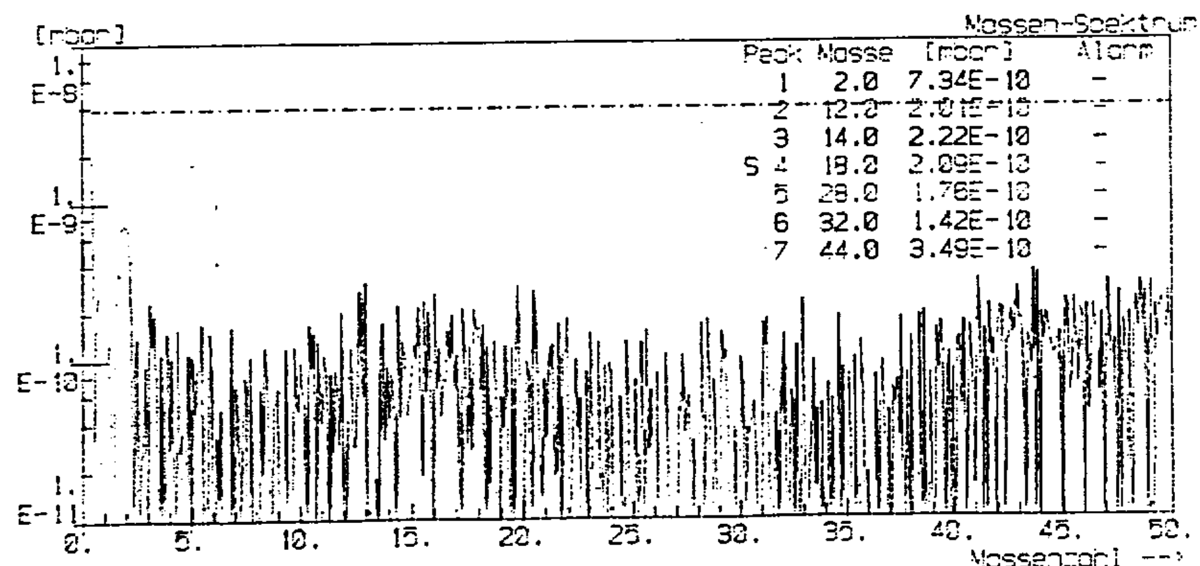

after coupler bake out

FIGURE 2. Massenspektrum der leeren Vakuumkammer bei ca. 25 °C nach dem Ausheizen der Kopplerkomponenten (Empfindlichkeit p = 10^{-9} mbar).

1) Cold parts before bake out

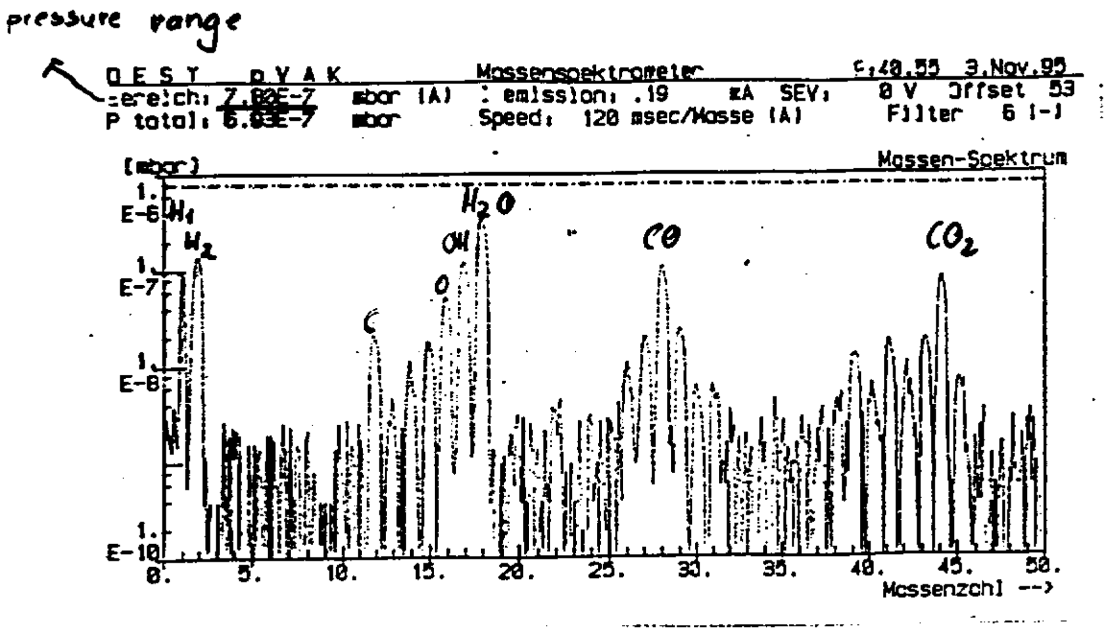

FERMILAB 1/2

50°C / 14 h

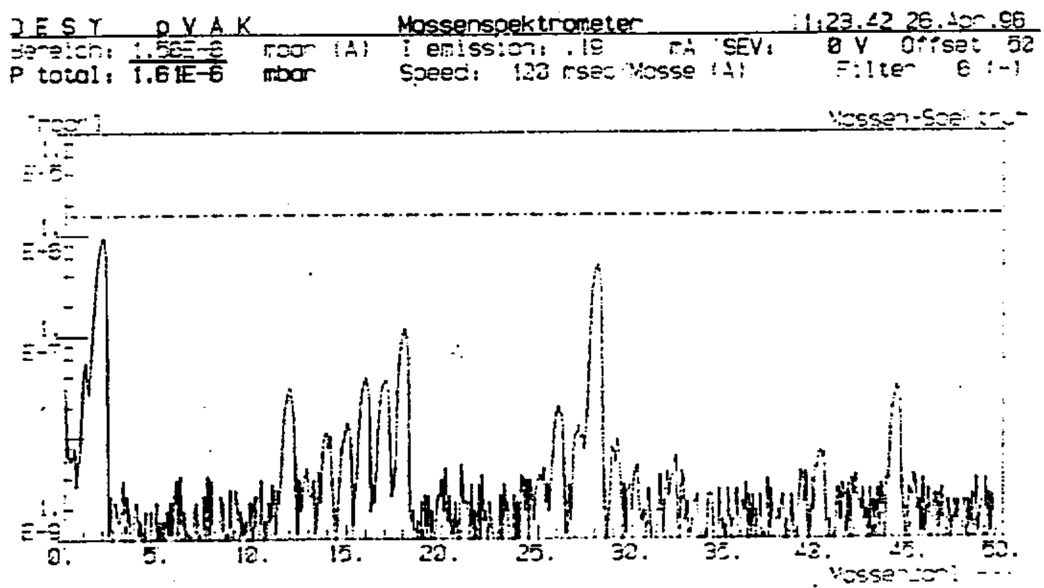

FERMILAB 3/4

36°C / 21 h

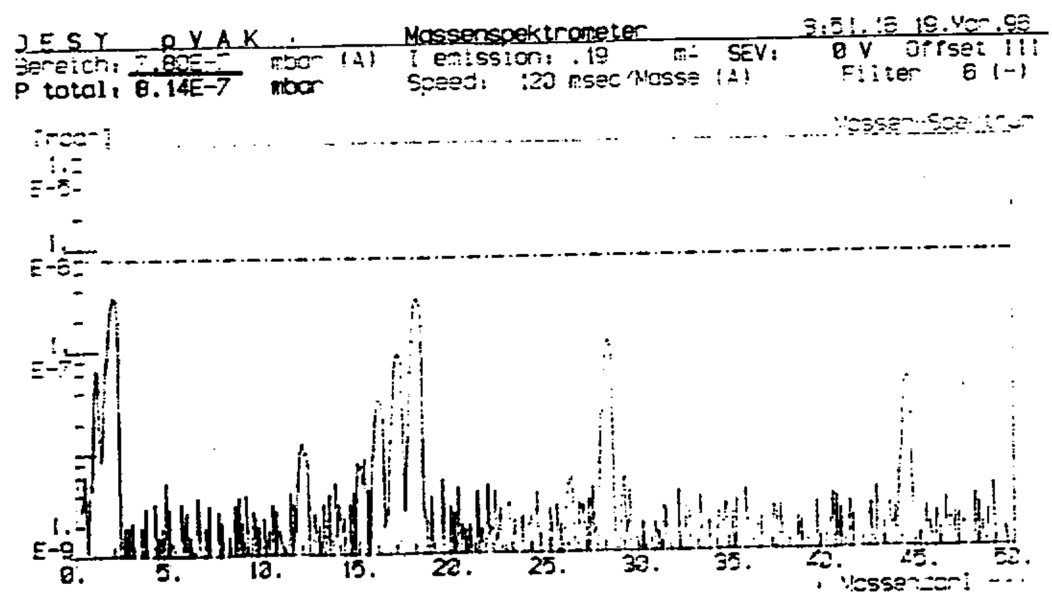

DESY 1/2

20°C / 19h

2) Cold parts during bake out

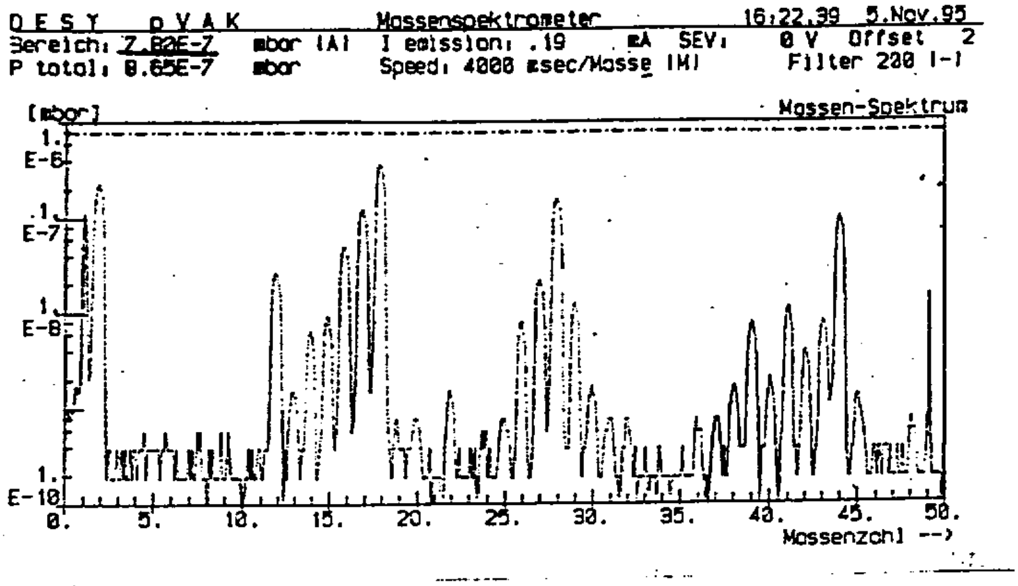

FERMILAB 1/2

215°C

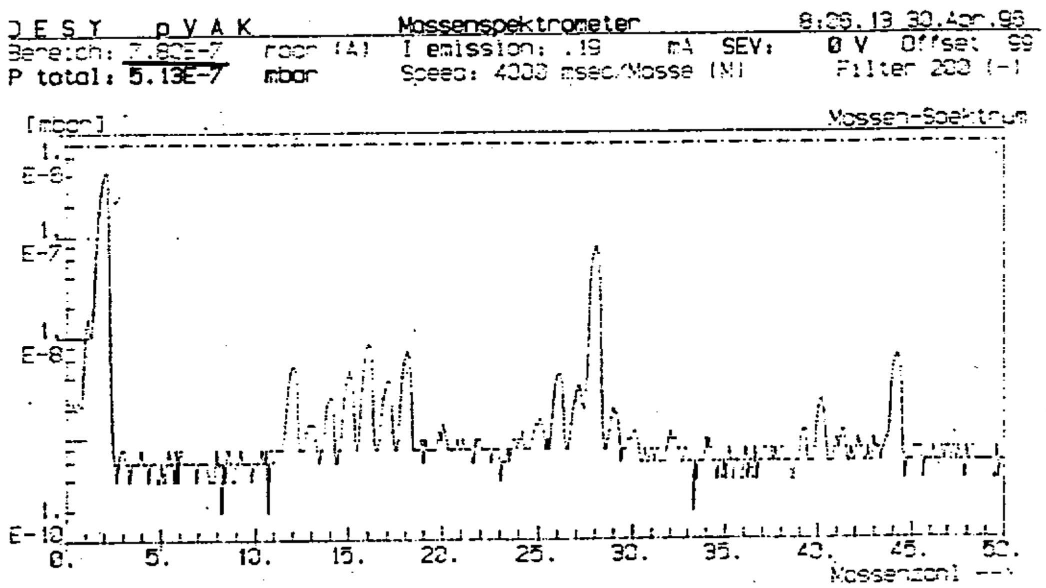

FERMILAB 3/4

300 °C

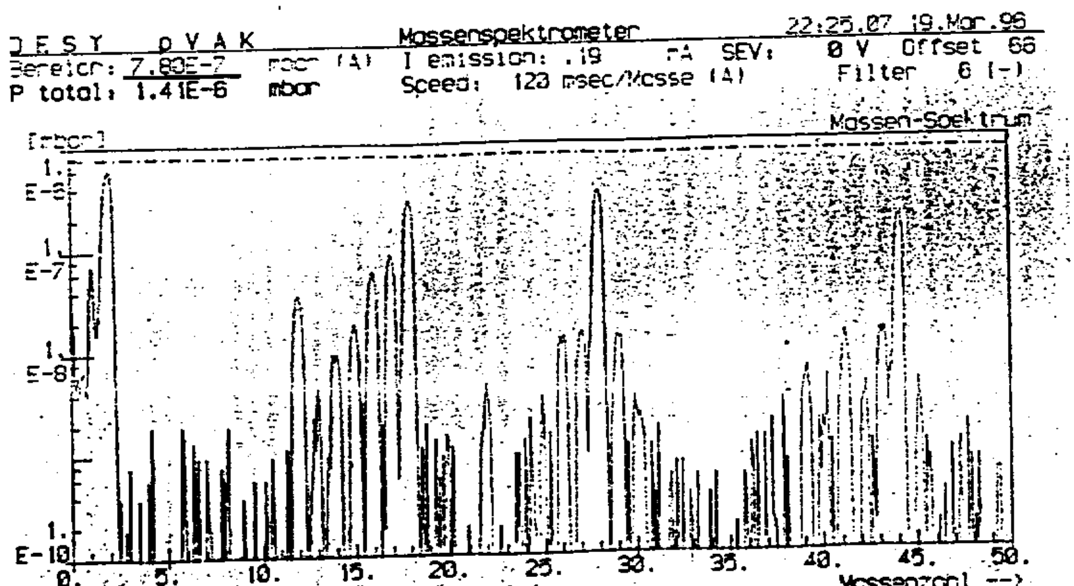

DESY 1/2

200 °C [crossed out]

3) Cold parts after bake out

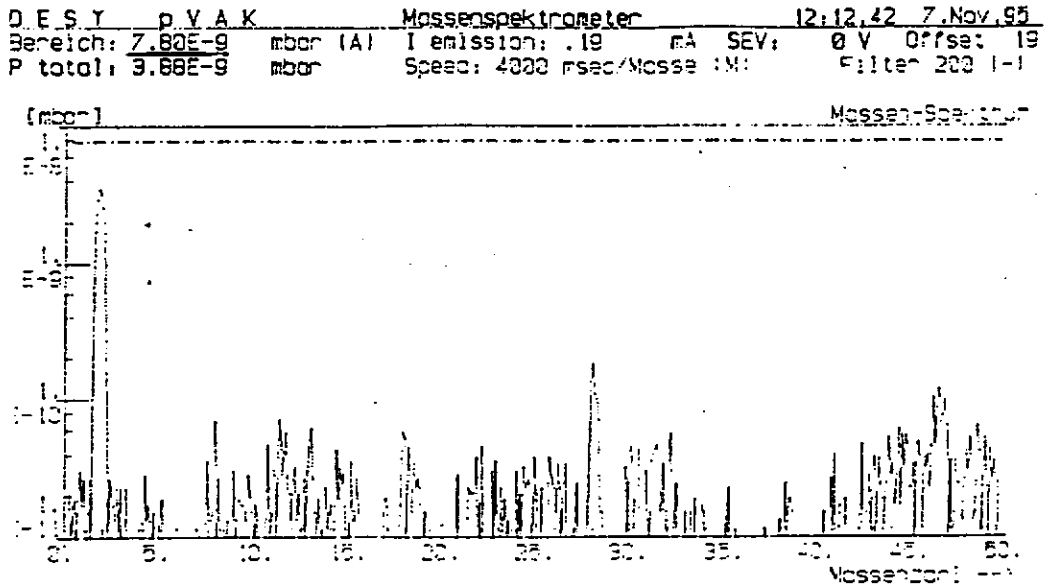

FERMILAB 1/2

24°C / 10 h after cooldown

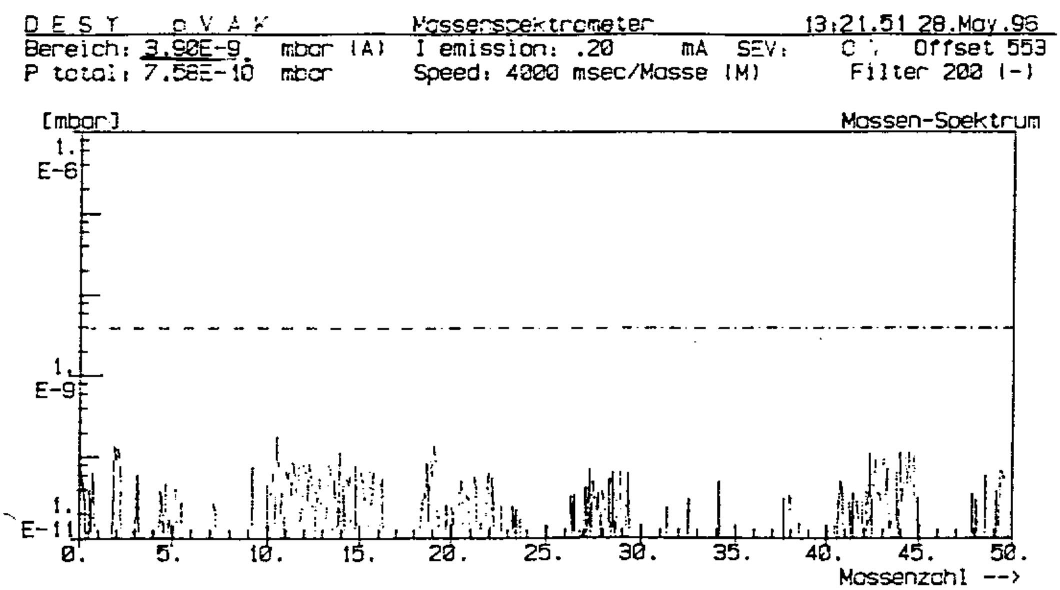

FERMILAB 3/4

50°C / 600 h after cool.

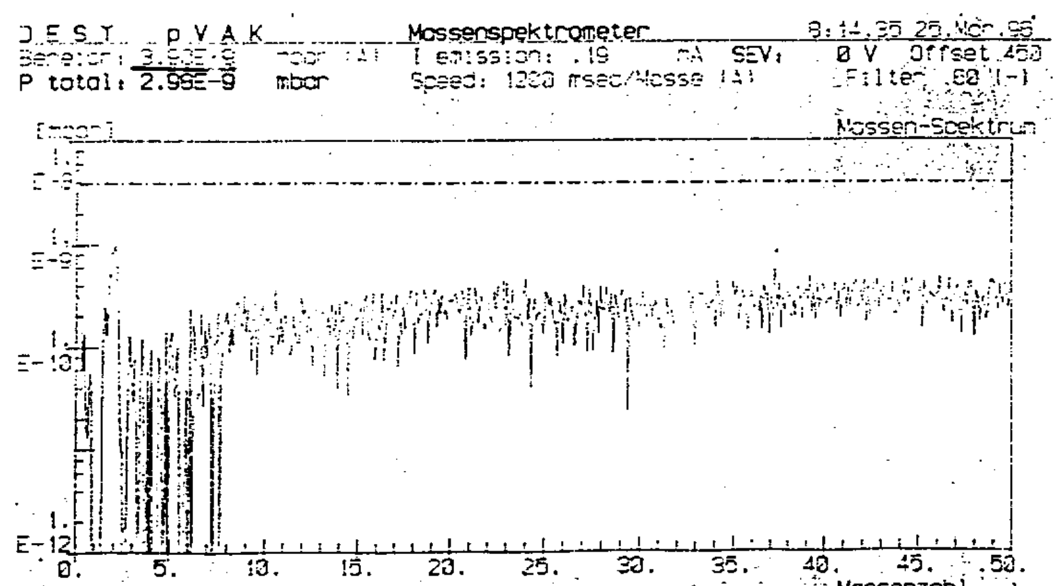

DESY 1/2

20°C 142 h after cooldown

11

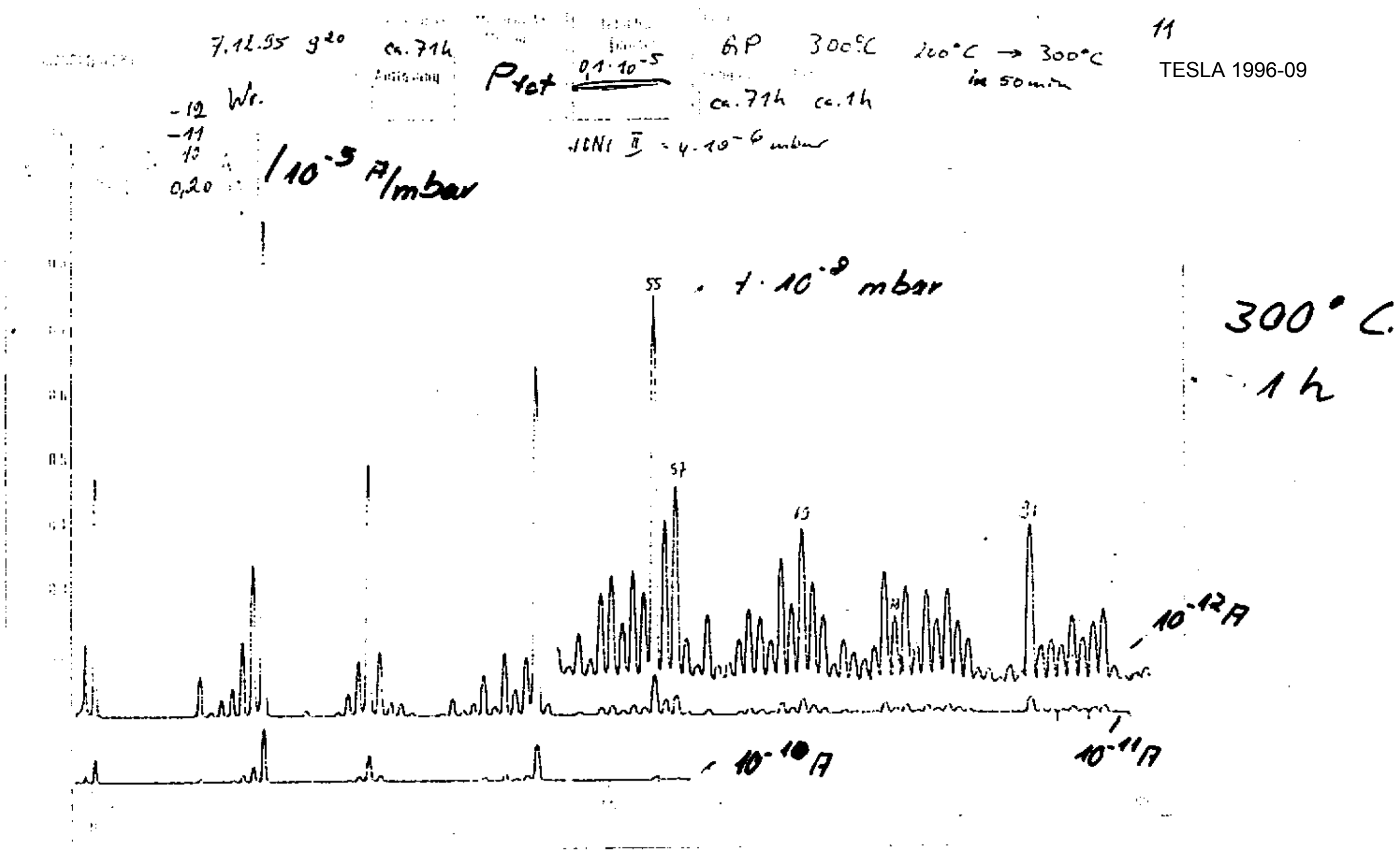

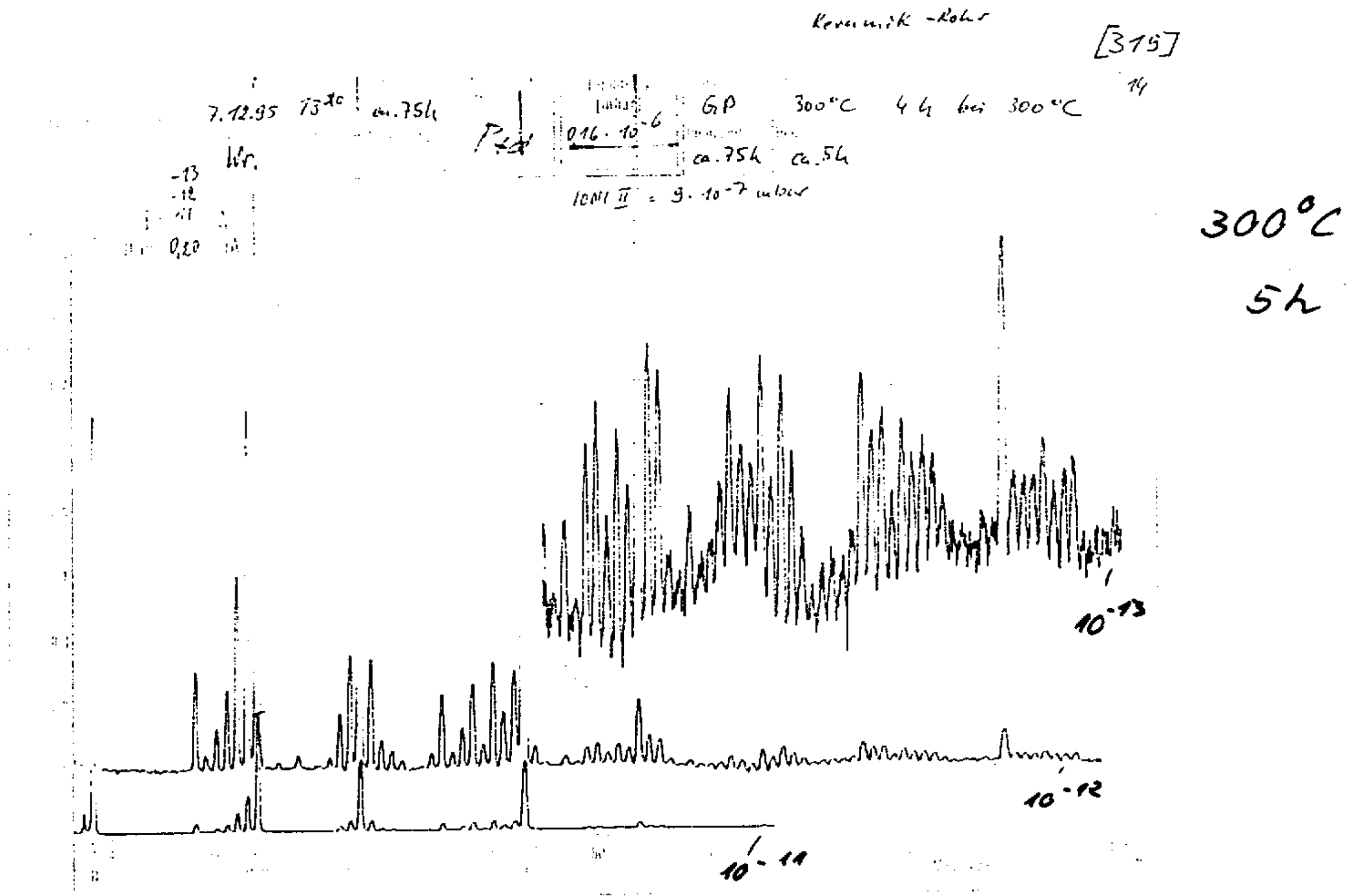

'pure' ceramics for DESY coupler

TESLA 1996-09

29. May. 1996

Experience with coupler processing (TTF-couplers)

Wolf-D. Möller
Mark Champion
Bernhard Dwersteg
André Gössel
⋮

Coupler teststand

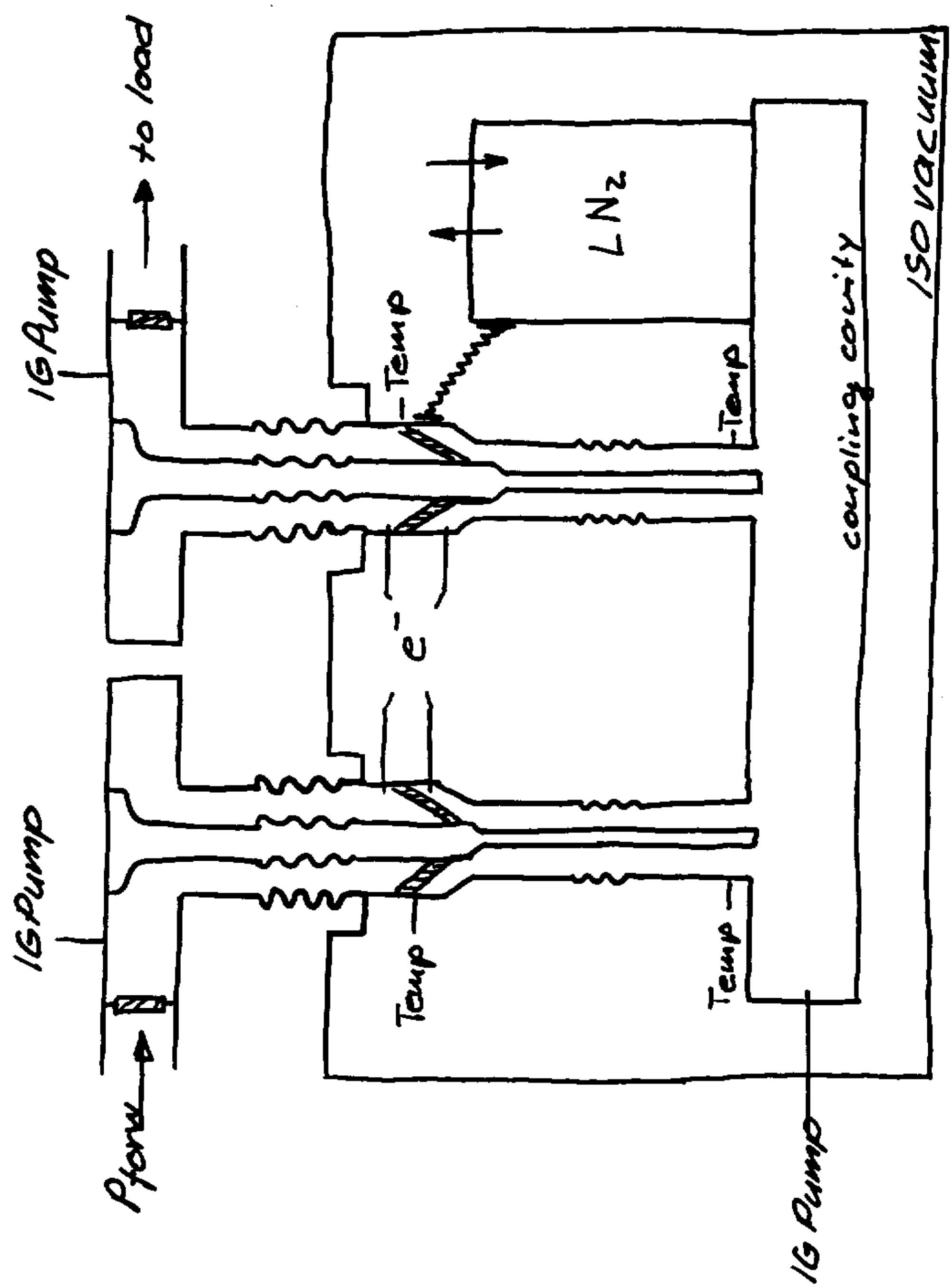

Fermi TTF coupler on CHECHIA

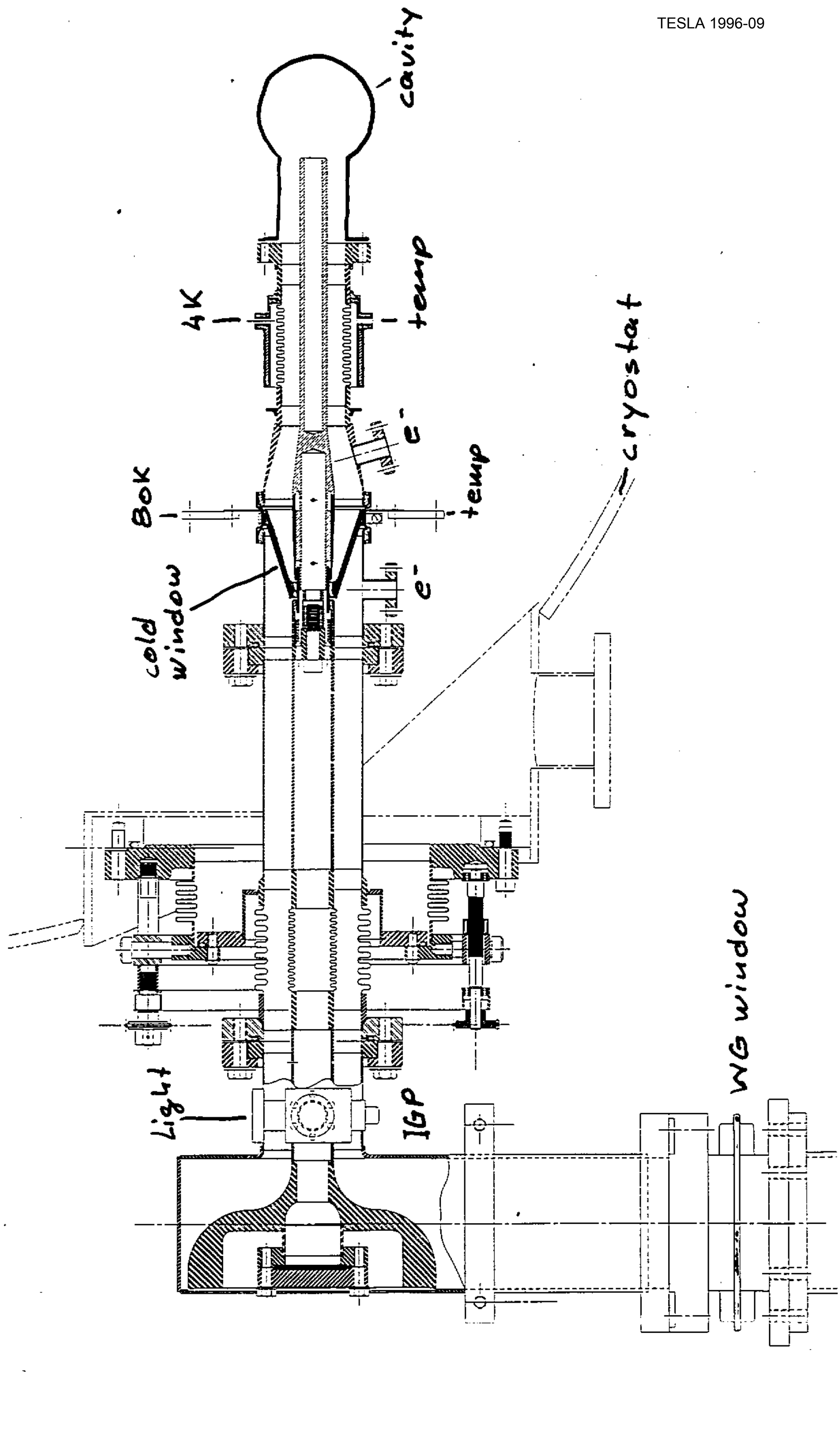

Sensors

pressure:	- IG pump
	- penning gauge
temperature:	- PT 1000
charged particles (e^-)	- pick up
	- 0-2V ≙ 0-30 μA
light:	- photomultiplier
	- 0-10V ≙ 0,1 Lux

Hardware Interlock

pressure	- in doorknob	$6 \cdot 10^{-7}$ mbar	HV off
	- out "	"	on
	- cavity	"	klystron
temp	- in coax window	150K	
	- out "	"	
	- in cavity flange	"	
	- out "	"	
light	- warm coax		
e^-	- in coax window 2x		
	- out "		
He level	(only CHECHIA)	55%	

↑ setpoints

coupler processing programm

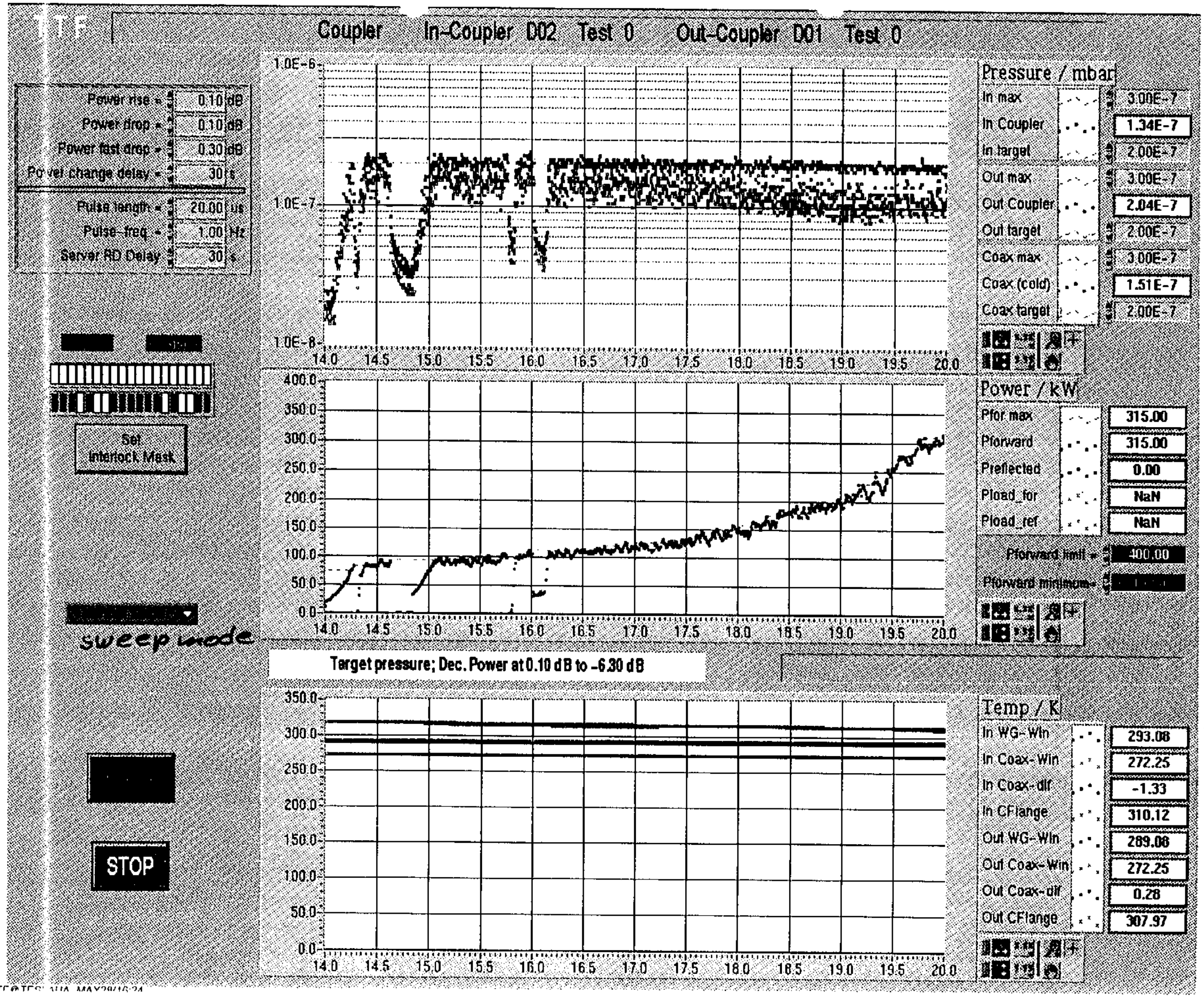

⑥

Goals of processing

1. on coupler test stand (traveling wave)

pulse: 1.3ms / 10Hz
power: 1MW

2. on cavity in CHECHIA

- cavity detuned

for operation: pulse: 1.3ms / 10Hz
power: 400kW

for HPP: pulse: 500µs / 1Hz
power: 1MW

- cavity on resonance

pulse: ≤ 1.3ms / 10Hz
power: up to cavity field limit

better: pulse: 2ms
power: 60kW
(Jaceks talk)

Processing procedure

at room temperature

- rise the power at short pulslength (20µ
  up to 1MW

- increase the pulslength for next rise

- sweep over the full power range
  for some hours

- sweep over power range with
  strong activities

cool down

- same procedure than at R.T

on cavity

- same procedure for standing
  wave and for cavity on resonance

Results

Fermi series coupler F01/F02 on coupler test stand

conditions:

- leak on F02 cold bellow into iso vac
- copper plating was stripped on outer coax between cold window and doorknob
- traveling wave

e⁻ activities during processing

pulse	F01 (output) cavity side	F01 (output) doorknob side	F02 (input) cavity side	F02 (input) doorknob side
(RT)				
20µs/1Hz		onset at 172kW up to 1MW		
50µs/1Hz	defect	170kW - 1MW	785 kW	70kW - 1MW
100µs/1Hz	defect	300kW - 1MW	300kW - 1MW	100kW - 1MW
(70K)				
1,4ms/10Hz	defect	160 - 400kW	188 - 400kW	160 - 400kW

conclusion

- we reached 1MW @ 500µs/1Hz
  400kW @ 1,4ms/10Hz
- e⁻ activities on all probes over wide range
- no power sweep, no e⁻ datalogging
- finished because of timeschedule

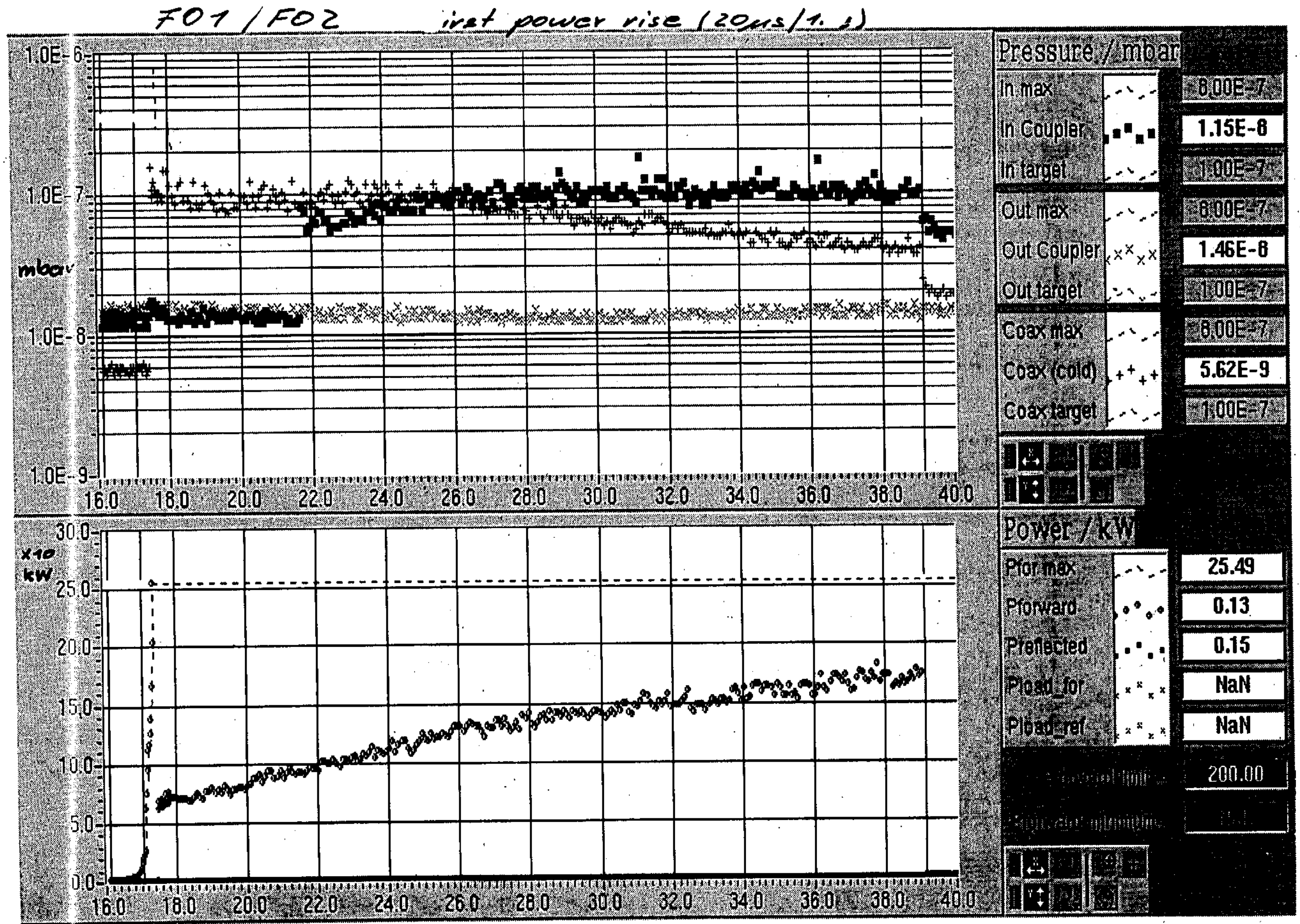

F01 / F02 irst power rise (20μs/1. s)
Pressure / mbar
In max
In Coupler
In target
Out max
Out Coupler
Out target
Coax max
Coax (cold)
Coax target
8.00E-7
1.15E-8
1.00E-7
8.00E-7
1.46E-8
1.00E-7
8.00E-7
5.62E-9
1.00E-7
1.0E-6
1.0E-7
mbar
1.0E-8
1.0E-9
16.0
18.0
20.0
22.0
24.0
26.0
28.0
30.0
32.0
34.0
36.0
38.0
40.0
Power / kW
Pfor max
Pforward
Preflected
Pload_for
Pload_ref
25.49
0.13
0.15
NaN
NaN
200.00
30.0
x10 kW
25.0
20.0
15.0
10.0
5.0
0.0

6B

Fermi series coupler F01 on C19 in CHECHIA

conditions:

- leak on the cold bellow to iso vac
- copper plating stripped on outer coax between cold window and doorknob
- cavity detuned

vacuum thresholds

at RT, 500μs, 200μs, 1Hz

in cavity vac: 60kW
125kW
240kW

180-220kW small activities

in doorknob: 150kW once

after cooldown

at 1Hz rep.rate: no vacuum reaction
10Hz ": some backout effects on WG

charged particles (e^-)

doorknob side: no e^-
cavity side: 60 - 80kW
190kW
240kW

F07 on C19 in CHECHIA

[mbar]

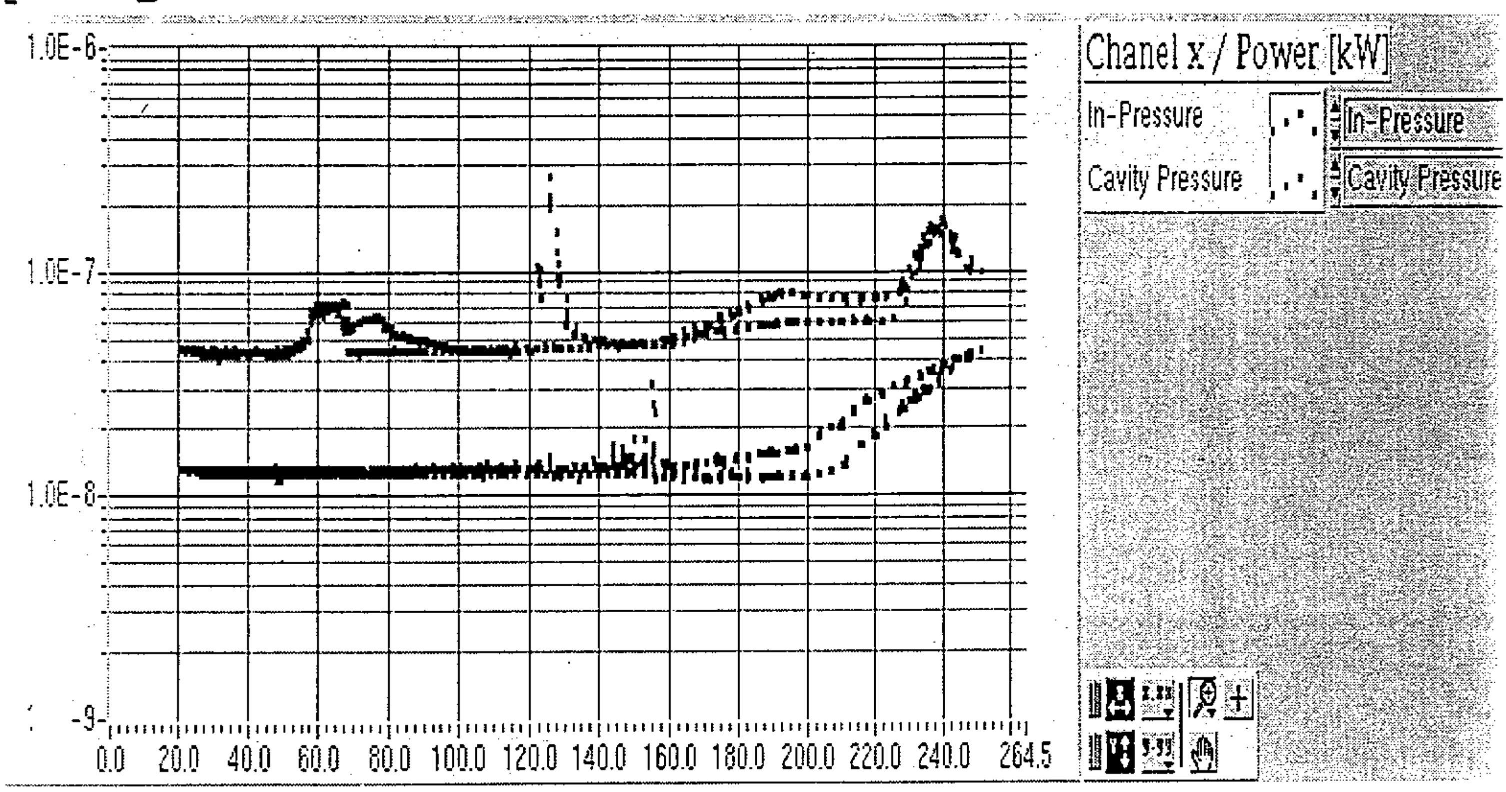

Pforw [kW]

- cavity detuned
- 200μs / 1Hz
- room temp
- power sweep

FO1 on C19 in CHECHIA

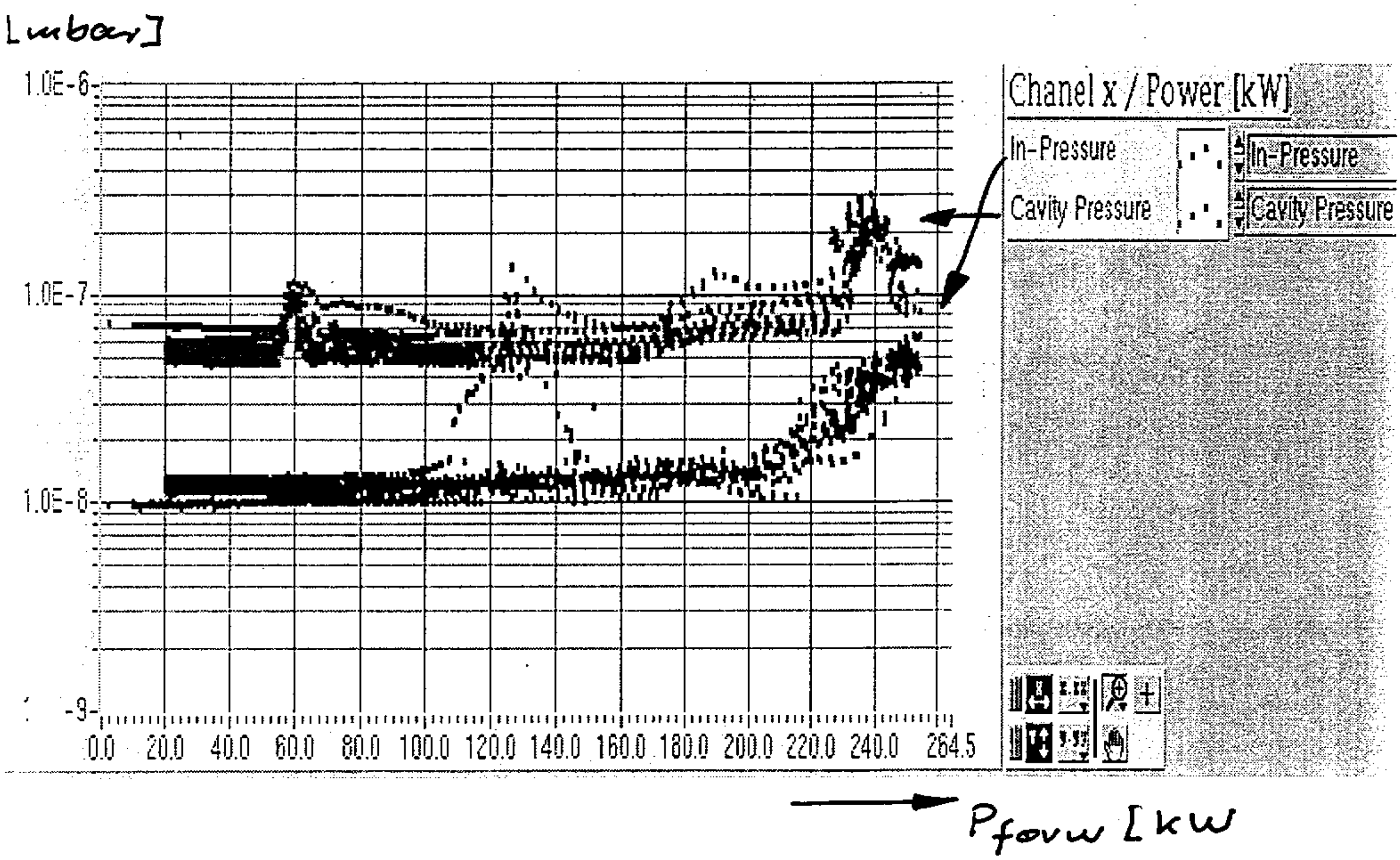

- cavity detuned
- 500µs / 1Hz
- room temperature
- power sweep

e- vs power (F01 on cavity side, RT, cavity detuned)

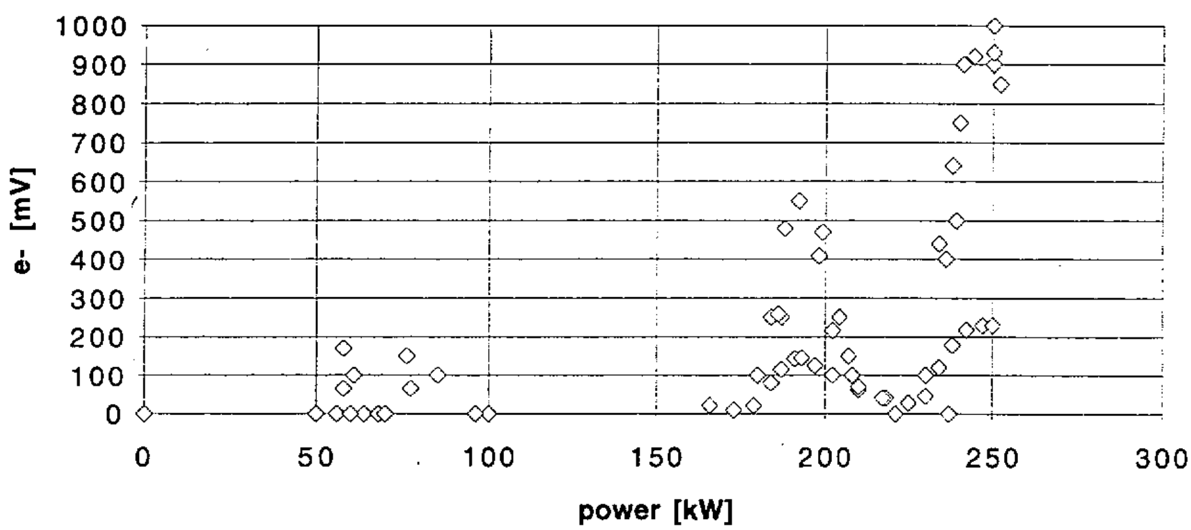

- 100µs and 200µs / 1Hz

- cavity on resonance ($Q_{ext} = 3 \cdot 10^6$)

500µs/1Hz , 18.3 MV/m , P_{forw} = 125kW

vacuum bursts in WG
small e⁻ — " —

1ms/1Hz , 21 MV/m , P_{forw} = 90kW

thermal break down
vac bursts + e⁻ in WG

conclusion:

we archieved off resonance, cold
- 250kW @ 500µs/10Hz
- 120kW @ 1.4ms/10Hz

on resonance cold
- still WG activities, no threshold
- no e⁻ on cavity side

more processing necessary for WG

Fermi series coupler F03 on C19 in CHECHIA

conditions:

- copperplating stripped on warm outer coax
- cavity detuned
- not preprocessed on teststand

thresholds on different power levels, room temp., 200μs, after 3d proc.

doorknob side			cavity side	
vac	e⁻	light	vac	e⁻
160		160	60	60
200	250	200	100	100
450		450	120	190
500			-400	240
630	650			320
			450	450
				650
				1000

1,8K/70K

160	–	160	–	–
330				

cavity detuned, RT
pulse: 200µs, 2Hz
after 3 days conditioning

cavity side

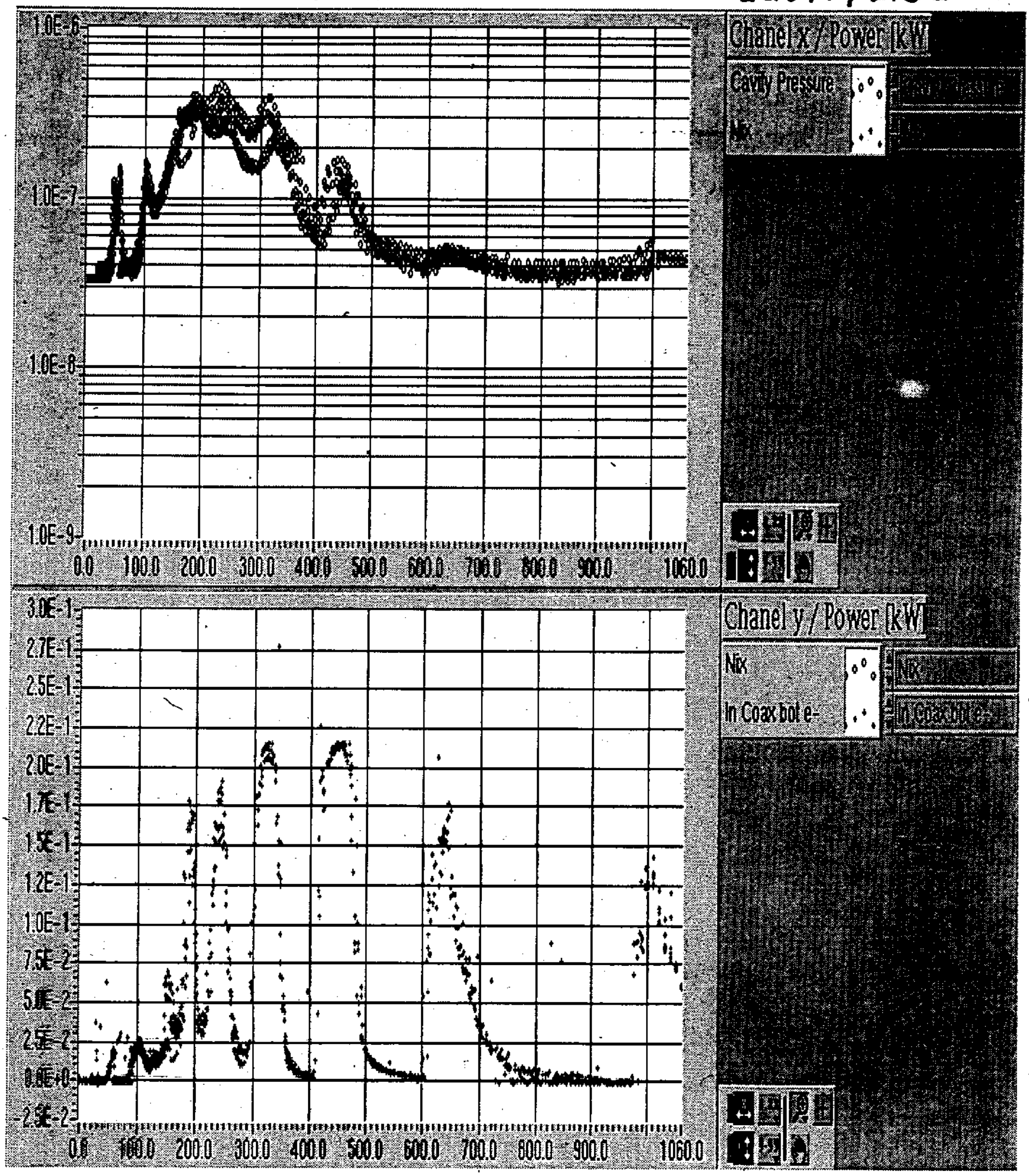

FO3 on C79
cavity detuned, RT
pulse: 200 µs, 2 Hz
after 3 day conditioning

doorknob side

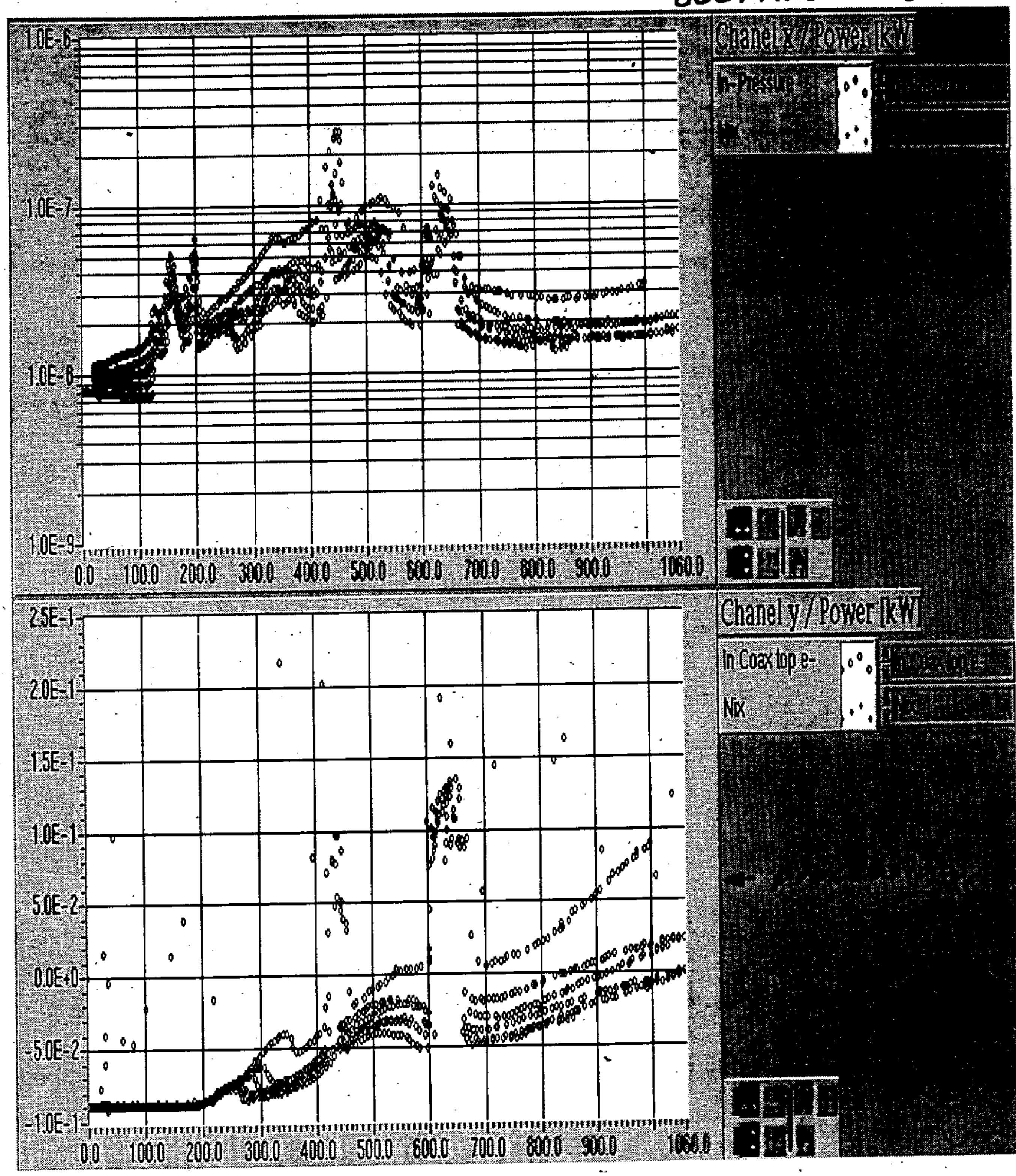

F03 on C17
cavity detuned, RT
pulse: 200μs, 2Hz
after 3days conditioning

doorknob side

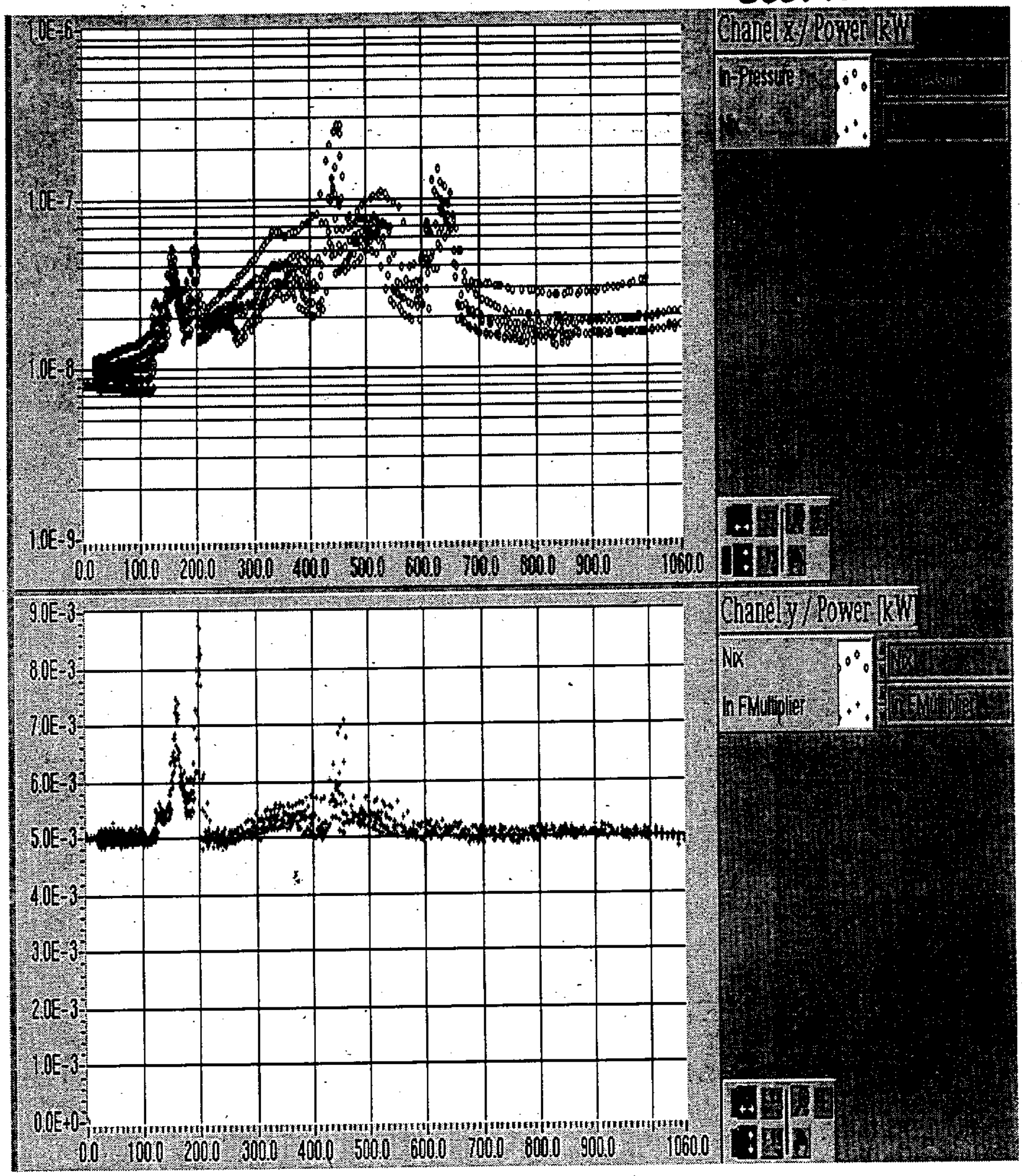

FPC on C11 . :-)

cavity detuned, 1.8K

pulse: 200-500µs, 2Hz

doorknob side

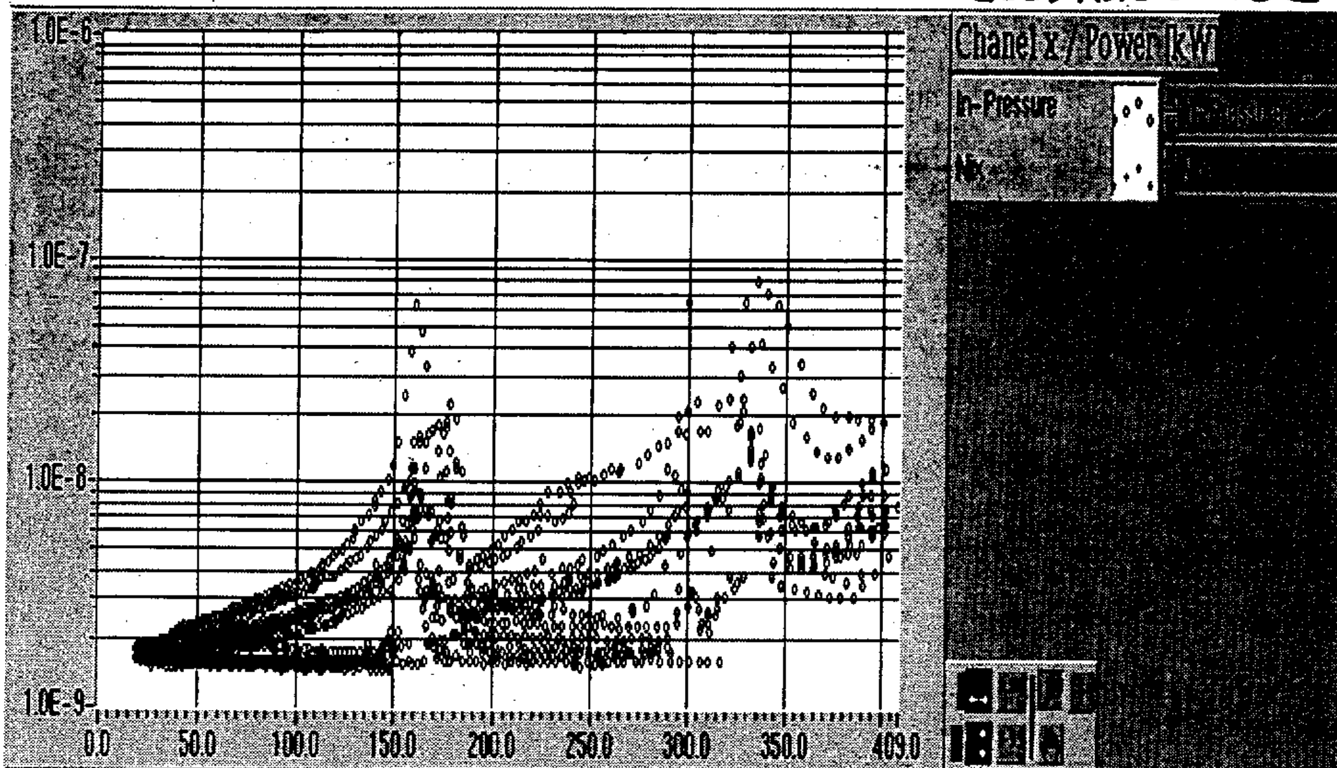

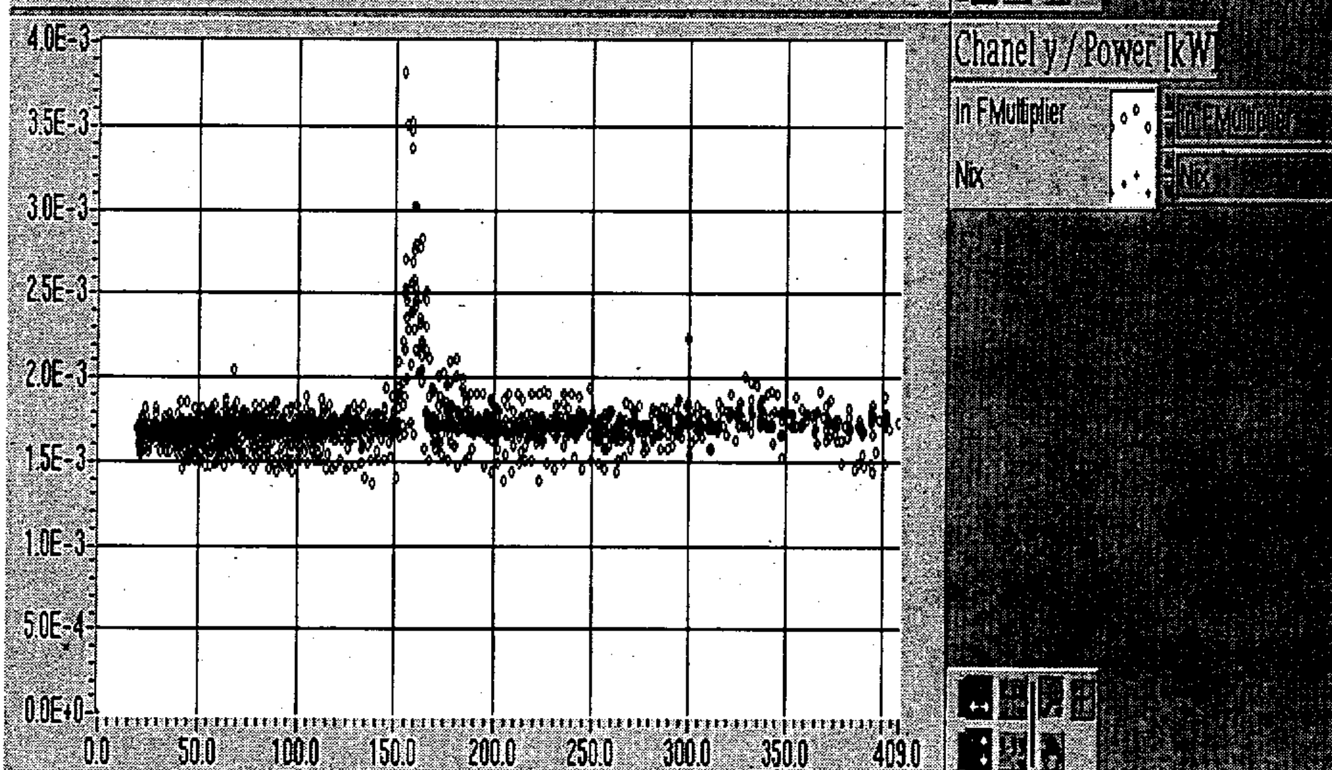

FO3 on C19
cavity detuned, 1.8K

doorknob side

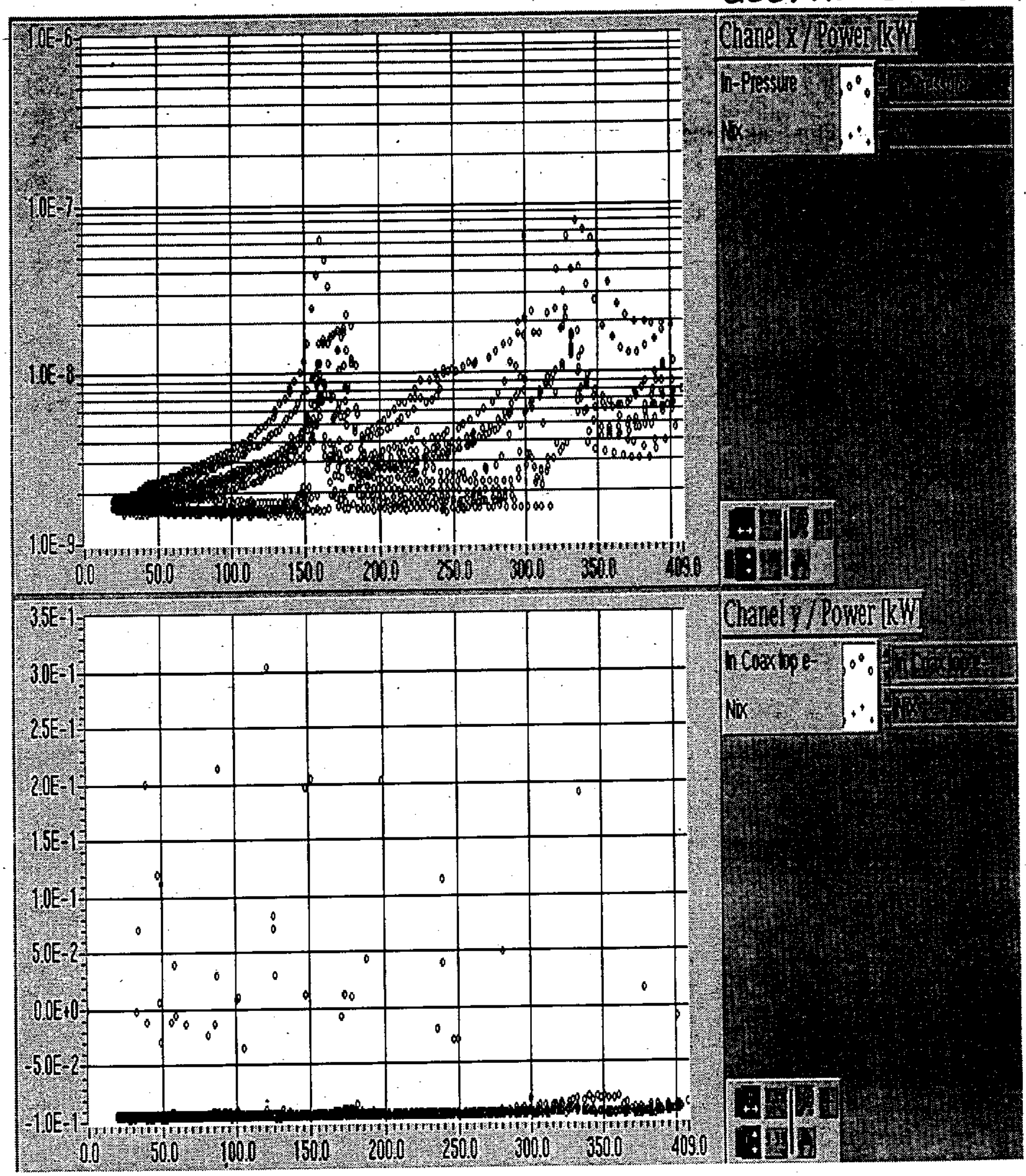

~~FUS~~ ~~...~~

cavity detuned, 1,8K

pulse: 200 - 500µs, 2Hz

cavity side

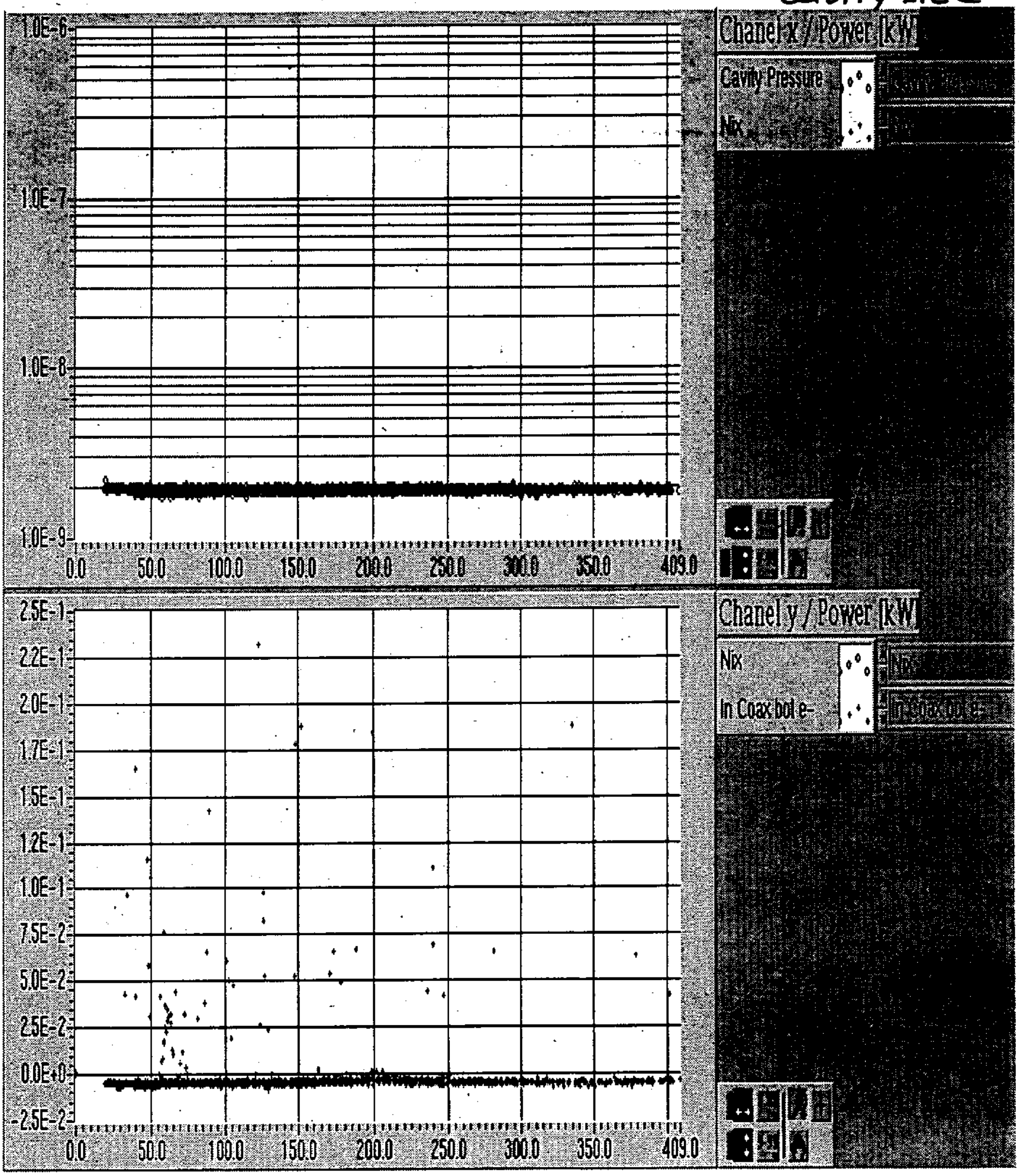

FO3 on C19
cavity detuned, 1.8K
pulse: 500μs / 2Hz

after 5d warm + 5d cold processing

doorknob side

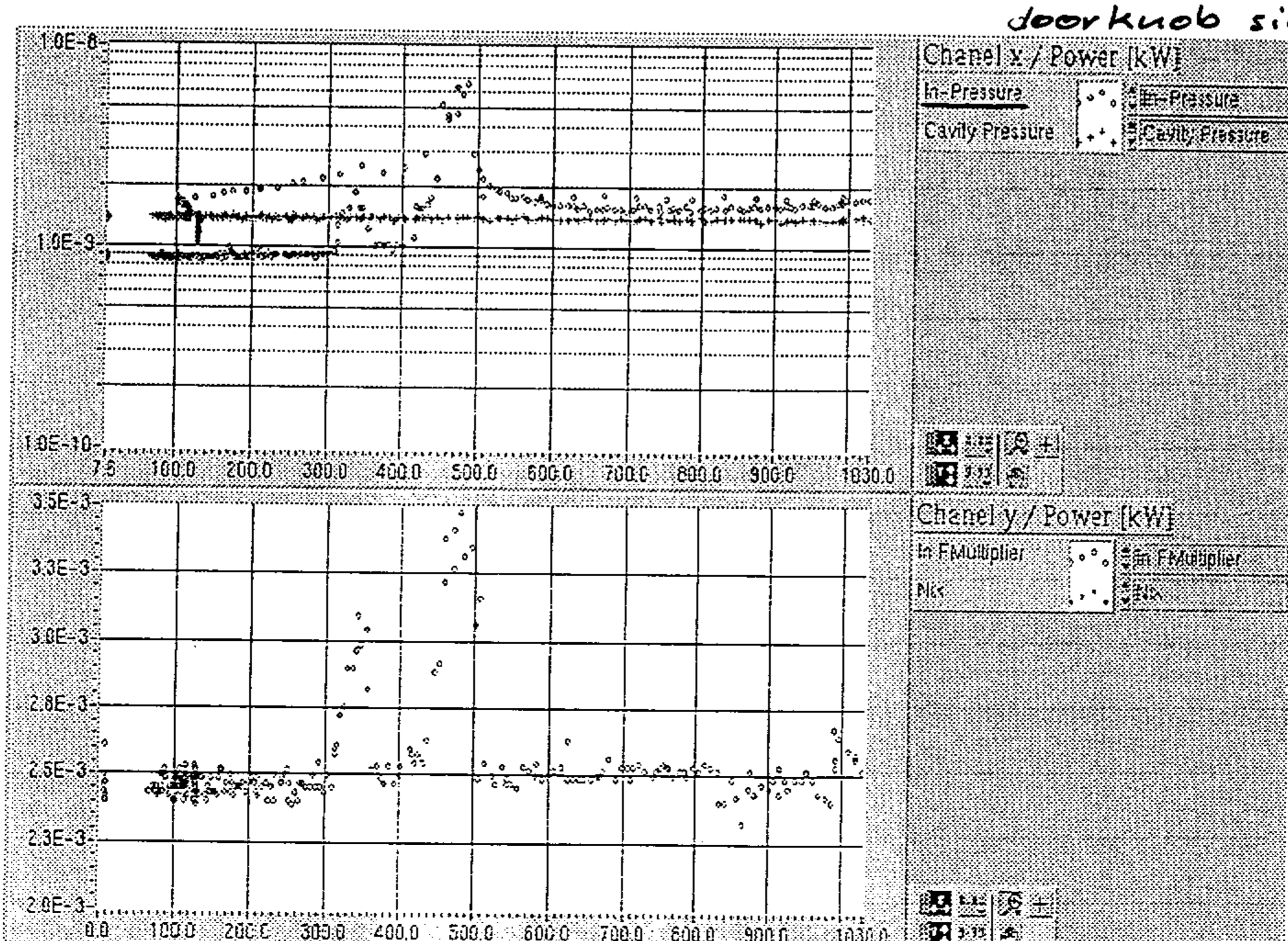

(25)

F03 on C19
cavity detuned, 1.8K
pulse 500μs / 2Hz

5d warm + 5d cold processing

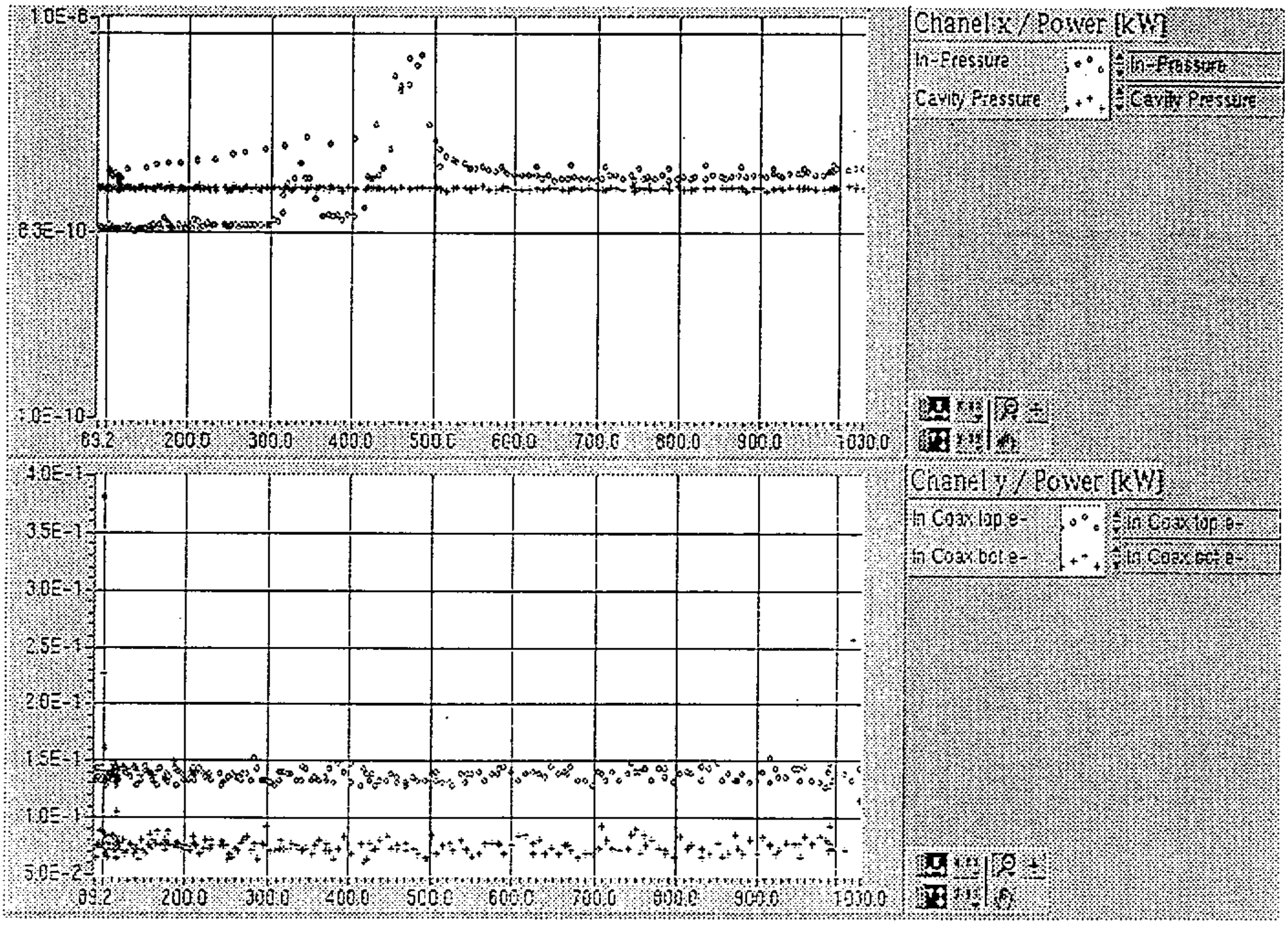

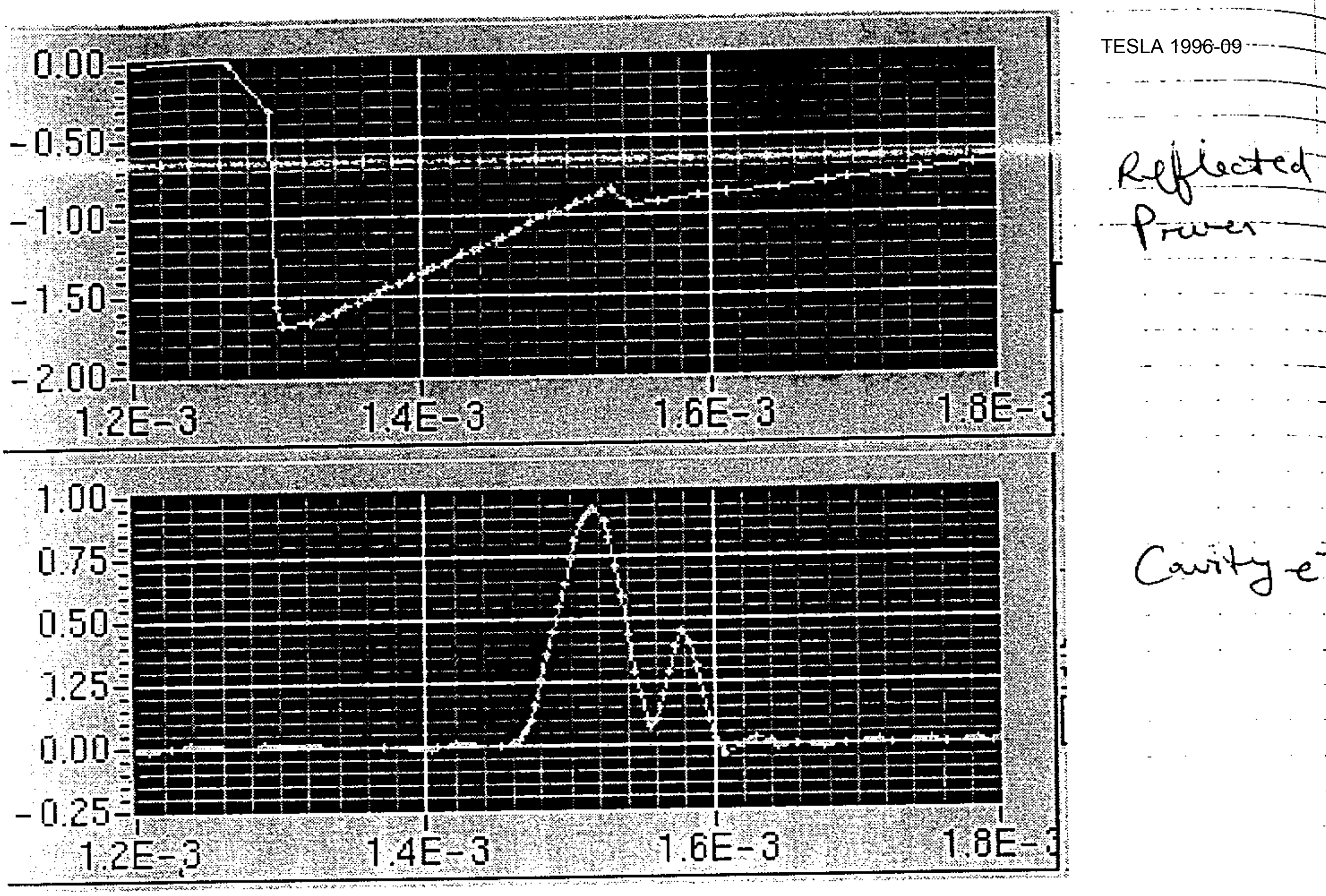

P_{ver} ~ 365 kW

Note e^- peaks before and after rf turn off.

- on resonance

- 250 μs / 2 Hz

e^- onset at 250 kW

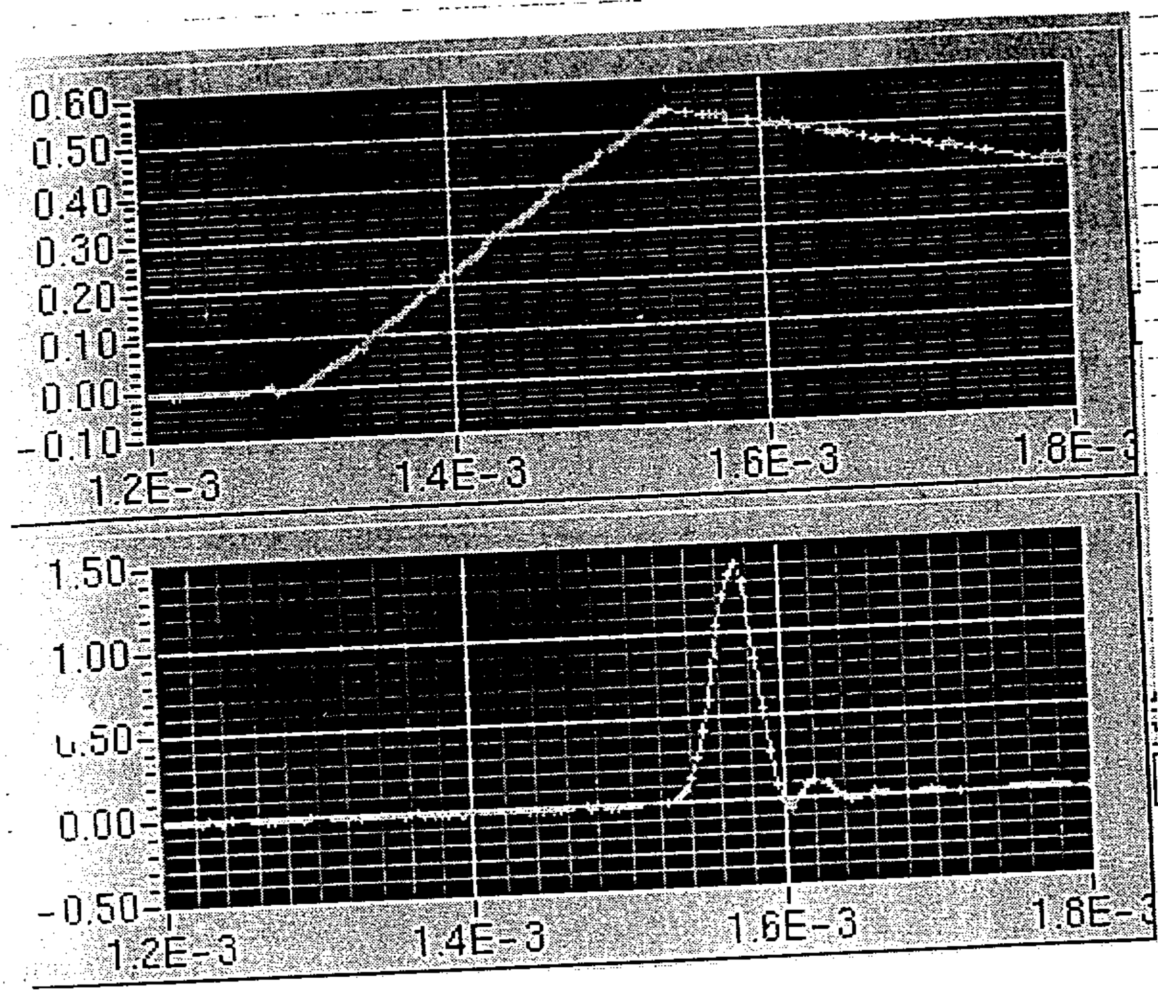

Cavity Voltage

Waveguide e⁻

18,45 P_{vcr} ~ <u>475 kW</u> at time of snap shot.

- on resonance
- 250 µs / 2 Hz

e⁻ onset at 250 kW

conclusion:

- coupler F03 is free of e^- and light up to 250kW at cavity on resonance

- at P_{forw} > 250kW there are e^--signals before and after phaseshift

- the system performance is limited by the cavity

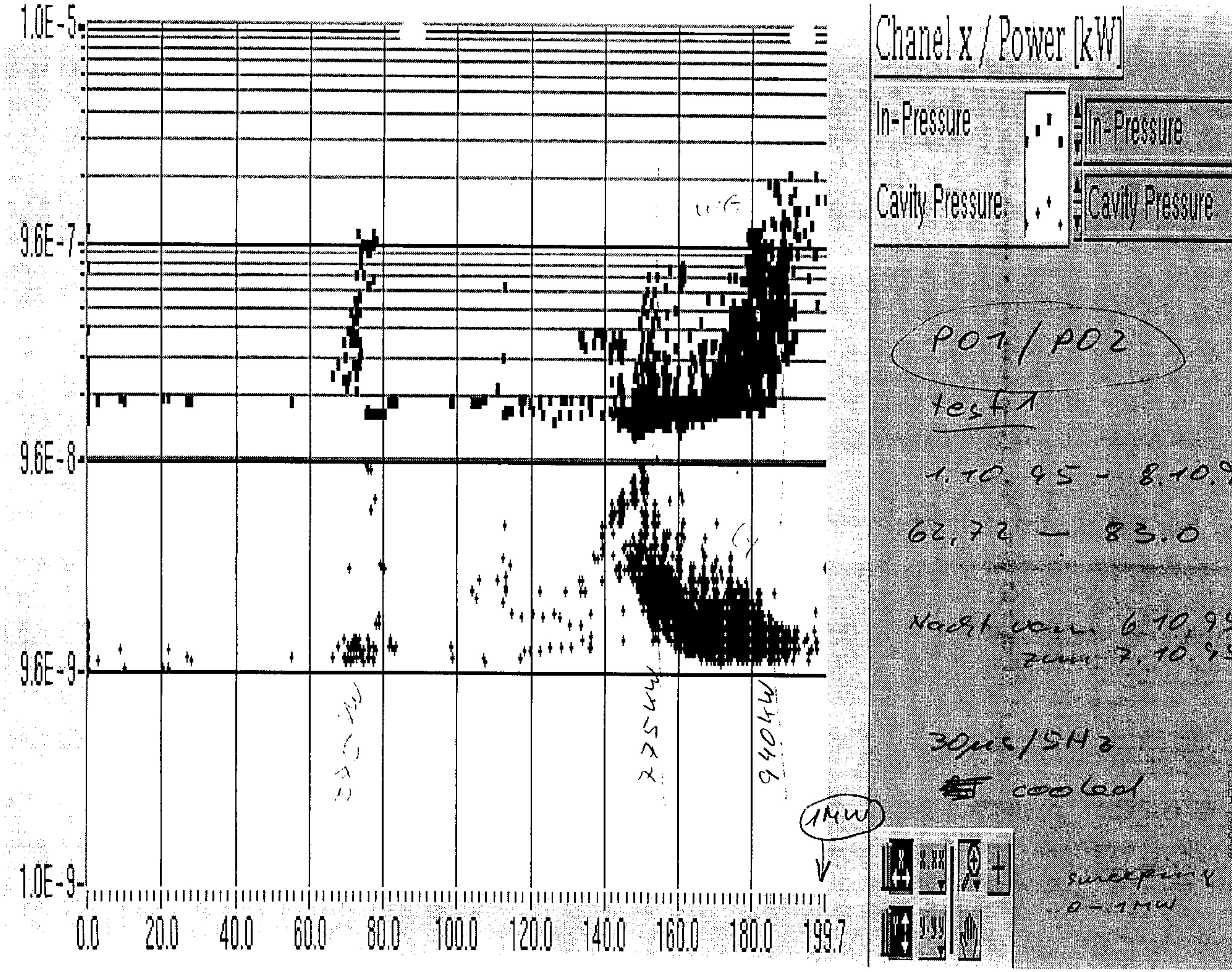
Chanel x / Power [kW]
In-Pressure
Cavity Pressure
1.0E-5
9.6E-7
9.6E-8
9.6E-9
1.0E-9
0.0
20.0
40.0
60.0
80.0
100.0
120.0
140.0
160.0
180.0
199.7
P01 / P02
test 1
1.10.95 – 8.10.95
62,72 – 83.0
Nacht vom 6.10.95
zum 7.10.95
30µs/5Hz
cooled
sweeping
0 – 1MW
1MW
775kW
940kW
TESLA 1996-09

Stored Coupler-Processing - Data

Setting :	Frequency / Hz Pulse-Length / us Pulse-Frequncy / Hz Program-Mode (Normal; Sweep; User-Controll)
Limit :	max In-Coupler-Pressure / mbar target In-Coupler-Pressure / mbar max Out-Coupler-Pressure / mbar target Out-Coupler-Pressure / mbar max Coax-Pressure / mbar target Coax-Pressure / mbar max Pforward / W min Pforward / W Interlock - Reset -Mask (19 Bit (Chanels))
Main value:	In-Coupler-Pressure / mbar Out-Coupler-Pressure / mbar Coax-Pressure / mbar Pforward / W Preflected / W Pforward_Load / W Preflected_Load / W Interlock-Event (19 Bit (Chanels)) First Interlock-Event
Temperature:	WG-Window In-Coupler / K Coax-Window In-Coupler / K Coax-Difference In-Coupler / K Coax-Flange In-Coupler / K WG-Window Out-Coupler / K Coax-Window Out-Coupler / K Coax-Difference Out-Coupler / K Coax-Flange Out-Coupler / K
Light&e-:	In-Coupler e- / V In-Coupler-Coax top e- / V In-Coupler-Coax bottom e- / V Out-Coupler e- / V Out-Coupler-Coax top e- / V Out-Coupler-Coax bot e- / V Photo-Multiplier In-Coupler / V Photodiode In-Coupler / V Photo-Multiplier Out-Coupler / V Photodiode Out-Coupler / V
Global:	Time in second Result [string] (Power increment; decrement; ...)

DESY 29-MAY-96 / Jukka Sarvas

TESLA 1996-09

PROGRESS IN MULTIPACTING ANALYSIS

PROJECT TEAM:

DESY: DIETER PROCH, JACEK SEKUTOWICZ

UNIV. OF HELSINKI: JUKKA SARVAS, PASI YLÄ-OIJALA, HANNU MÄKIÖ

1. ANALYSIS METHOD

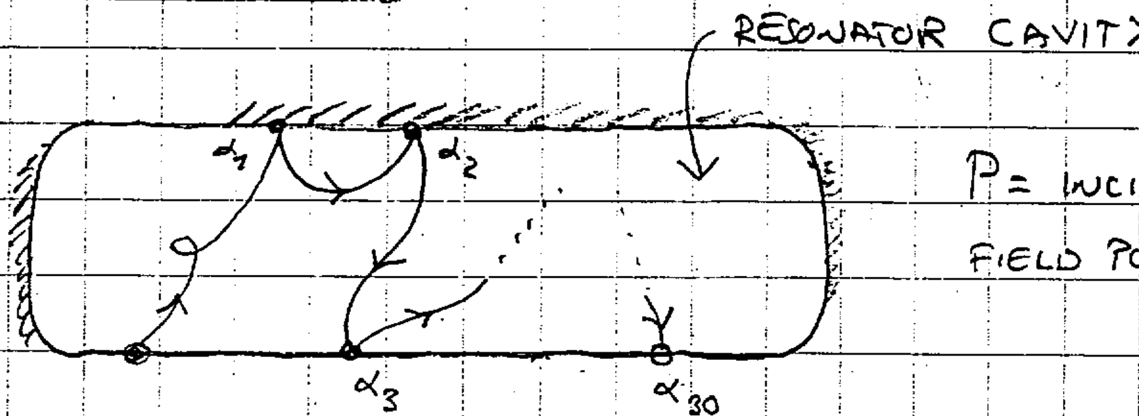

P = INCIDENT FIELD POWER

- Send electrons uniformly
- Follow (relativistic) electron trajectory up to 30 wall hits (if survives so long)

$$c_{30}(P) = \frac{\#\text{ of surviving electrons}}{\#\text{ of initial electrons}}$$

$$\alpha_{30}(P) = \frac{\#\text{ of secondary electrons}}{\#\text{ of initial electrons}}$$

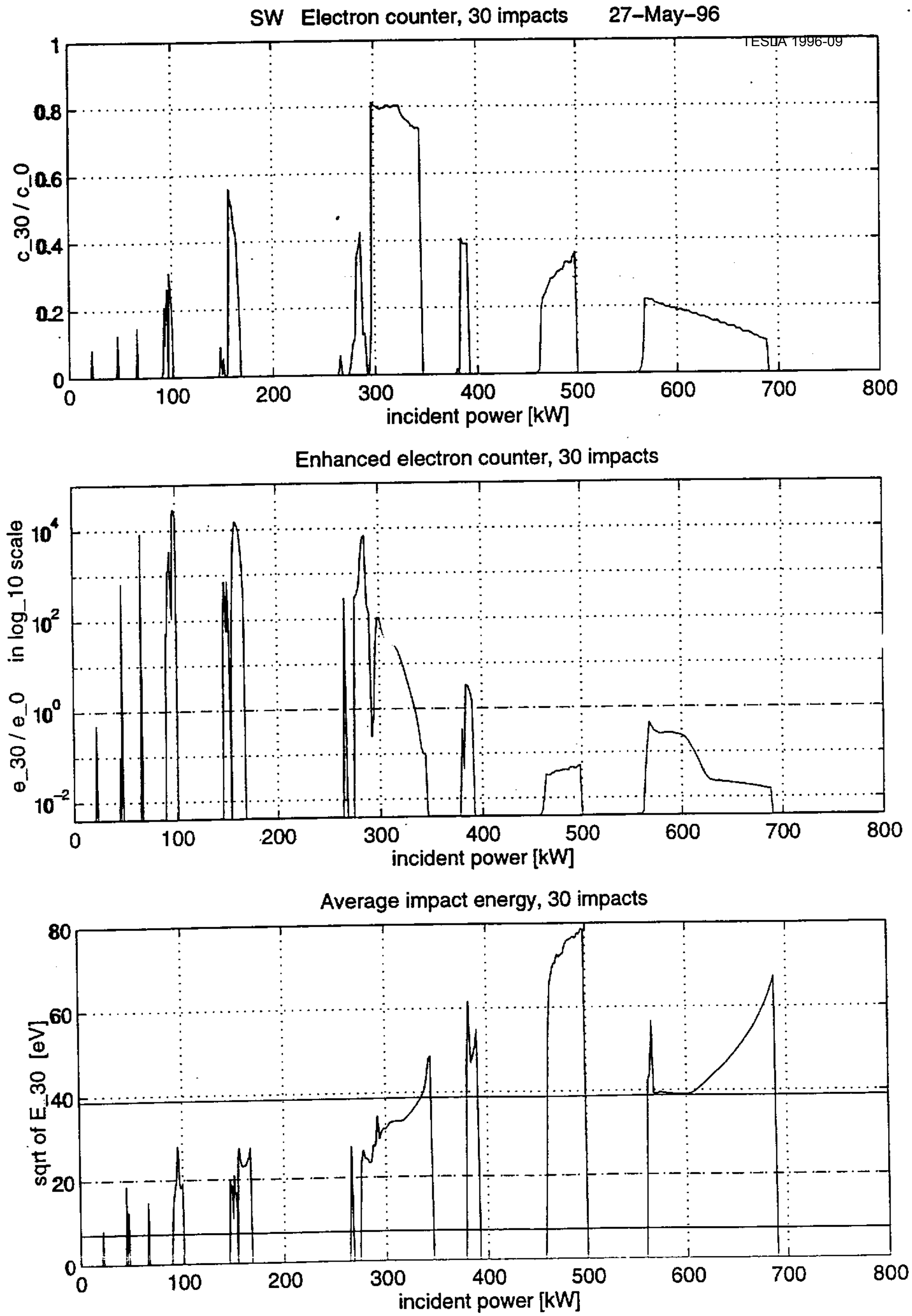
SW Electron counter, 30 impacts 27–May–96
c_30 / c_0
incident power [kW]
Enhanced electron counter, 30 impacts
e_30 / e_0 in log_10 scale
incident power [kW]
Average impact energy, 30 impacts
sqrt of E_30 [eV]
incident power [kW]

3. COAXIAL LINE

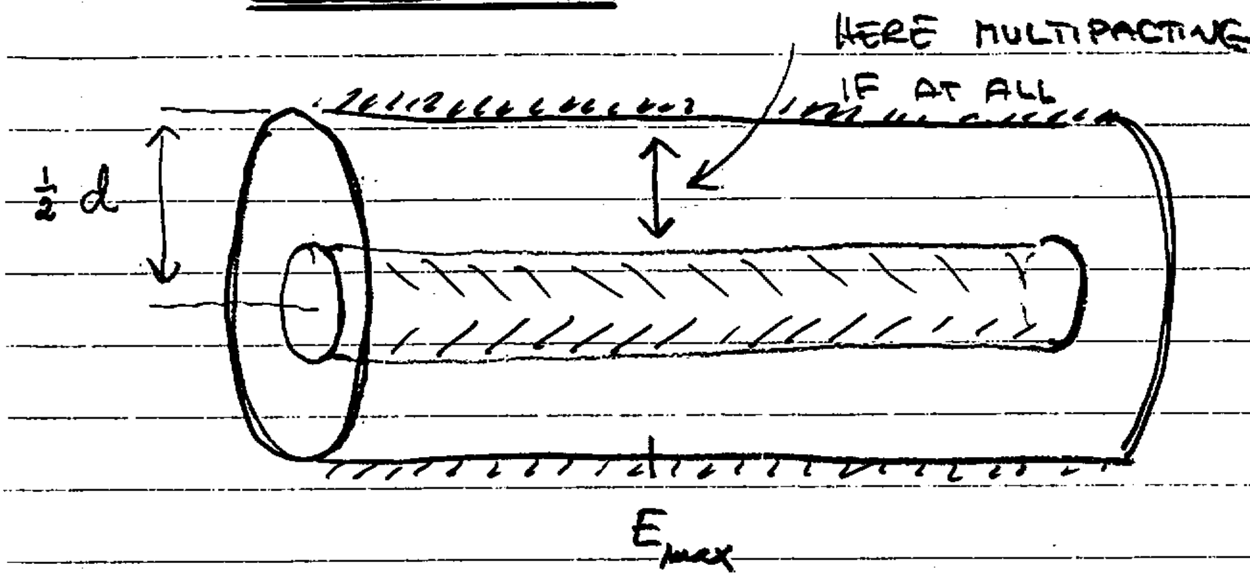

Standing wave : Multipacting occurs at max of E with certain field powers

Scaling laws :

$$P_{\text{one-point}} \sim (fd)^4 Z$$

$$P_{\text{two-point}} \sim (fd)^4 Z^2$$

Travelling wave :

$$P_{TW} = 4 P_{SW}$$

Mixture of SW and TW : Not as expected !

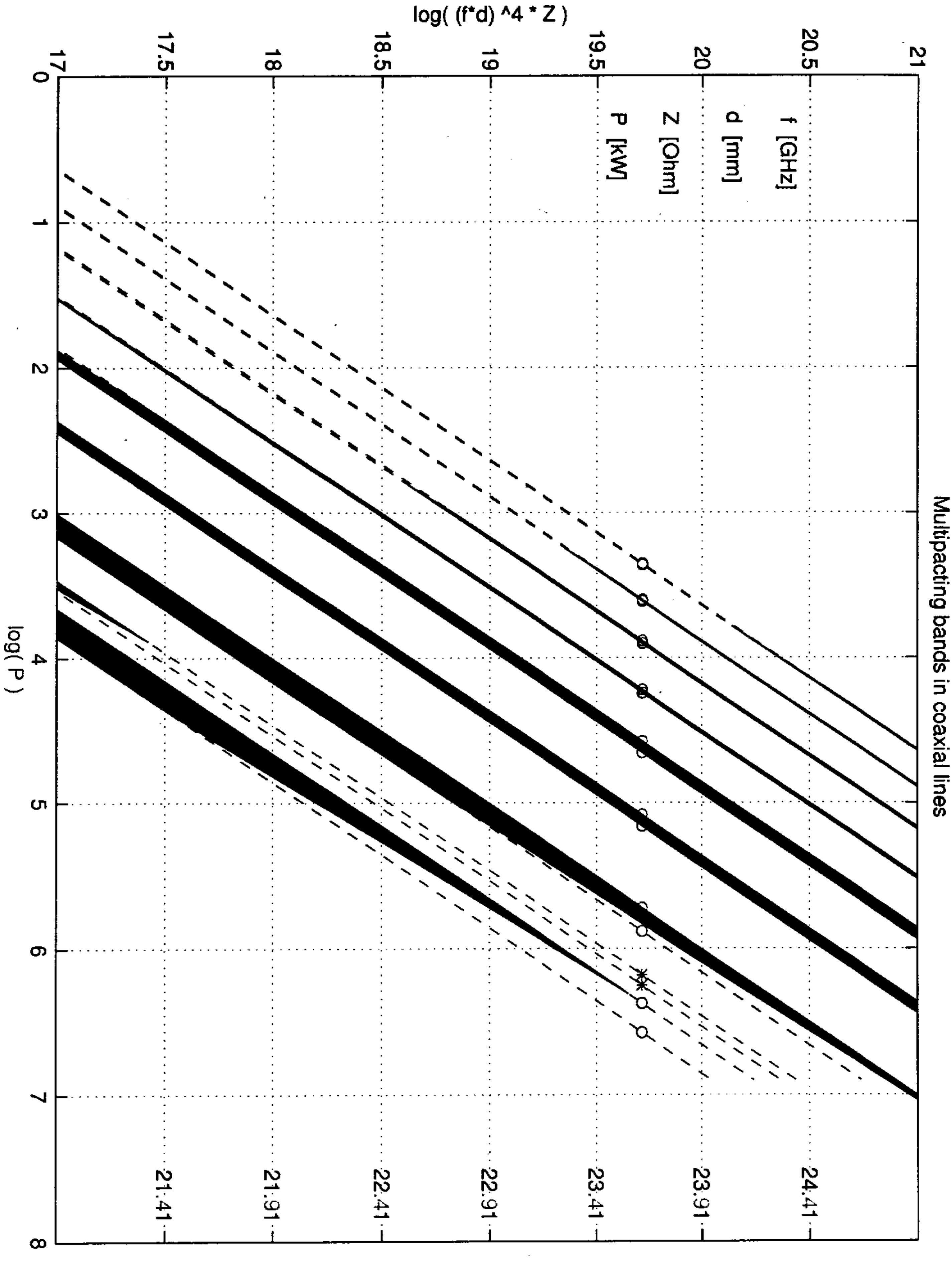
Multipacting bands in coaxial lines
log((f*d) ^4 * Z)
log(P)
f [GHz]
d [mm]
Z [Ohm]
P [kW]
17
17.5
18
18.5
19
19.5
20
20.5
21
0
1
2
3
4
5
6
7
8
21.41
21.91
22.41
22.91
23.41
23.91
24.41

Other analized structures:

- CONICAL WINDOW:
  - standing wave

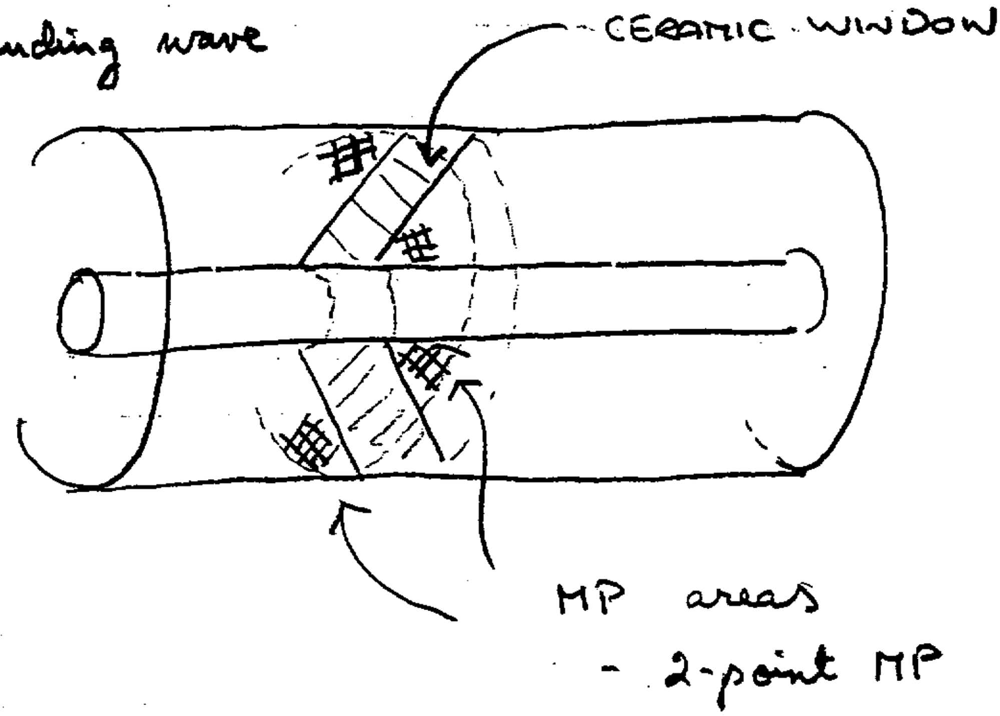

- THE DWERSTEG WINDOW: no MP observed (SW)

- TAPERED LINE, standing wave

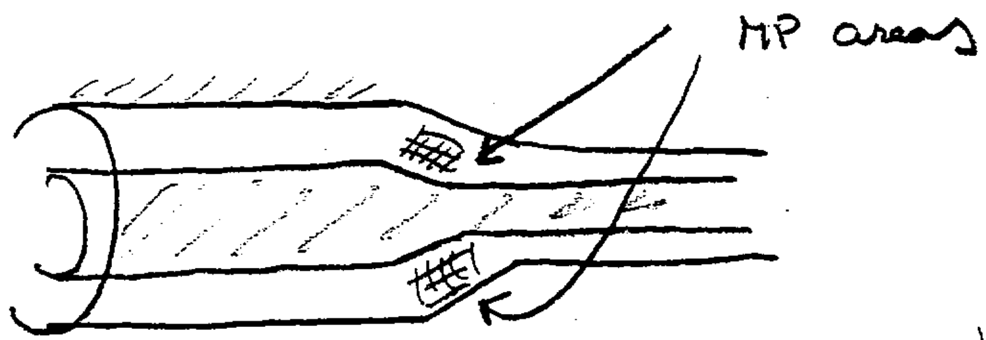

- IMPEDANCE STEP:
  - SW

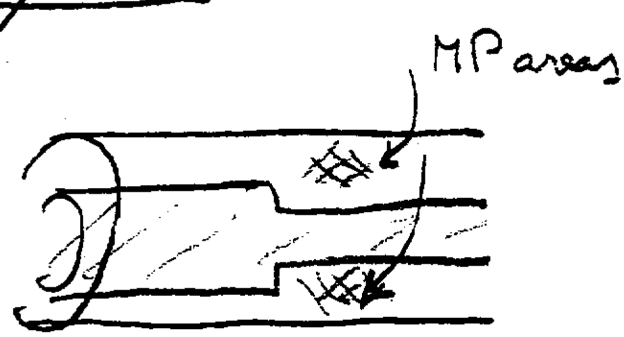

4, METHODS SUPPRESSING MP

General idea : Either perturb the field or the conductor geometry in order to break the MP trajectory pattern

1) DC - BIAS IN COAXIAL LINE

- DC voltage between conductors
- SW

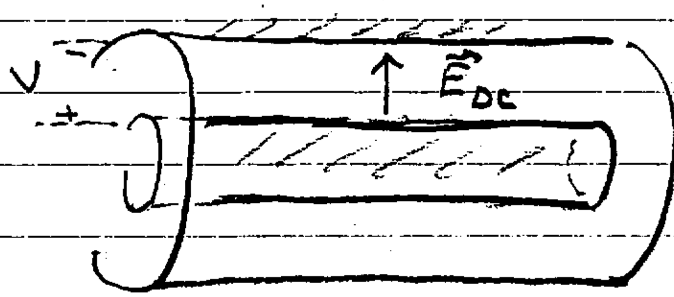

- How to use : 'Navigation chart'

2) STATIC MAGNETIC BIAS (works)

- permanent magnet pieces
- coil and wire systems

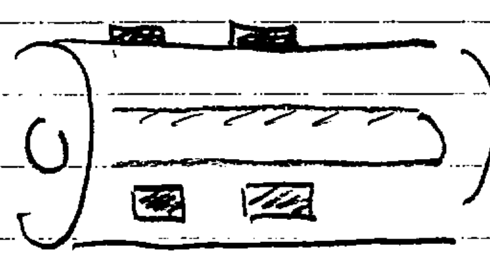

3) GROOVING

- works

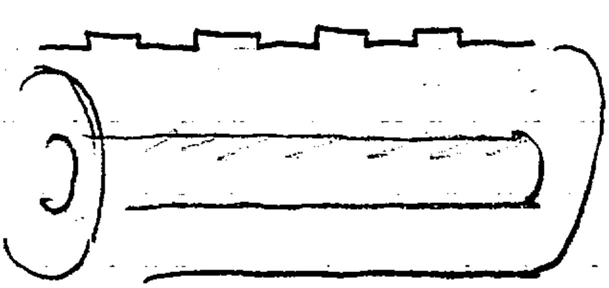


Enhanced electr ounter 30 impacts
ay-96
incident RF power [kW]
DC voltage [V]
900
800
700
600
500
400
300
200
100
-2500
-2000
-1500
-1000
-500
0
500
1000
1500
2000
4
3
2
1
0
-1
-2
1. order
2 points
2. order

TESLA 1996-09

ANALYSIS OF MULTIPACTING IN COAXIAL LINES

PART TWO: THE RESULTS

Pasi Ylä-Oijala
Rolf Nevanlinna Institute
University of Helsinki, Finland
May 29, 1996

Geometry:

- 500 MHz, 50 Ω coaxial line, outer diameter is 103 mm

Standing waves :

- in SW multipacting seems to be predominantly due to the electric field only
- multipacting appears clos to the maximum of the electric field, called as electric–multipacting (EMP)

Traveling waves:

- in TW multipacting is due to both the electric and magnetic field
- the wall impacts of the multipacting electrons appear close to the maximum of the electric field
- the electrons are traveling along with the wave, to the same direction as the wave propagates
- traveling is quite slow, typically a couple of mm between wall impacts

Mixed waves:

- in mixed waves or partially reflected waves the situation is more complicated
- both electric– and magnetic–multipacting (EMP) and (MMP) appear
- MMP appears close to the maximum of the magnetic field

Mixed waves:

- consider a combination of a superposition of the SW and TW fields

$$\begin{aligned}\vec{E}_R &= R\,\vec{E}_{SW} + (1-R)\,\vec{E}_{TW},\\ \vec{B}_R &= R\,\vec{B}_{SW} + (1-R)\,\vec{B}_{TW},\end{aligned}$$

- where R, $0 \le R \le 1$, is the reflection coefficient
- if $R = 1$ we have the SW fields and if $R = 0$ we have the TW fields

Scaling law for EMP:

- approximate scaling law for EMP power levels

$$P_R^{EMP} \sim \frac{1}{(1+R)^2} P_{TW} = \frac{4}{(1+R)^2} P_{SW}.$$

Scaling laws:

- in SW we have found some scaling laws for the field frequency, the diameter of the line and the impedance of the line

$$P_{\text{one-point}} \sim (f\,d)^4\,Z, \quad P_{\text{two-point}} \sim (f\,d)^4\,Z^2.$$

- f is the frequency of the field, d is the outer diameter and Z is the impedance of the line

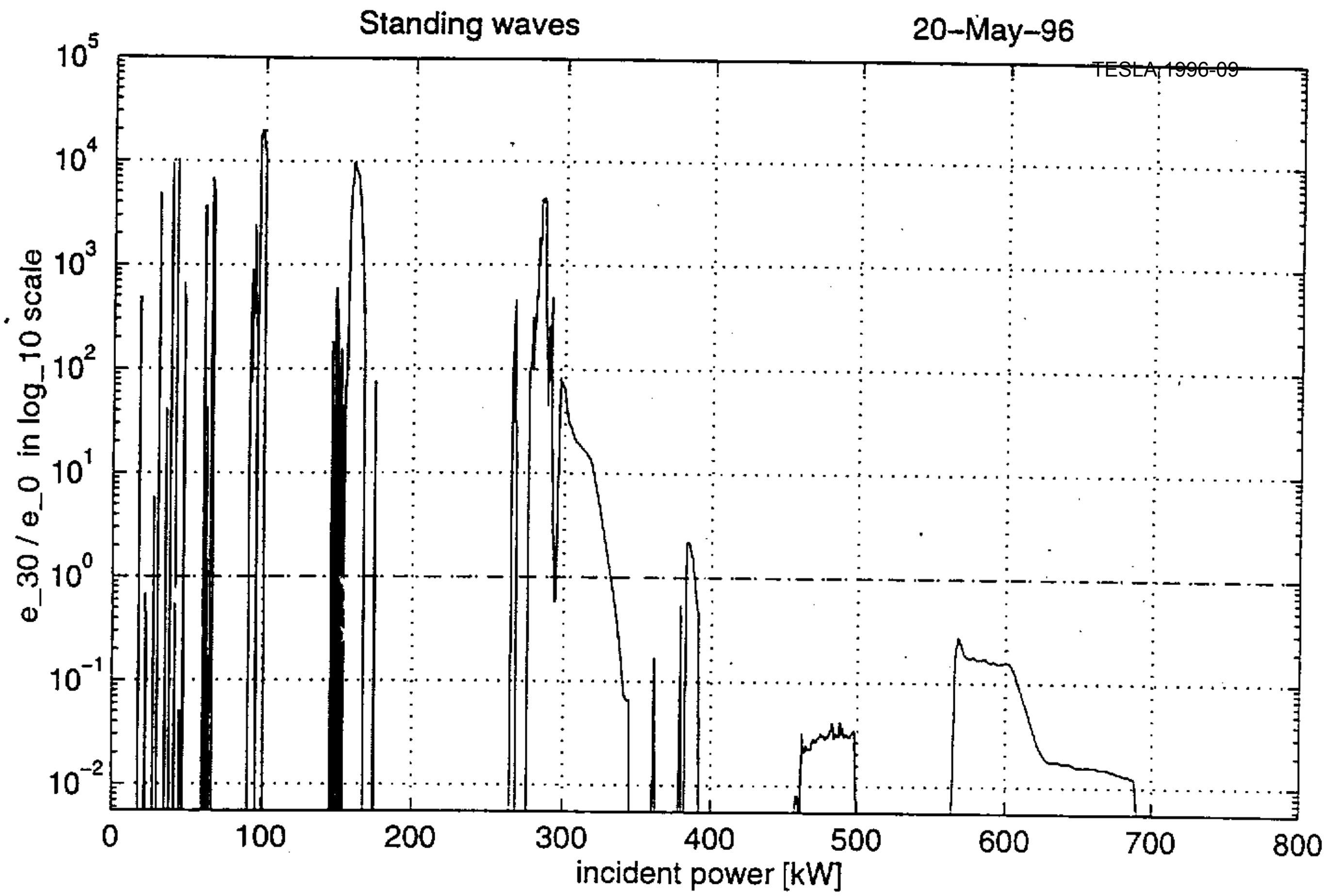
Standing waves
20-May-96
TESLA 1996-09
e_30 / e_0 in log_10 scale
incident power [kW]
0
100
200
300
400
500
600
700
800

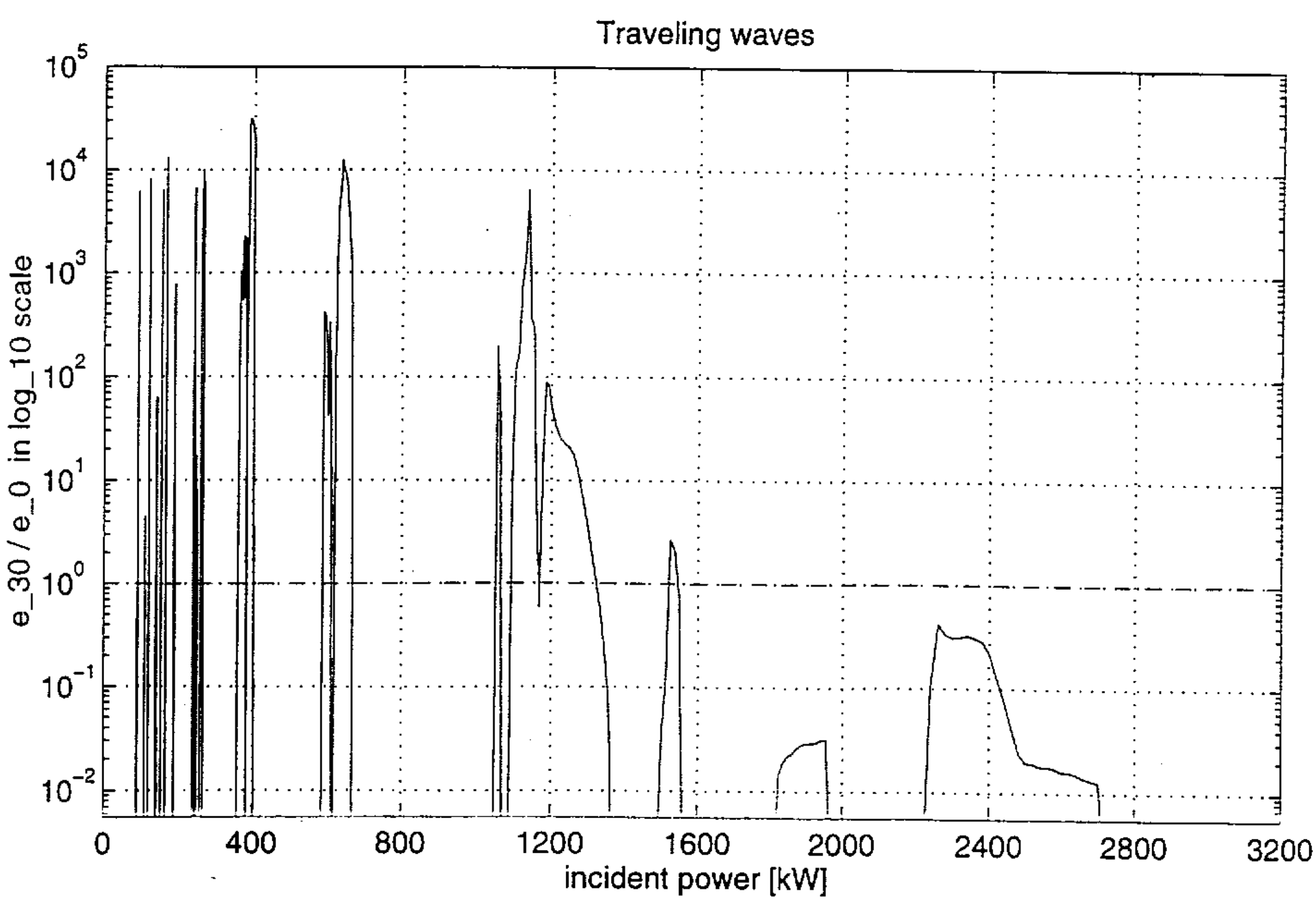
Traveling waves
e_30 / e_0 in log_10 scale
incident power [kW]
0
400
800
1200
1600
2000
2400
2800
3200

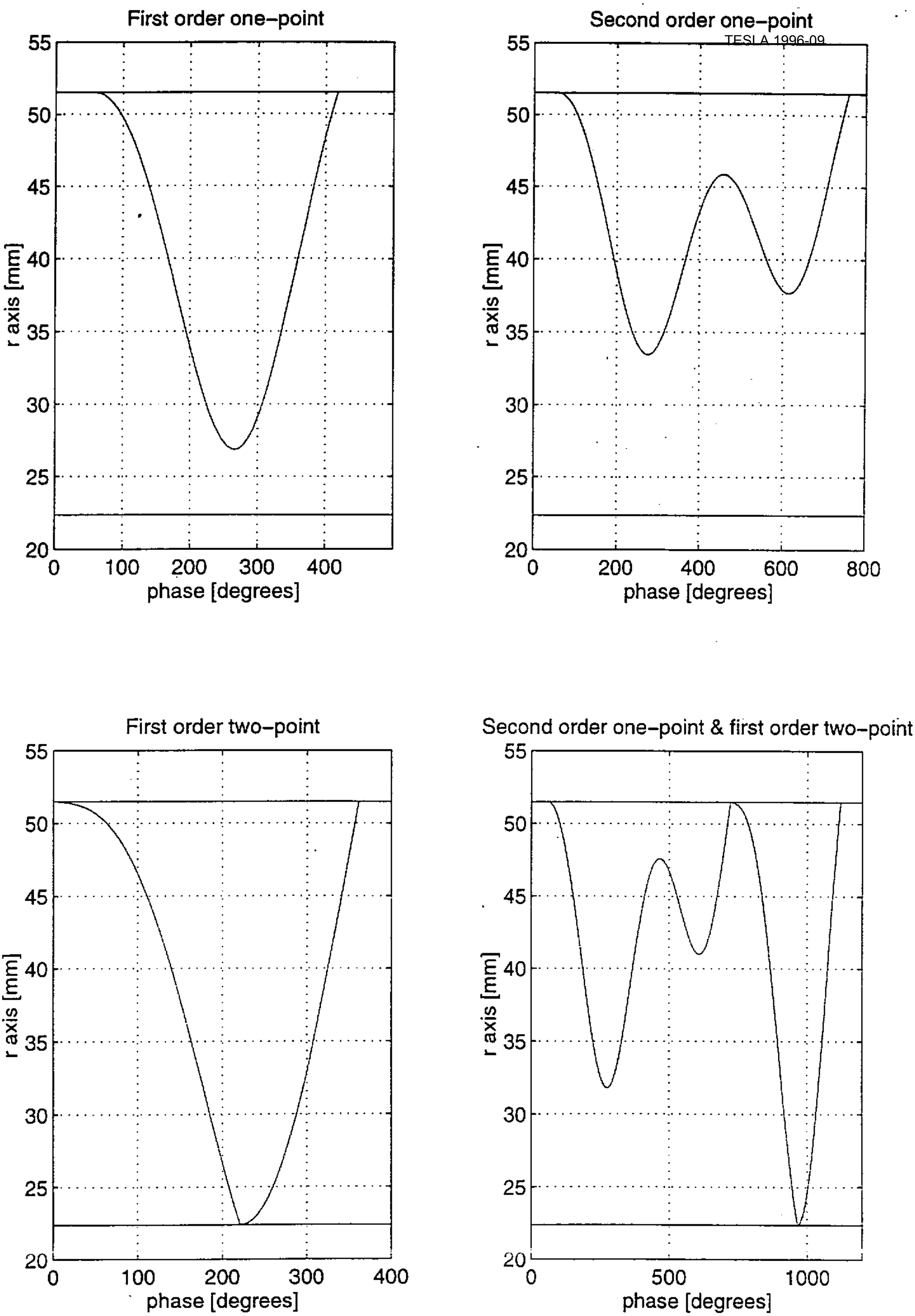
First order one-point
Second order one-point
First order two-point
Second order one-point & first order two-point
r axis [mm]
phase [degrees]
55
50
45
40
35
30
25
20
0
100
200
300
400
500
600
800
1000

First order one-point

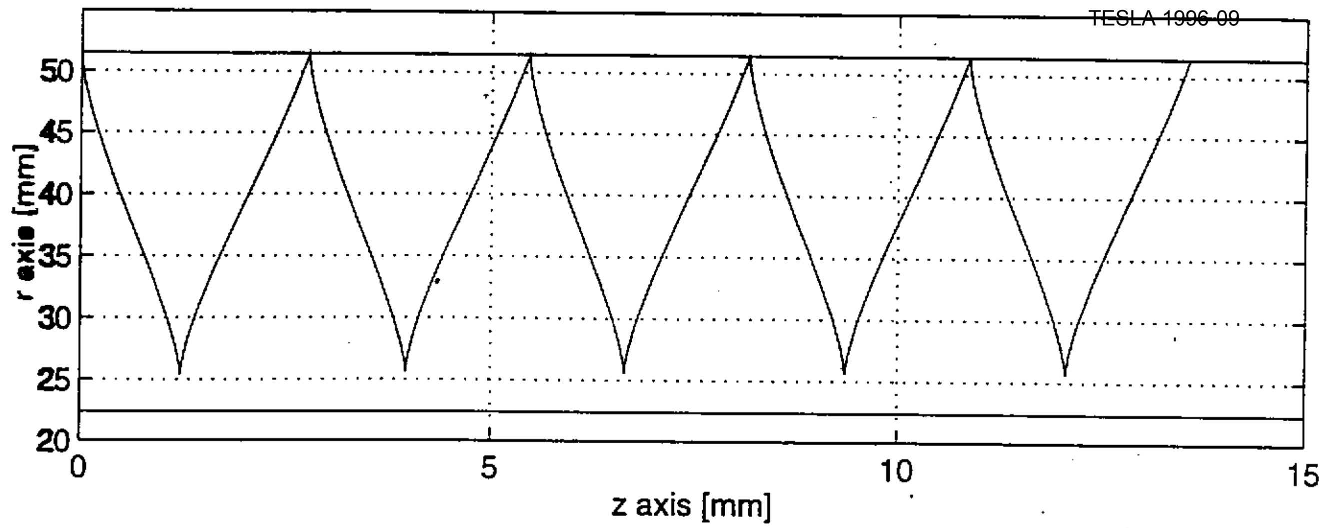

Second order one-point

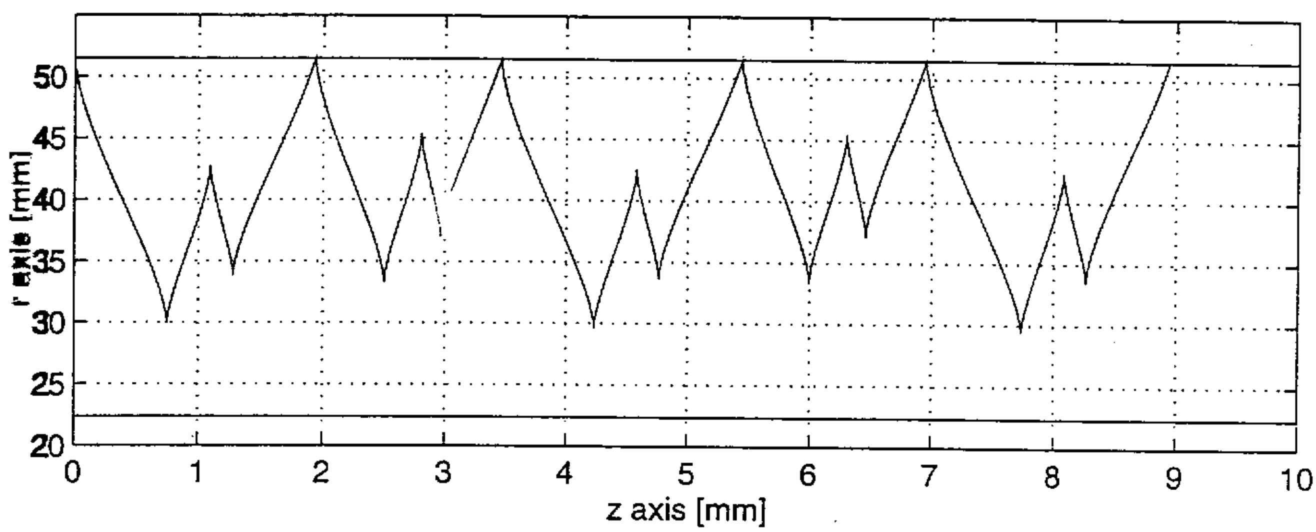

First order two-point

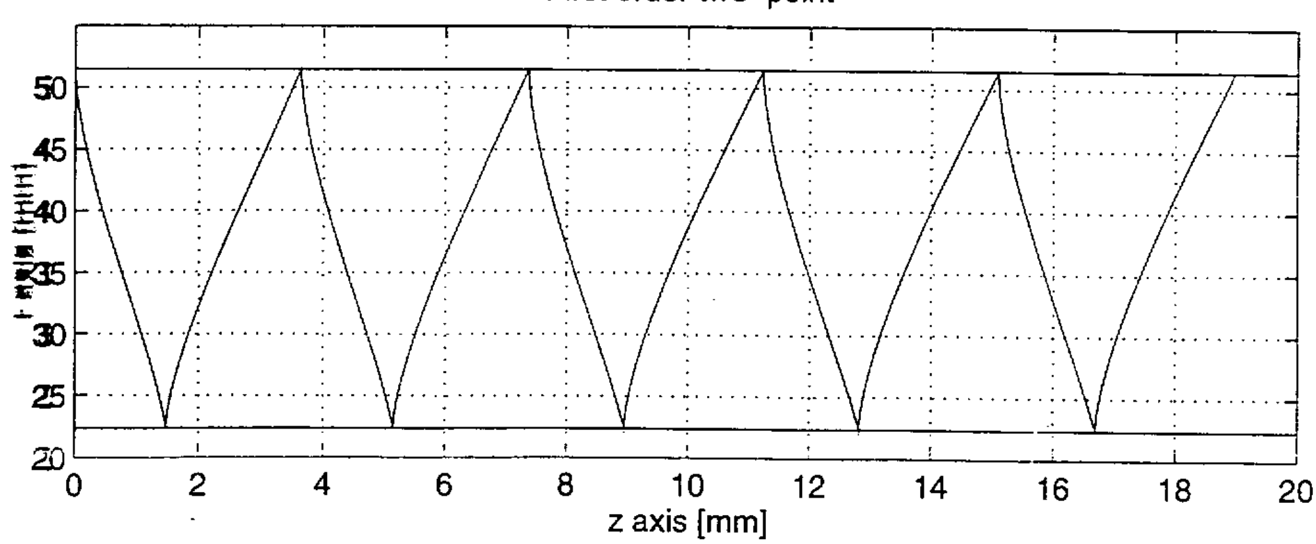

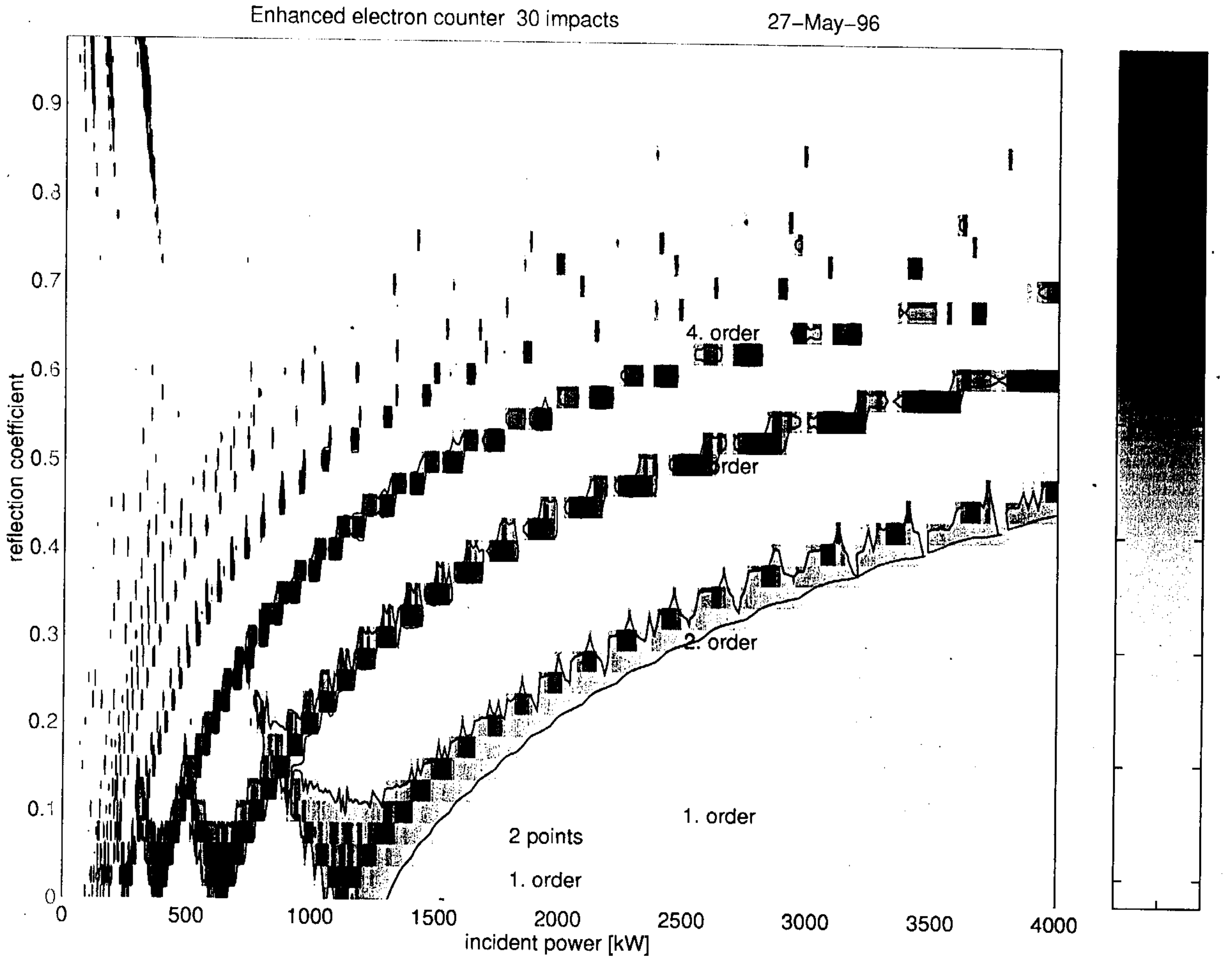
Enhanced electron counter 30 impacts
27–May–96
reflection coefficient
0.9
0.8
0.7
0.6
0.5
0.4
0.3
0.2
0.1
0
incident power [kW]
0
500
1000
1500
2000
2500
3000
3500
4000
4. order
3. order
2. order
1. order
2 points
1. order
4
3
2
1
0
−1
−2
−3

1. order

DESY coax R = 0.25 P = 1665 [kW] (EMP) 23-May-96

TESLA 1996-09

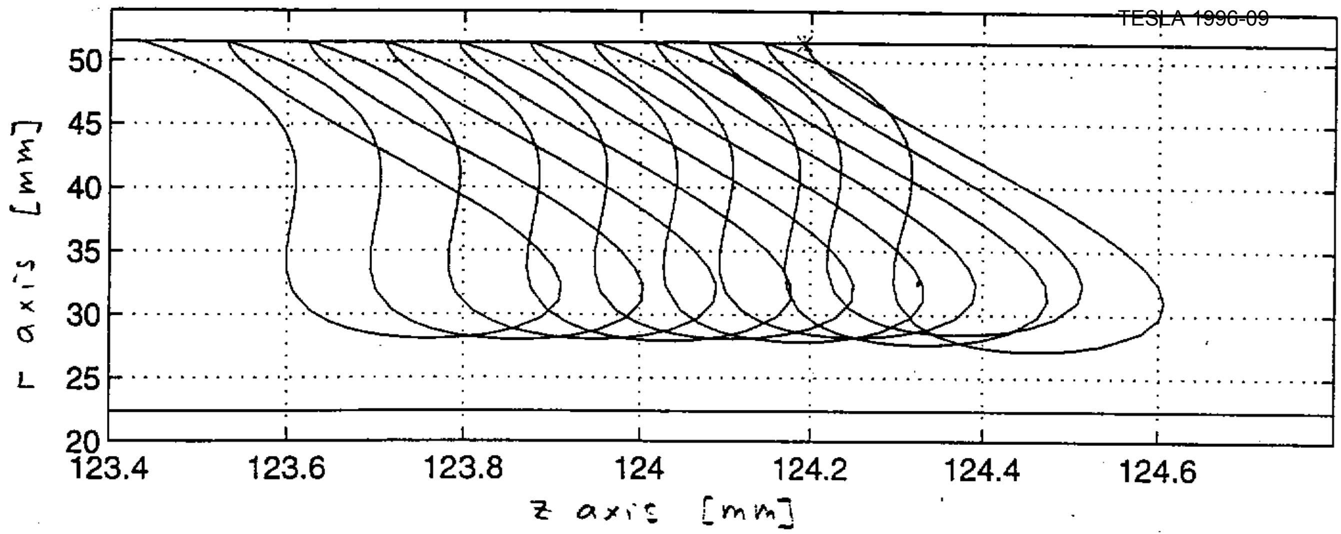

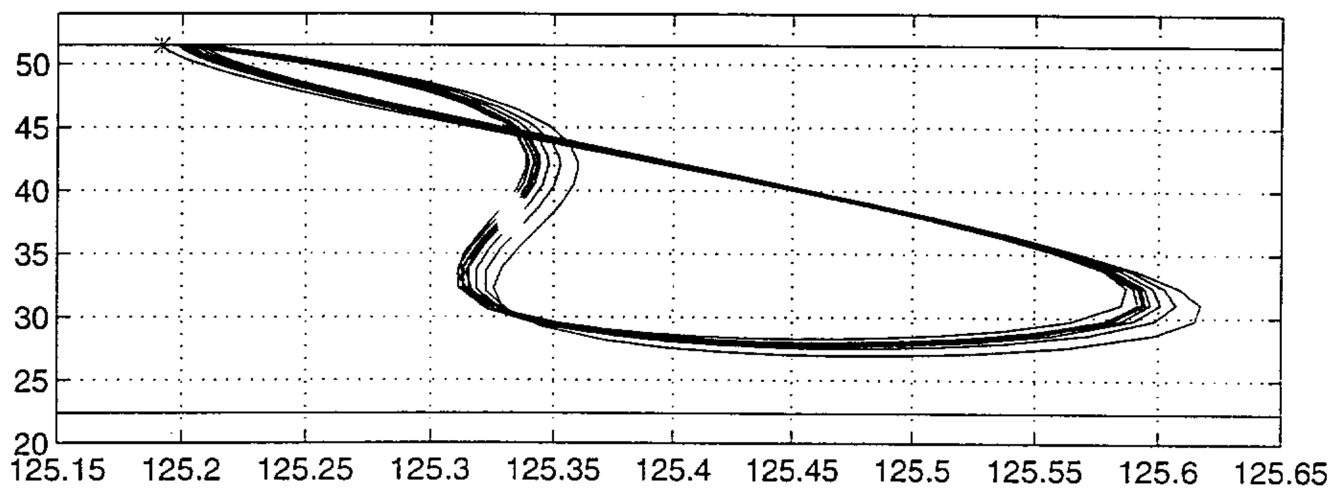

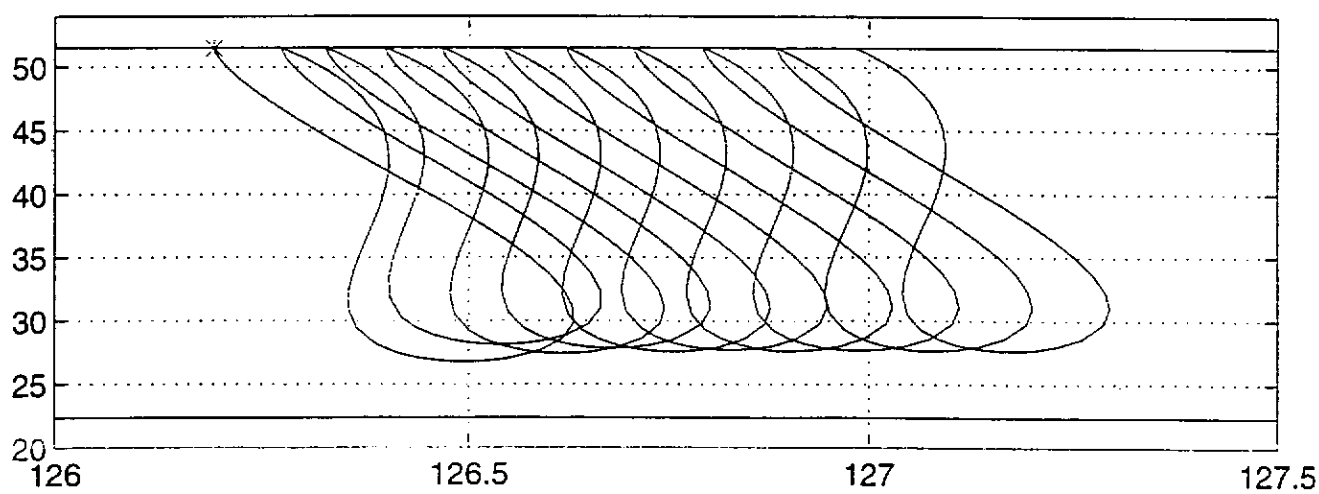

DESY coax R = 0.25 P = 4000 [kW] (MMP) 24-May-96

TESLA 1996-09

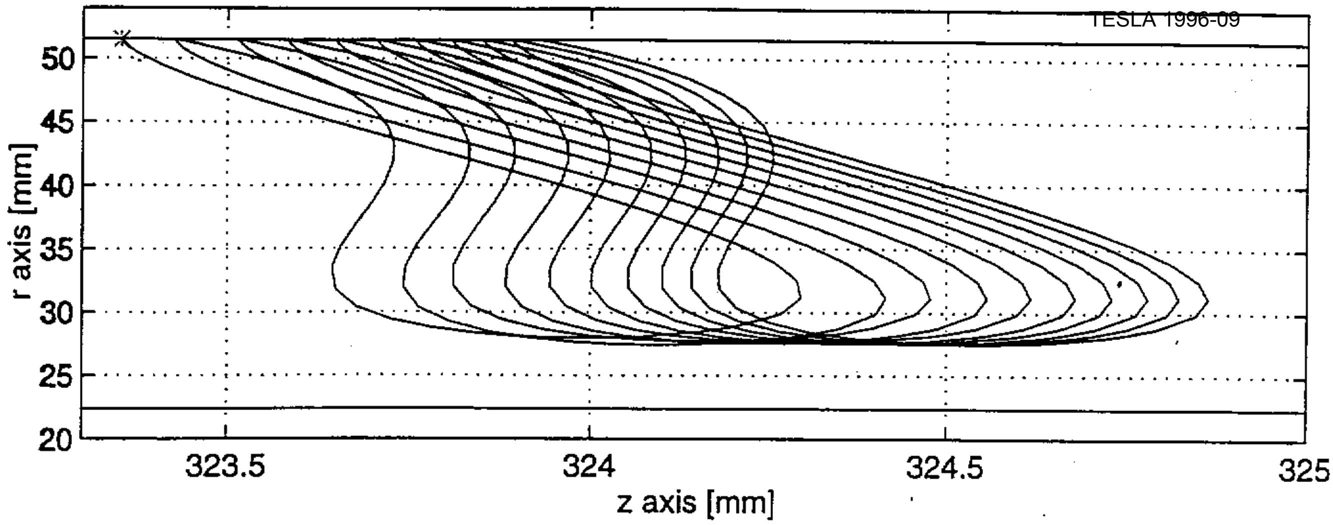

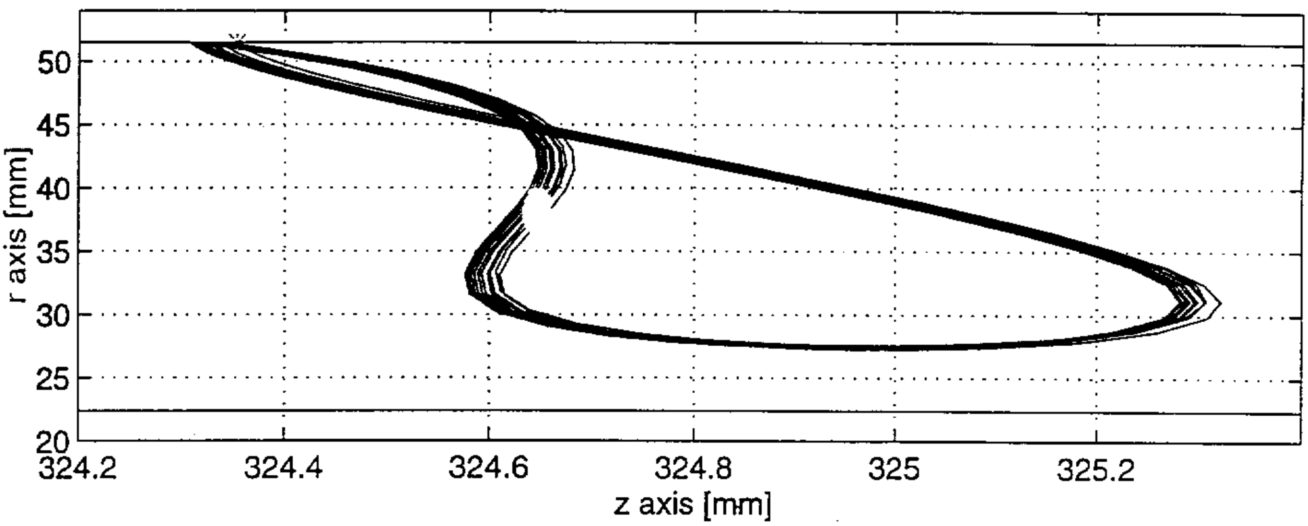

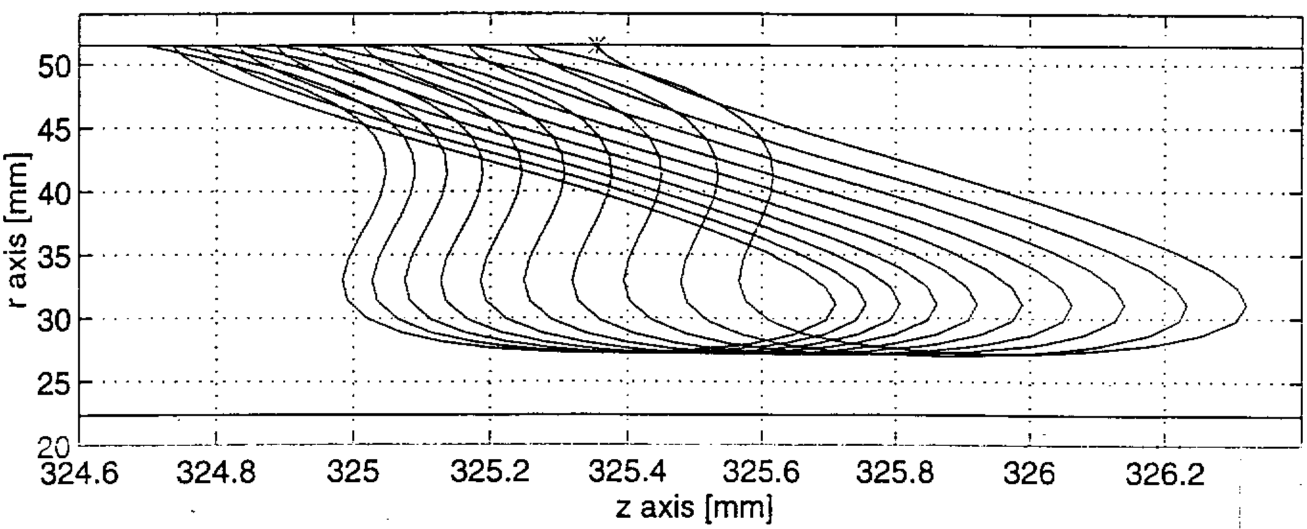

Multipacting Calculations.

A. Mosnier.

TESLA 1996-09

- focus on ē multipacting induced in the vicinity of windows
- Numerical code : uses the field distributions computed by Urmel-T

  SW mode : voltage max & voltage min simulation

  TW mode : time-dependant field obtained by addition of 2 SW fields with a 90° phase shift

A primary ē is first emitted from the alumina surface
when the ē impinges a wall (ceramic or copper part) secondary ē are emitted
the total number of re-emitted ē is computed after N impacts.
→ Scan of alumina surface, power & phase | gives an idea of the width & of the strength of MP.

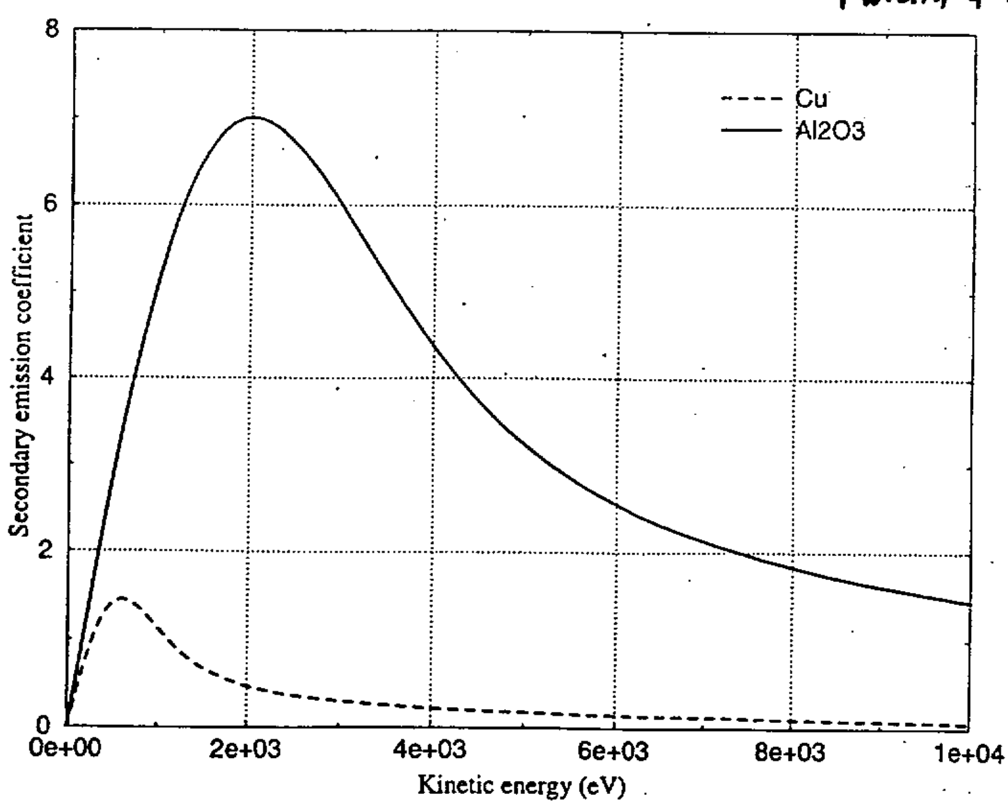

Example of SEC used for calculations.

Power : 1 → 400 kW

Phase : step = 2°.

1°- Example : Fermilab's conical window.

upstream & downstream sides were scanned

Scan of the alumina surface : 9 equidistant initial points (10% → 90%)

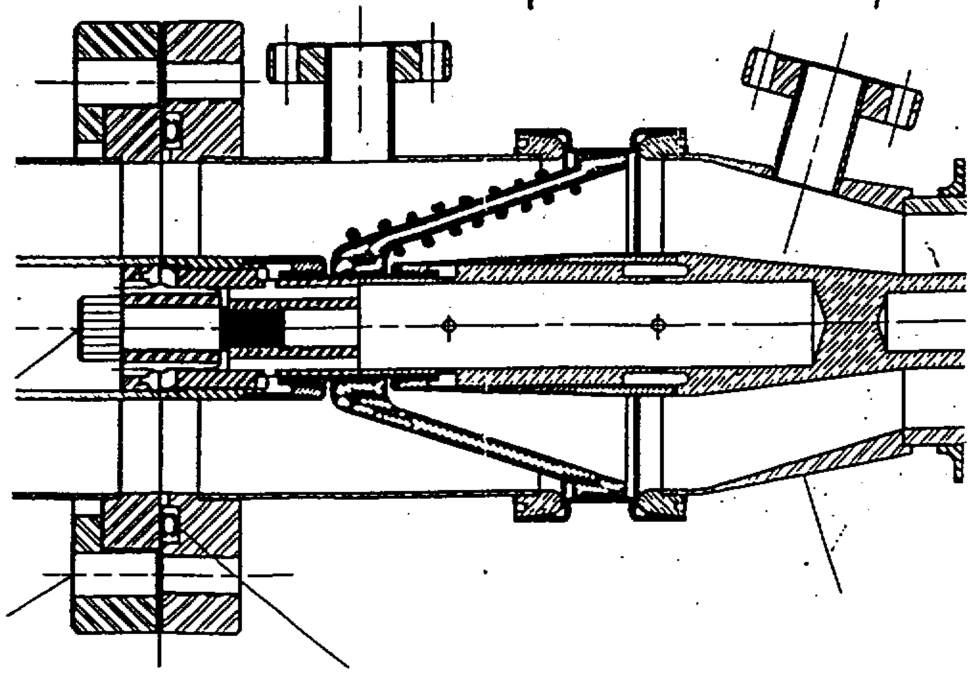

Example of Radial Electric Field at half radius. (R = 22 mm) (P = 200 kW)

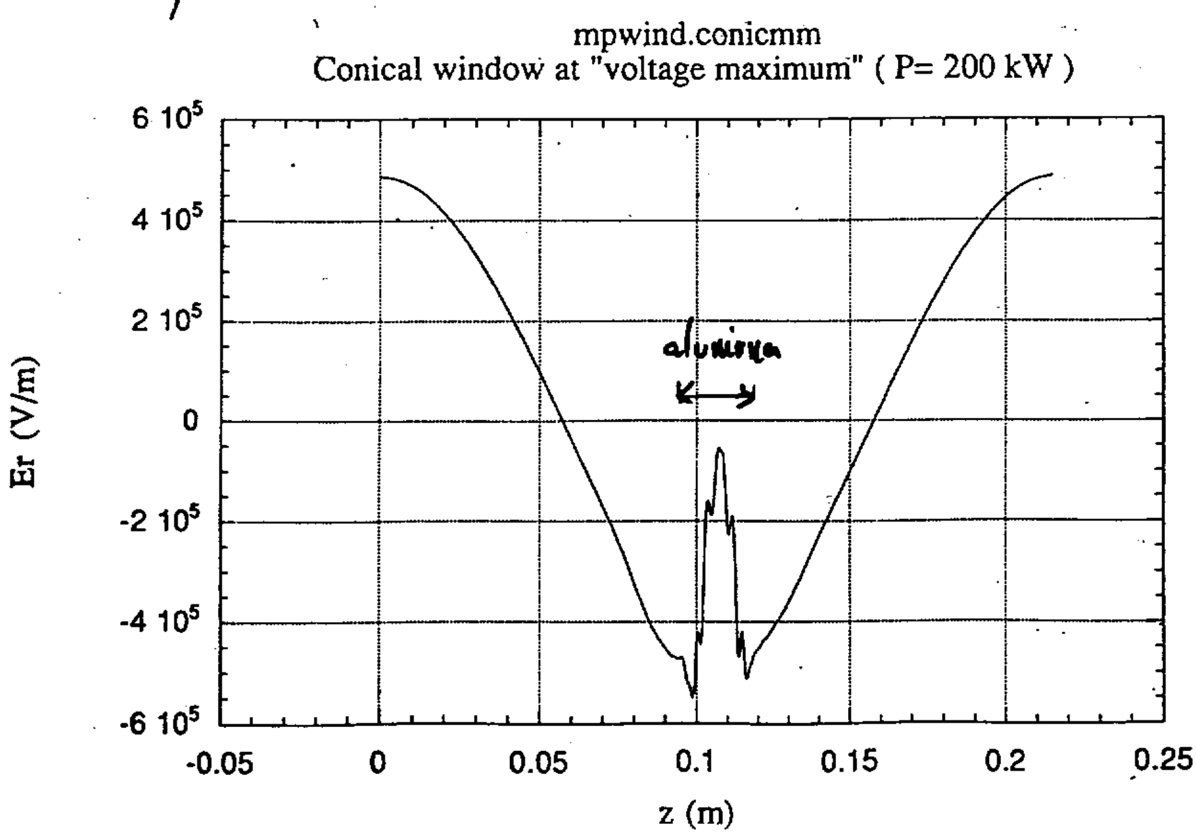

ceramic at voltage maximum

conic 'voltage max' upstream

conicmmL

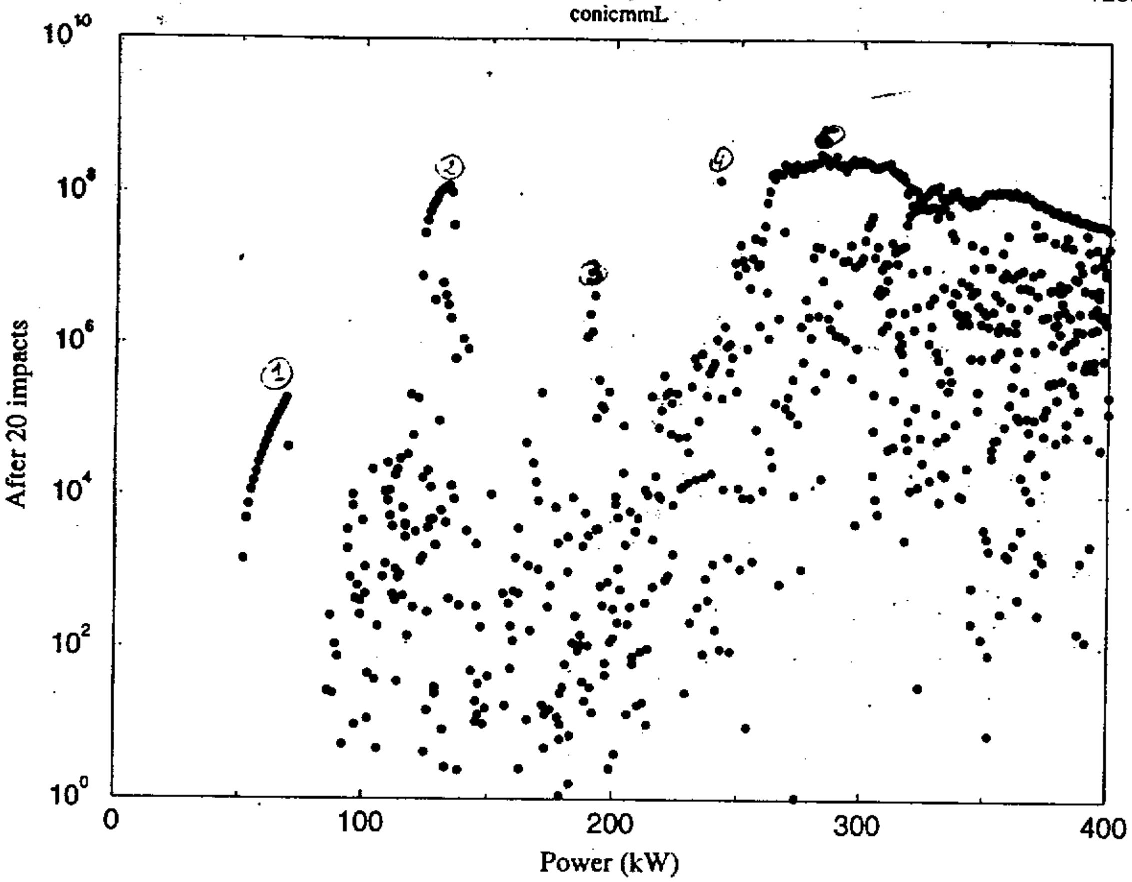

upstream

conic 'voltage max' downstream

conicmmR

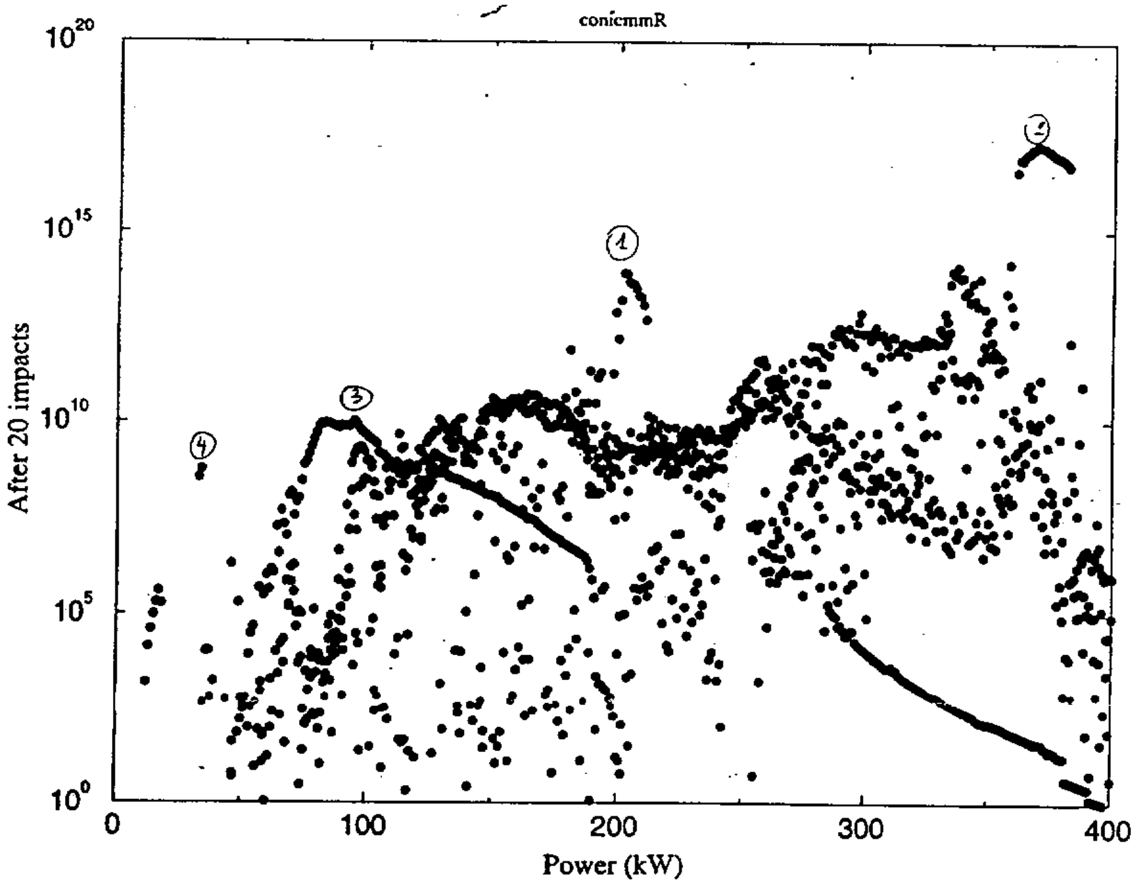

downstream

>

stronger multipack

conic 'voltage min' upstream

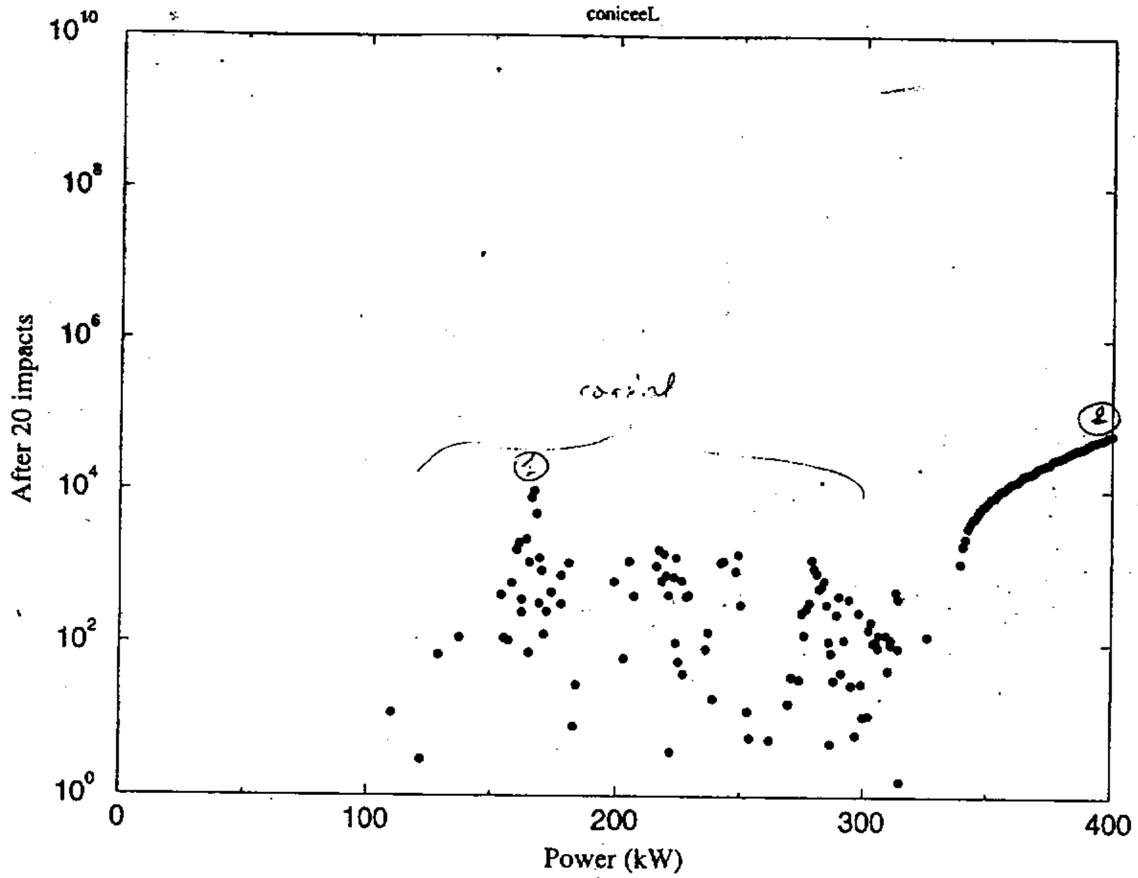

upstream

conic 'voltage min' downstream

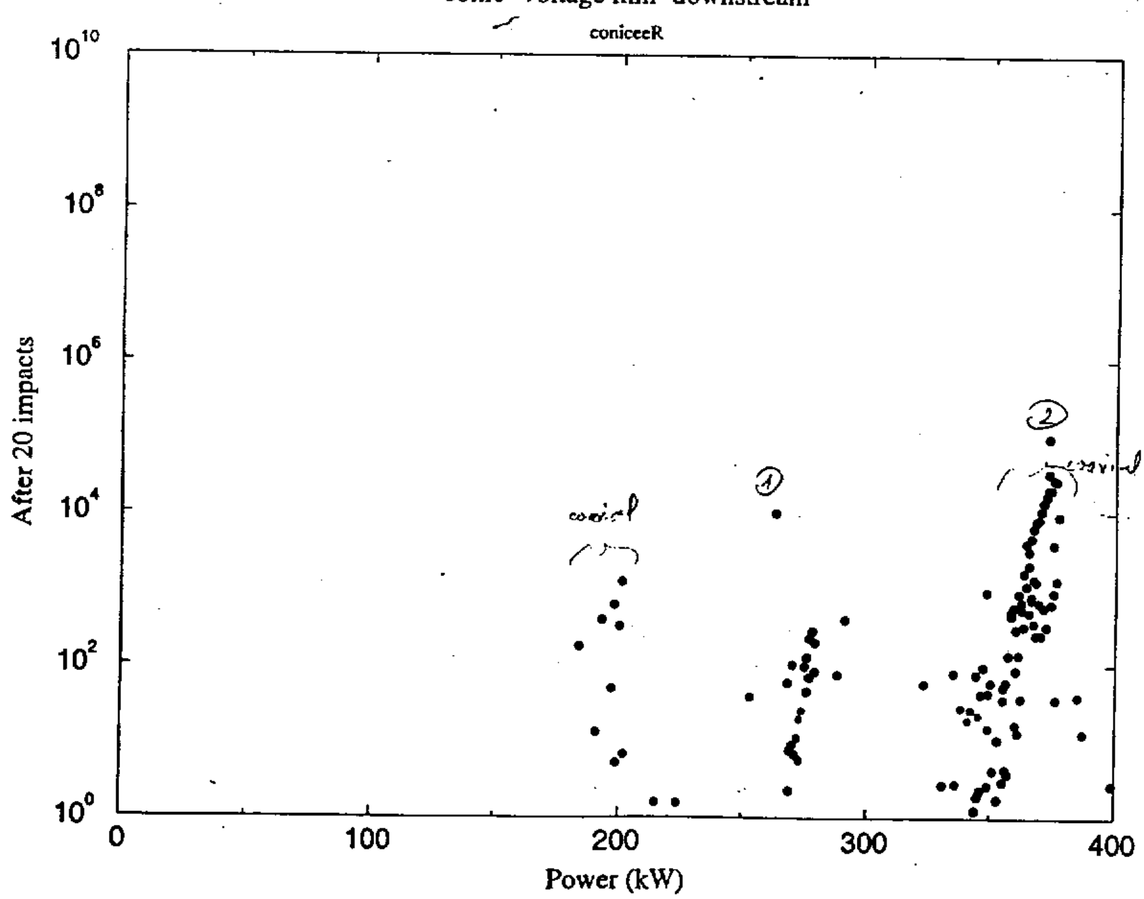

downstream

TW calculations

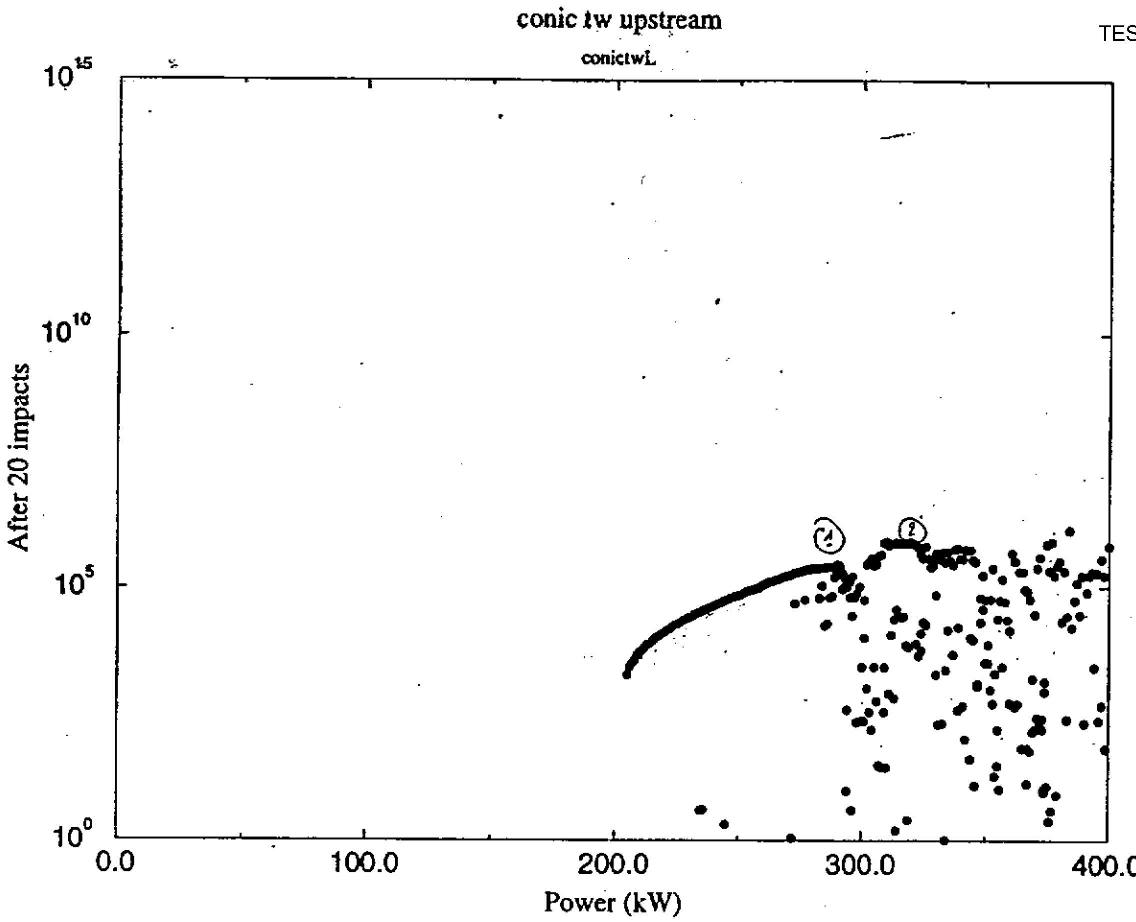

upstream

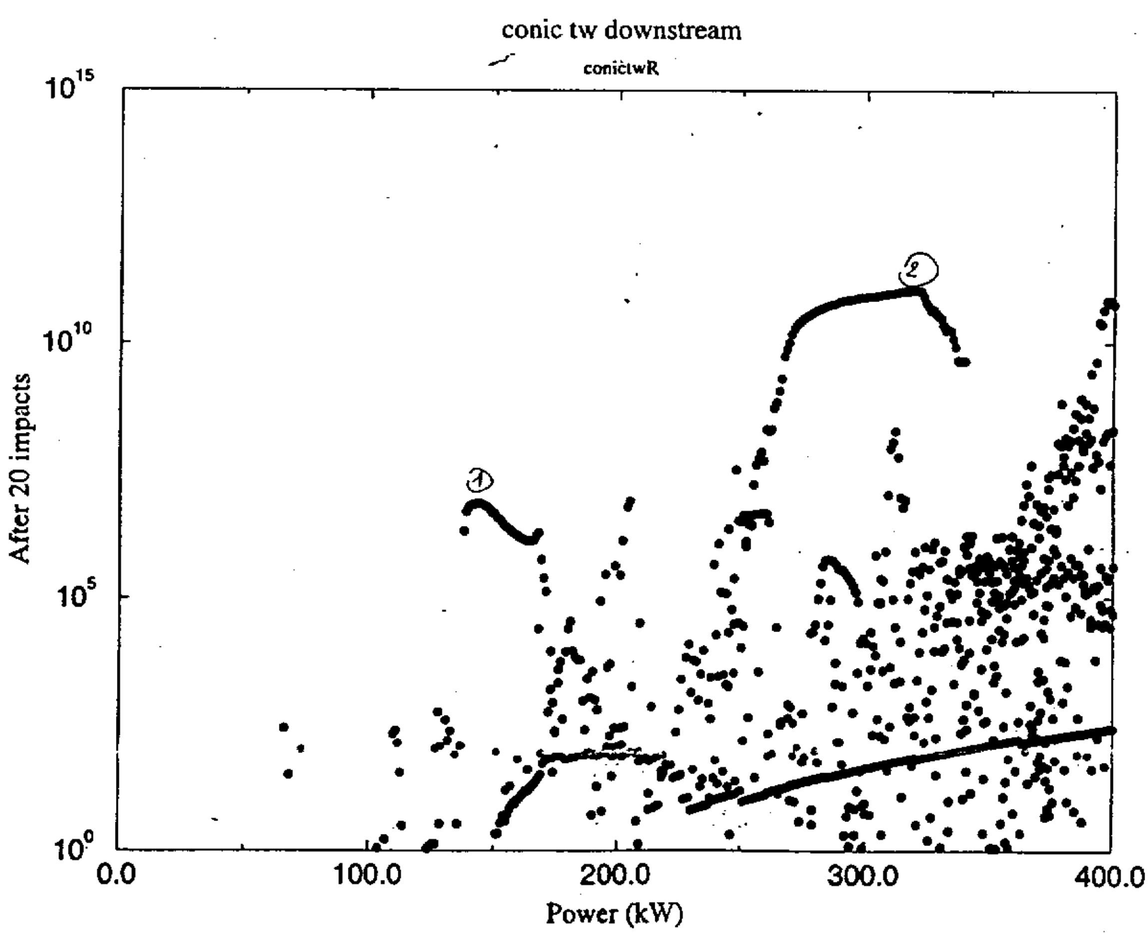

downstream

Voltage Maximum upstream side.

③ P = 192 kW order 3

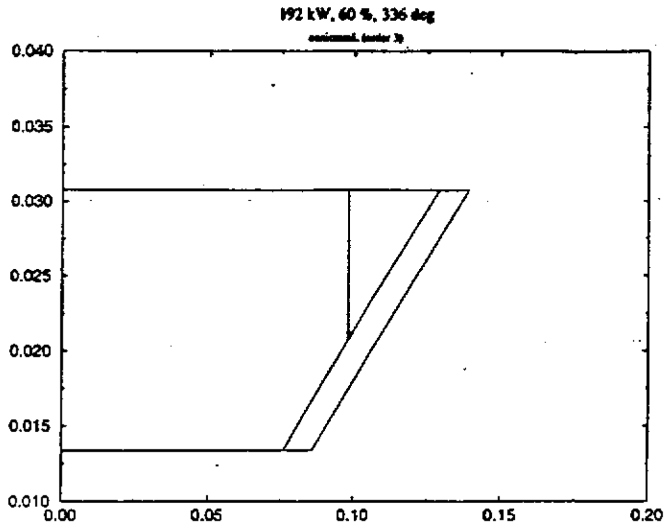

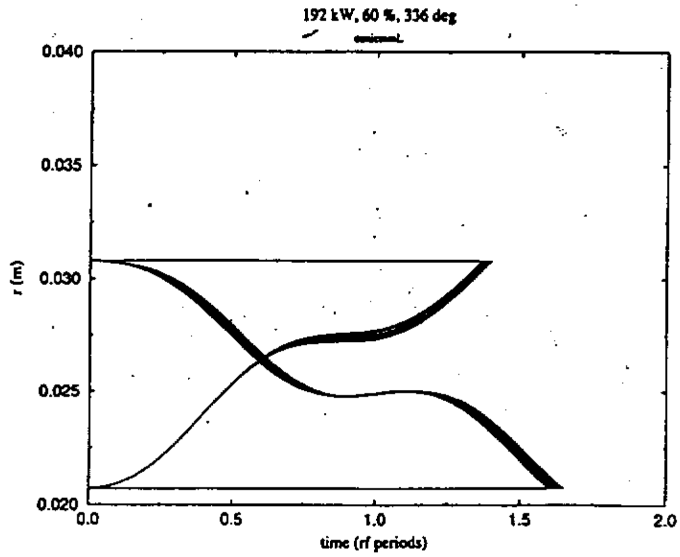

⑤ P = 283 kW order 1

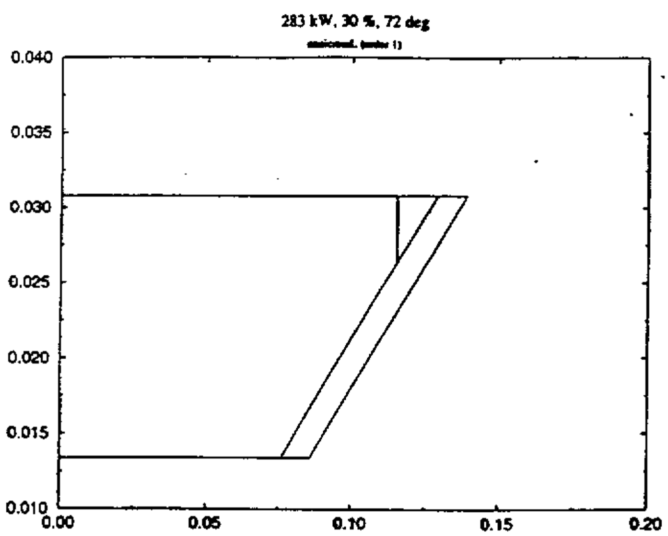

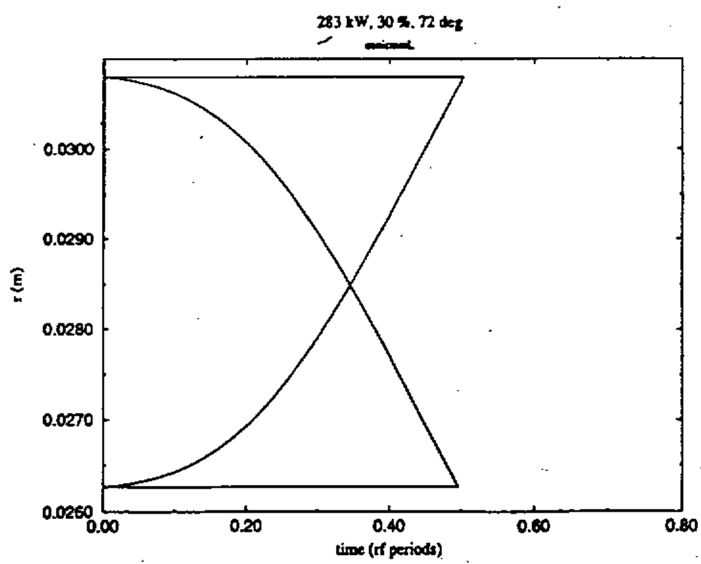

(1) P= 69 kW order 1

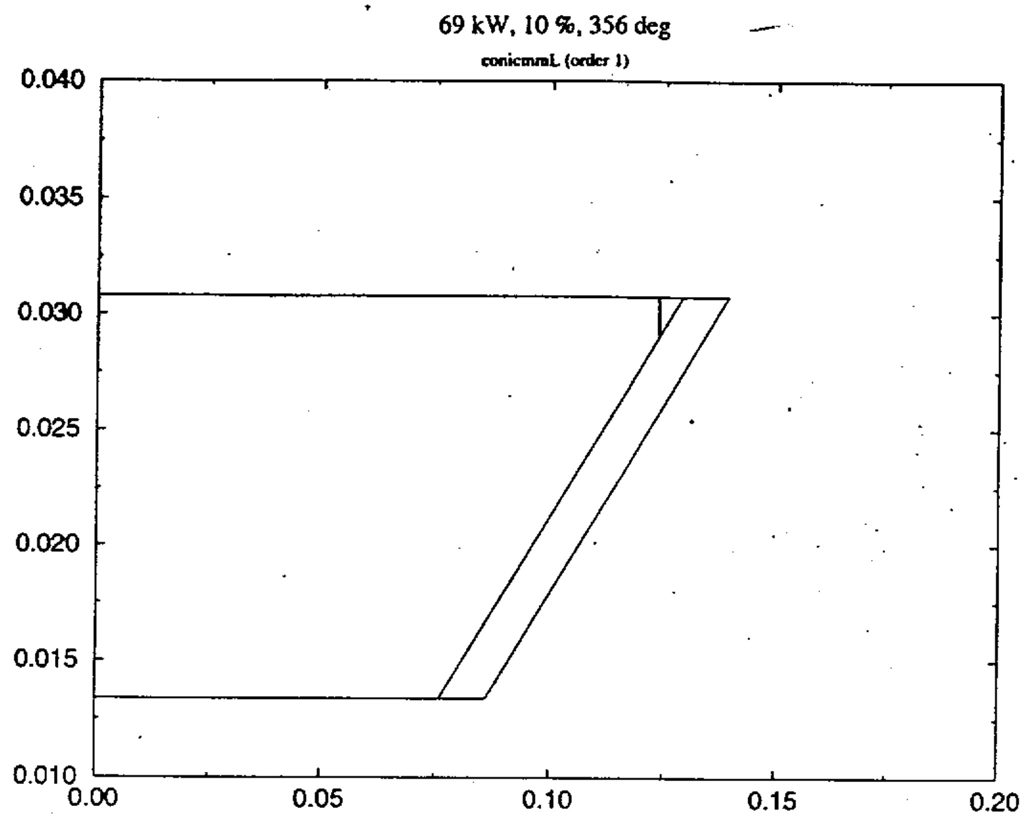

(2) P= 133 kW order 1

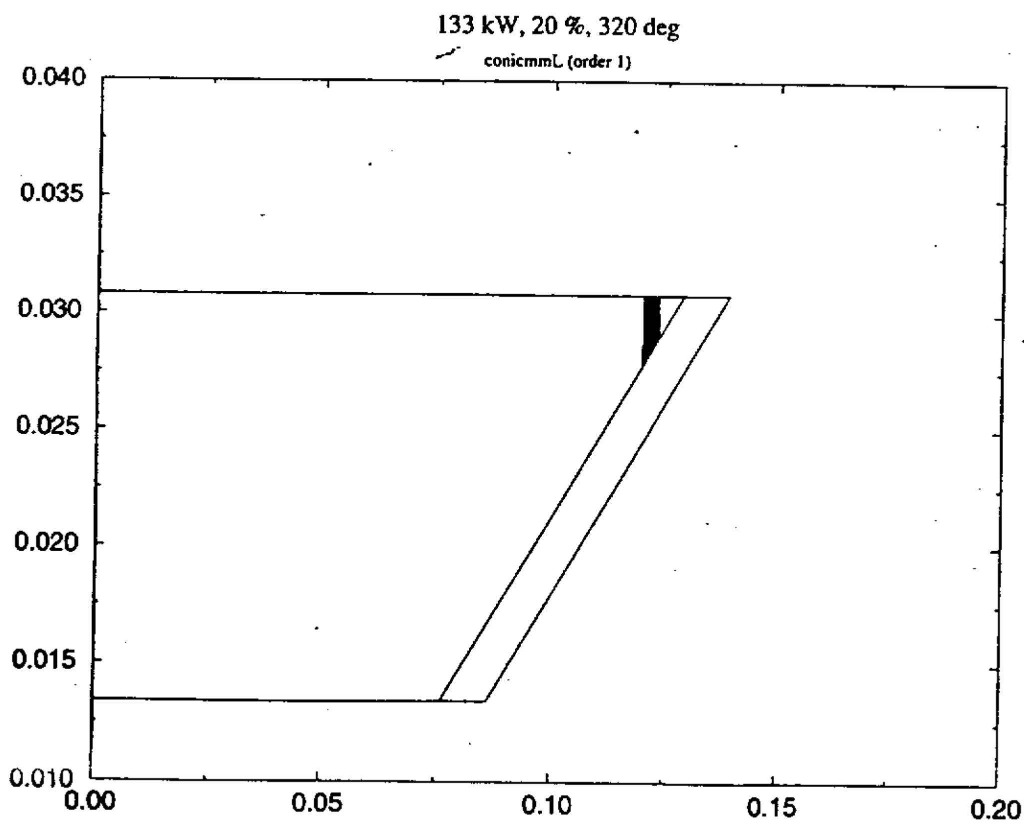

Voltage Maximum downstream

(3) P=95kW order 1 → involves ceramics + copper

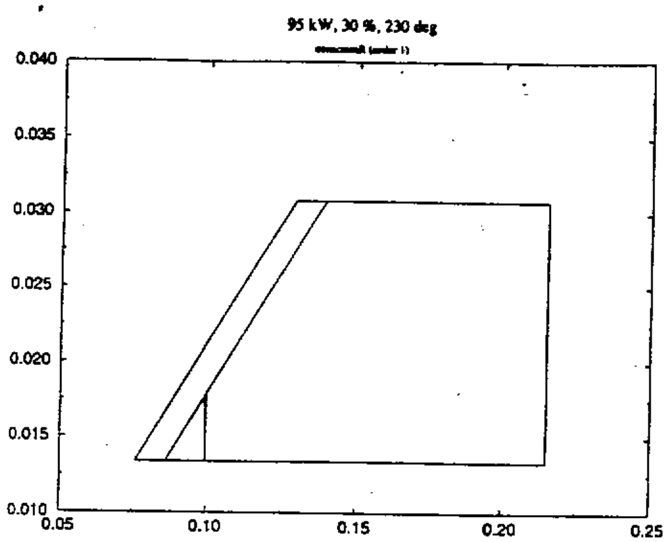

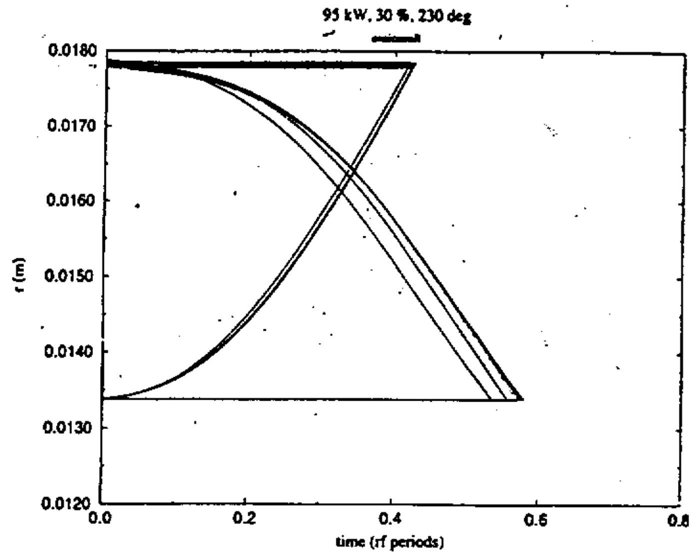

(1) P=202kW order 4 → involves ceramics only

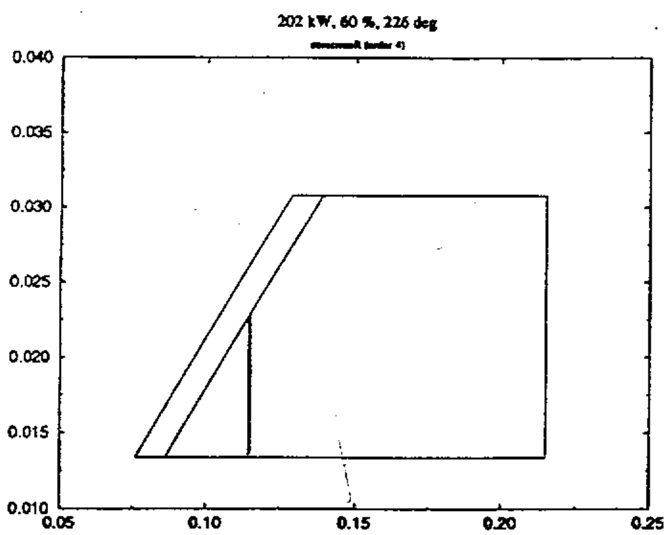

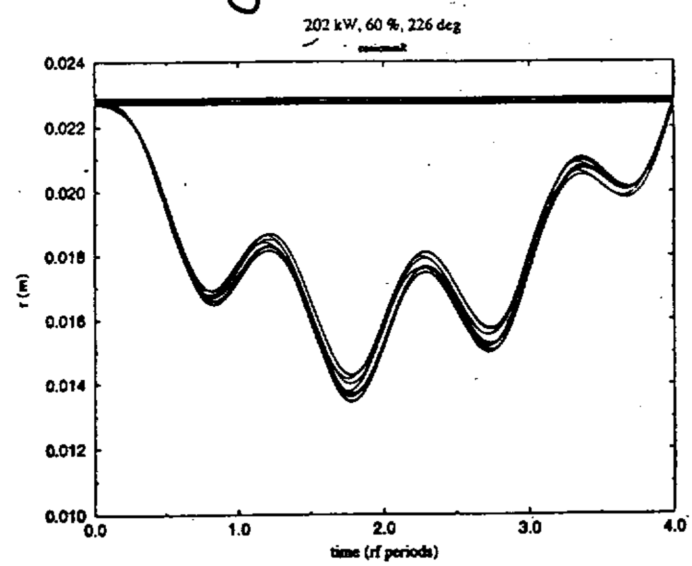

② P = 369 kW order 3

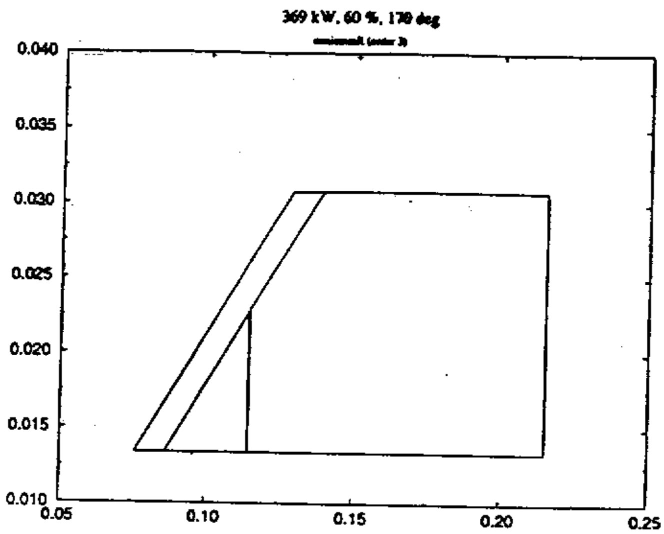

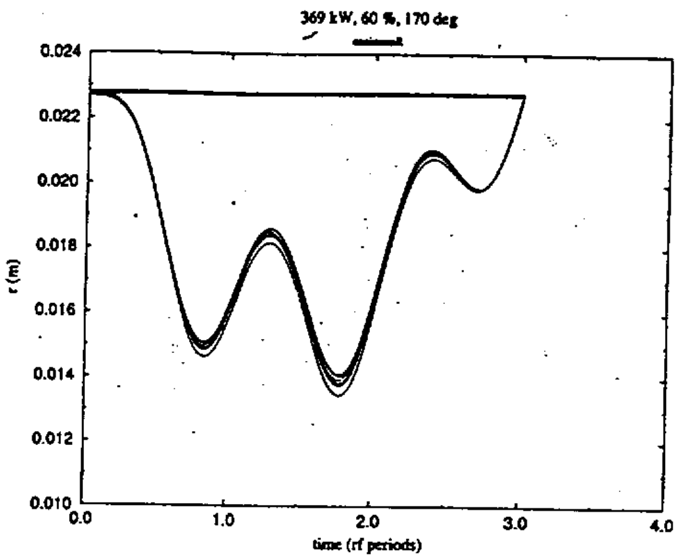

④ P = 34 kW.

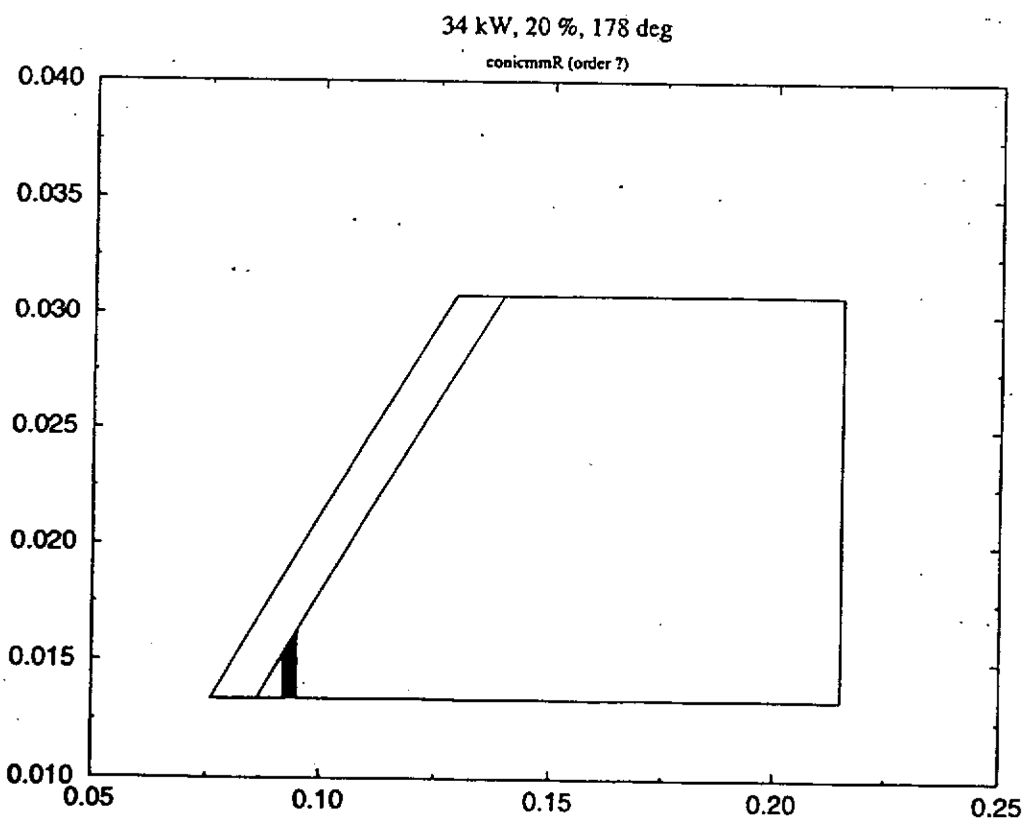

Voltage minimum upstream wae.

(1) P= 166 kW ends up with coaxial MP → order 8

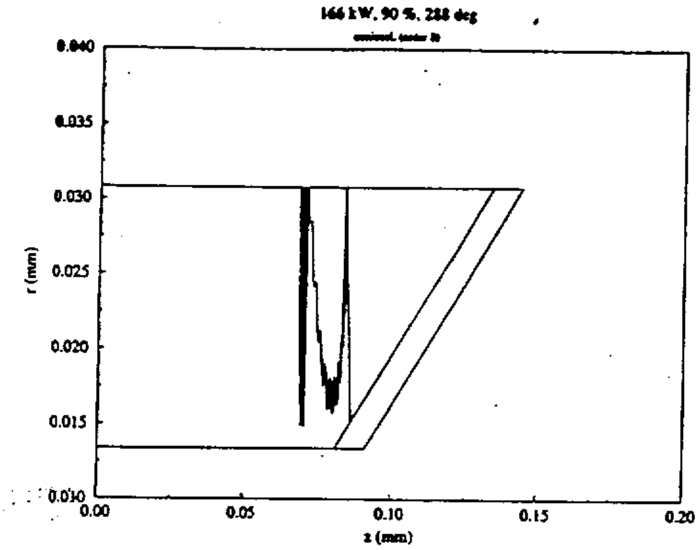

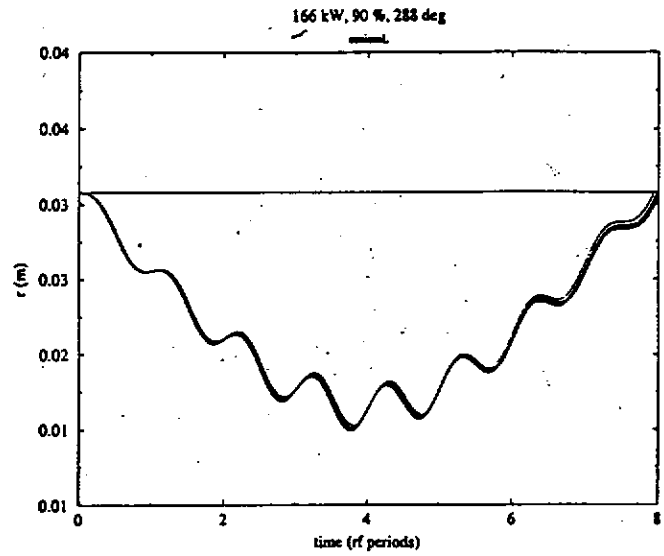

(2) P= 400 kW order 1

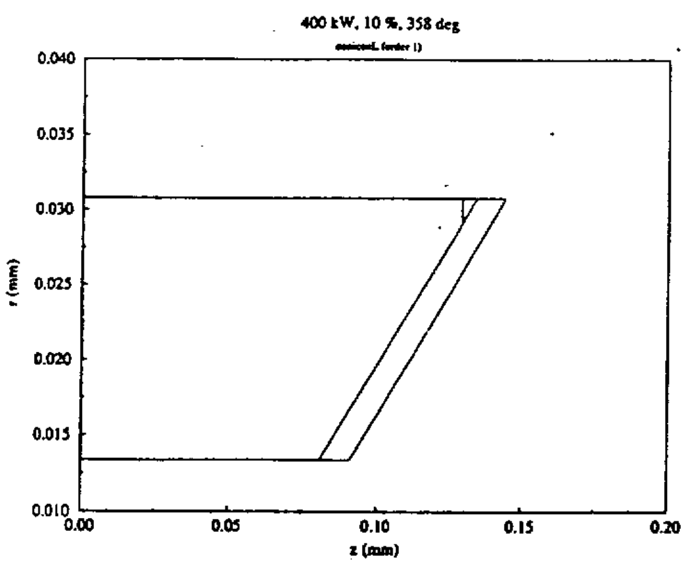

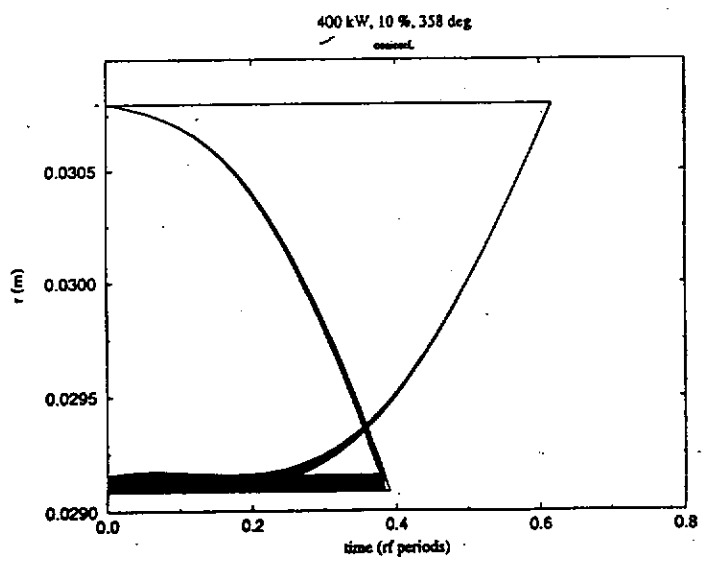

① P= 263 kW

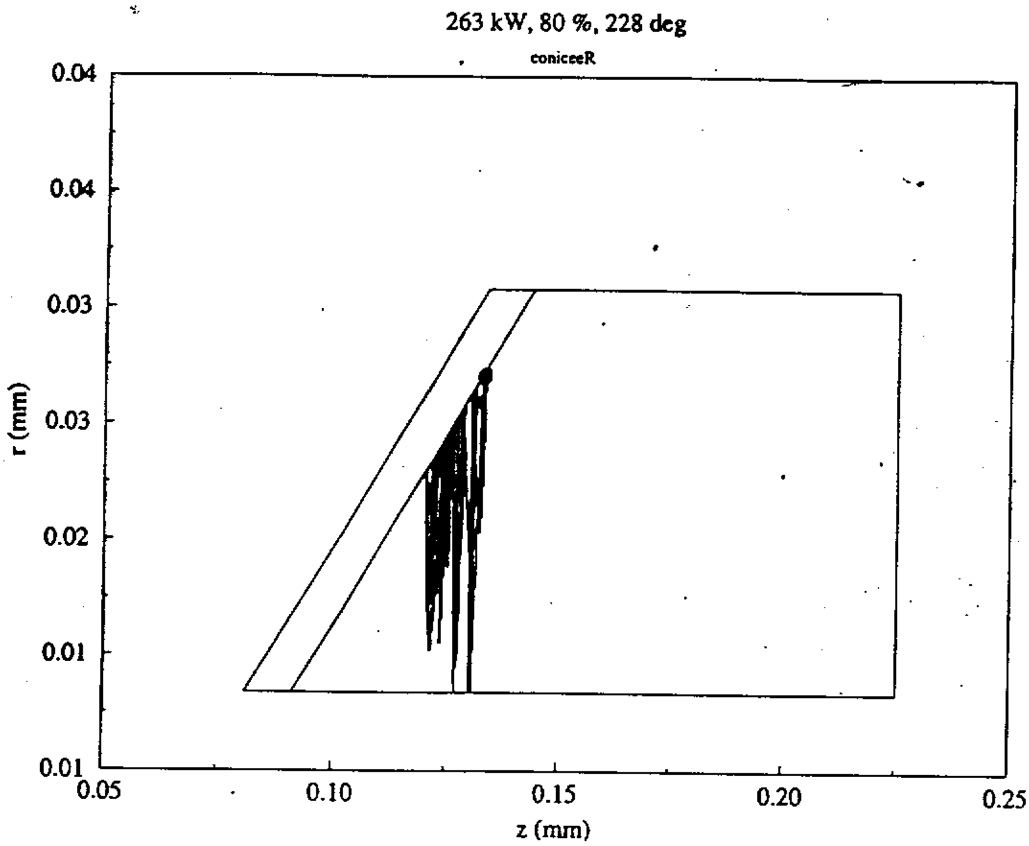

② P= 373 kW

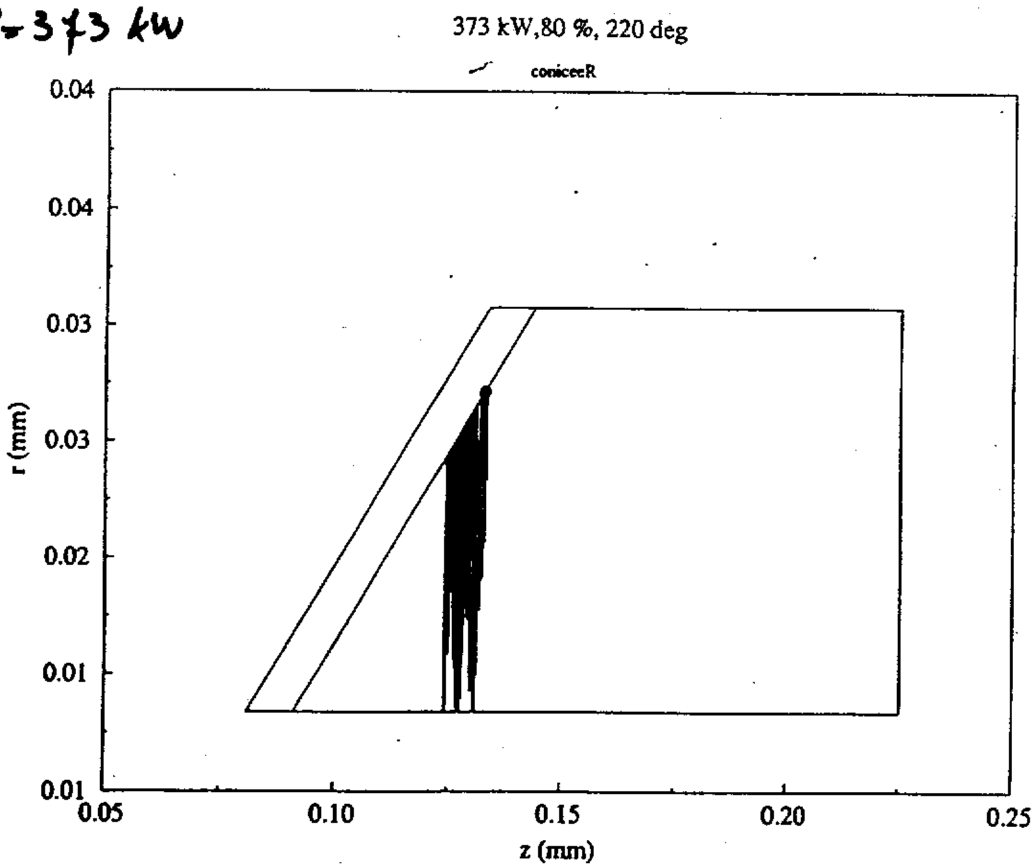

IW upstream

① P= 286 kW order 1

286 kW, 10 %, 250 deg

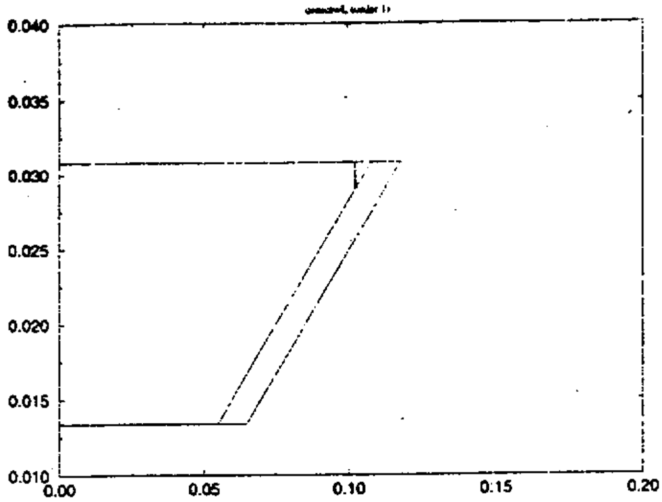

286 kW, 10 %, 250 deg

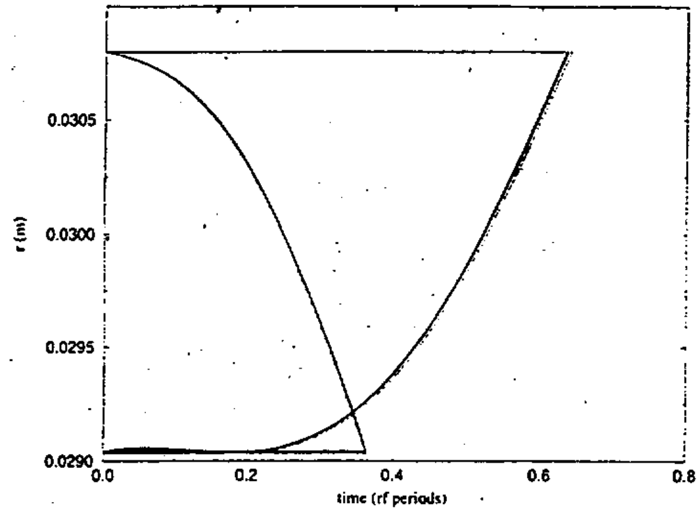

② P= 320 kW order 3 at beginning

320 kW, 60 %, 290 deg

conictwL

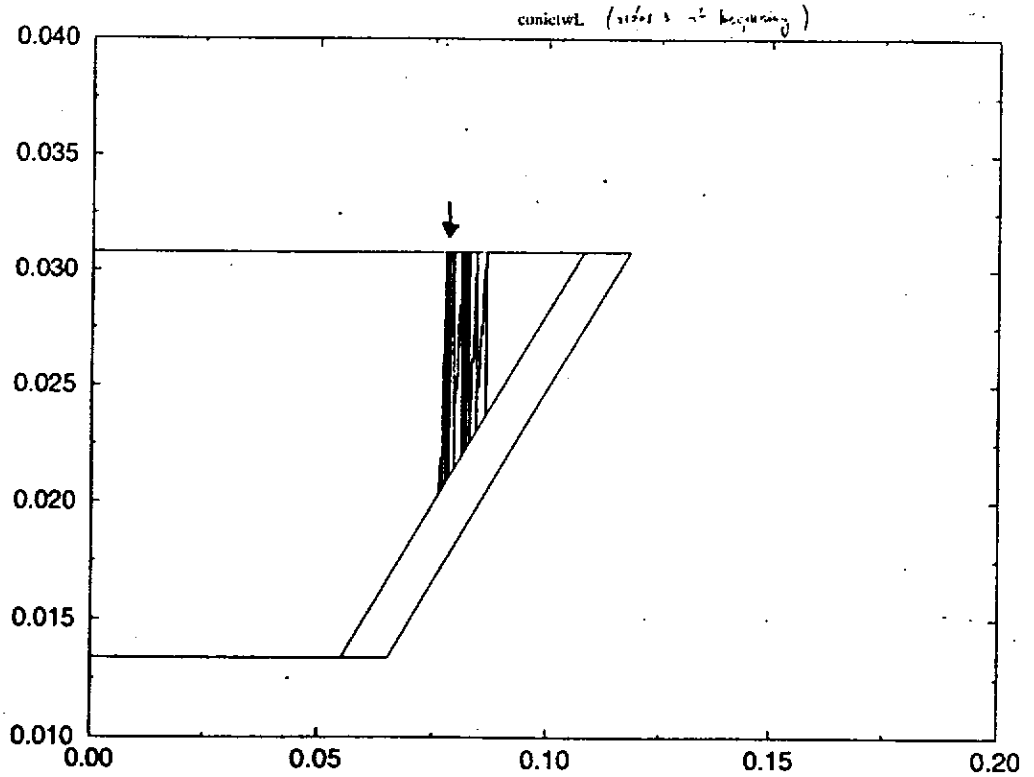

① P = 144 kW order 3

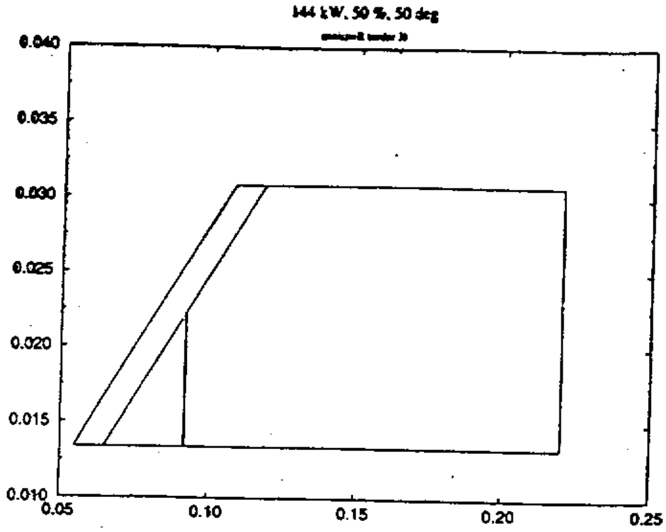

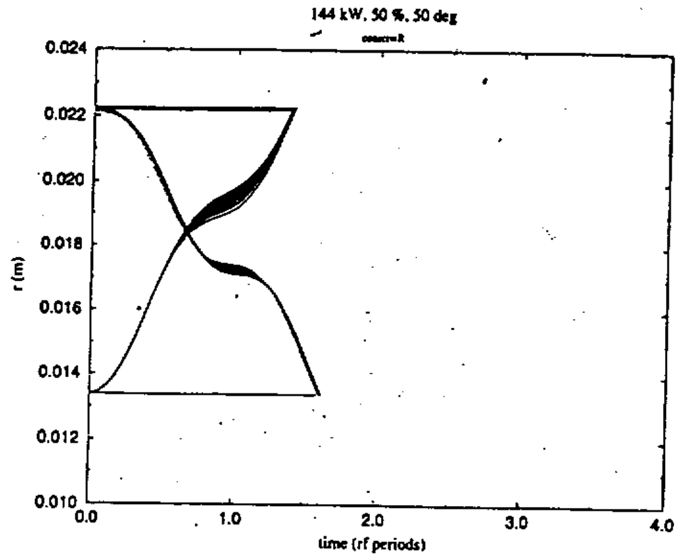

② P = 320 kW order 2

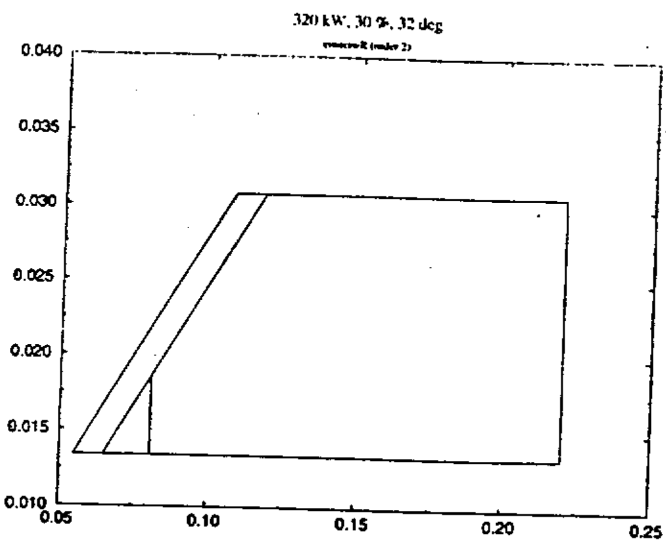

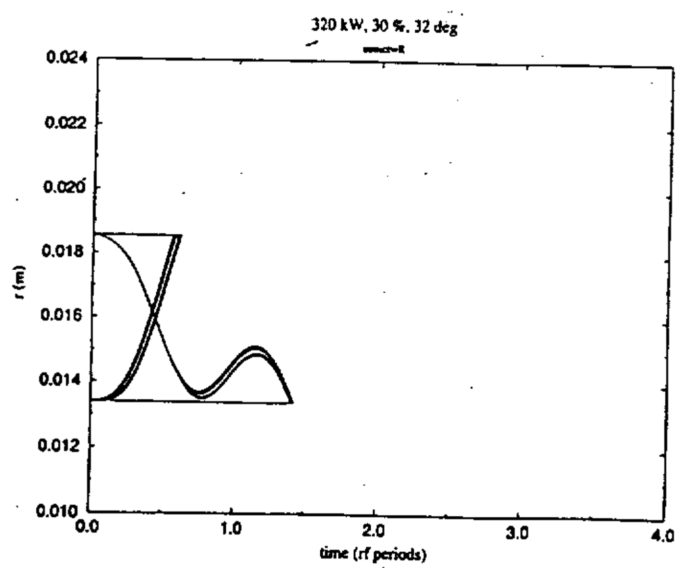

Example 2: The cylindrical DESY window

both surfaces were scanned (9 points x2)

power: 0 → 400 kW

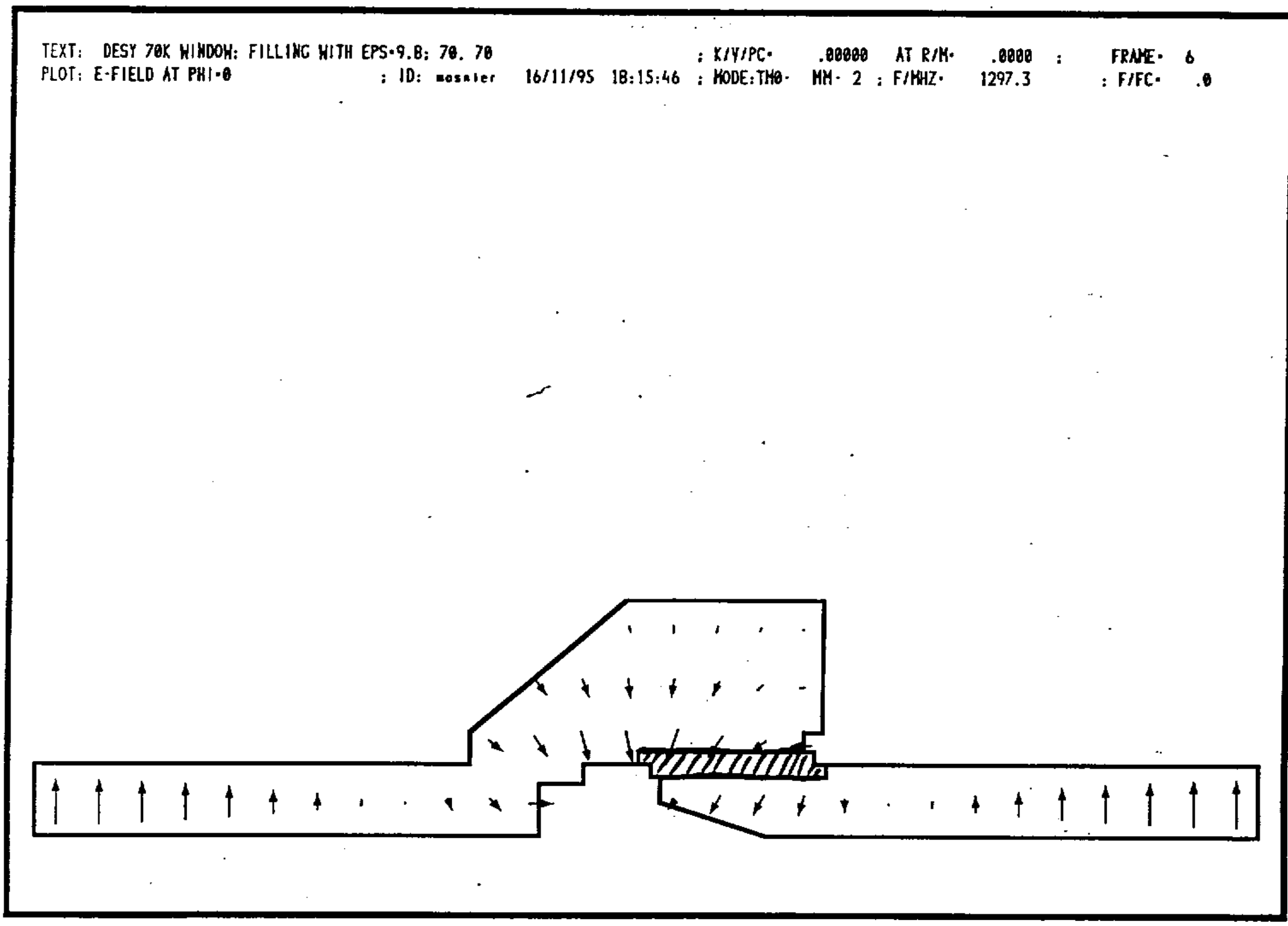

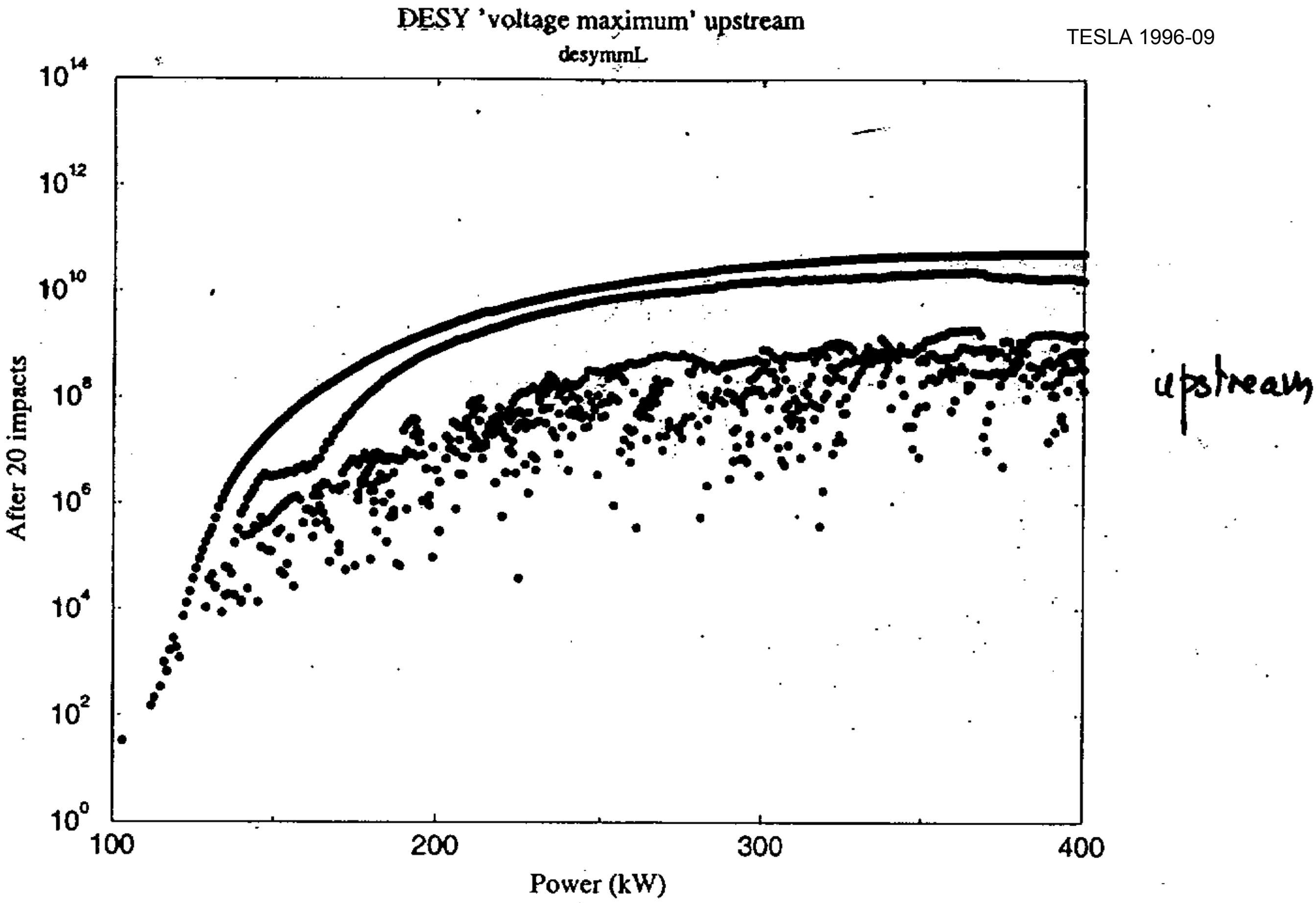
DESY 'voltage maximum' upstream
desymmL
After 20 impacts
Power (kW)
upstream

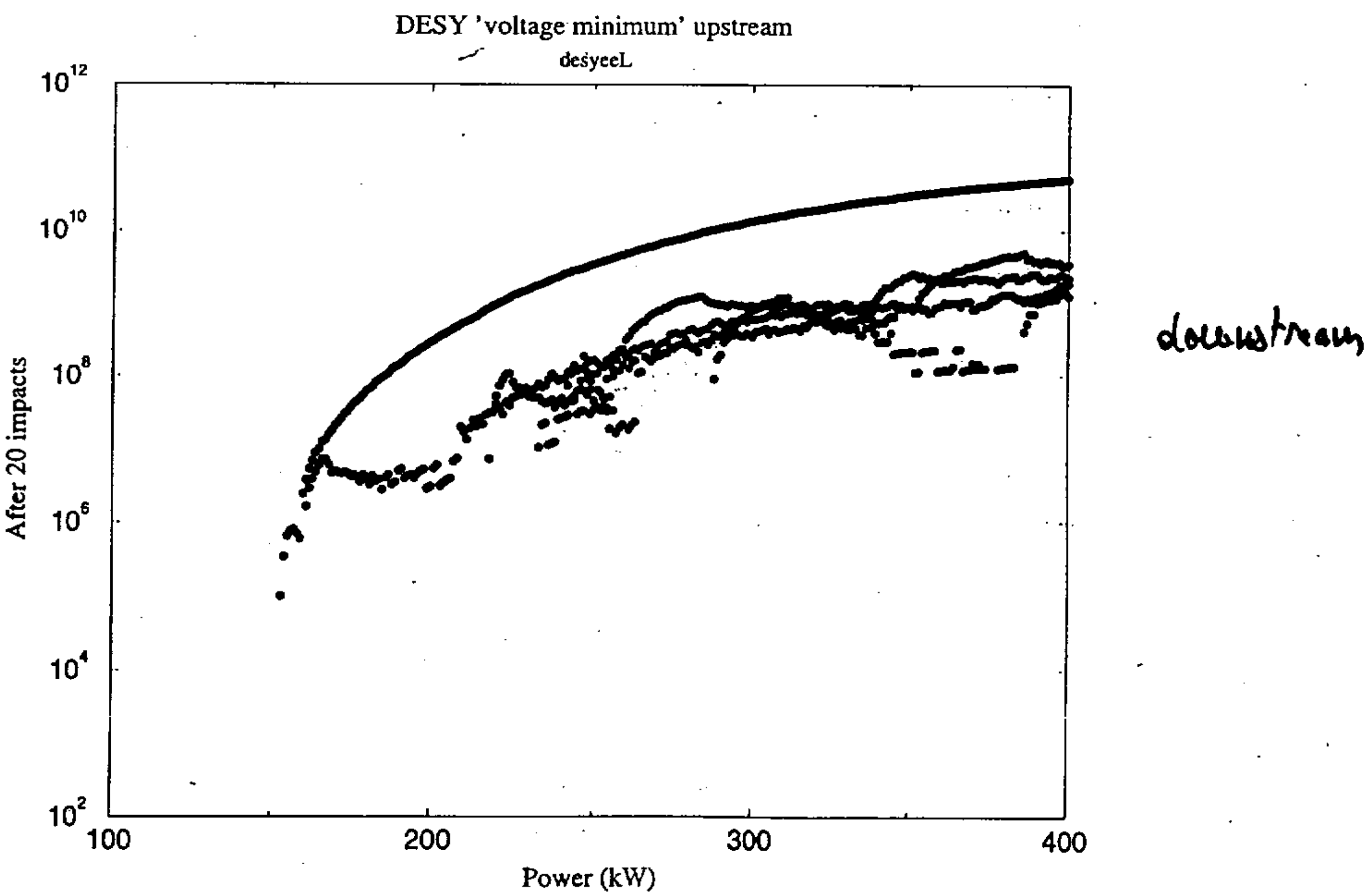
DESY 'voltage minimum' upstream
desyeeL
After 20 impacts
Power (kW)
downstream

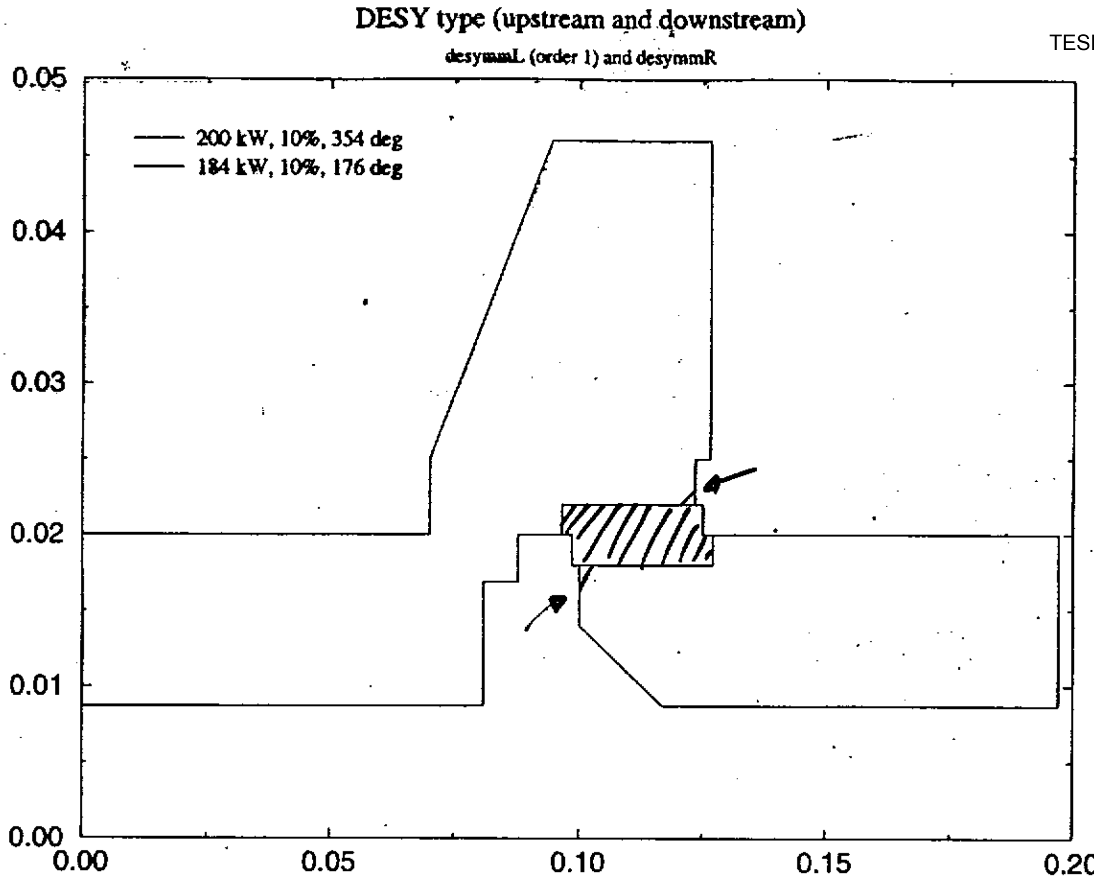

→ 2 main multipacting trajectories.

upstream } → order 1

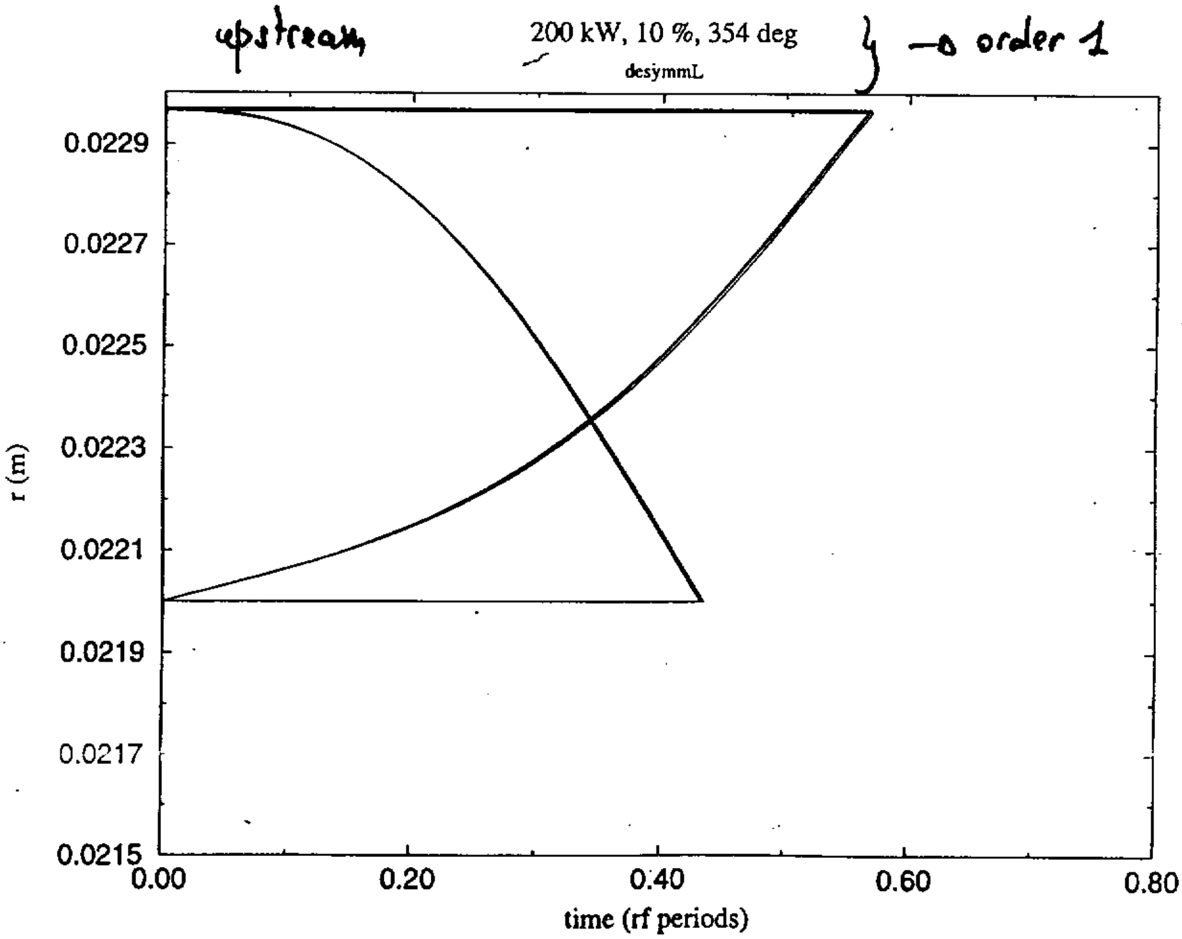

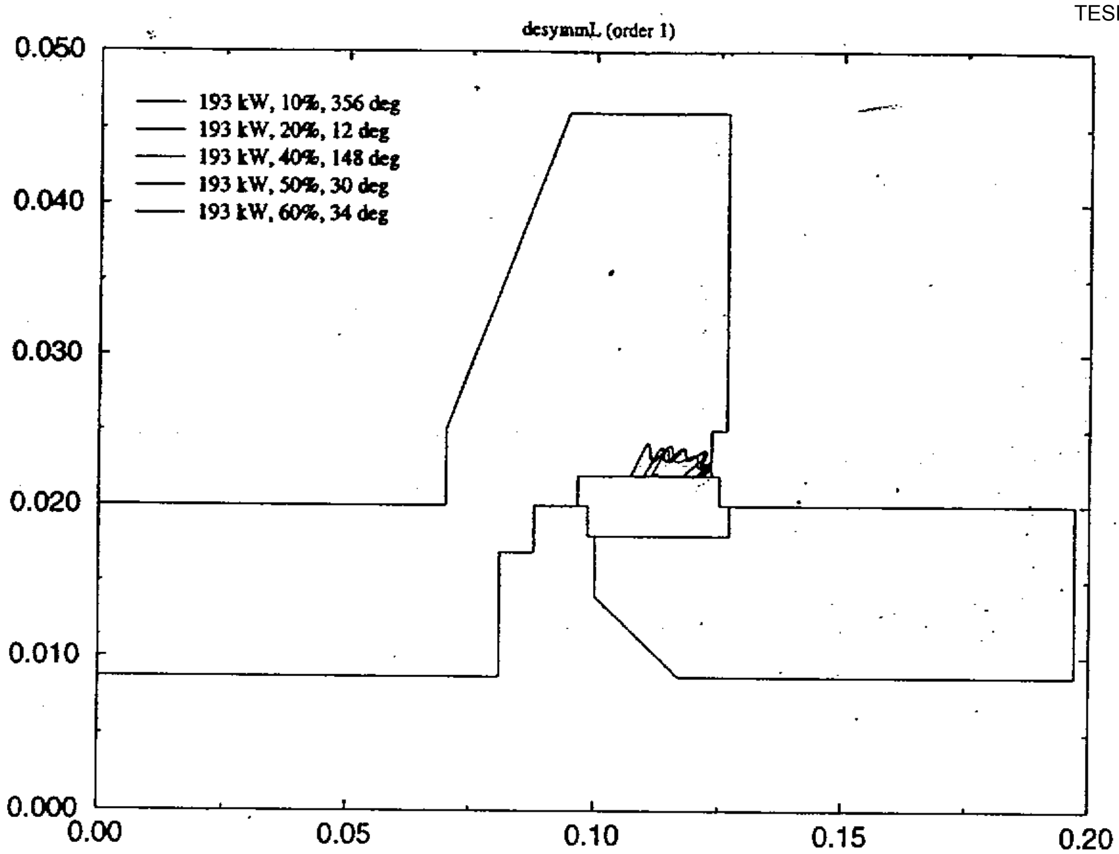

5 examples of trajectories (P = 193 kW)
starting at ≠ locations on the ceramic
converge to this 2-point multipacting between metal + ceramic

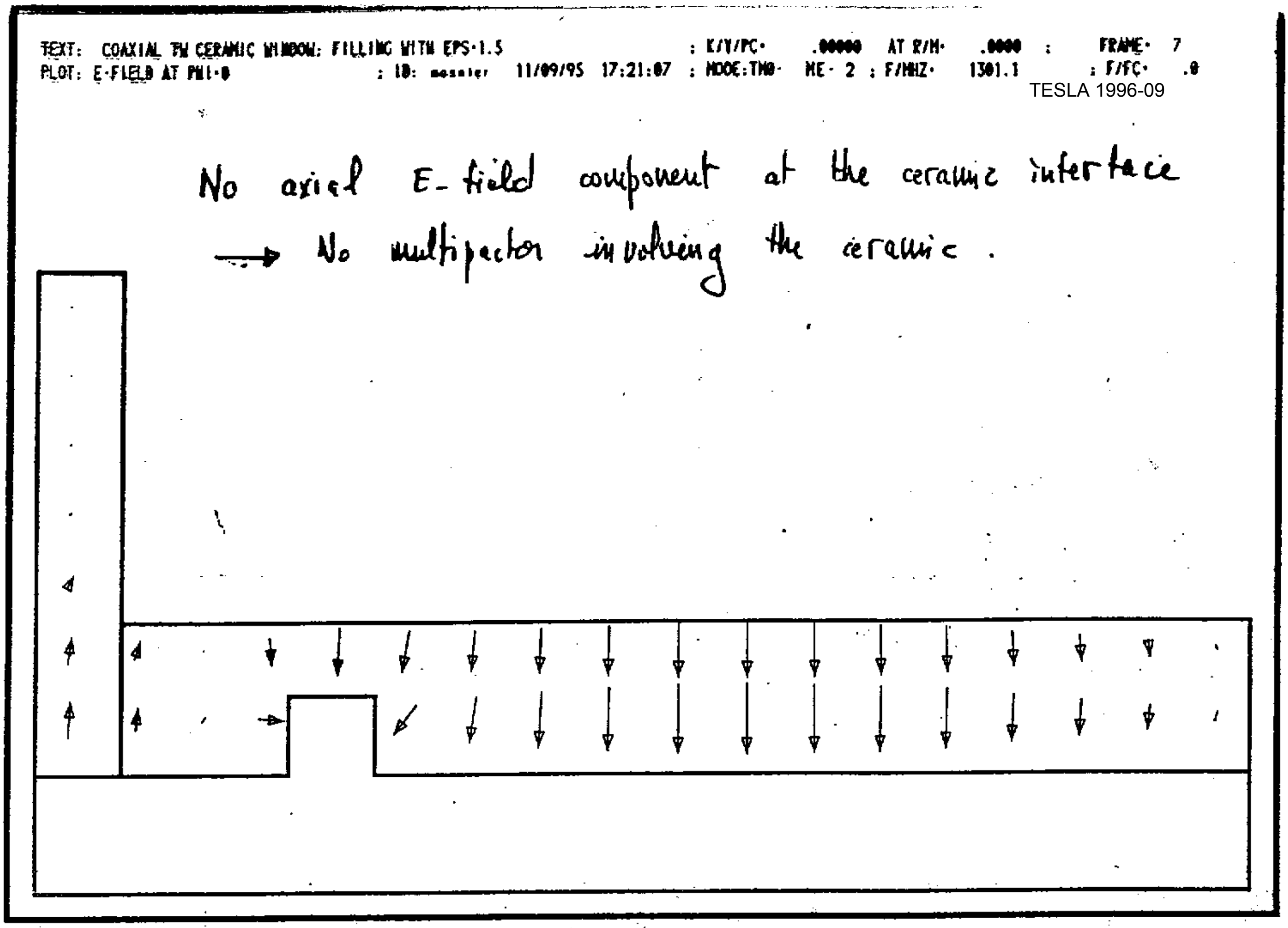

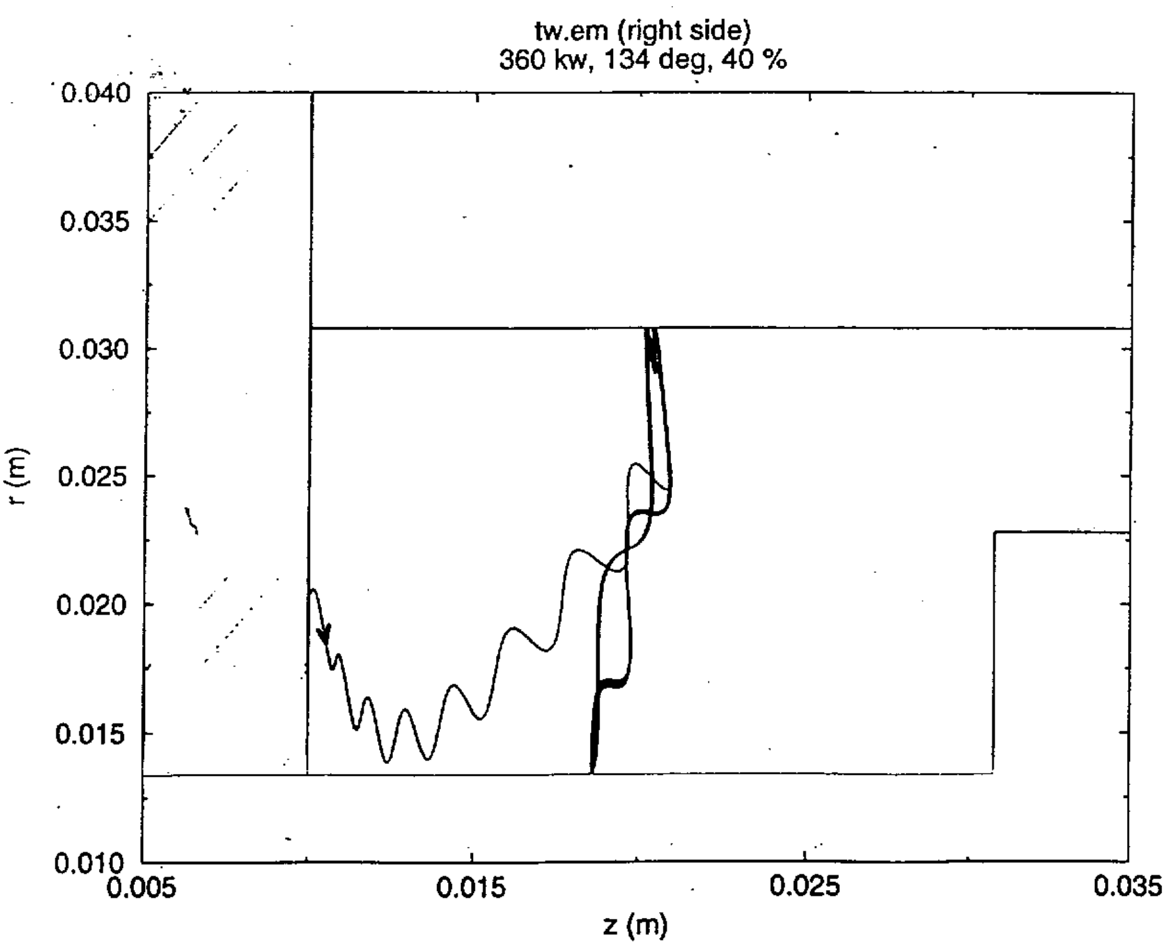

MP trajectories found at high incident power (> 350 kW) but only between inner and outer copper conductors.

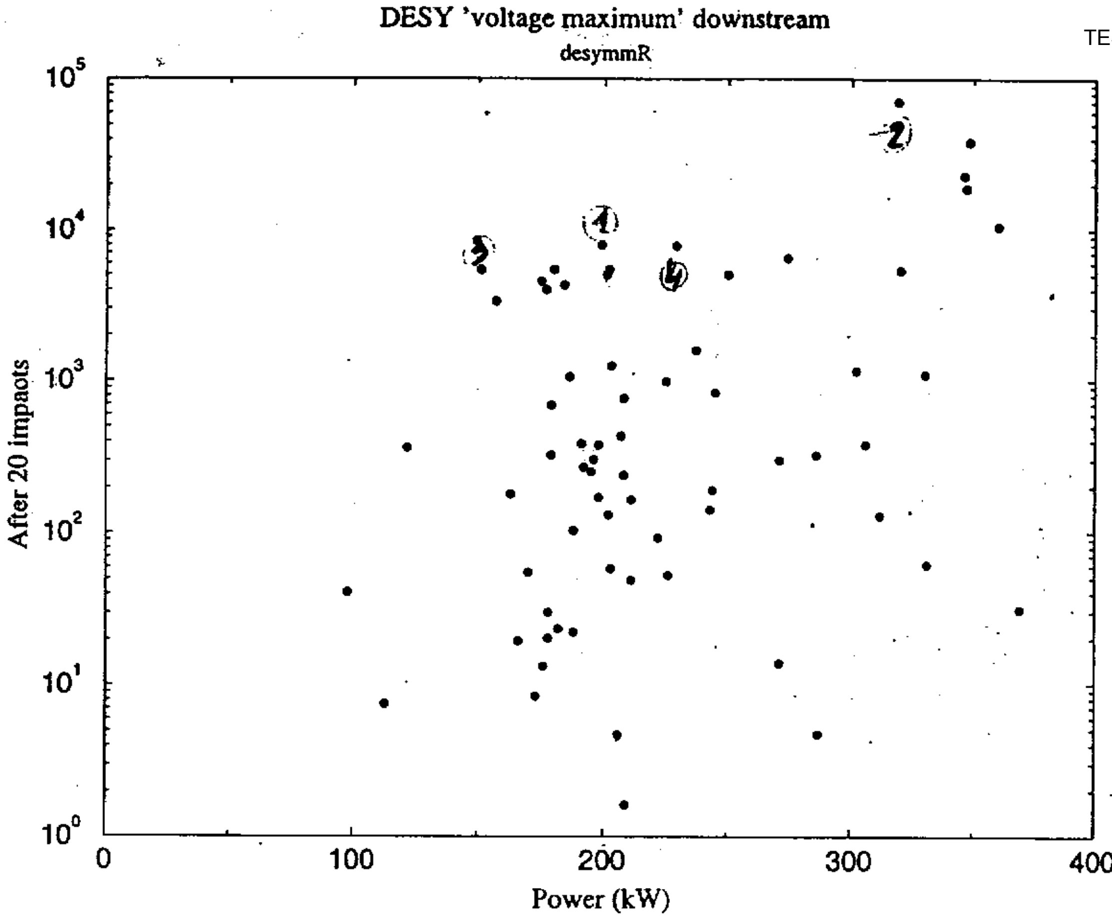
DESY 'voltage maximum' downstream
desymmR
After 20 impaots
Power (kW)
10^5
10^4
10^3
10^2
10^1
10^0
0
100
200
300
400
1
2
3
4

downstream

199 kW, 10 %, 162 deg

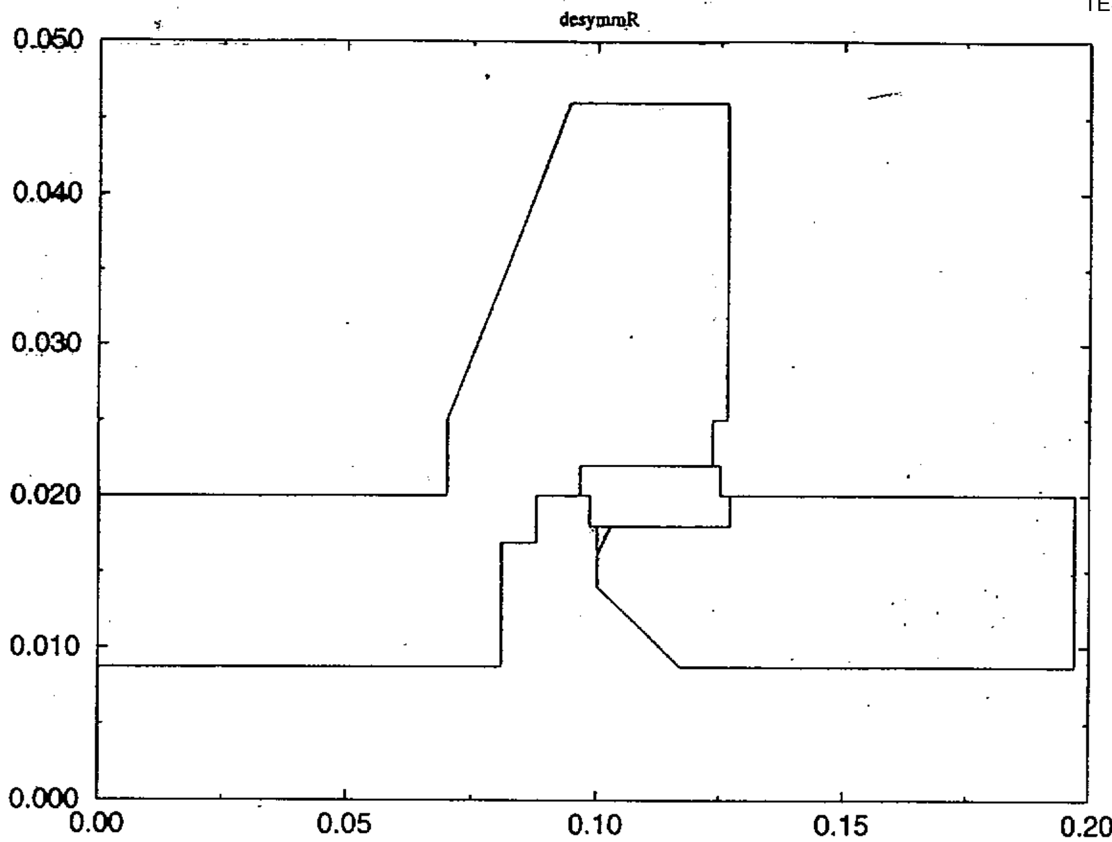

319 kW, 10 %, 138 deg

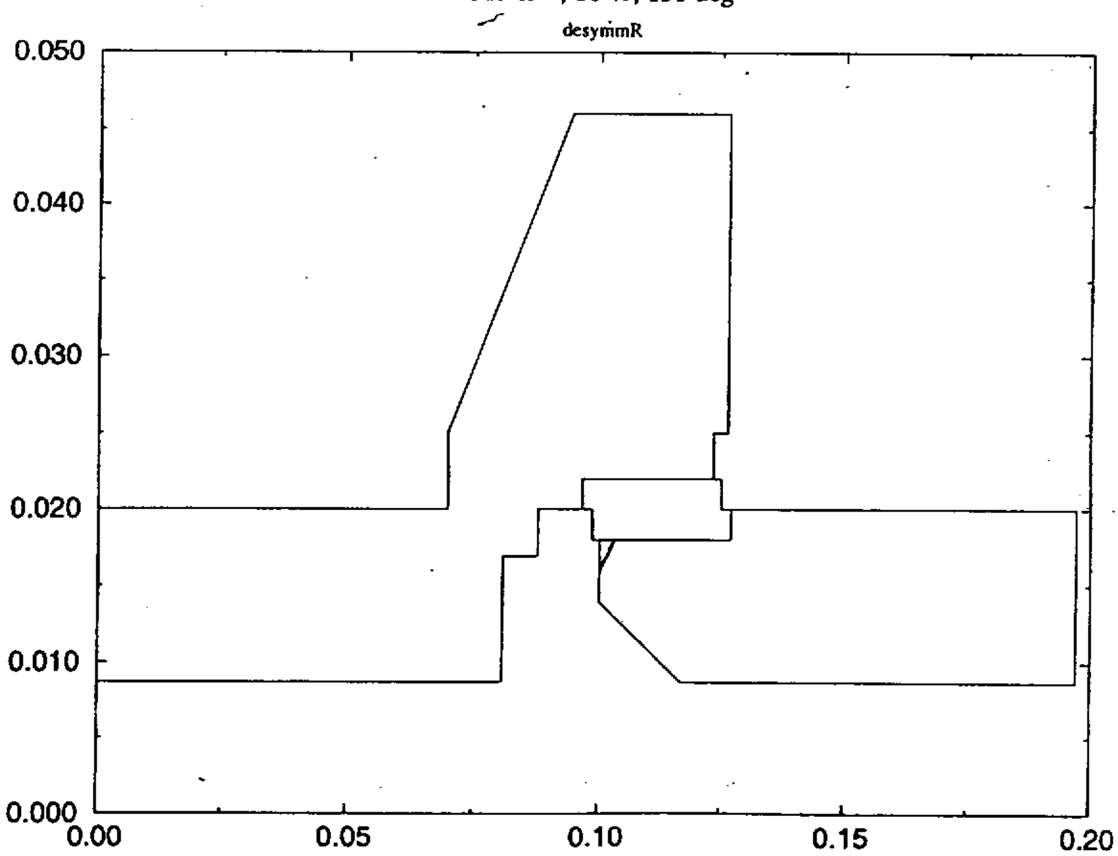

151 kW, 70 %, 244 deg

desymmR

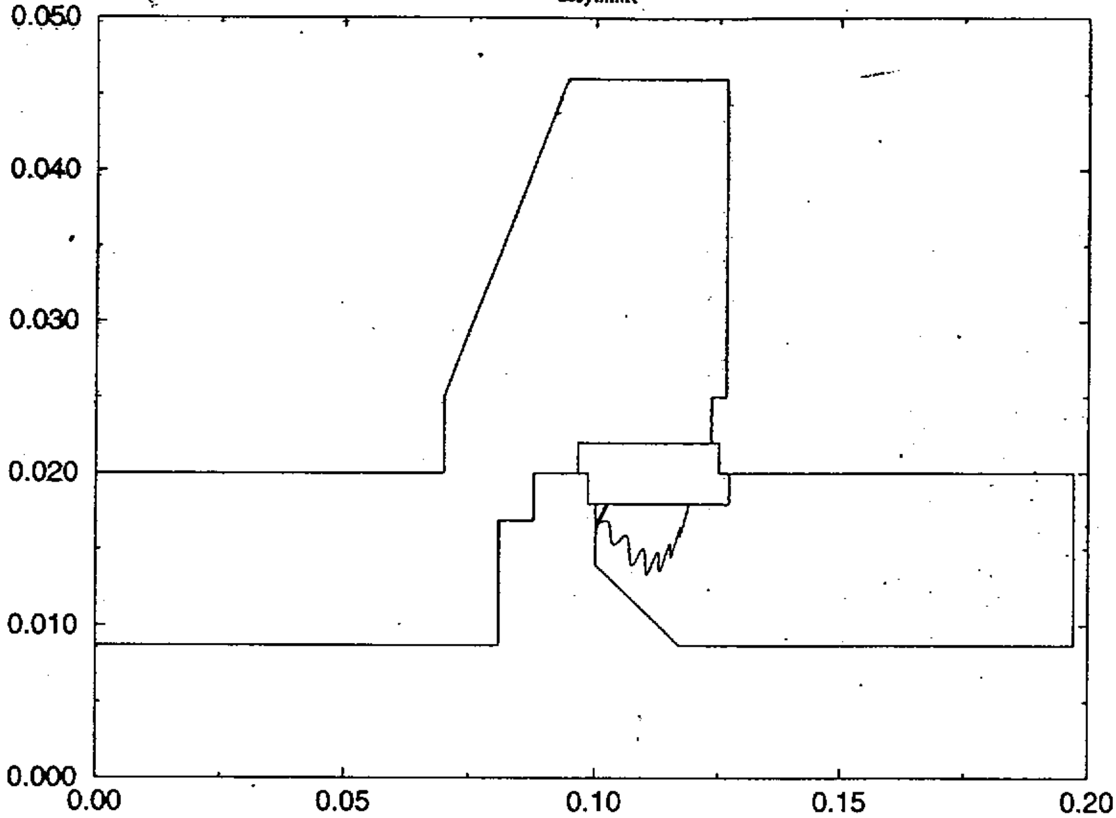

④

229 kW, 80 %, 196 deg

desymmR

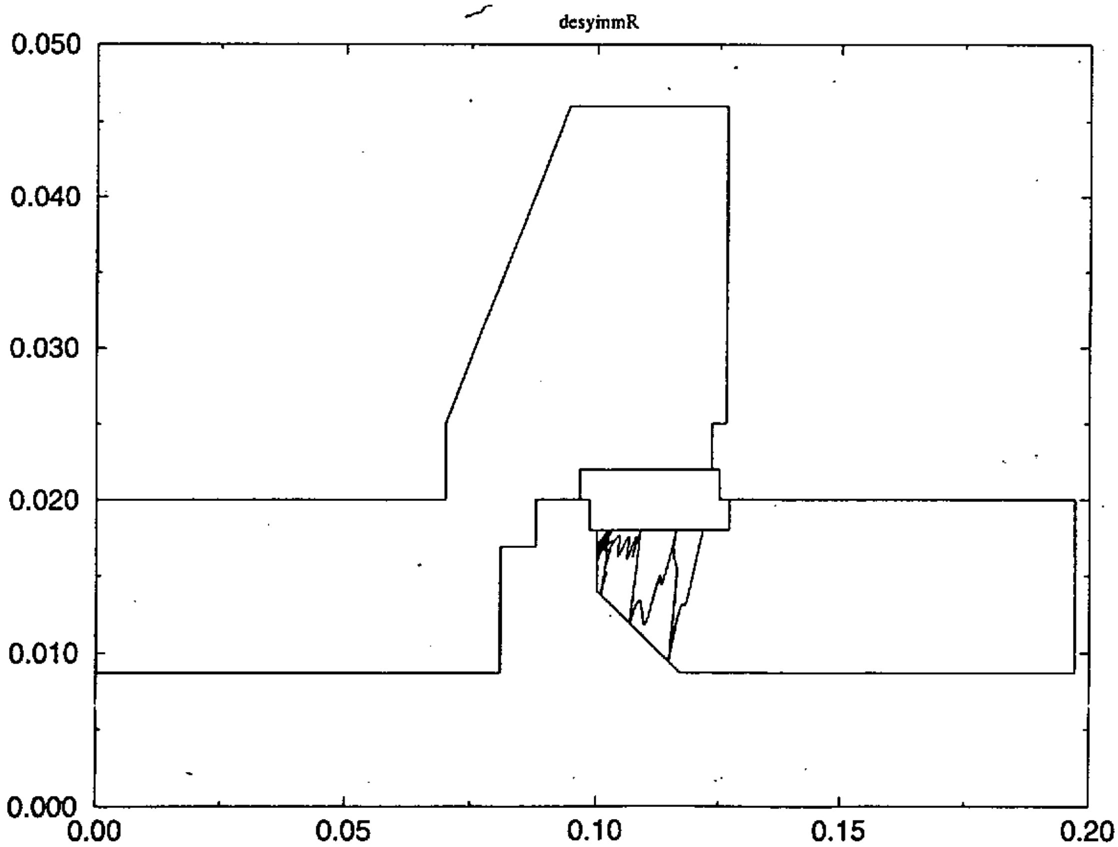

Example 3. The TW disc window

Principle: Each side of the ceramic disc is matched with a capacitive element.

→ pure TW in the ceramic

→ the field at the interface and inside the ceramic is lower than for a global matching

→ matching independent of the thickness of ceramic (can be choosen sufficiently thick)

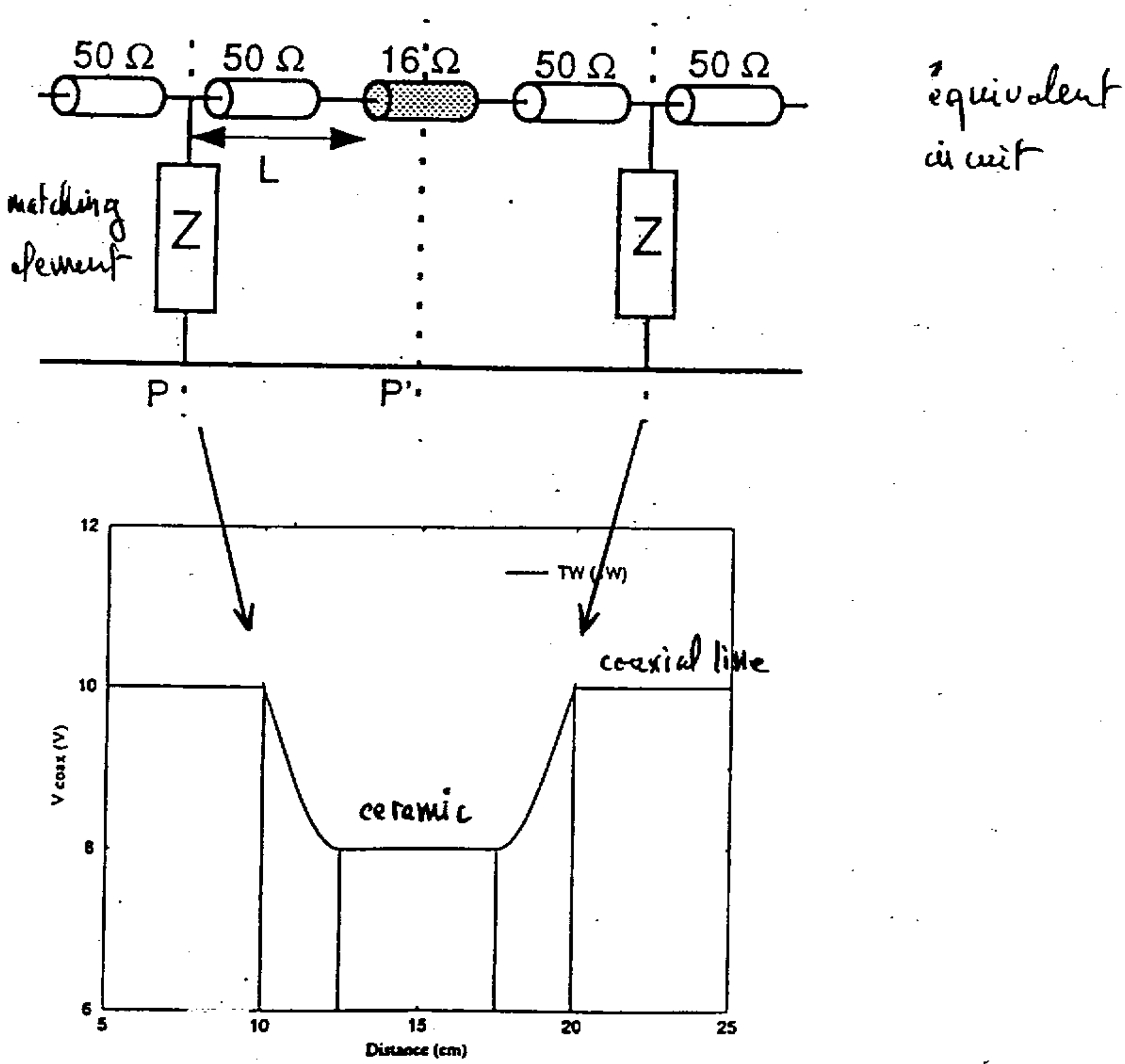

Voltage along a coaxial guide with a 5 cm thick ceramic and matching irises

HFSS simulations

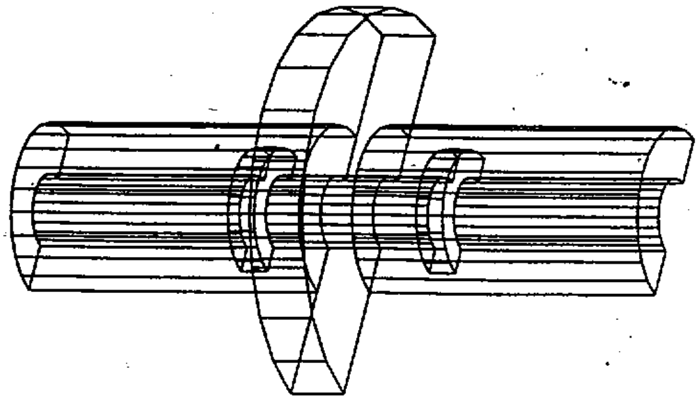

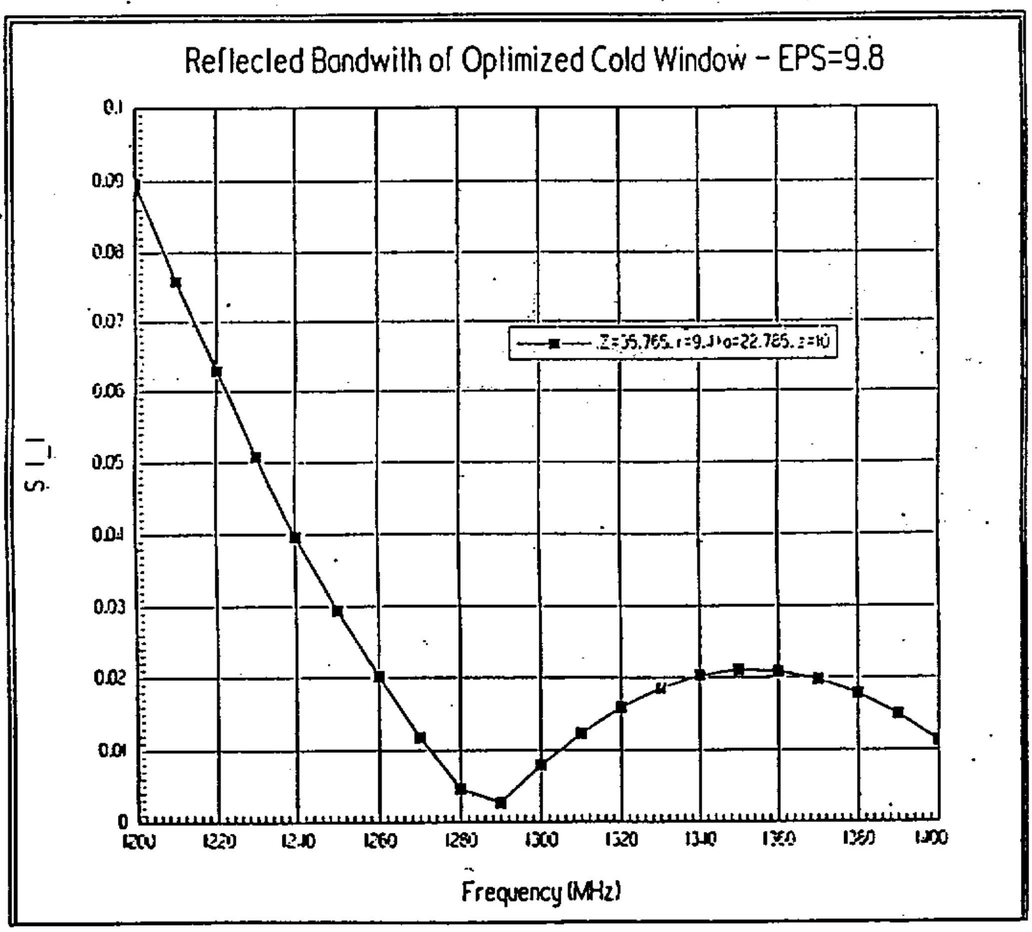

TESLA 1996-09

ANALYSIS OF TTF COUPLER PROCESSING BEHAVIOR

J. Sekutowicz
DESY, MHF-SL
Notkestraße 85, 22607 Hamburg, FRG

1. Reflection during pulse operation

2. Comparison between computed and observed multipacting levels of :
   - coaxial lines
   - tapered coaxial line
   - conical ceramic window

Measurements have been done by :
M. Champion
B. Dwersteg
A. Gössel
W-D. Möller

Computations have been done by:
H. Mäkiö
D. Proch
J. Sarvas
E. Somersalo
P. Ylä-Oijala

1. Reflection during pulse operation

We should remember that reflection of RF power will take place for:

a) **40 %** of TESLA RF on time, during the operation,

b) **100 %** of time, during conditioning of cavities and couplers.

At pulse operation, standing wave (SW) pattern in FM couplers and waveguides varies vs. time. In particular, positions of planes with maximum voltage, at which multipacting process take place, move along input line vs. time.

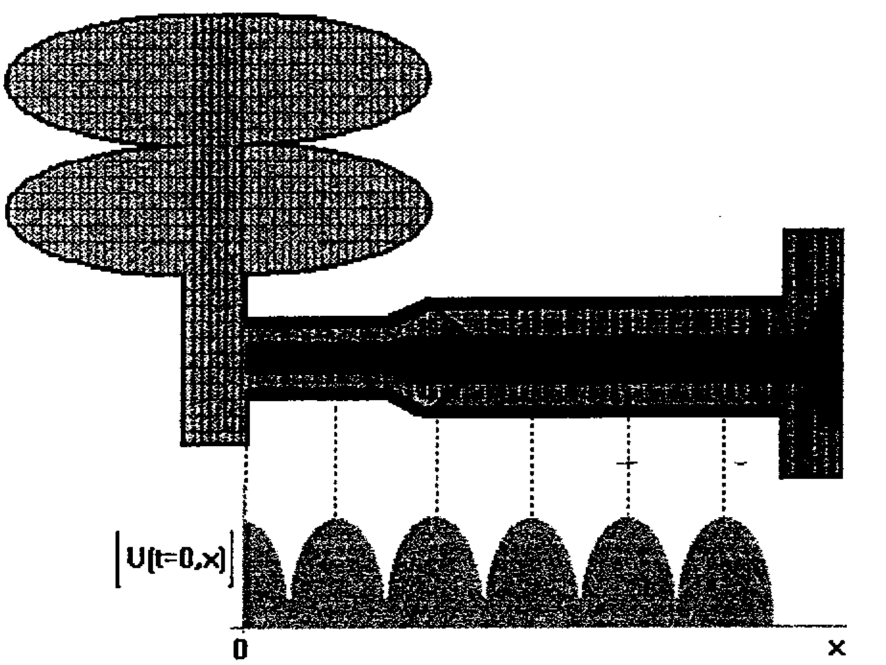

Fig.1 Voltage SW pattern at the beginning of RF pulse (t=0)

Time development of the SW pattern depends on relation between:

- resonant frequency of a cavity Fo and frequency of the source F,
- Qo and Qext .

SC cavities are usually strongly overcoupled (Qext << Qo). For the TTF accelerator :

$$Qext = 3\ 10^6 \text{ and } Qo = 5\ 10^9$$

$$\beta = 1667 \quad \text{and} \quad BW_{-3dB} = 434 \text{ Hz} .$$

Three cases shown below illustrate how SW pattern depends on the relation between Fo and F.

Case I (on resonance and small detuning < BW)

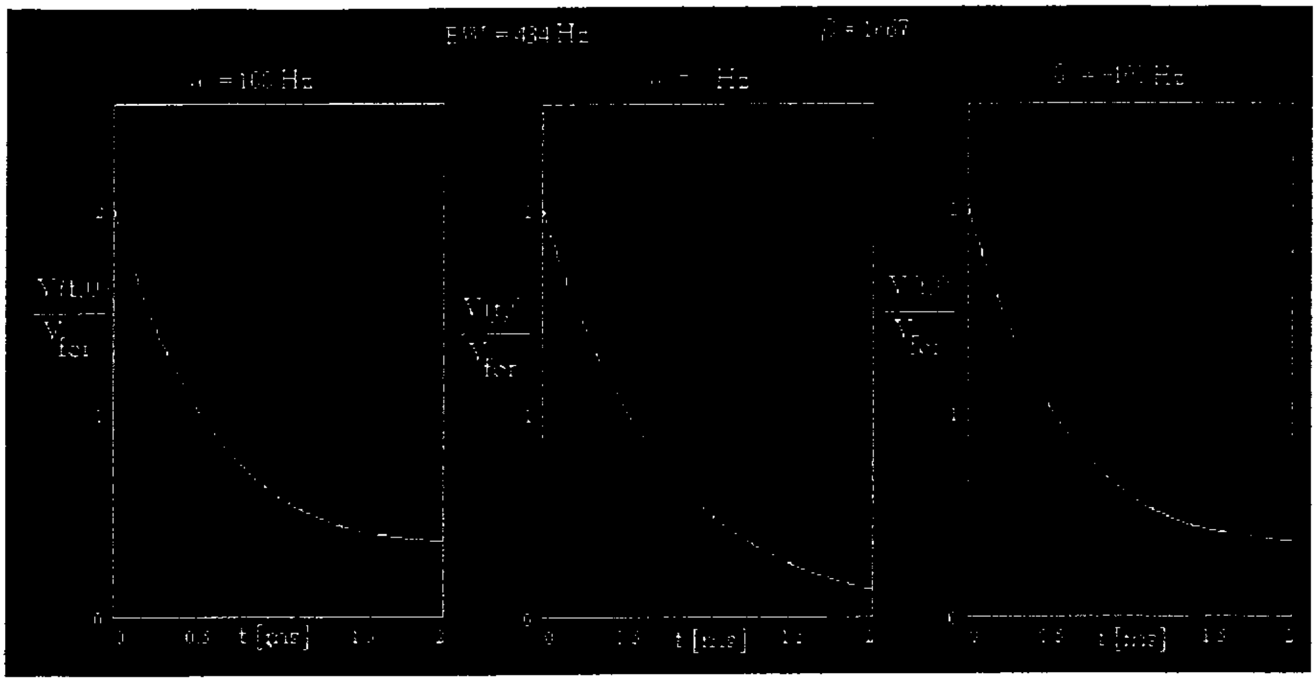

Fig.2 Voltage at the antenna tip for the detuning $\delta = \pm$ BW/4 and at resonance Fo = F

At t=0 forward and reflected wave are in phase. Total voltage is scalar sum $V=V_{back}+V_{for}= 2*V_{for}$. and standing wave pattern has maximum at the antenna tip. Then, reflection drops to 0 at t = 540 μs and <u>changes phase</u> $V=V_{back}-V_{for}$. For Fo = F voltage V is scalar difference of both amplitudes.

Case II (detuning ≥ 5*BW)

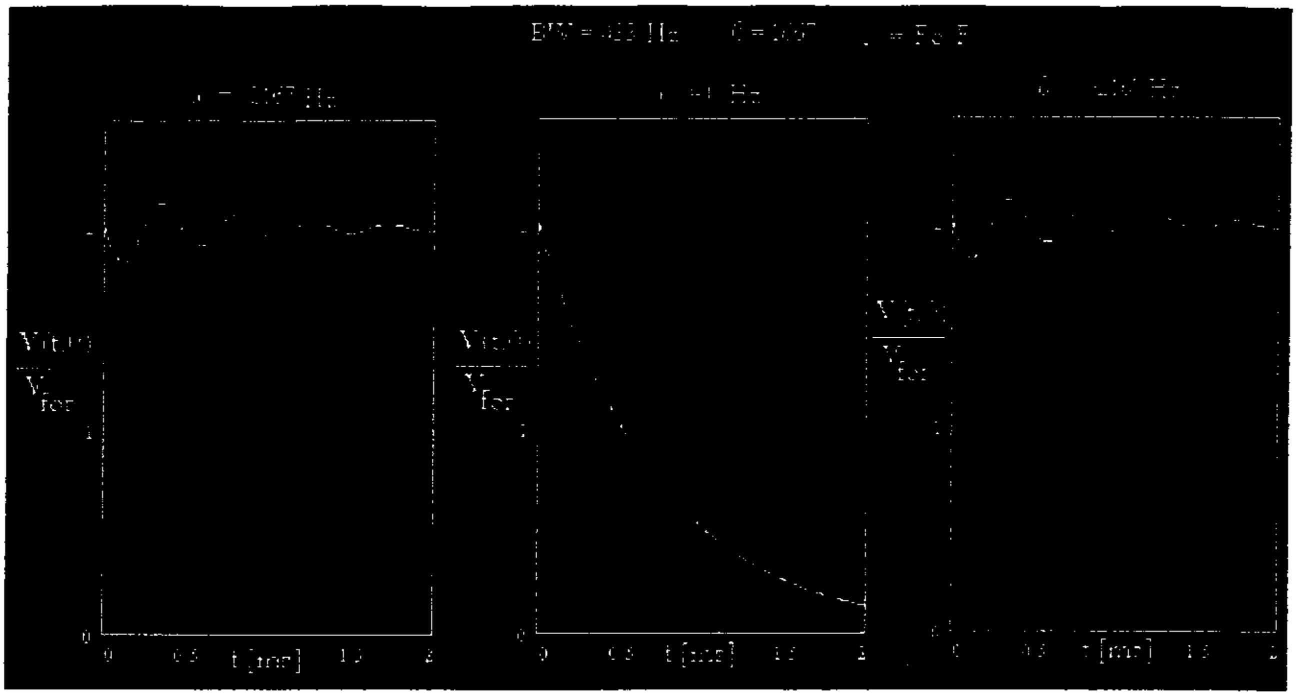

Fig.3 Voltage at the antenna tip for the detuning $\delta = \pm 5$*BW

As for case I, at t=0 V= 2* V_{for}, but after 250 μs maximum voltage at the antenna tip and all maxima in the coupler exceed that value, since

„ backward wave = reflected wave + radiated wave"

That effect we can use for better conditioning of FM couplers when attached to sc cavities.

Case III (strong detuning ≥ 30*BW)

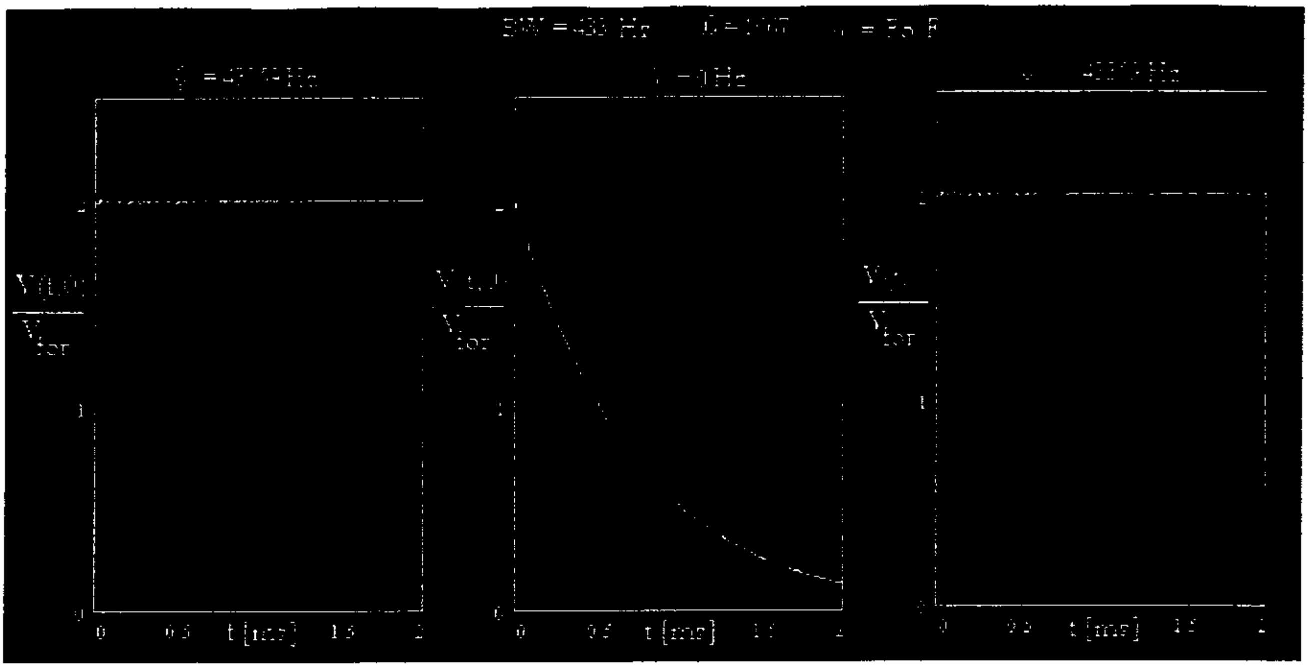

Fig.4 Voltage at the antenna tip for the detuning $\delta = \pm$ 100*BW

Here, as expected for the electric coupling and strong detuned cavity, SW pattern is constant for whole RF pulse and has maximum voltage $V = V_{refl} + V_{for} = 2^* \, V_{for}$ at the antenna tip.

2. Comparison between computed and observed multipacting levels

2.1 Standing wave pattern in FM couplers

DESY FM coupler

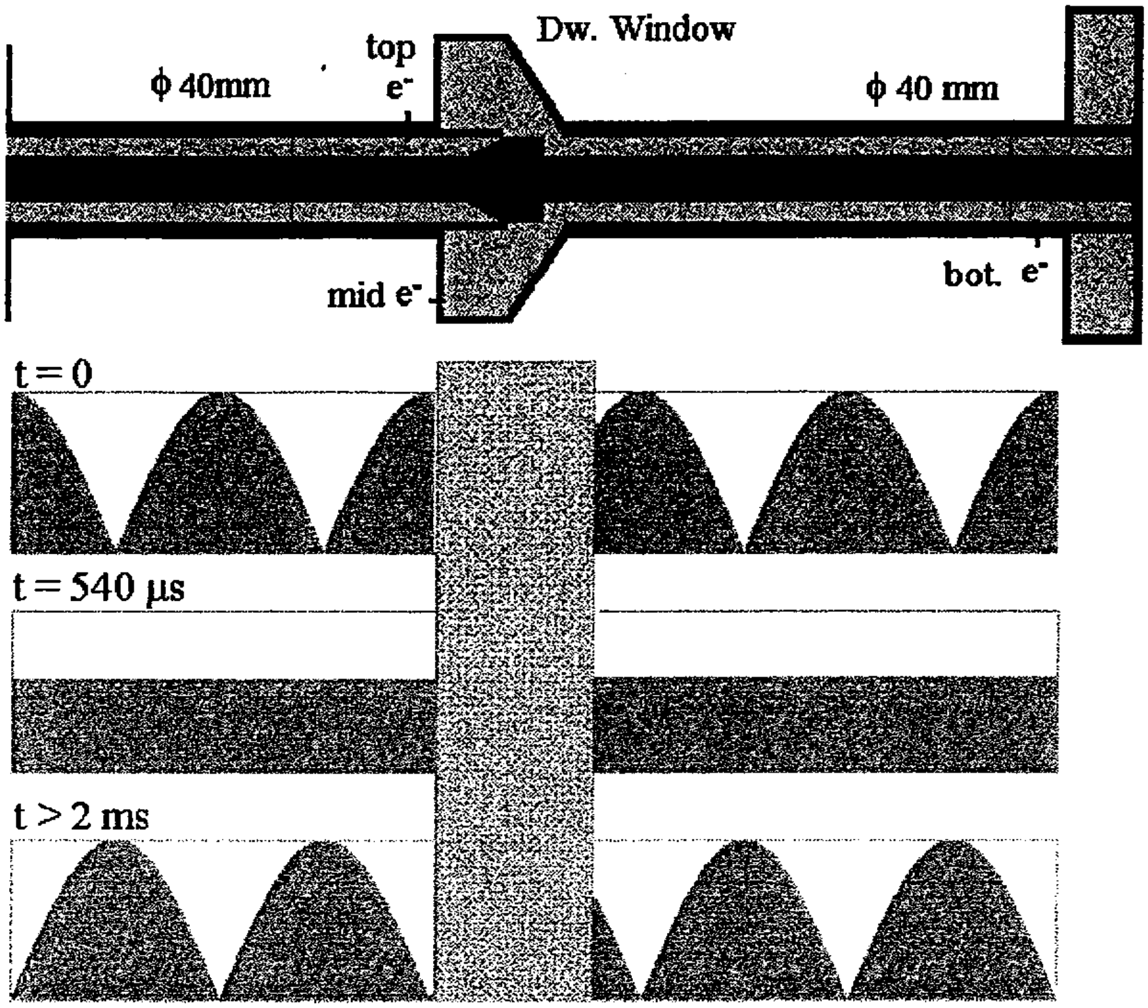

Fig.5 Voltage SW pattern along the DESY FM coupler (Fo = F)

Notice : there are 6 maximum voltage planes at the beginning of the pulse, t=0.

Summary of the computations and tests in respect to the multipacting phenomenon

- Computations showed that Dwersteg window should not have multipacting,

- Fig. 6 presents computed multipacting levels of ϕ 40 mm coaxial line for SW (upper scale) and TW (lower scale). Numbers give order of the one side multipacting process.

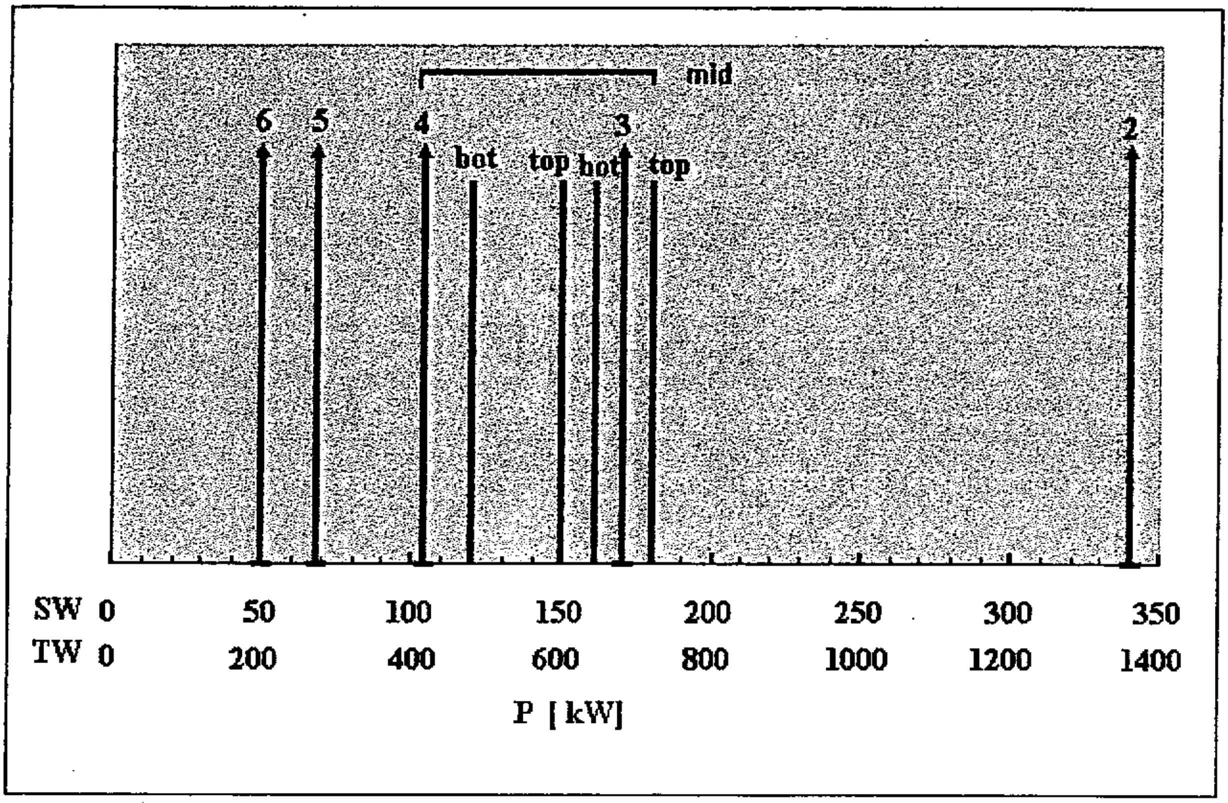

Fig. 6 Computed multipacting levels and measured electron activities in ϕ 40 mm coaxial line (DESY).

Test of 2 DESY couplers assembled to the test stand, was started two weeks ago.

In standing wave mode with pulse length of 100 μs, enhanced resonant electron activities have been observed by the top e^- detector of the coupler No. 1 and the bottom e^- detector of the coupler No. 2. (see Fig.6)

In addition, mid e^- detector of the coupler No. 2 showed continuously electron activities for the power range from 100 kW to 185 kW.

FNAL FM coupler

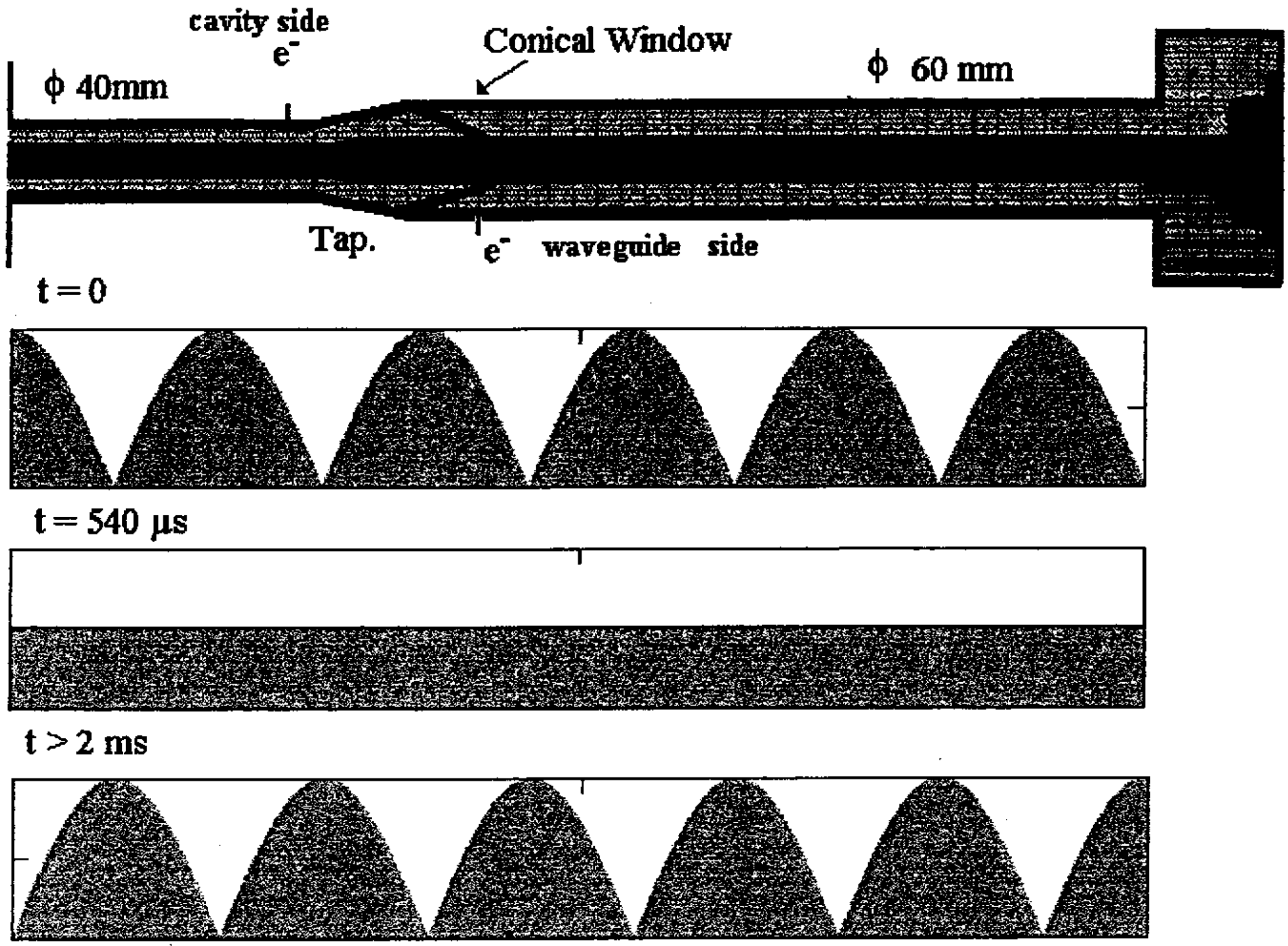

Fig.7 Voltage SW pattern along the FNAL FM coupler (Fo = F).

Notice : there are 6 maximum voltage planes at the beginning of the pulse t=0.

Summary of the computations and tests in respect to the multipacting phenomenon

Three FNAL couplers have been tested up to now. Couplers F01 and F02 have been tested on test stand. Additionally, coupler F01 and coupler F03 have been tested on cavity C19.

Multipacting levels for all components on the cavity side

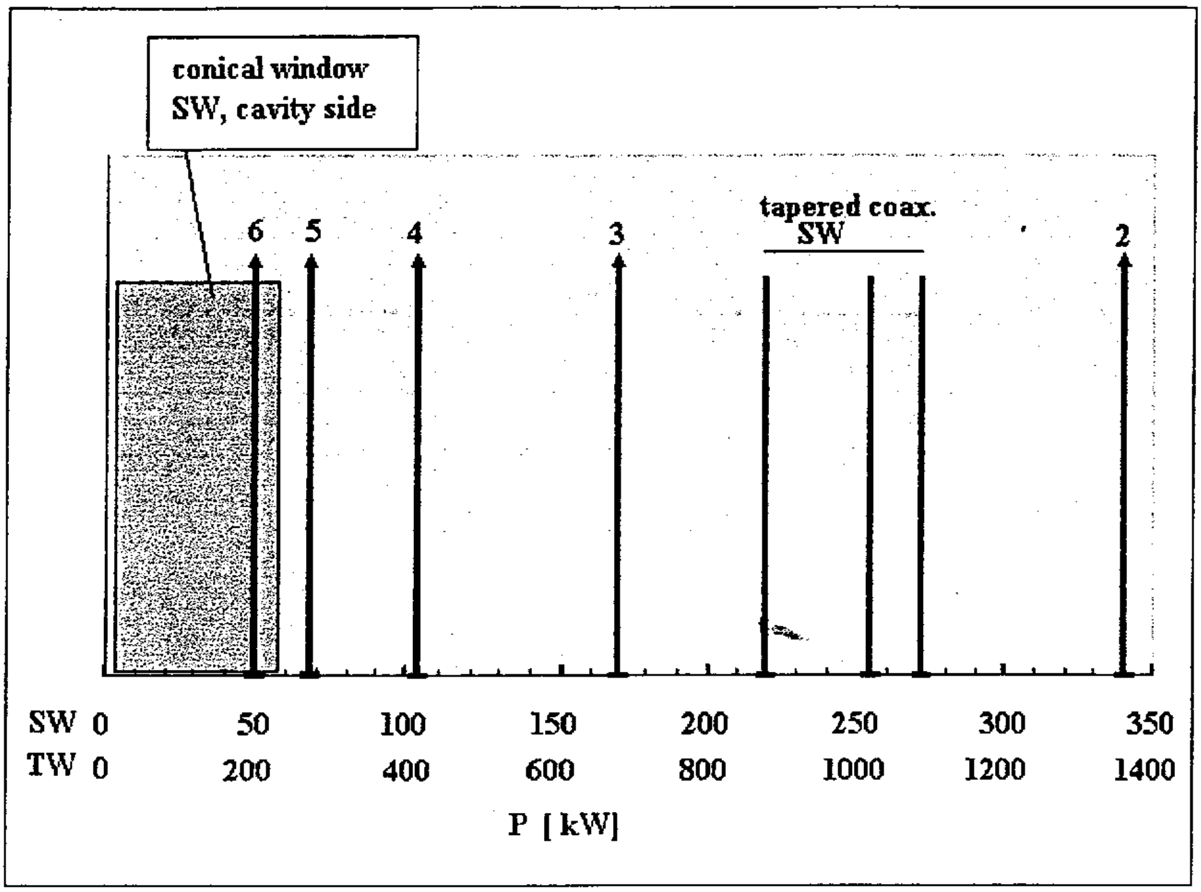

Fig.8 Computed multipacting levels in : ϕ 40 mm coaxial line, tapered coaxial line and conical window on the cavity side (FNAL)

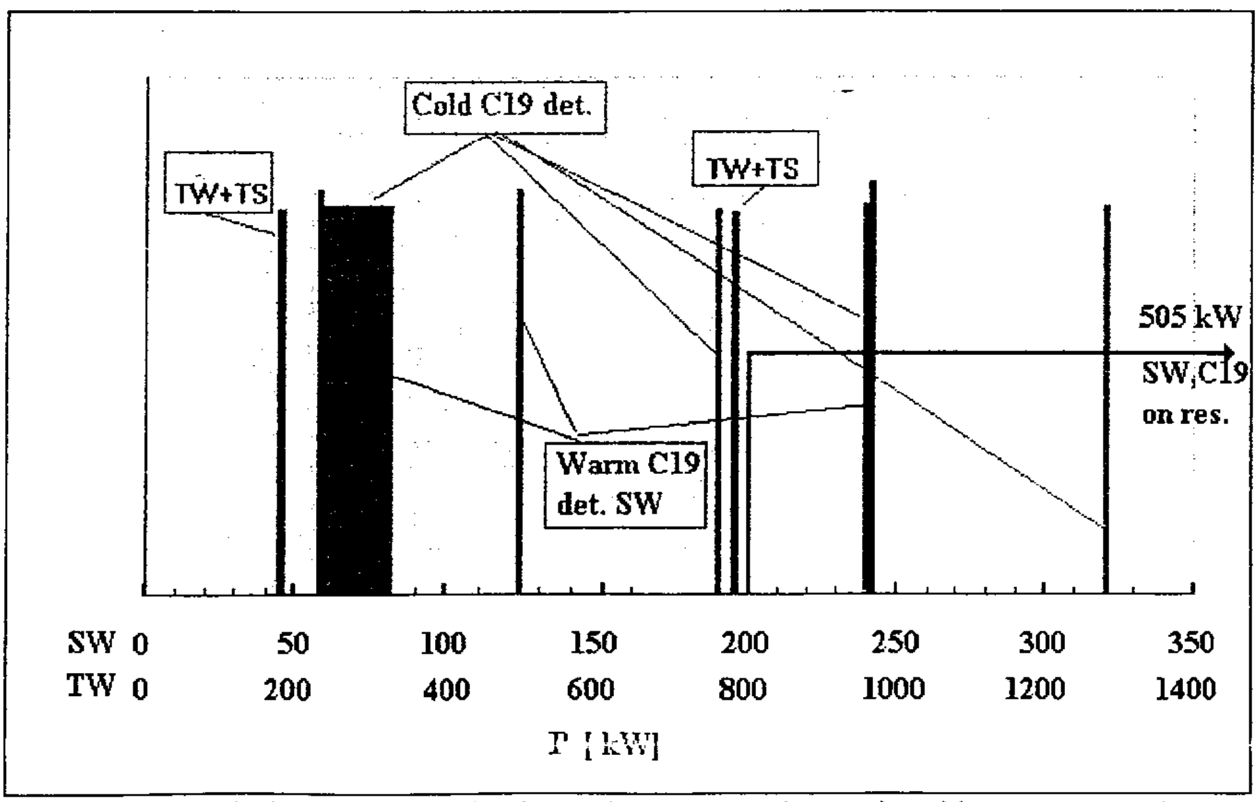

Fig. 9 Measured electron activities by e^- detector on the cavity side vs. power (FNAL).

Multipacting levels for all components on the doorknob side

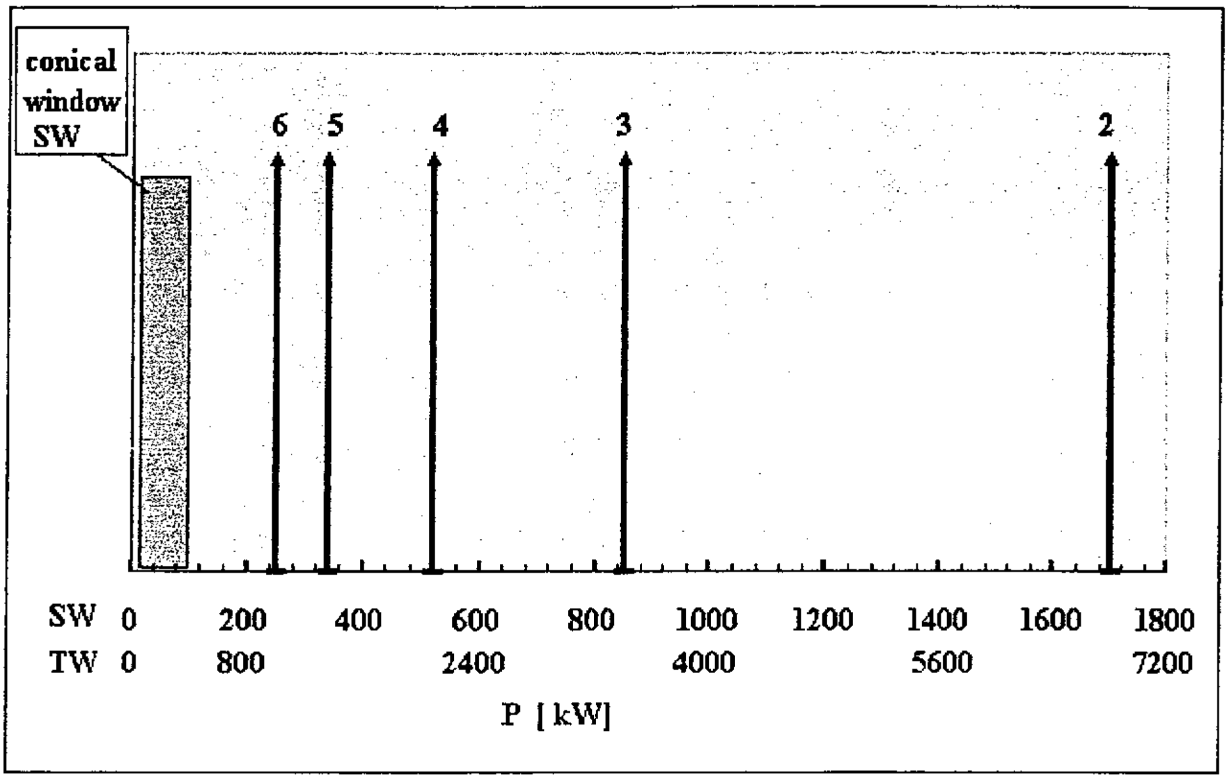

Fig. 10 Computed multipacting levels in: ϕ 60 mm coaxial line and conical window on the doorknob side (FNAL).

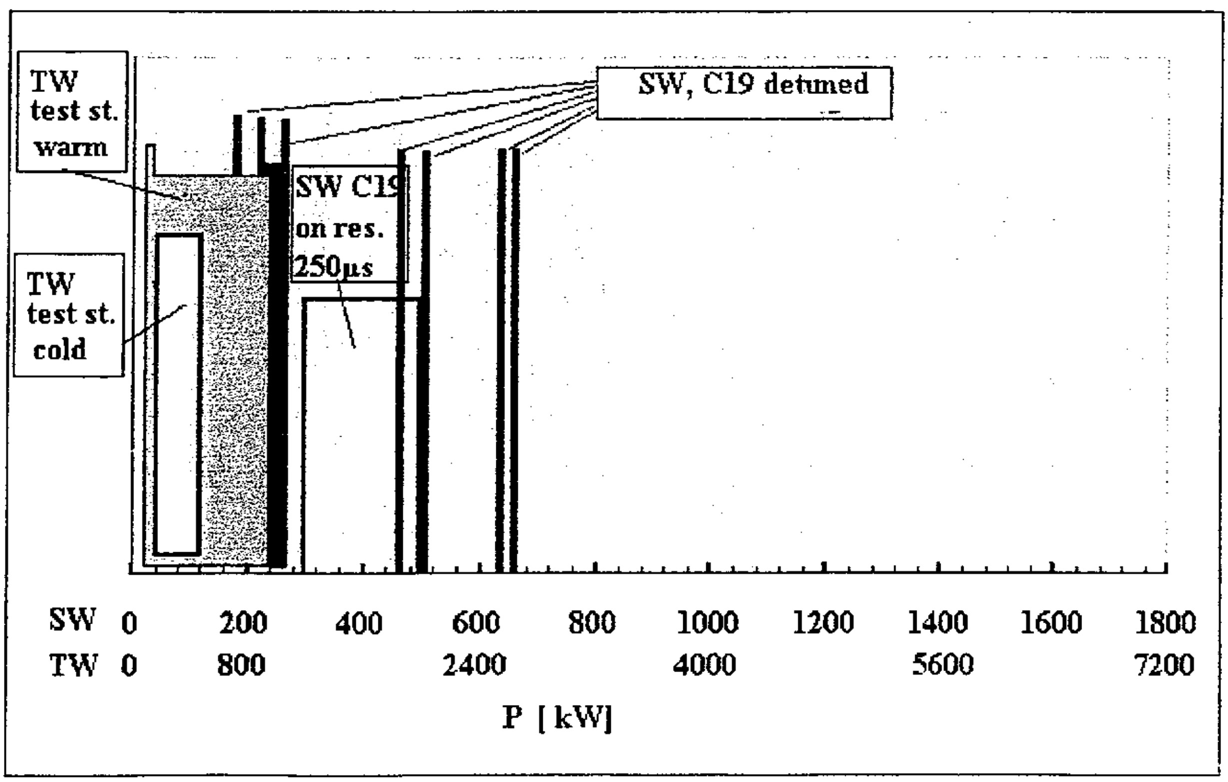

Fig. 11 Measured electron activities on the doorknob side (FNAL).

END REMARKS

DESY coupler

- test was stopped for discharging reason, so we have not enough data,
- observed electron activities agree with computed one with accuracy of

$$|Pcomp. - Pobserved| < 15\%$$

for the voltage error is of the order of 8%.

- unexpected are activities in the cold window region, but they have not resonant character.

FNAL coupler

cavity side :

- 6-th order multipacting (50 kW) is in good agreement with computation, but it showed up only during the traveling wave test on the test stand (TS) ?
- 5-th order can be seen when cavity is warm and detuned,
- 4-th order seems to be shifted from 104 kW to 120 kW (16 % error),
- 3-rd order is probably shifted from 170 kW to 190 kW,
- 2-nd order is shifted from 340 kW to 320 kW,

- tapered coaxial line shows one level of multipacting instead of three,

- conical window on that side has no multipacting for the computed region from 5 kW to 60 kW.
  There is measured band of the electron activities at cold test, near to 5-th order multipacting, but it is difficult to find out if it is caused by the conical window.
- very wide region of electron activities from 200 kW to 505 kW has been found at the cold test on resonance with pulses up to 250 μs.
  One possible explanation is cleaning of those areas which have zero voltage at the beginning of pulse.

doorknob side:

- conical window multipacting measured for traveling wave with cold test stand , agrees well with computation,

-two wide regions of electron activities have been measured for TW with warm test stand and SW with cold cavity on resonance ????

- in regions of 6-th and 4-th order multipacting some electron current was measured, but rest of computed levels could not be found.

Processing:

- TW processing cleans whole surface in the coupler but can be performed only on the test stand (coupler will be expose to air for final assembling),

- SW processing with detuned cavity does not clean whole surface of the coupler, since SW pattern stays constant during the pulse.

- processing on resonance with pulse time of the order of 500 μs cleans mainly maximum voltage regions. Notches are conditioned with half of that voltage for a short time at the end of the pulse.

- SW processing with sc cavity on resonance and pulse longer then 1.3 ms gives processing of whole surface with the voltage 40% higher that the voltage of the incident wave. But cavity performance may limit this power.

(we should discuss it to find optimum processing of the couplers)

TESLA 1996-09

Experience with Input Couplers at CERN

E. Haebel
H.P. Kindermann
M. Stirbel
V. Vechtcherevich

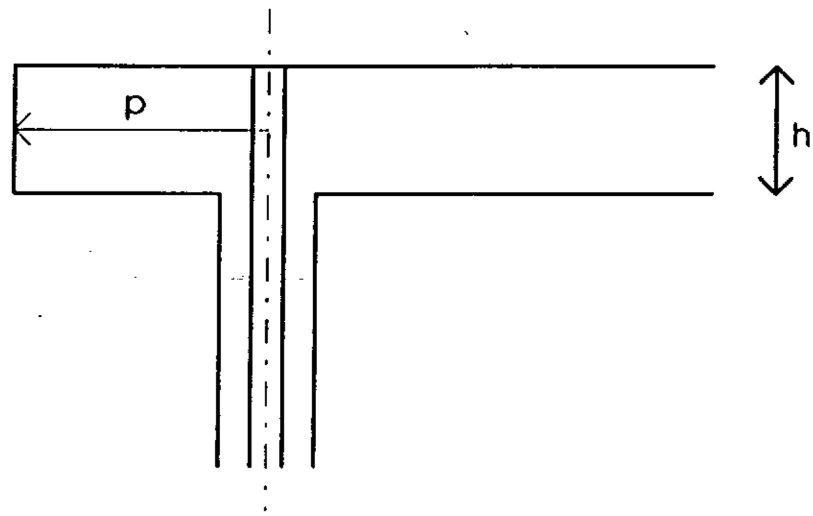
p
h

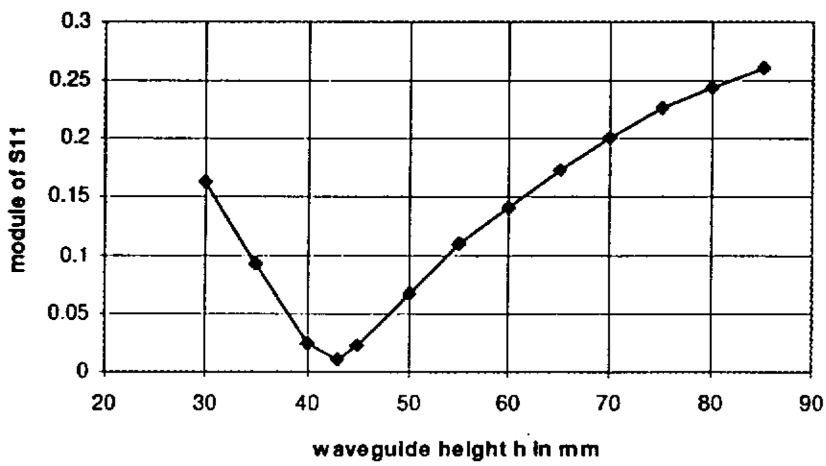
module of S11
0.3
0.25
0.2
0.15
0.1
0.05
0
20
30
40
50
60
70
80
90
waveguide height h in mm

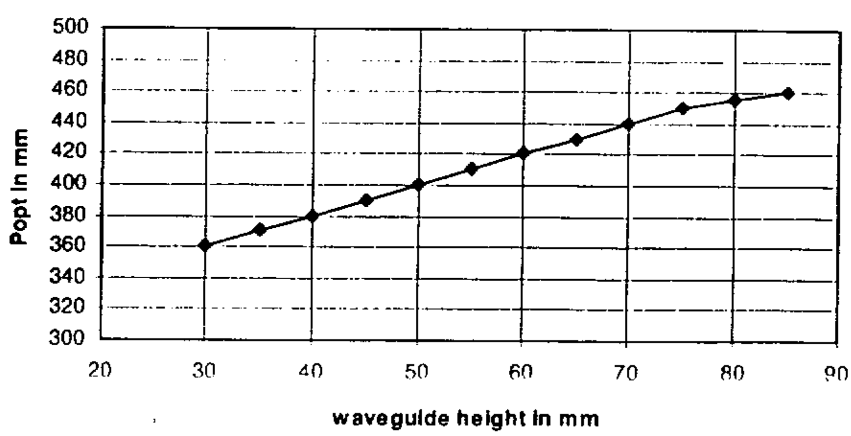
Popt in mm
500
480
460
440
420
400
380
360
340
320
300
20
30
40
50
60
70
80
90
waveguide height in mm

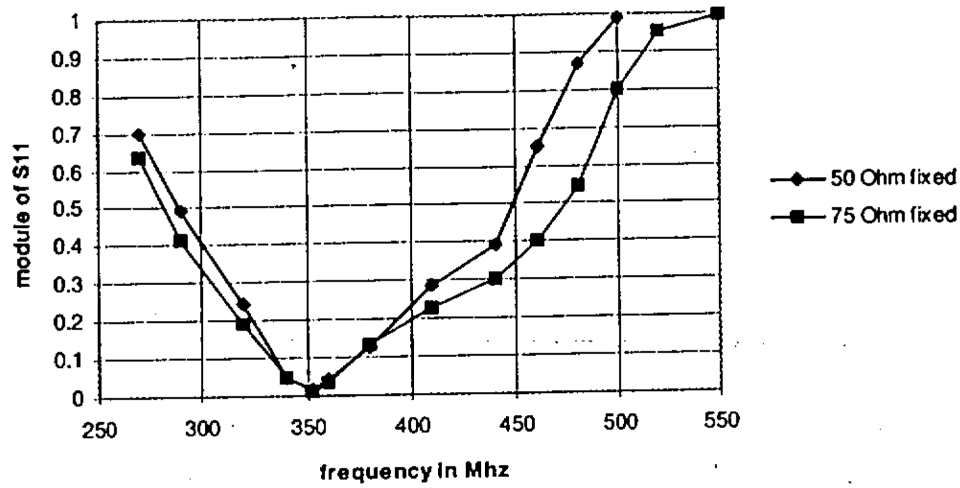

Frequency dependence of $|S_{11}|$ for 50 Ω and 75 Ω fixed couplers.

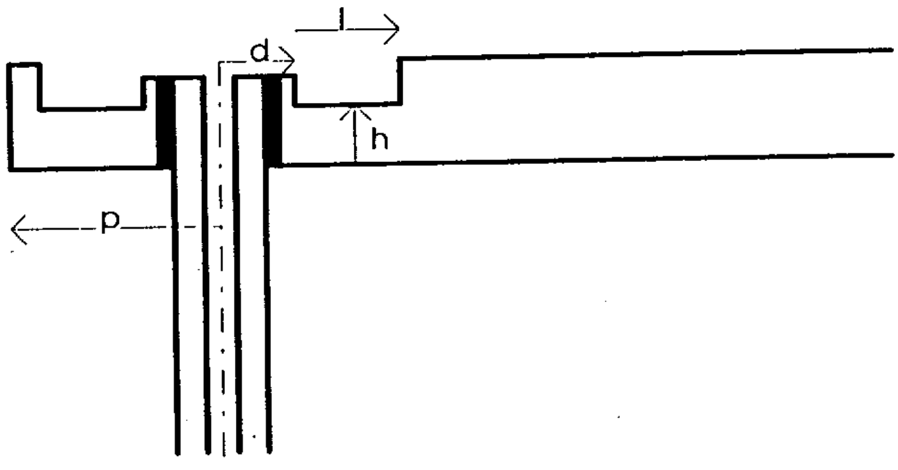

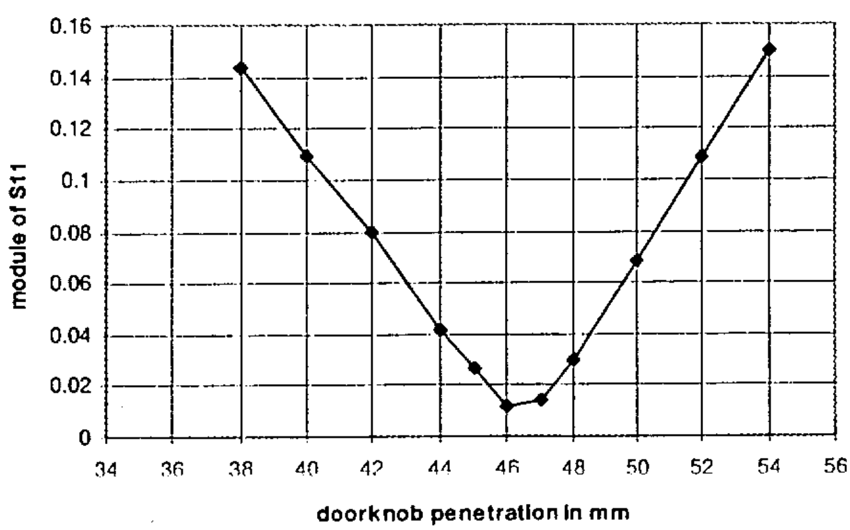

Influence of doorknob penetration for 75 Ω fixed coupler.

Scatter of coupling Qex

Data from 24 vertically tested cavities (W. Weingarten)

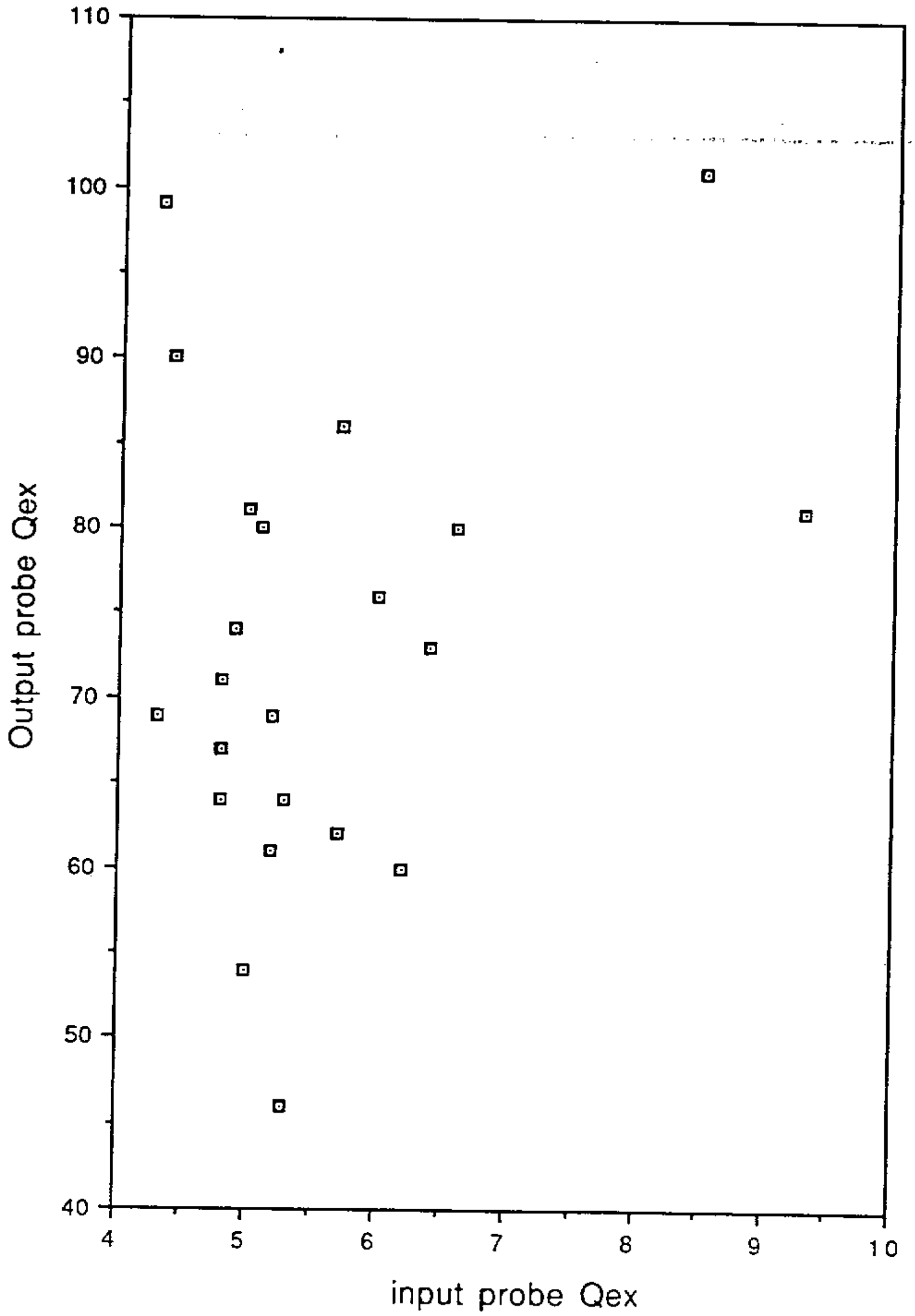

Itac

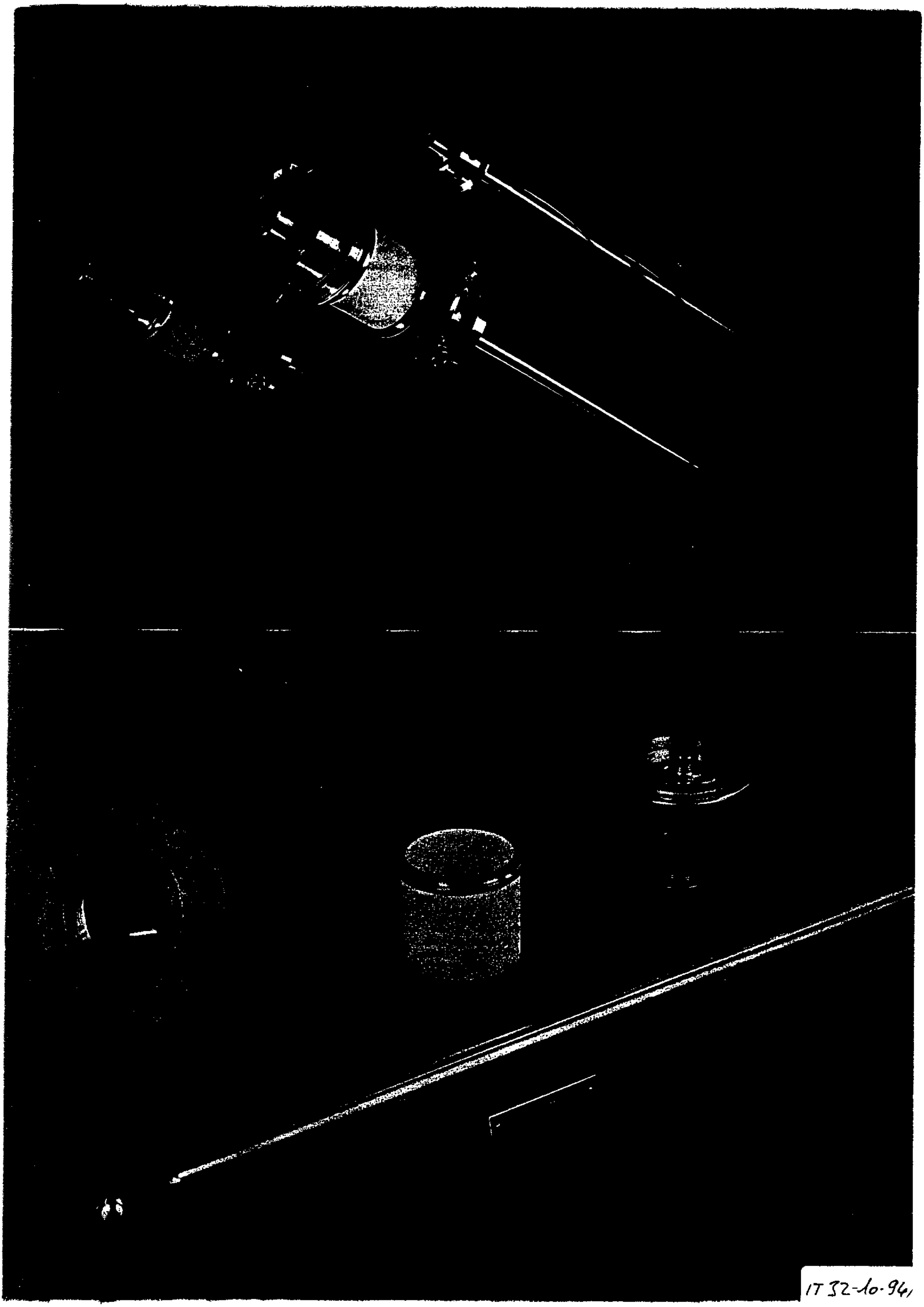

IT 32-10-94

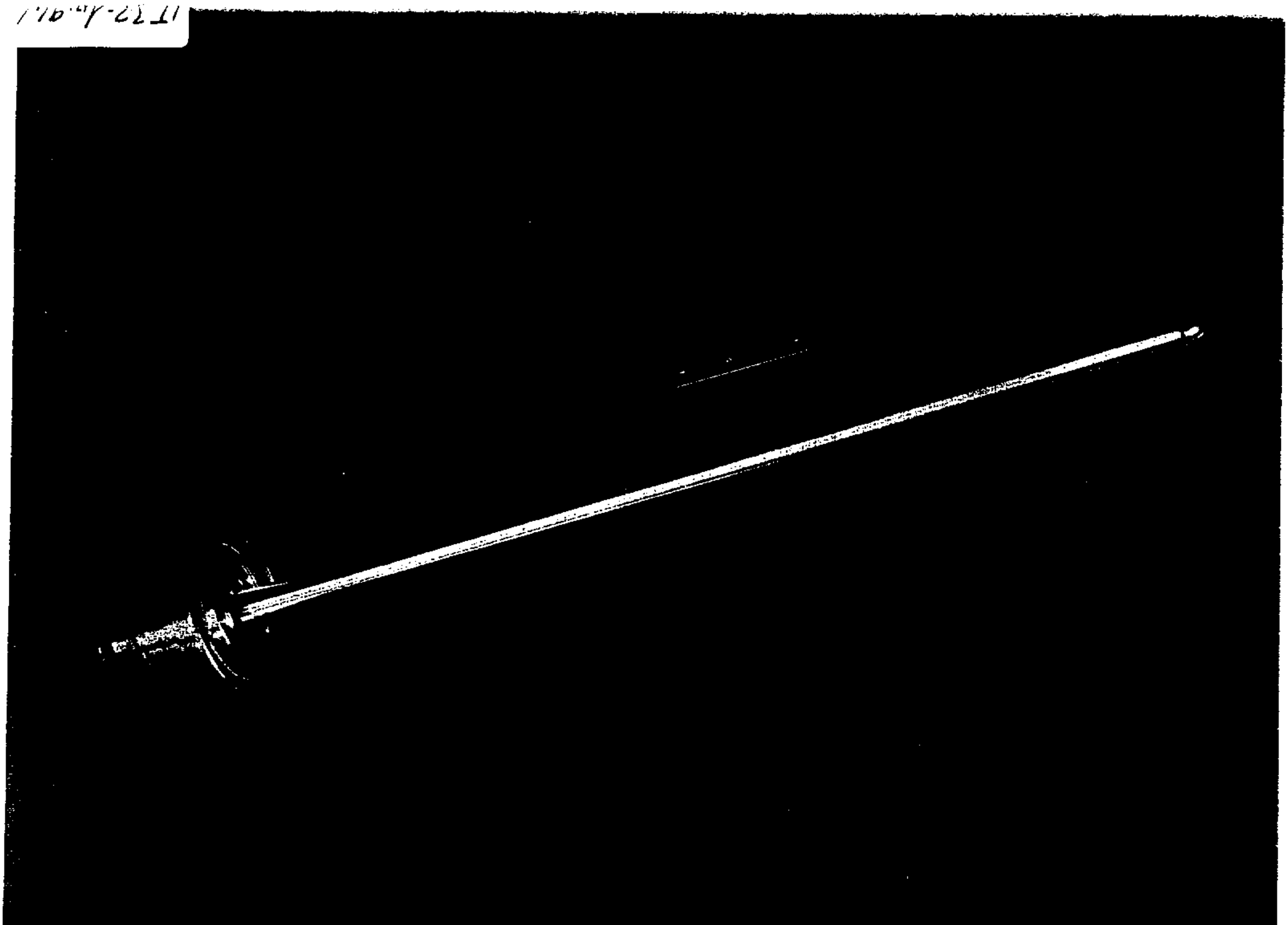

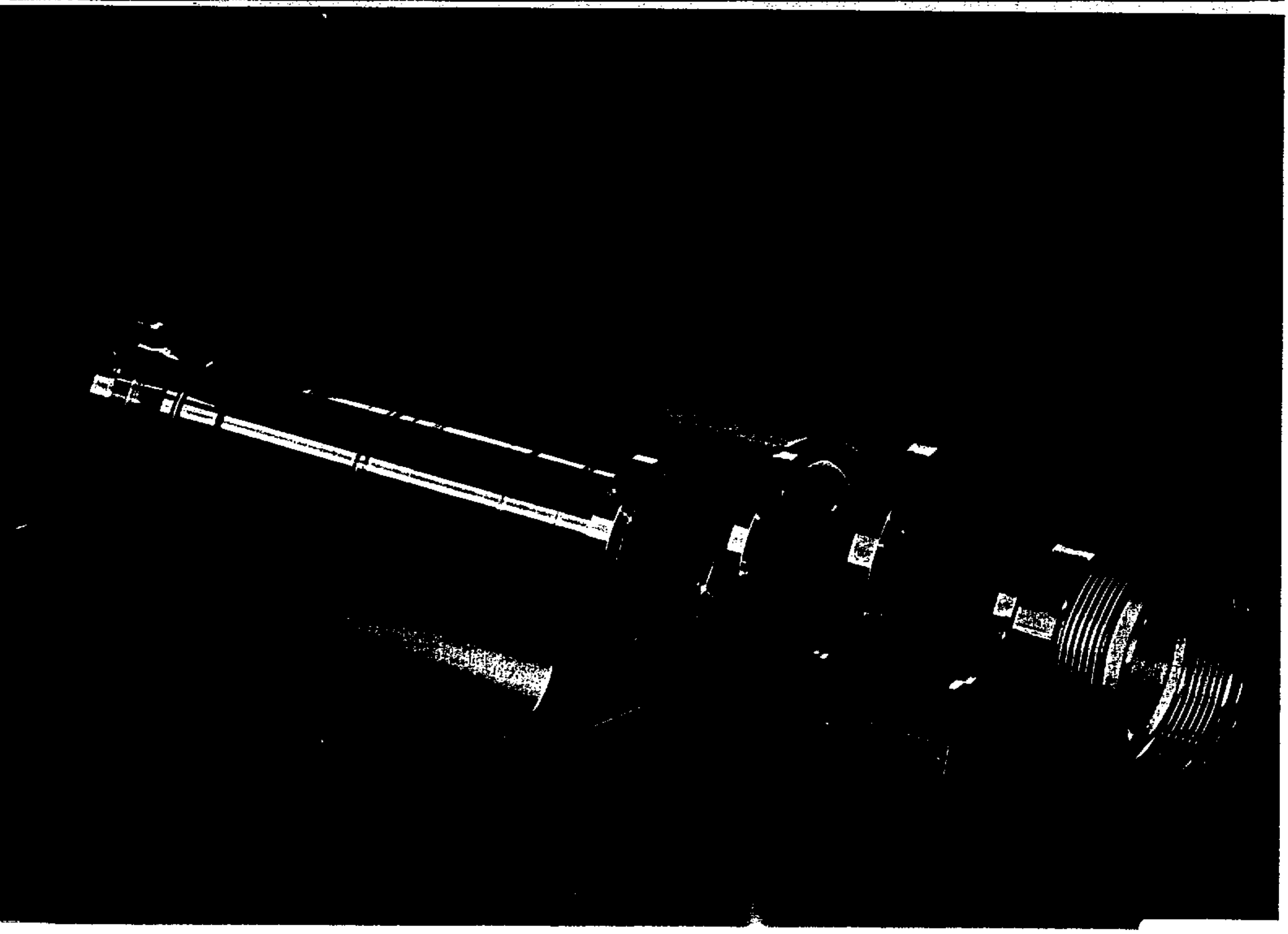


10 CM
Ac 27-5-96/

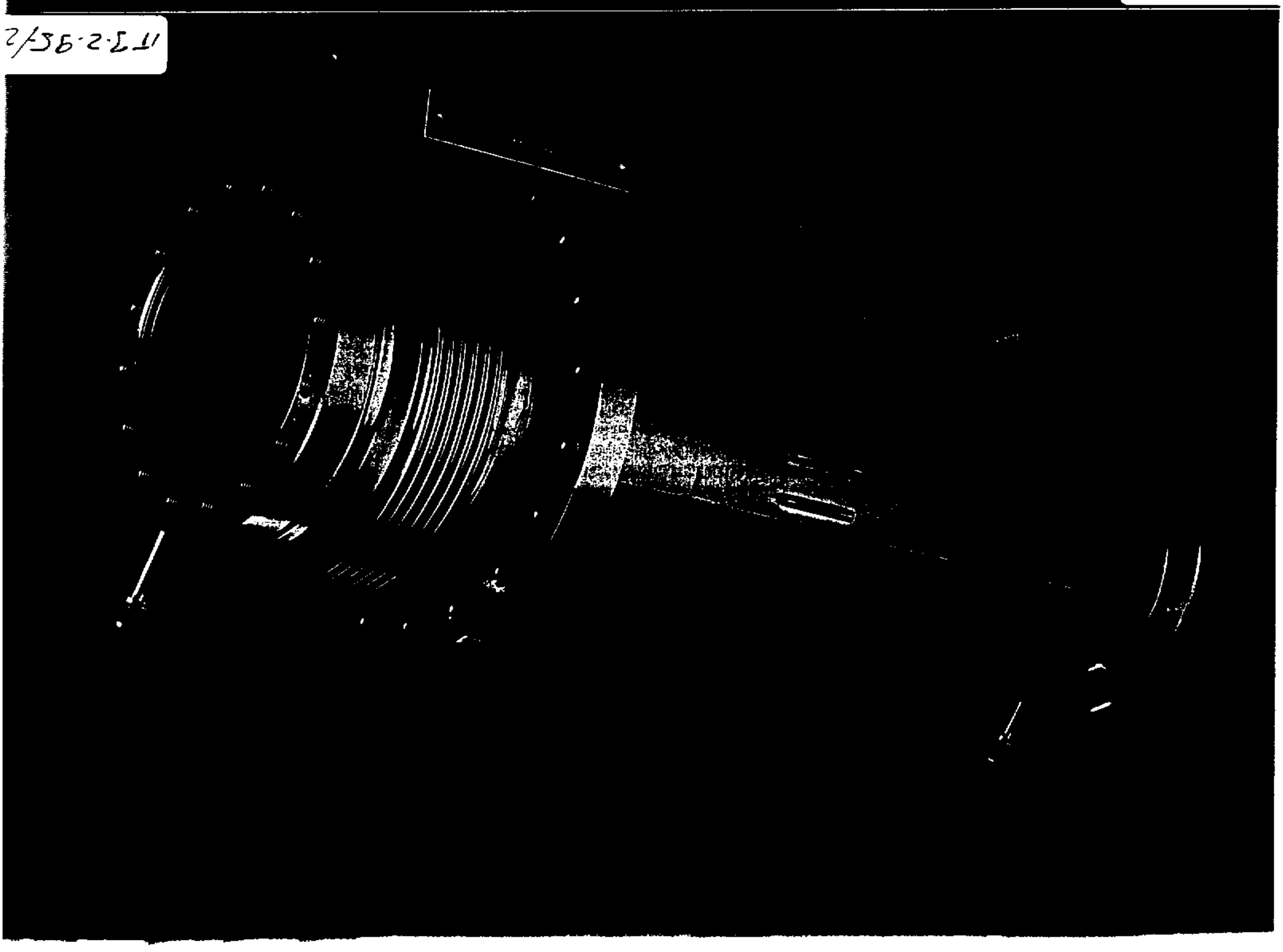

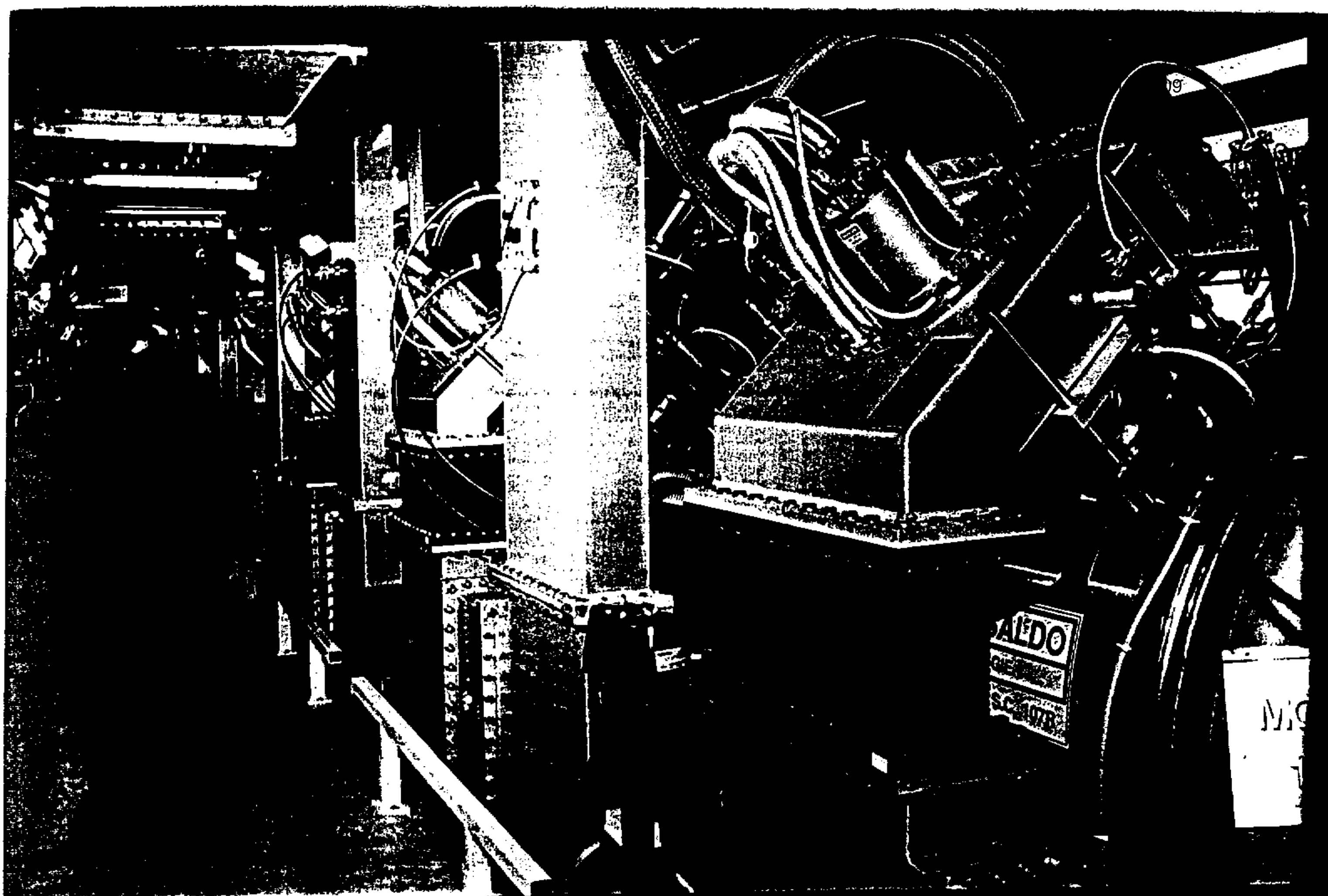

Ac 27-5-96

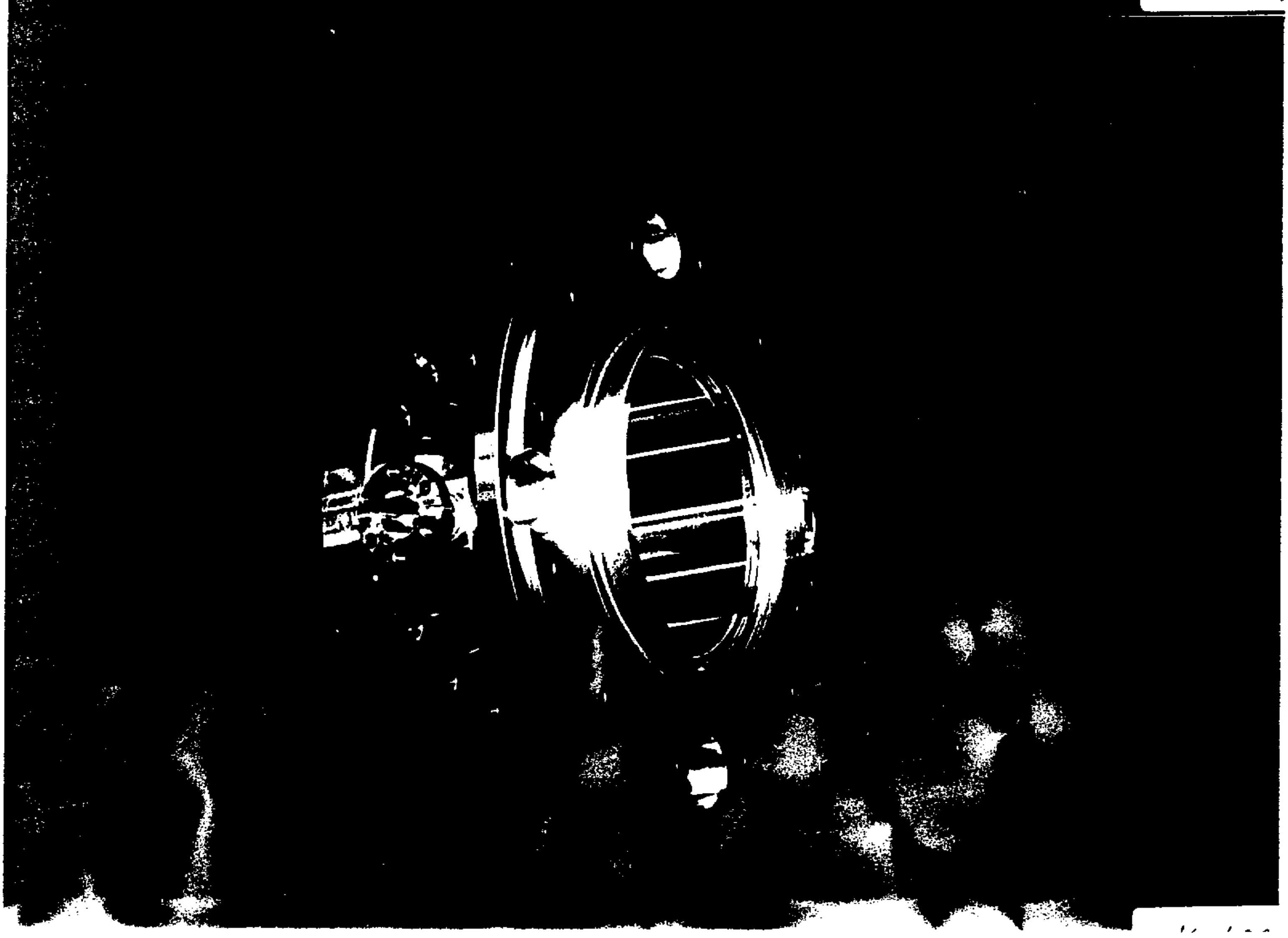

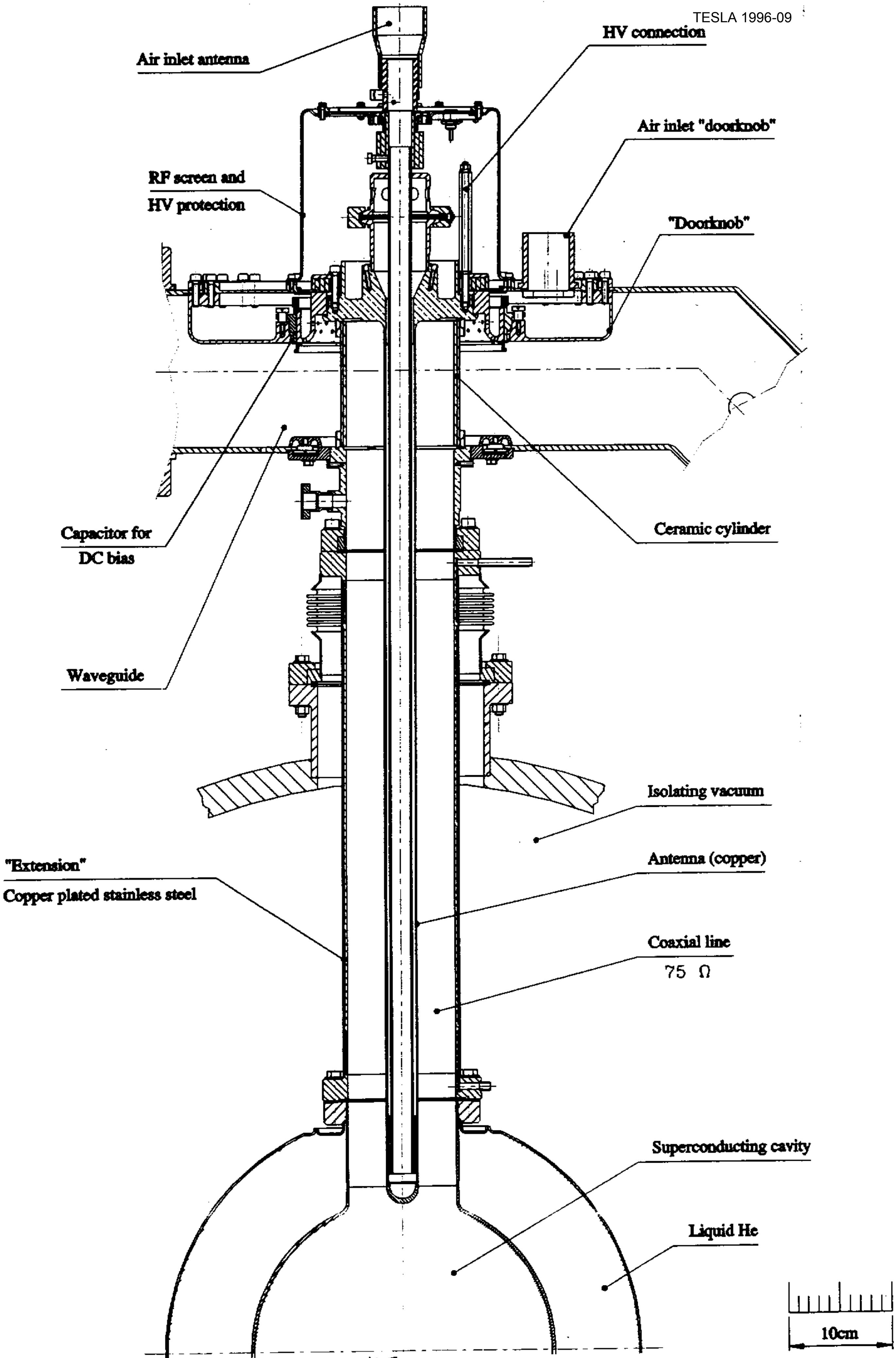
Air inlet antenna
HV connection
Air inlet "doorknob"
RF screen and
HV protection
"Doorknob"
Capacitor for
DC bias
Ceramic cylinder
Waveguide
Isolating vacuum
"Extension"
Copper plated stainless steel
Antenna (copper)
Coaxial line
75 Ω
Superconducting cavity
Liquid He
10cm

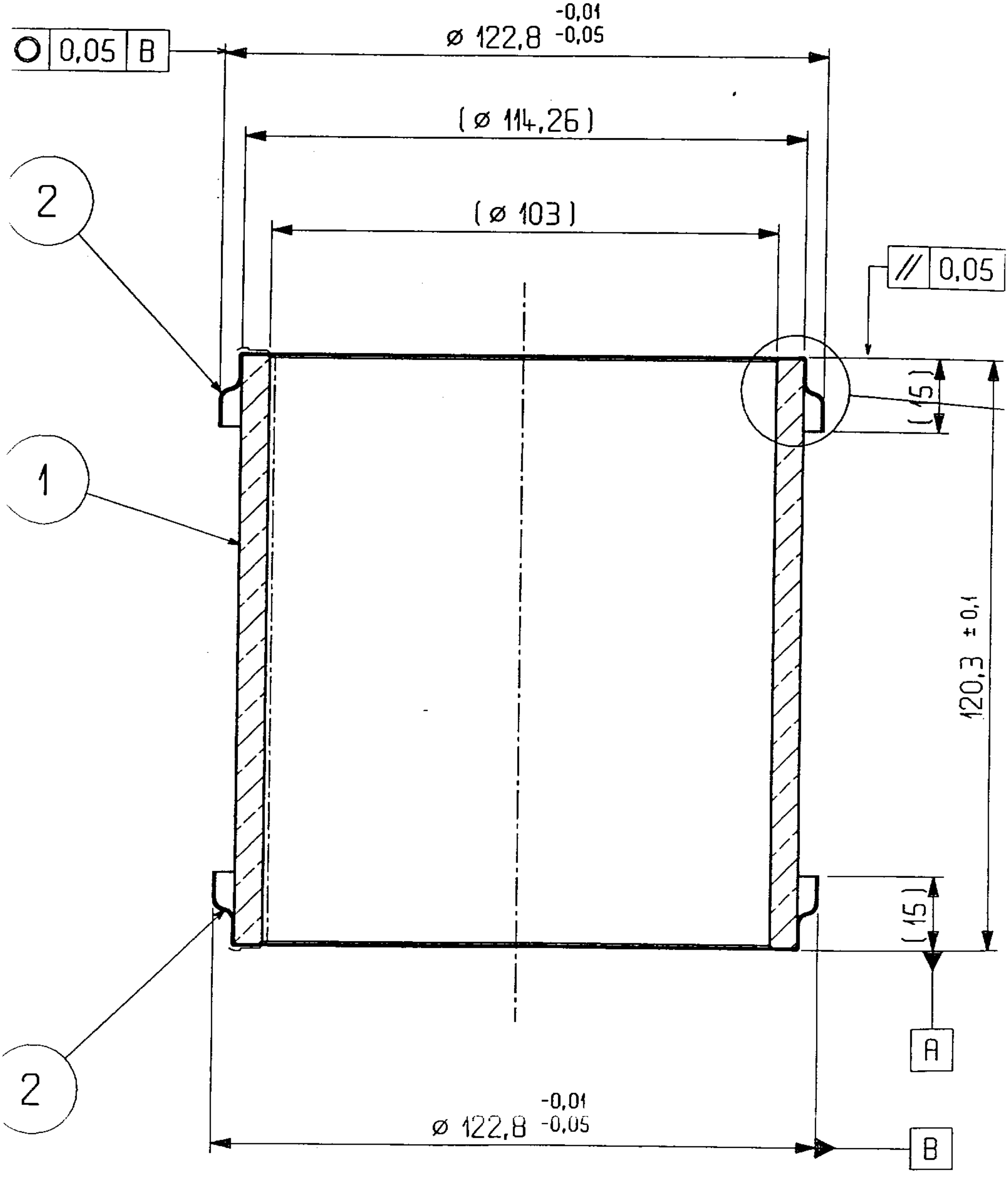

O 0,05 B
ø 122,8 -0,01 -0,05
(ø 114,26)
(ø 103)
// 0,05
2
1
(15)
120,3 ±0,1
(15)
2
A
ø 122,8 -0,01 -0,05
B

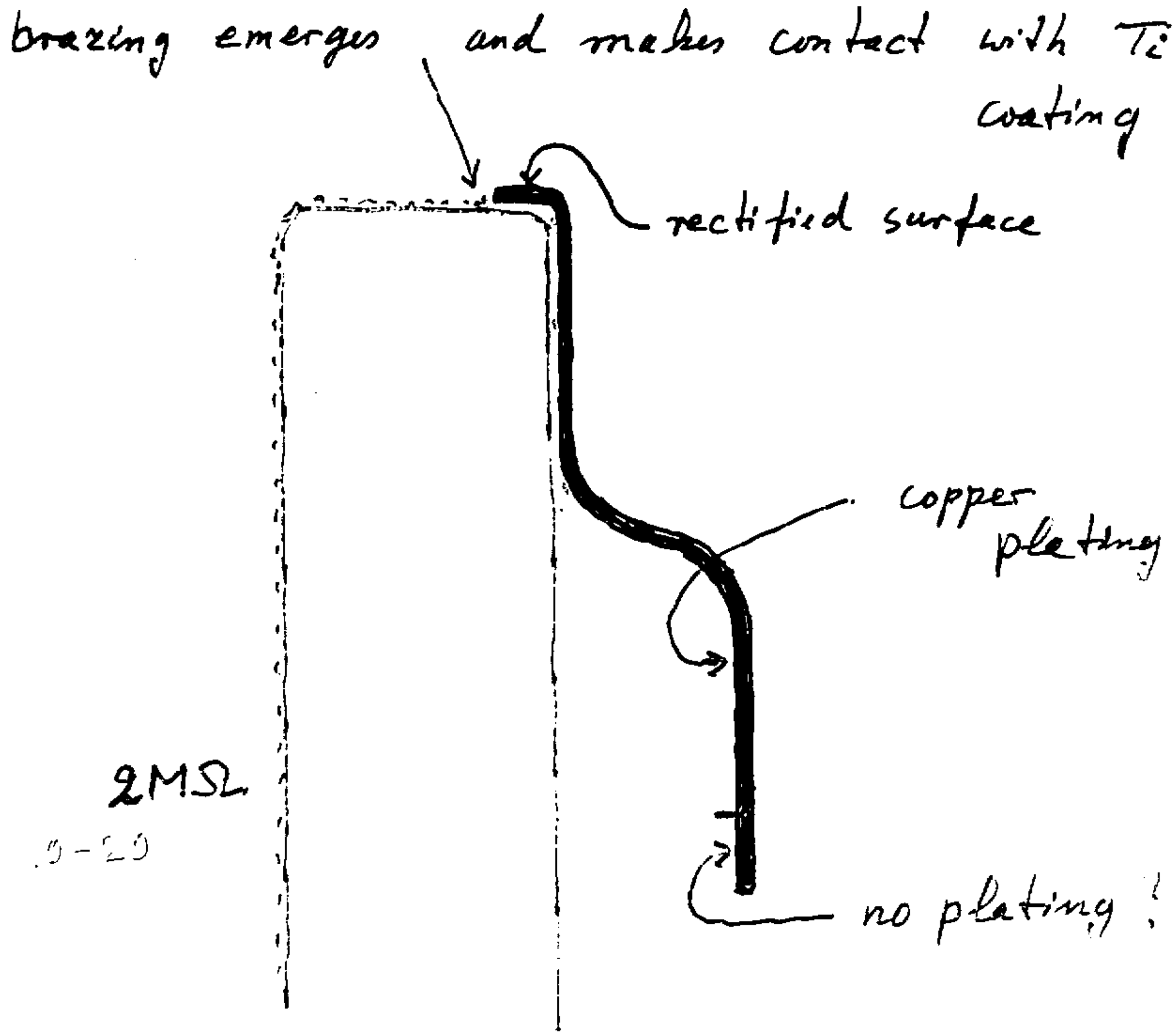
brazing emerges and makes contact with Ti coating
rectified surface
copper plating
no plating!
2MΩ

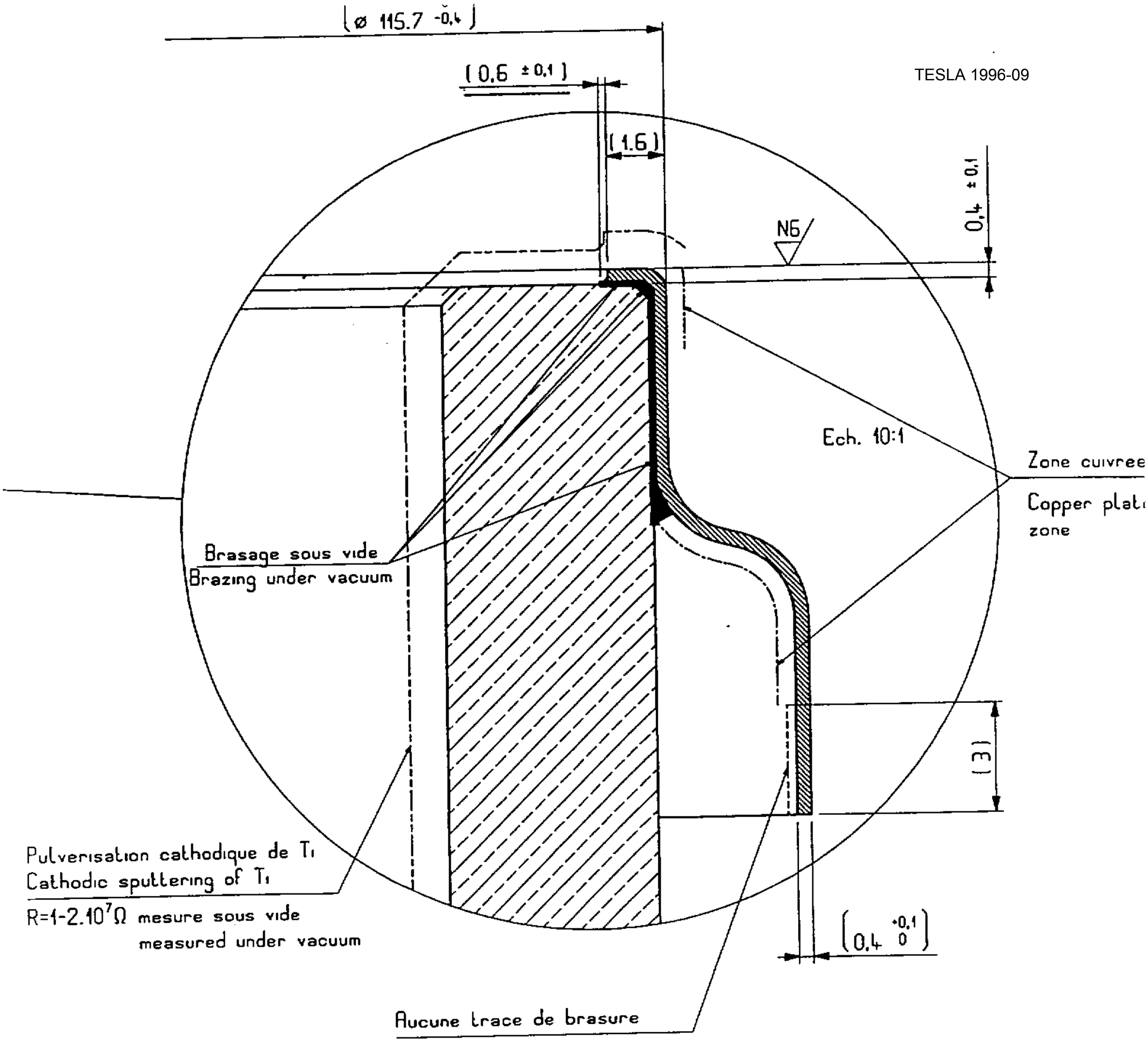
(ø 115.7 -0.4)
(0.6 ±0.1)
(1.6)
0.4 ±0.1
N6
Ech. 10:1
Zone cuivree
Copper plat
zone
Brasage sous vide
Brazing under vacuum
(3)
Pulverisation cathodique de Ti
Cathodic sputtering of Ti
R=1-2.10⁷Ω mesure sous vide
measured under vacuum
(0.4 +0.1 0)
Aucune trace de brasure

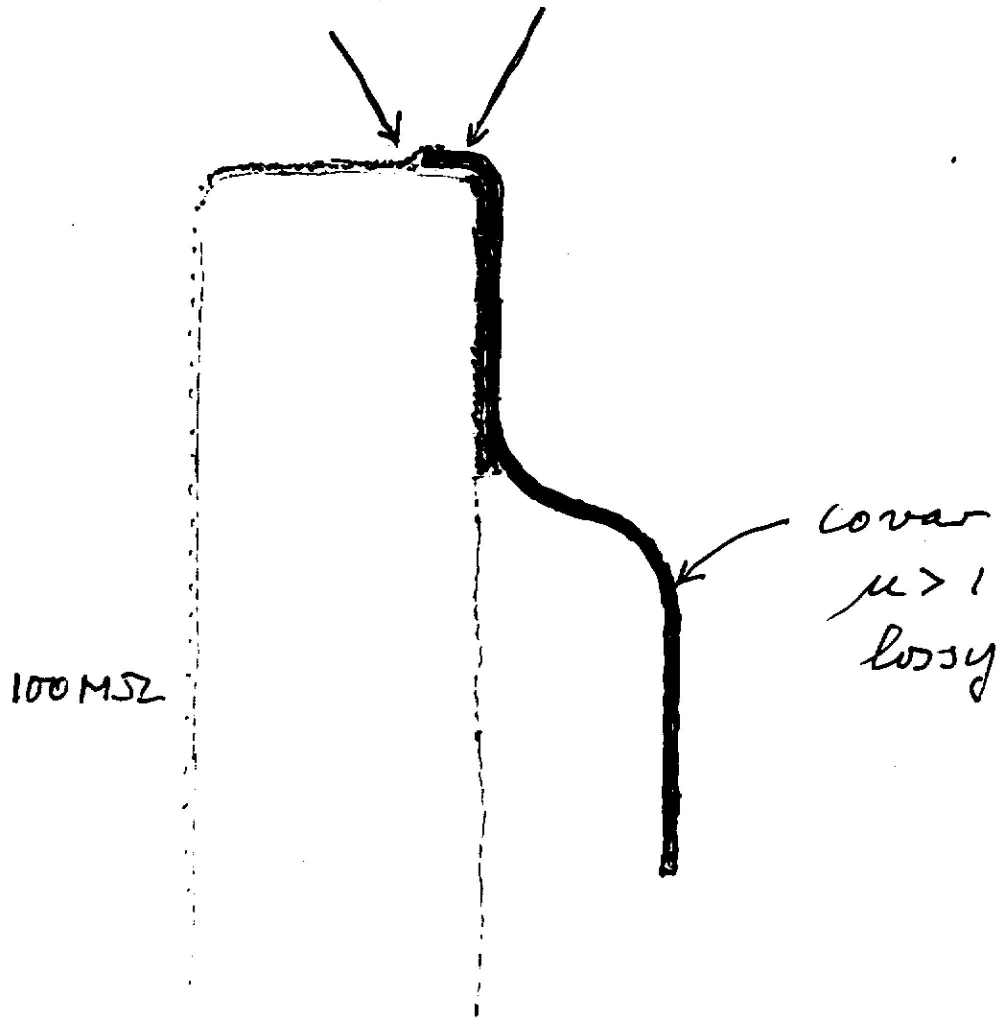
100 MΩ
covar
μ > 1
lossy

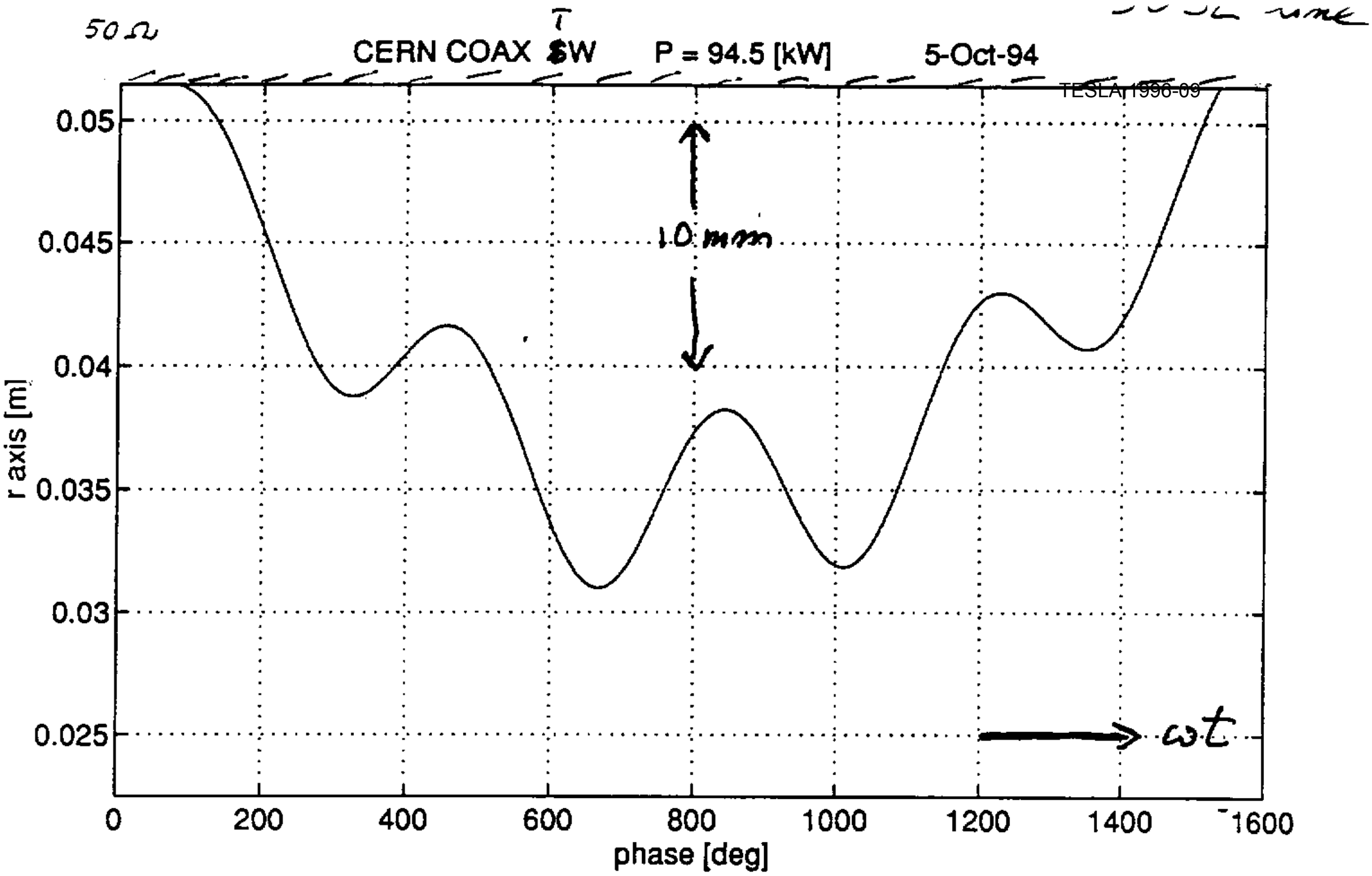
50 Ω
CERN COAX TW P = 94.5 [kW] 5-Oct-94
TESLA 1996-09
10 mm
ωt
r axis [m]
0.05
0.045
0.04
0.035
0.03
0.025
0
200
400
600
800
1000
1200
1400
1600
phase [deg]

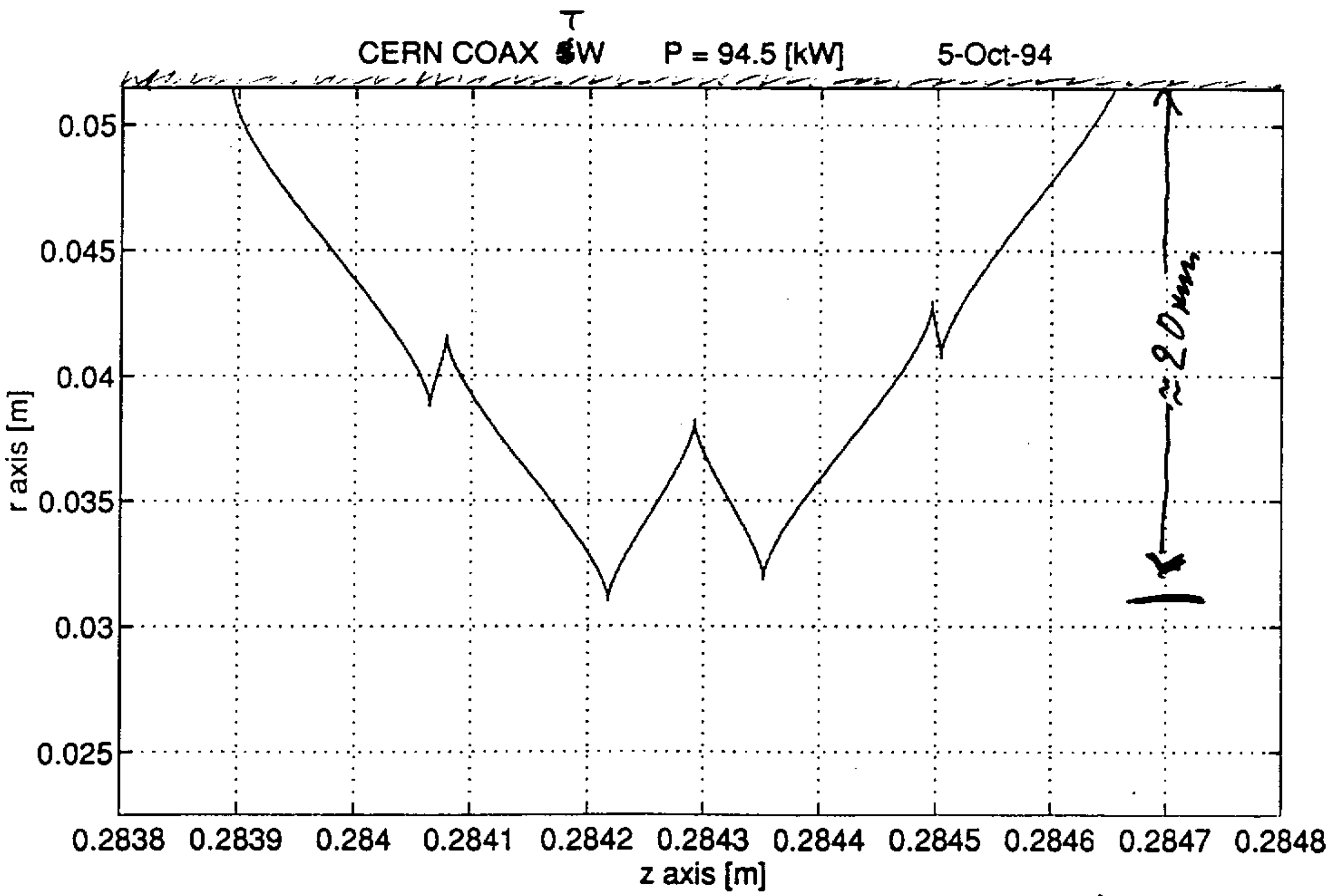
CERN COAX TW P = 94.5 [kW] 5-Oct-94
≈ 20 mm
r axis [m]
0.05
0.045
0.04
0.035
0.03
0.025
0.2838
0.2839
0.284
0.2841
0.2842
0.2843
0.2844
0.2845
0.2846
0.2847
0.2848
z axis [m]
.65 mm

FIGURE 32

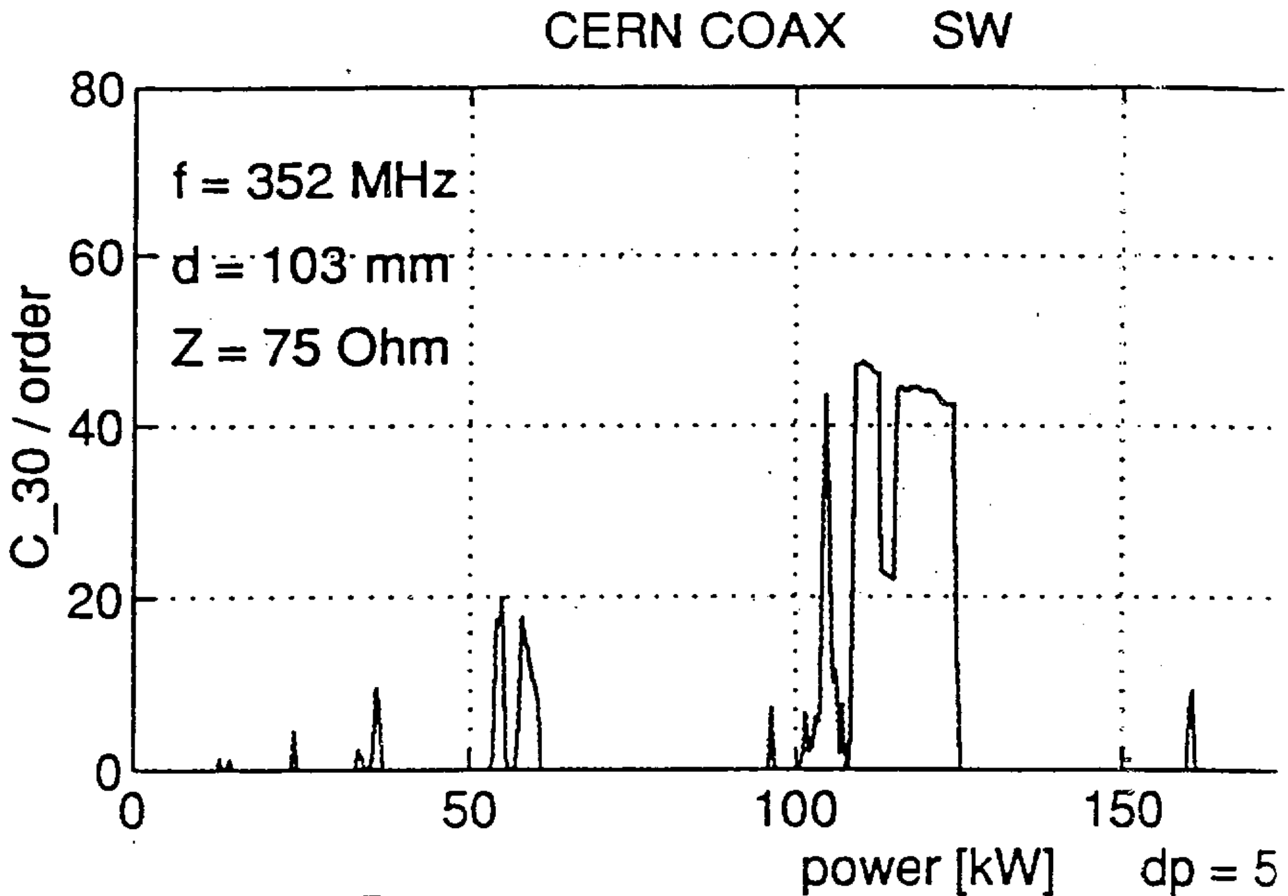

52 91 135 218 / 57 146 240 → TW power [kW]

64 112 167 270 / 70 181 300 → displayed power [kW]

100 150 400 900 / 200 300 400 1000 → impact energy [eV]

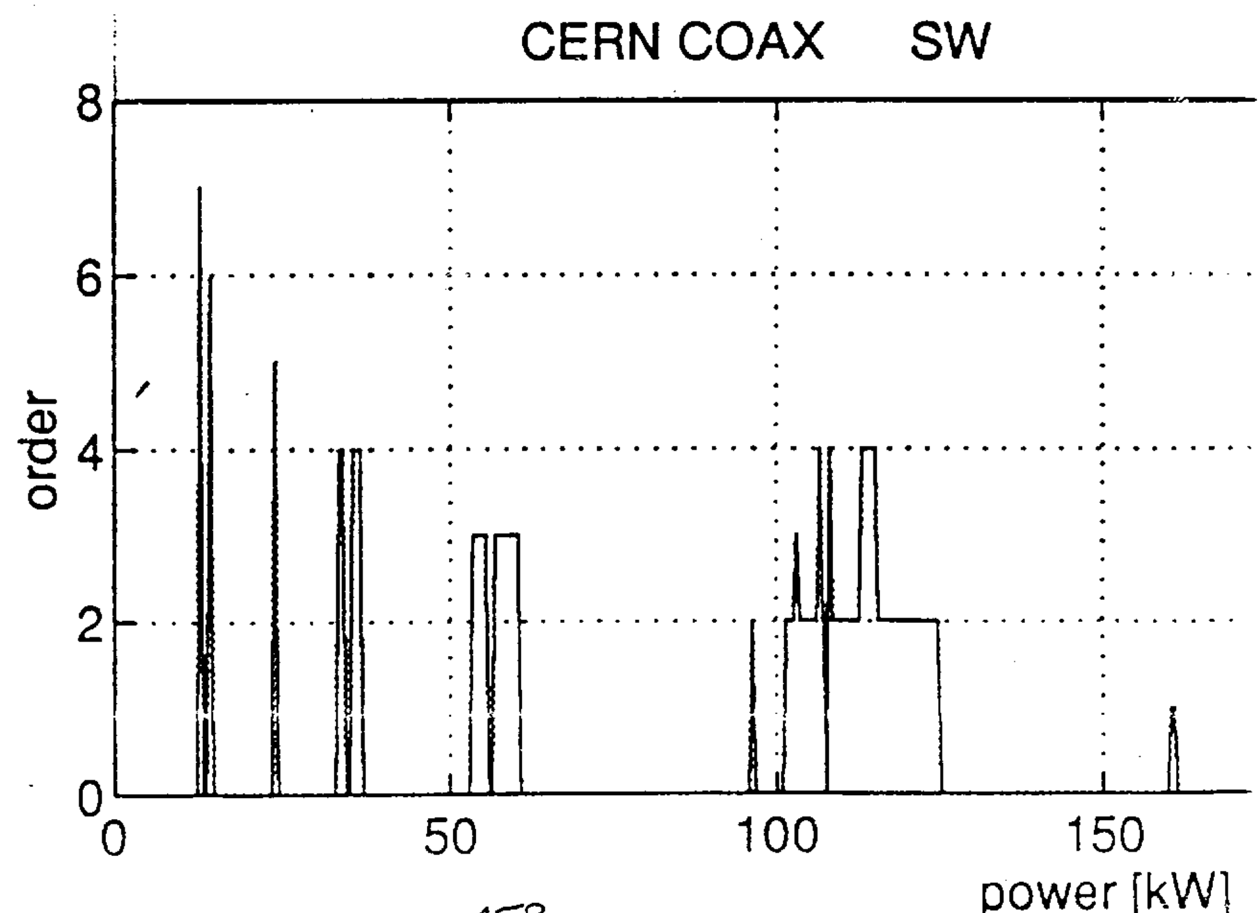

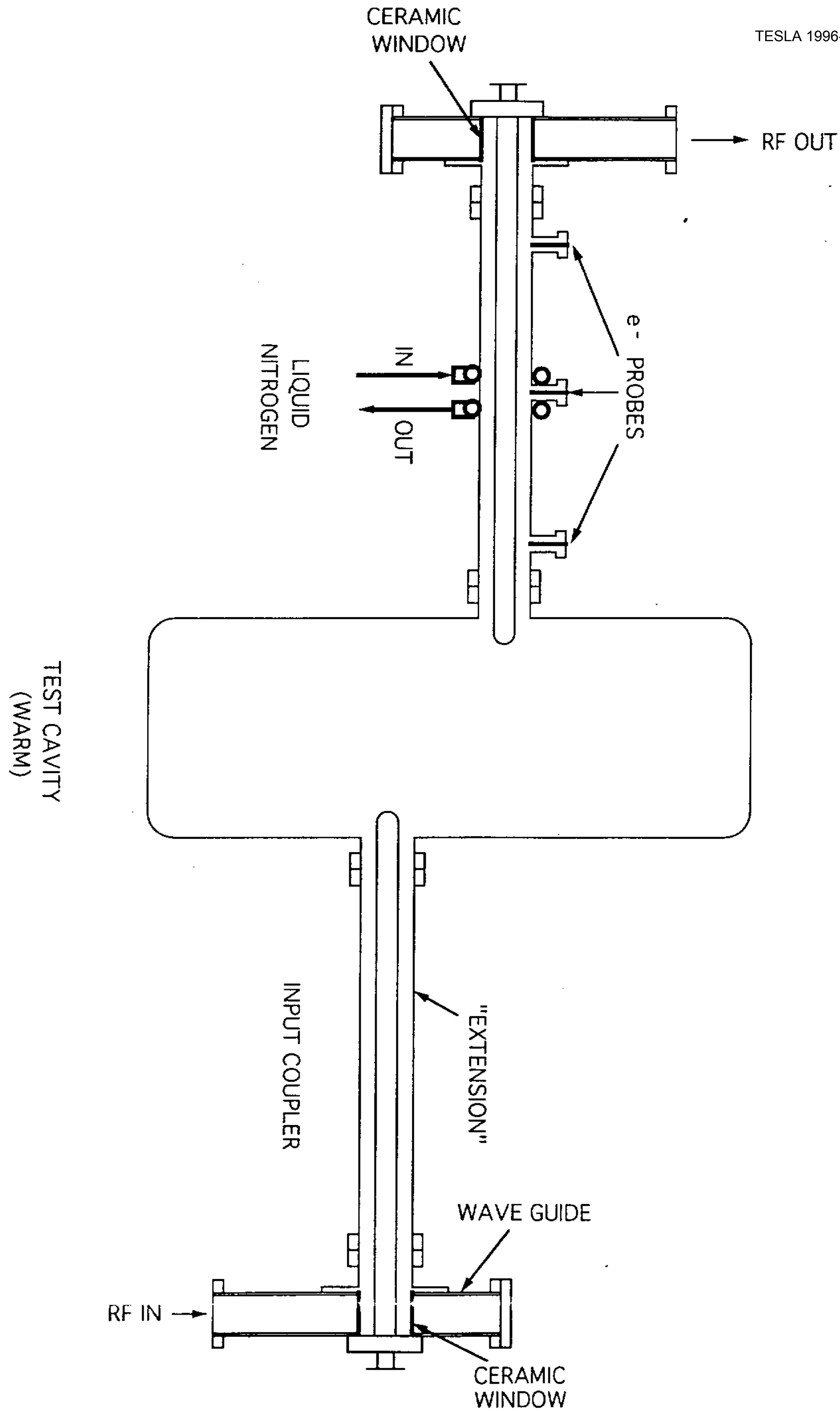
CERAMIC WINDOW
RF OUT
e - PROBES
LIQUID NITROGEN
IN
OUT
TEST CAVITY (WARM)
INPUT COUPLER
"EXTENSION"
WAVE GUIDE
RF IN
CERAMIC WINDOW

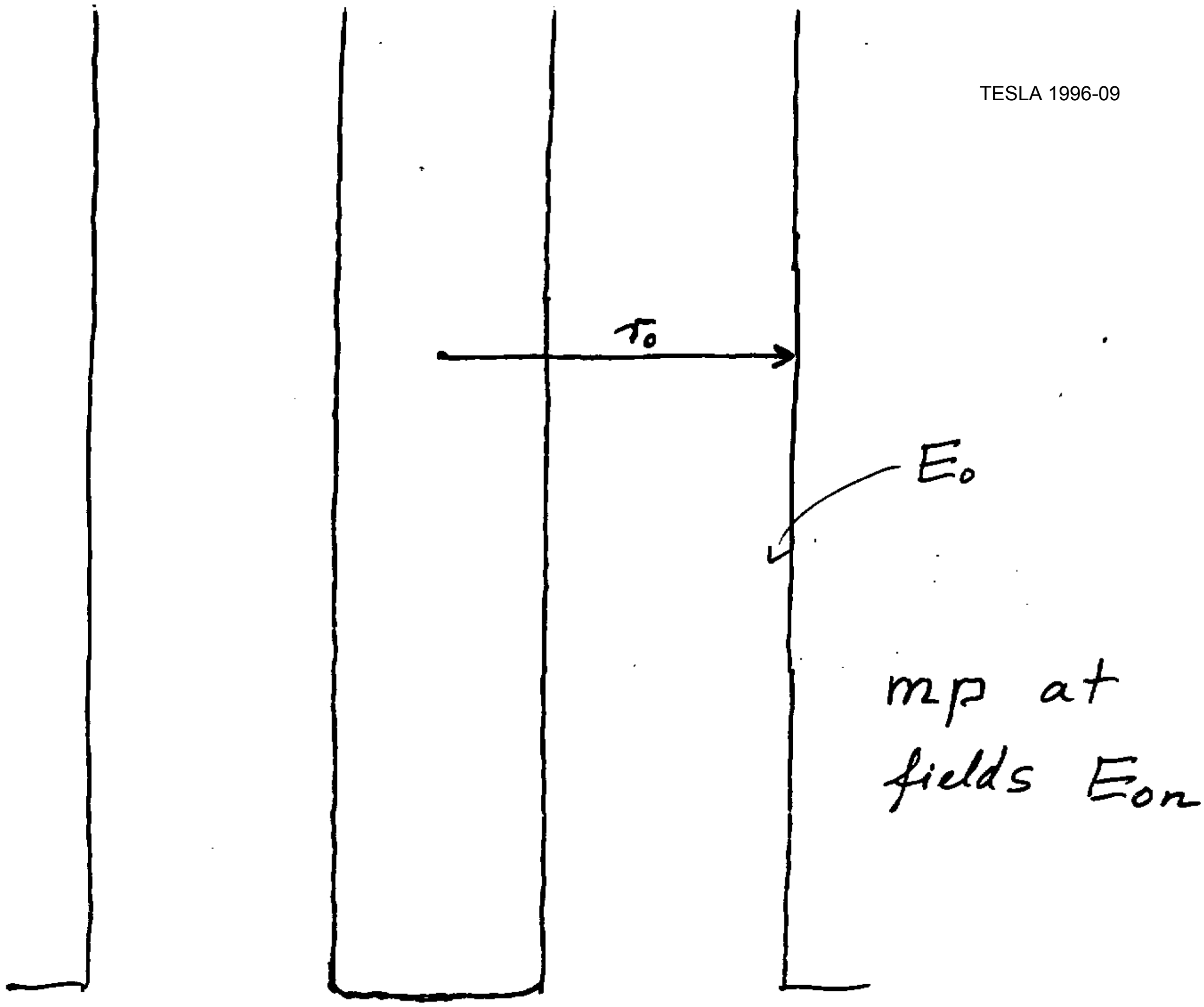

$$E = E_0 \frac{r_0}{r}$$

$$P_n = \frac{1}{2}\left(\frac{E_{on} r_0}{60}\right)^2 Z_w$$

make Z_w as big as possible!

EXPERIENCE WITH INPUT COUPLERS AT NOVOSIBIRSK

(Budker Institute of Nuclear Physics)

We have an experience with input power couplers only for room temperature copper cavities in the frequency range 25–700 MHz.

At low frequencies (4–55 MHz) we also have an experience with ceramic windows placed in the accelerating gaps of the cavities.

The most interesting is the experience at the frequency around 180 MHz.

CERAMICS USED FOR RF WINDOWS

We never used a high purity alumina ceramics.

The ceramics we used (commercial names 22HS, VK94−1) has 94−95% of Al_2O_3. Its properties are listed below:

Specific gravity 3.65 g/cm^3

Thermal elongation coefficient $\alpha = 5.7...6.7 \cdot 10^{-6}$
(per 1° C at 20...200° C)

Thermal conductivity $\lambda = 135$ mW/(cm·deg) at 20° C
104 mW/(cm·deg) at 200° C

Tensile strength 3700 kg/cm^2

Electric permittivity $\varepsilon = 10$

Dielectric losses $\tan(\delta) = 3 \cdot 10^{-4}$

Secondary emission coefficient $k_{max} = 3.7$
(at $E = 0.5$ keV of primary electron energy)

BONDING TECHNIQUE

We used only ceramic cylinders for RF windows (no experience with planar windows).

For connection of ceramic parts with metal parts we used the diffusion bonding technique.

For bonding copper and ceramic parts are clamped together with the strength of 1.5 kg/mm^2, heated to the temperature 980^o C in a hydrogen oven and kept so for few hours.

After that the copper-ceramic unit is brazed with other components in a vacuum oven using the silver-copper eutectic alloy.

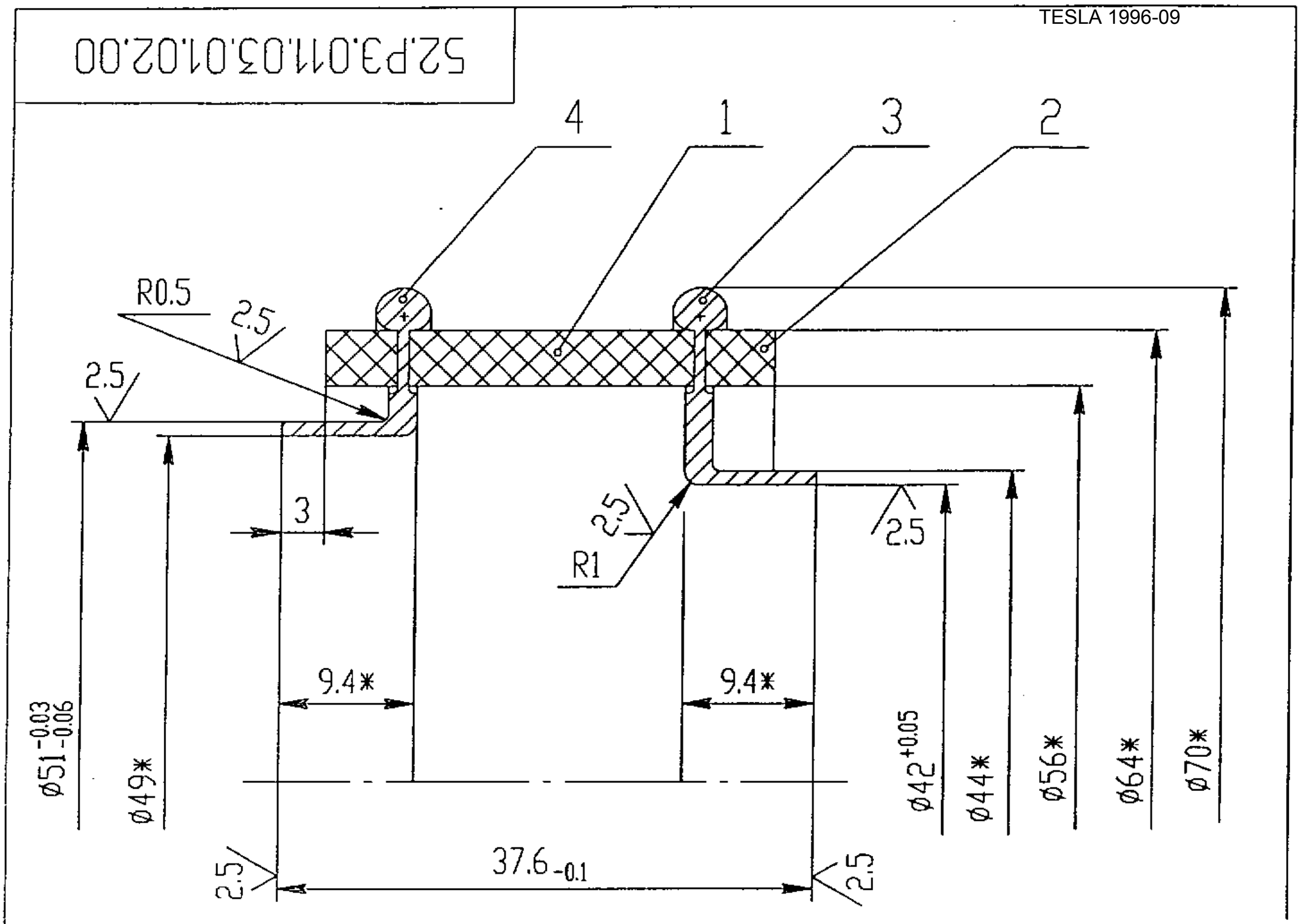

An Example of a Ceramic Window (Diffusion Bonded)

TESTS OF CERAMICS

We were interested to learn whether it was possible to build RF windows from the ceramics available for the power level around 1 MW or even higher – at the frequency of 180 MHz. (That was at the time when the RF system based on the new type of RF power amplifier – gyrocon – was designing for the VEPP–4 collider capable to operate to the energy above 7 GeV).

Several ceramic windows were (sequentially) tested in a specially designed coaxial cavity where they were placed in the place of maximum electrical field. A d.c. polarizing voltage was applied to the ceramic window for suppressing multipacting. All the windows ran successfully up to the peak RF voltage around 25 kV that corresponded to the TW power level above 4 MW in a 75 Ohm coaxial line.

COUPLER DESIGNS

After that the input coupler for VEPP–4 cavities and the output coupler for the gyrocon have been designed and built. They had different designs but in both types of couplers a d.c. biasing was used. The coupling loop was not short circuited. There was a capacitor at its end and a d.c. voltage was applied to the loop. The value of the capacitance was adjusted to reduce RF electric fields at the ceramic window.

Couplers of the VEPP–4 cavities were tested up to the power level 220 kW in TW mode with the cavity tuned on (VSWR around 1.1). They were also tested with the cavity tuned off up to the fields corresponding to TW power level above 500 kW.

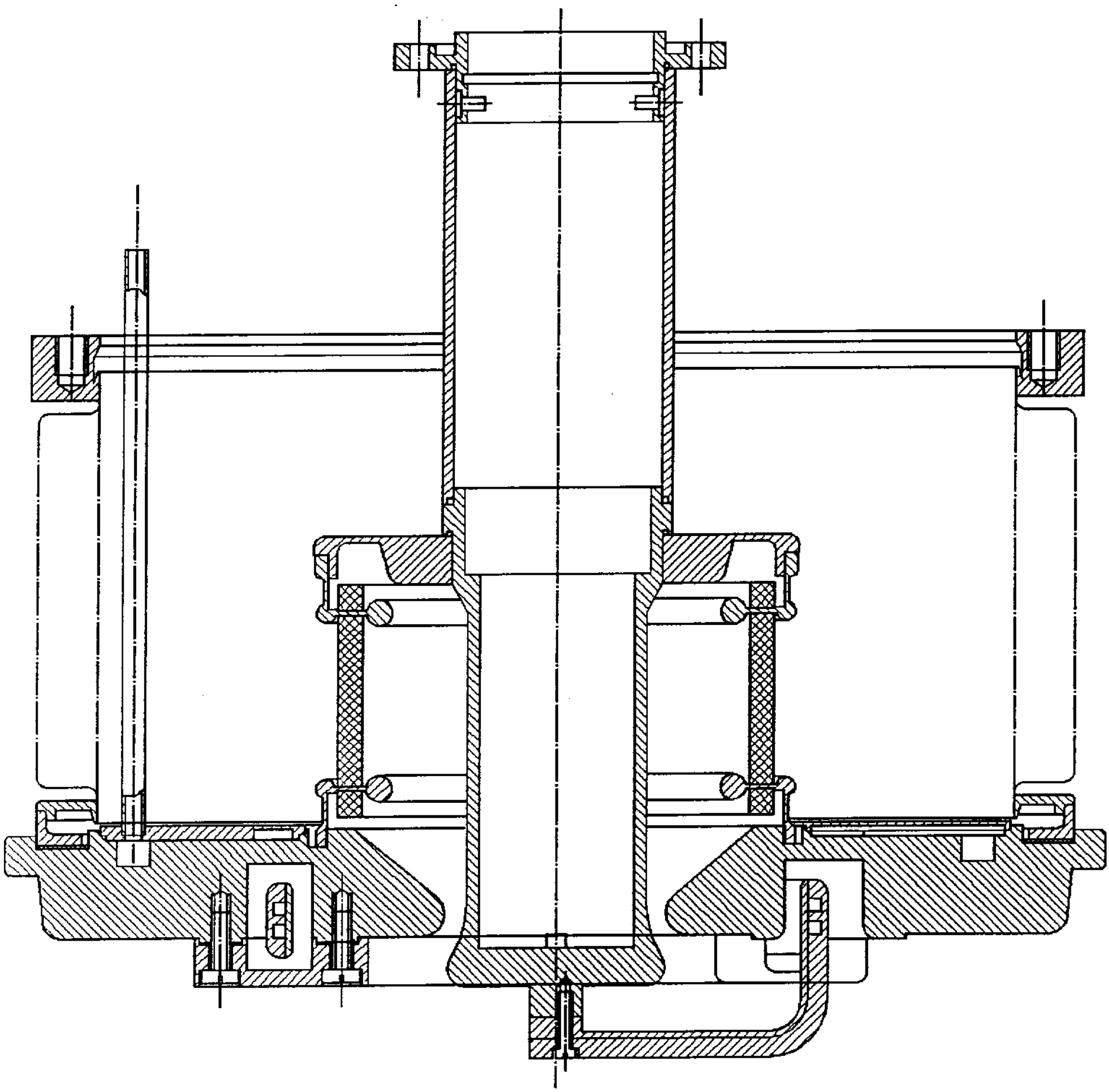

THE POLARIZED VEPP-4 COUPLER (180 MHZ)

The d.c. biasing is a very effective way to suppress multipacting in RF couplers (as well as in RF cavities) but the design is rather sophisticated. It is better not to use it when possible.

At low frequencies (or at low power levels) it is possible to avoid multipacting choosing gaps between electrodes and between electrodes and ceramic small enough for multipacting. When it is impossible, the other way out is to find a geometry that is not good for multipacting. So, for years we use a delta-like shape of coupling loops (not polarized). The multipacting is unlikely to appear in that type of loops due to drift of electrons. Recently we applied similar approach to the general design of input couplers for the frequency ranges 500 MHz and 700 MHz.

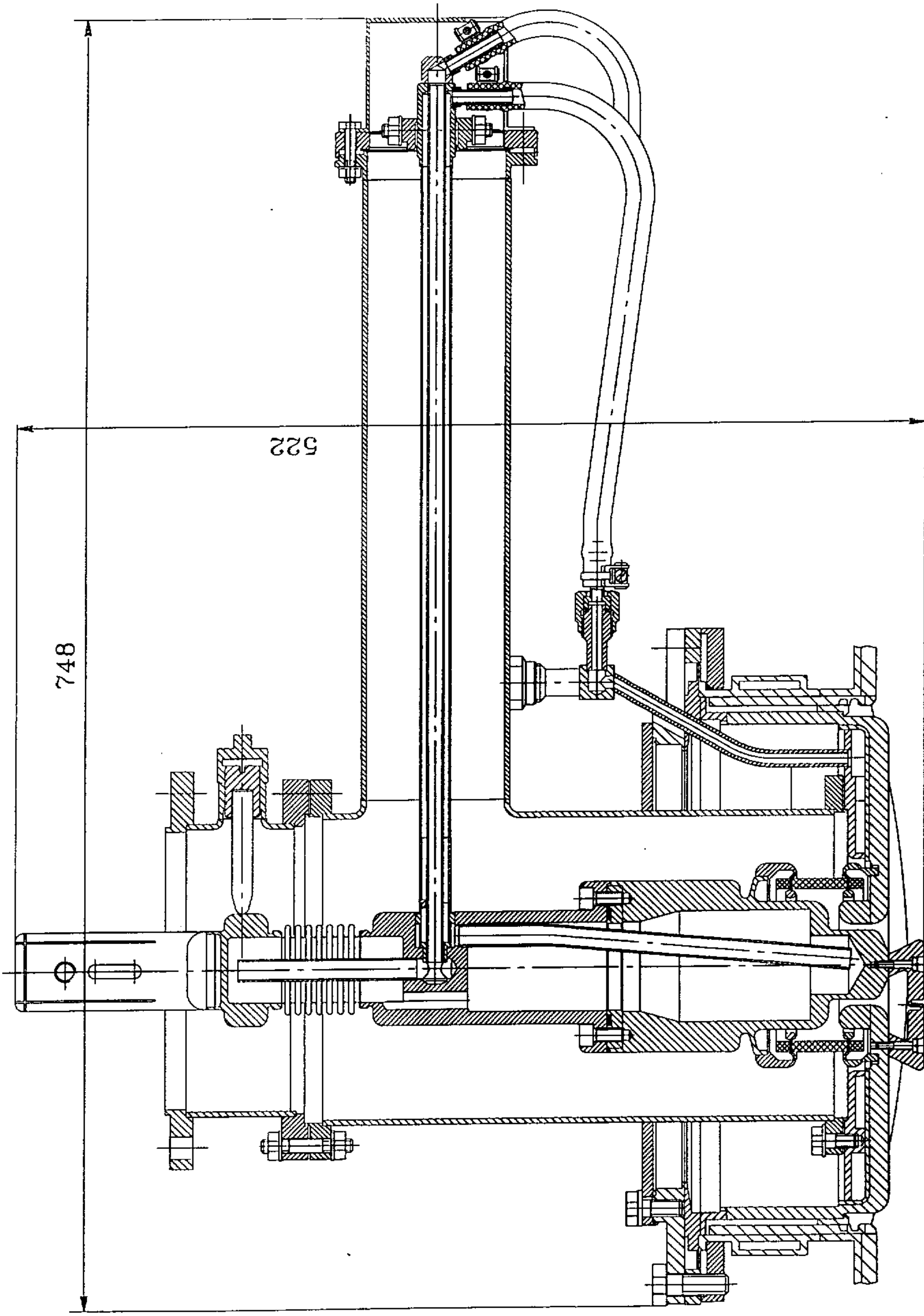

The RTMR Main Coupler (180 MHz)

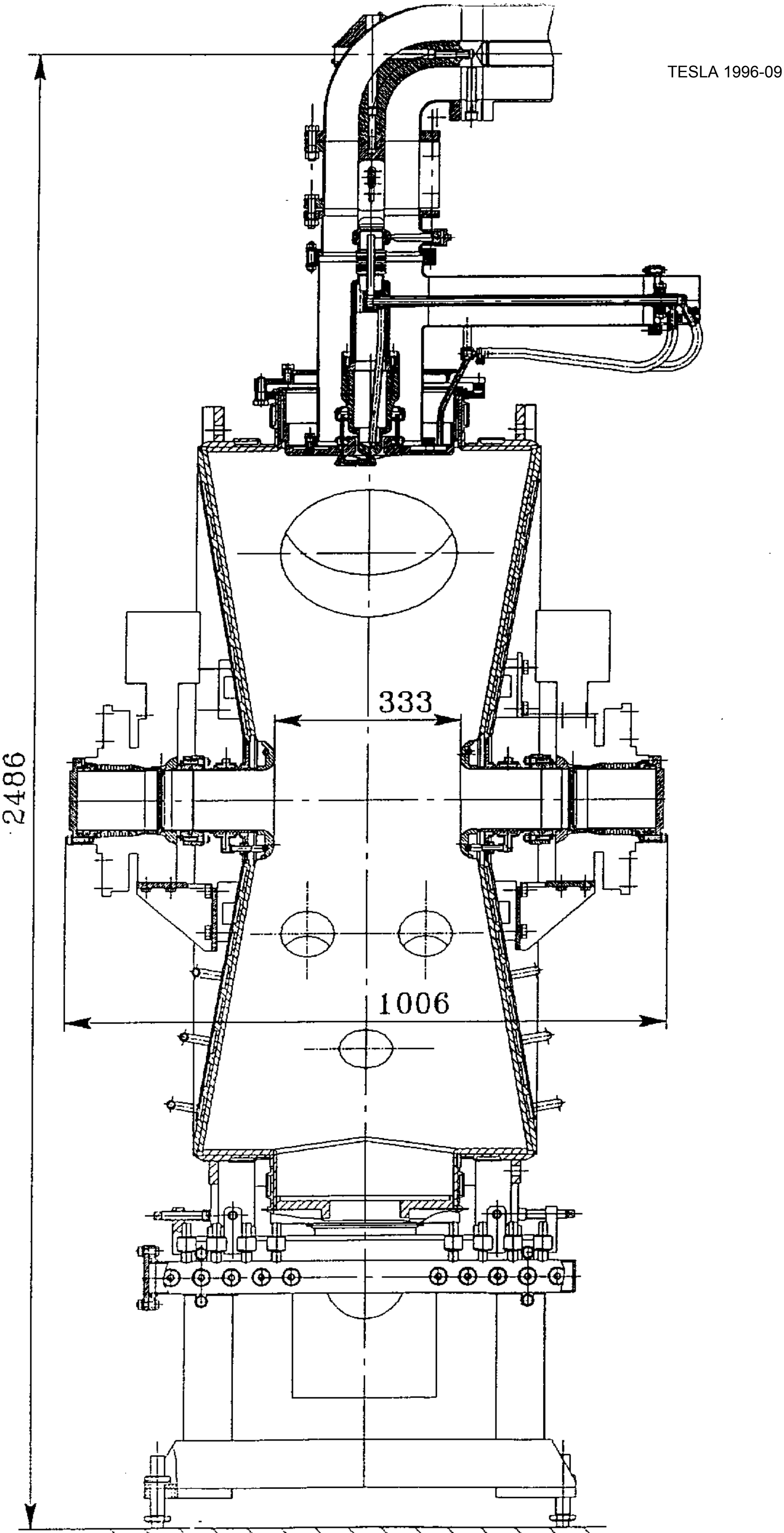

A RTMR CAVITY (180 MHz)

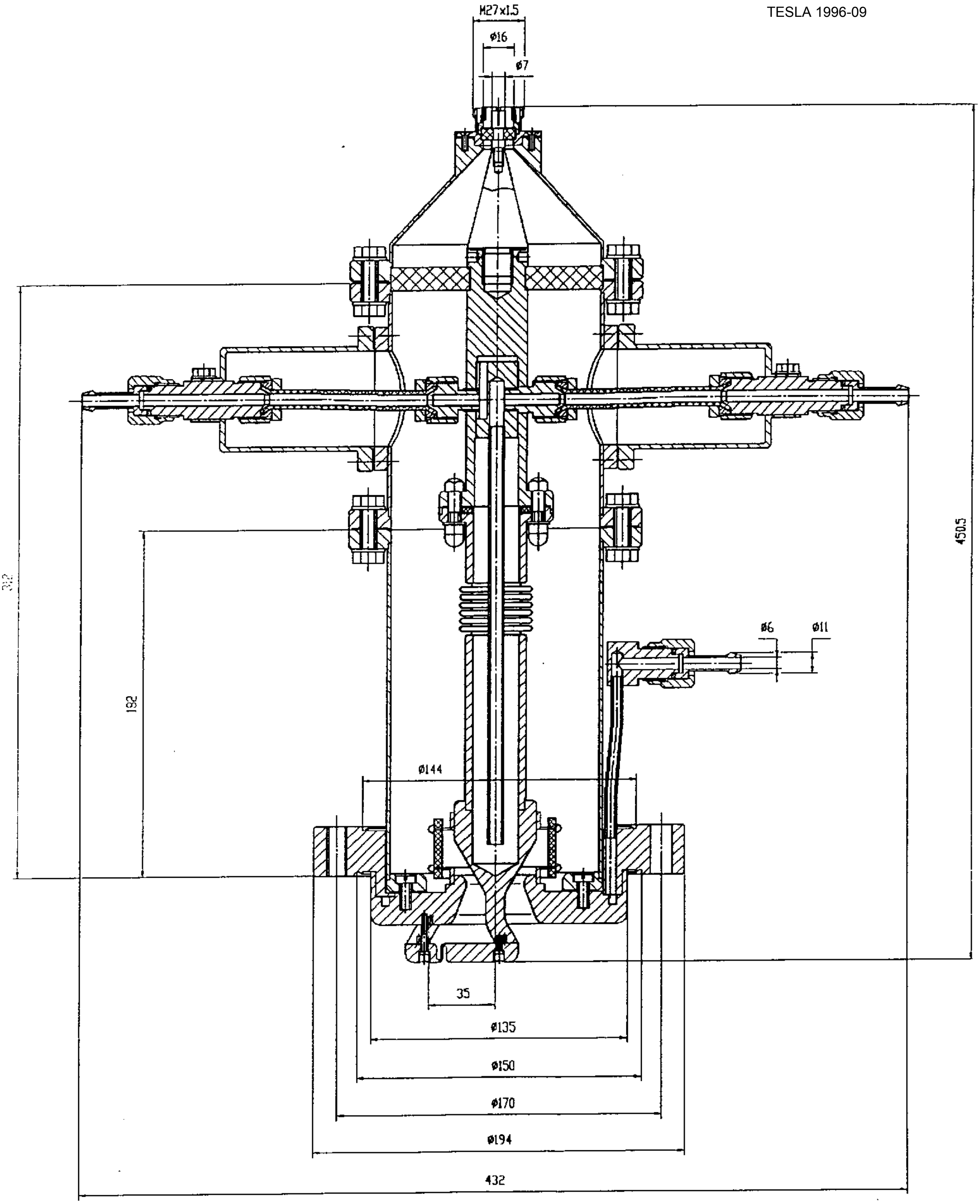

THE MAIN COUPLER FOR A 540 MHZ CAVITY

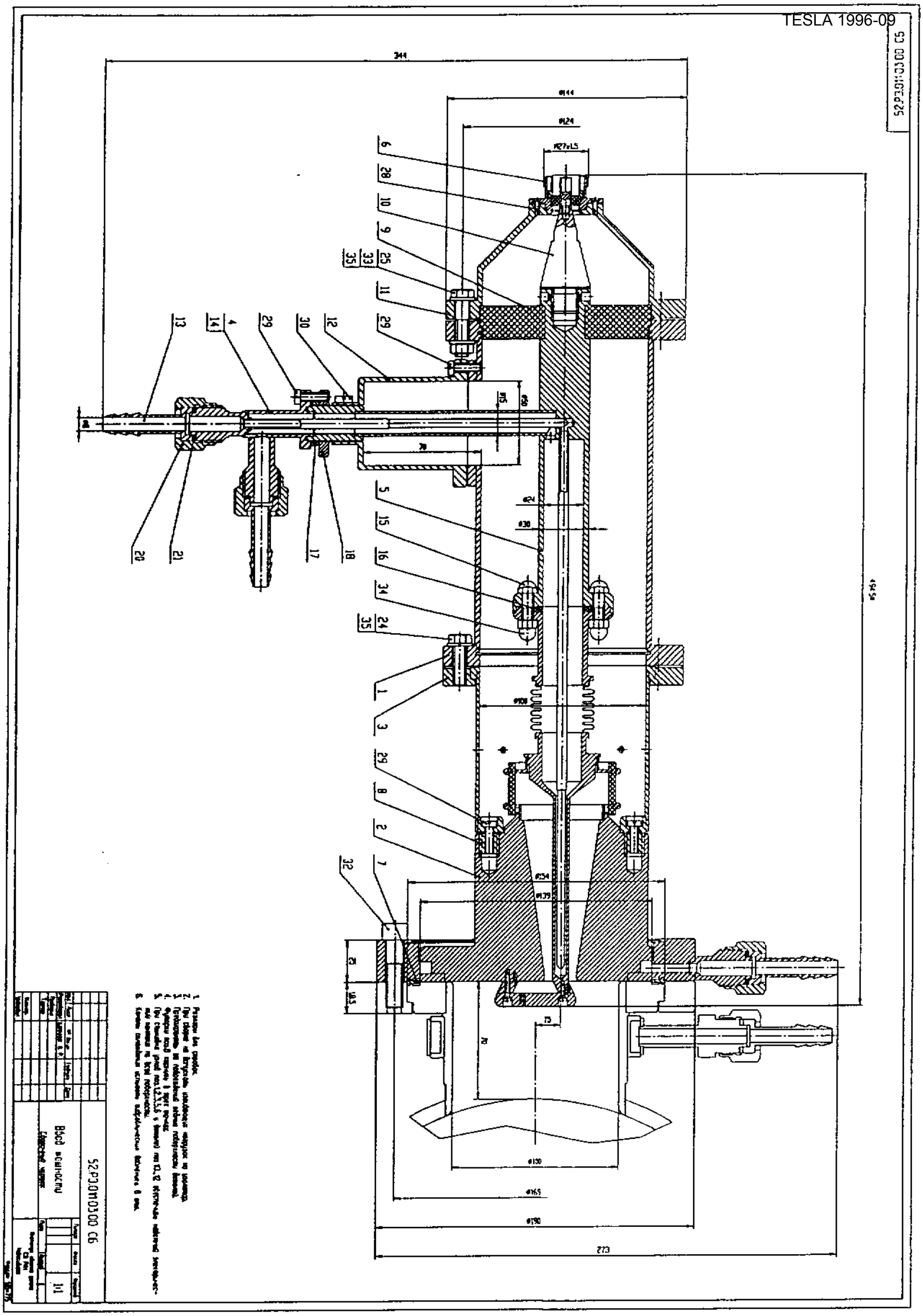

THE MAIN COUPLER
FOR THE DAMPING RING CAVITY (700 MHz)

EXPERIMENTS WITH GLOWING DISCHARGE

We had a dramatic experience with trying to clean the couplers (together with the cavity) by the low pressure glowing discharge. We tried twice to do it but both times the windows cracked after that at RF power applied. The cause was the copper sputtering on the ceramic window by glowing discharge. Heating of this copper layer by RF power caused excessive mechanical stresses in the ceramic and its destroying.

Telescopic - type coupler for TESLA

Bienvenue G., Garvey T., Mace M., Panvier R., Soliak N.
LAL, IN2P3, Orsay, France.
(on leave BINP,Protvino,Russia)

Motivation: RF coupler is one of the critical elements of TESLA approach to LC (one/meter). At present time neither of existing designs: Fermilab and DESY satisfy completely all requirements, so, still a lot of work to improve them.

The main problems can be identified with following most critical elements of coupler:`

- *cold and warm windows*
- *bellows inside the coaxial line*

Aims of new solution are: to suppress cold window and bellows in co-axial line, to simplify it's mounting inside cryostat and to reduce the manufacturing cost.

The idea : coupler can be mounted with SC cavity in folded position and then extended, like telescope, to be attached to feeder waveguide outside the cryomodule. Coupler vacuum is common with that of cavity, isolated by warm window or vacuum valve.

Problems: sliding rf contacts, ...

Possible solution - to use materials with different coefficients of thermal expansion (*10 $^{-6}$):
Cu = 17 or ss =16.5; Ti = 8.9; W=4.5 for receiving good rf contact at 70 K.

Test of rf contacts at telescopic junction at high power level on RF test bench at Saclay: *1.3 GHz, 1 MW, 2 ms, 0.1 Hz.*-1 Hz

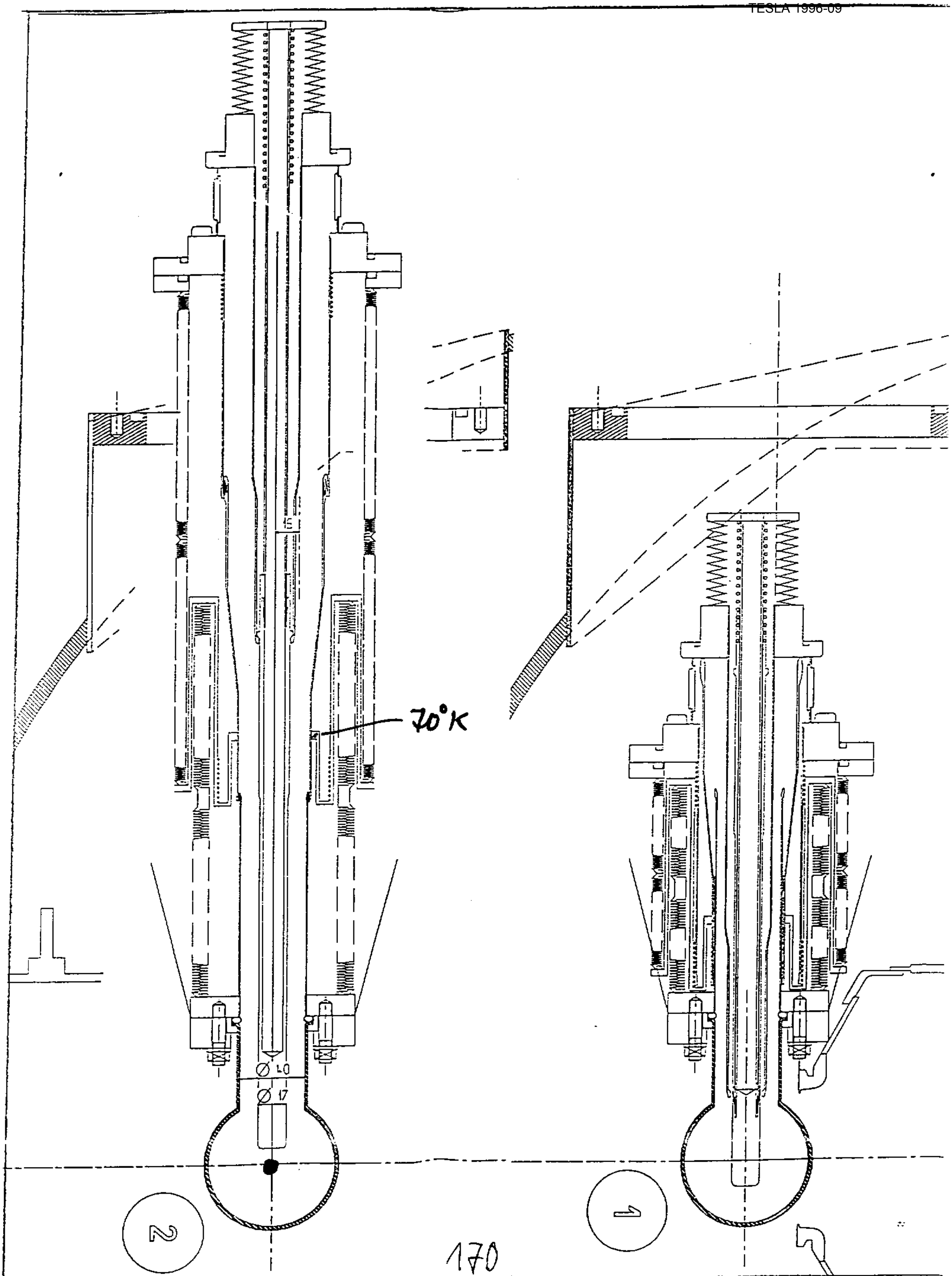
15
70°K
Ø 40
Ø 17
2
1

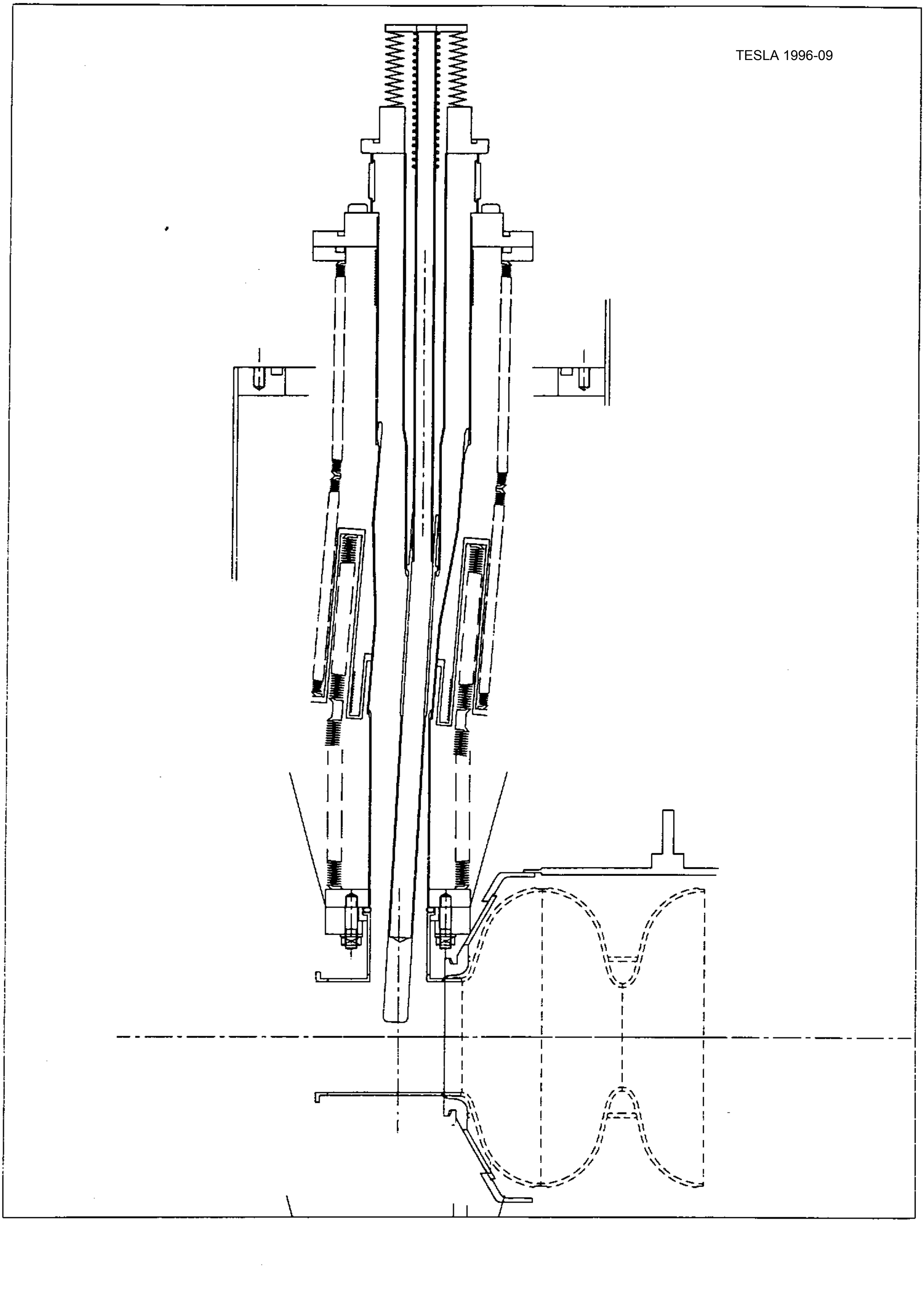

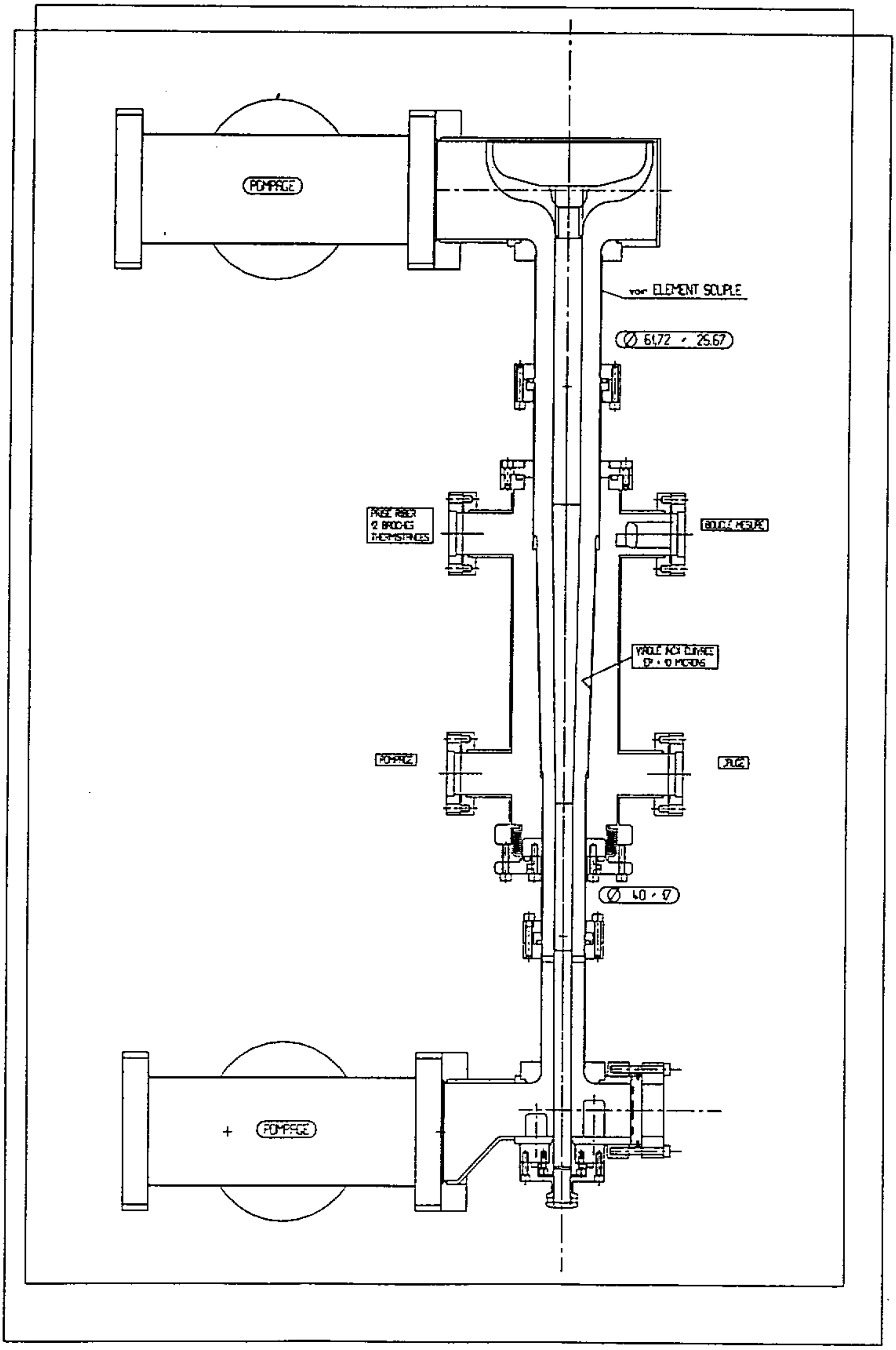

Figure 2: *Setup for testing of RF contact in telescopic coupler.*

WG-coax transition (Ø40 mm)

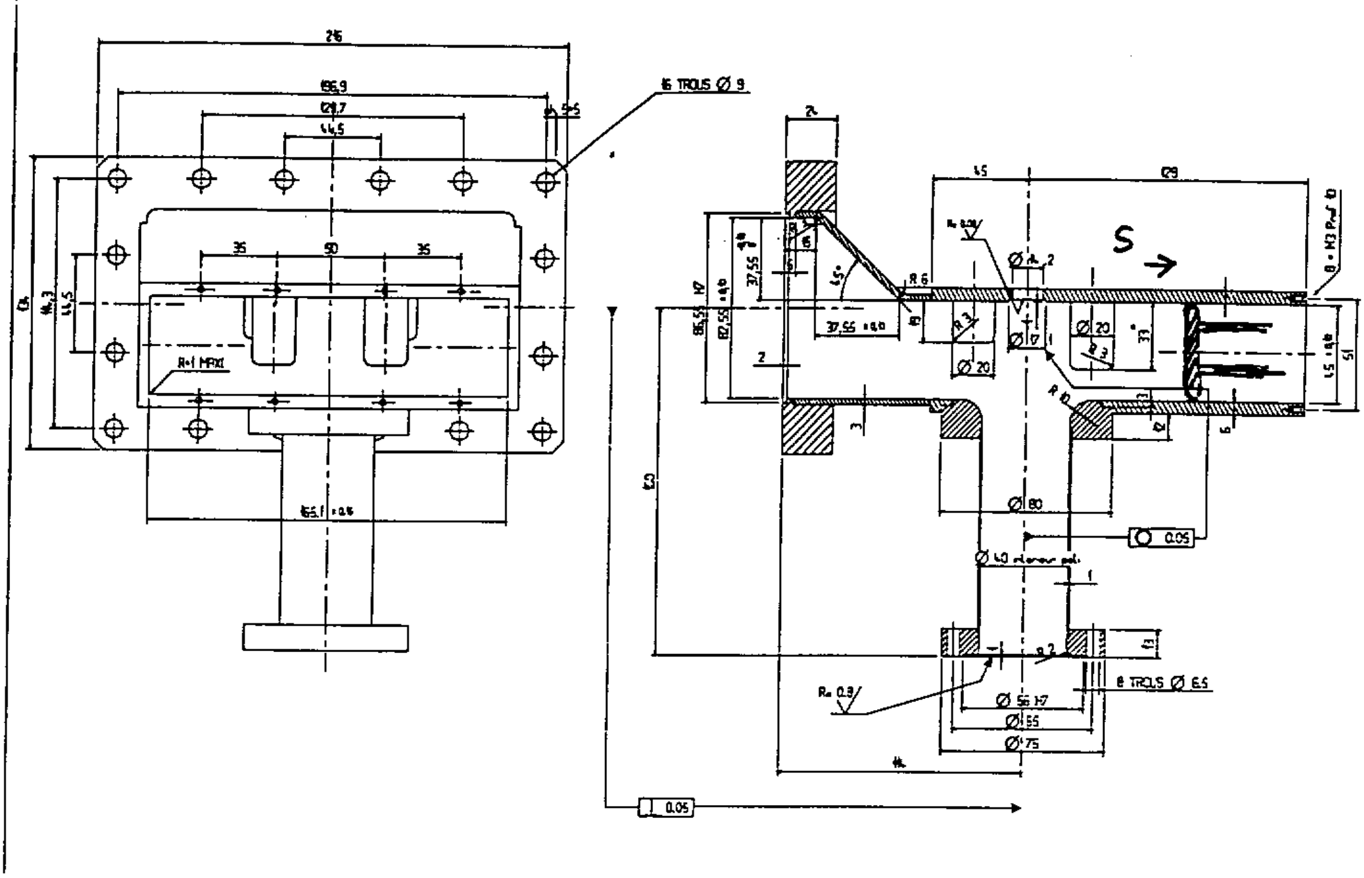

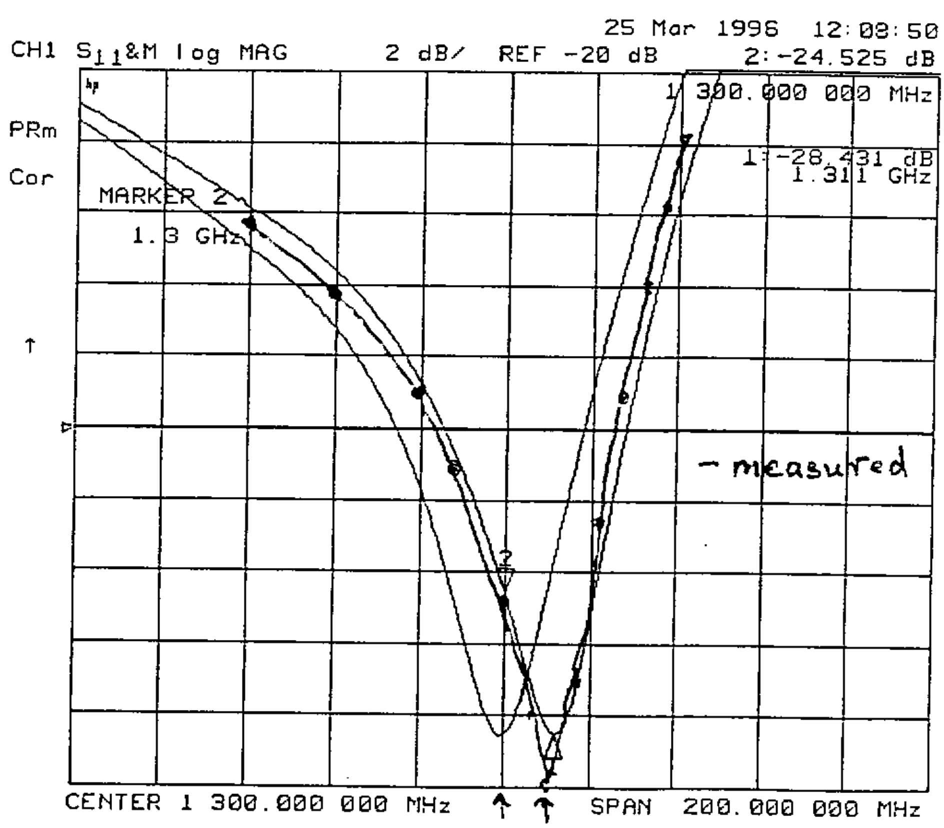

$$\frac{\Delta F}{\Delta S} = 11 \frac{MHz}{mm}$$

bias

DC polarisation for TTF coupler

Garvey T., Mosnier A., Panvier R, Chel S, Soliak N.
LAL,IN2P3, Orsay; France; CEA,Saclay,France:
(on leave of absence from BINP, Protvino,Russia)

On-side MP can be dangerous for any design of coupler as predicted by simulation. Though high power test of simple 40 mm coaxial line at DESY contradict with simulation, nevetheless the risk of MP high enough in real geometry of coupler.

There are few well-known possibilities to reduce MP:

- *Geometry: P ~(f*d)^4*Z; f-freq,d-gap, Z-impedance*
- *Eccentric coax*
- *Coating Ti, TiN,... to reduce secondary emission*
- *Injection of perturbing RF*
- *Electric DC bias (-1.5+2.5 kV)*

Two possible designs of WG-coax transition were simulated by HFSS, both for Ø 62 mm coaxial line and reduced height of WG (45 mm).

1. DESY-type with cylindrical warm window. DC bias like in CERN design by Kapton foil on air side.

2. Fermilab simple doorknob transition with choke cavity.

DESY-type WG-coax transition for Ø65 mm coaxial line

TESLA 1996-09

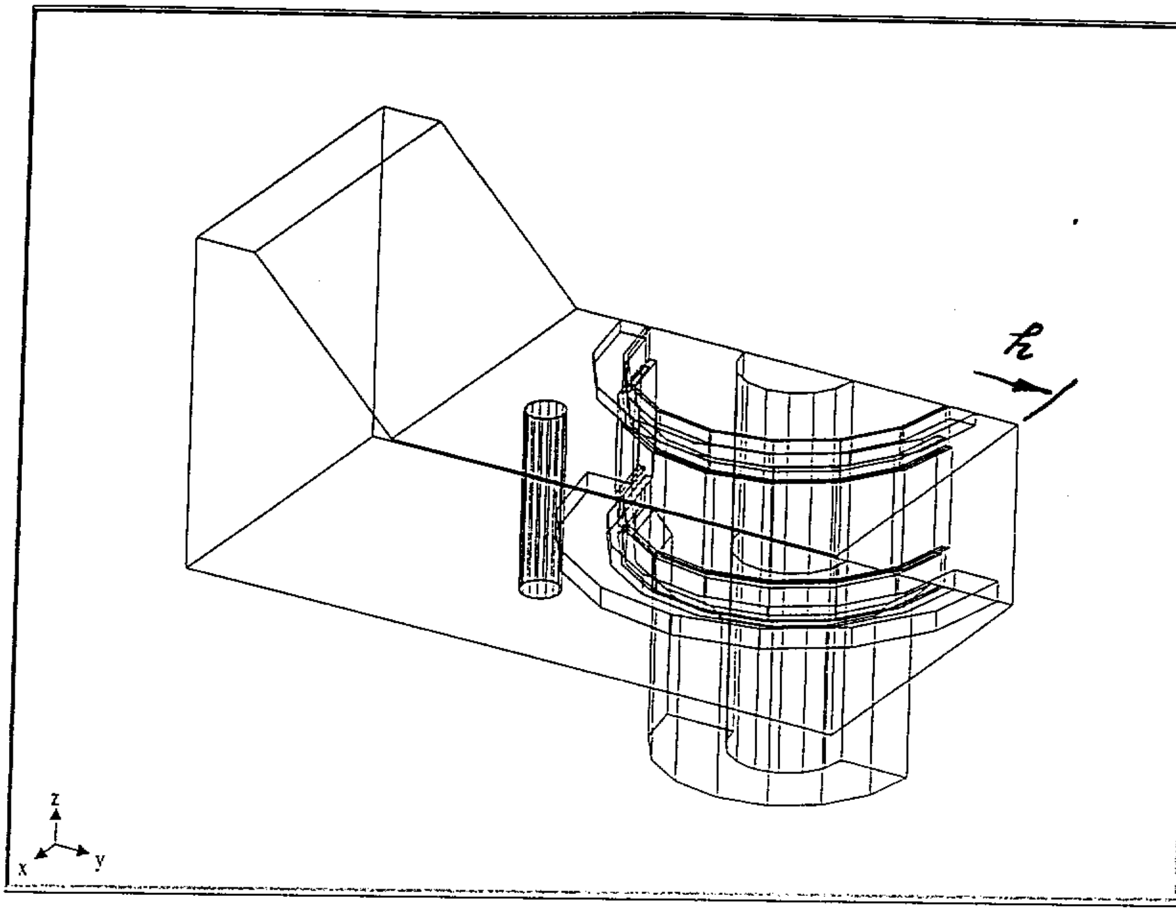

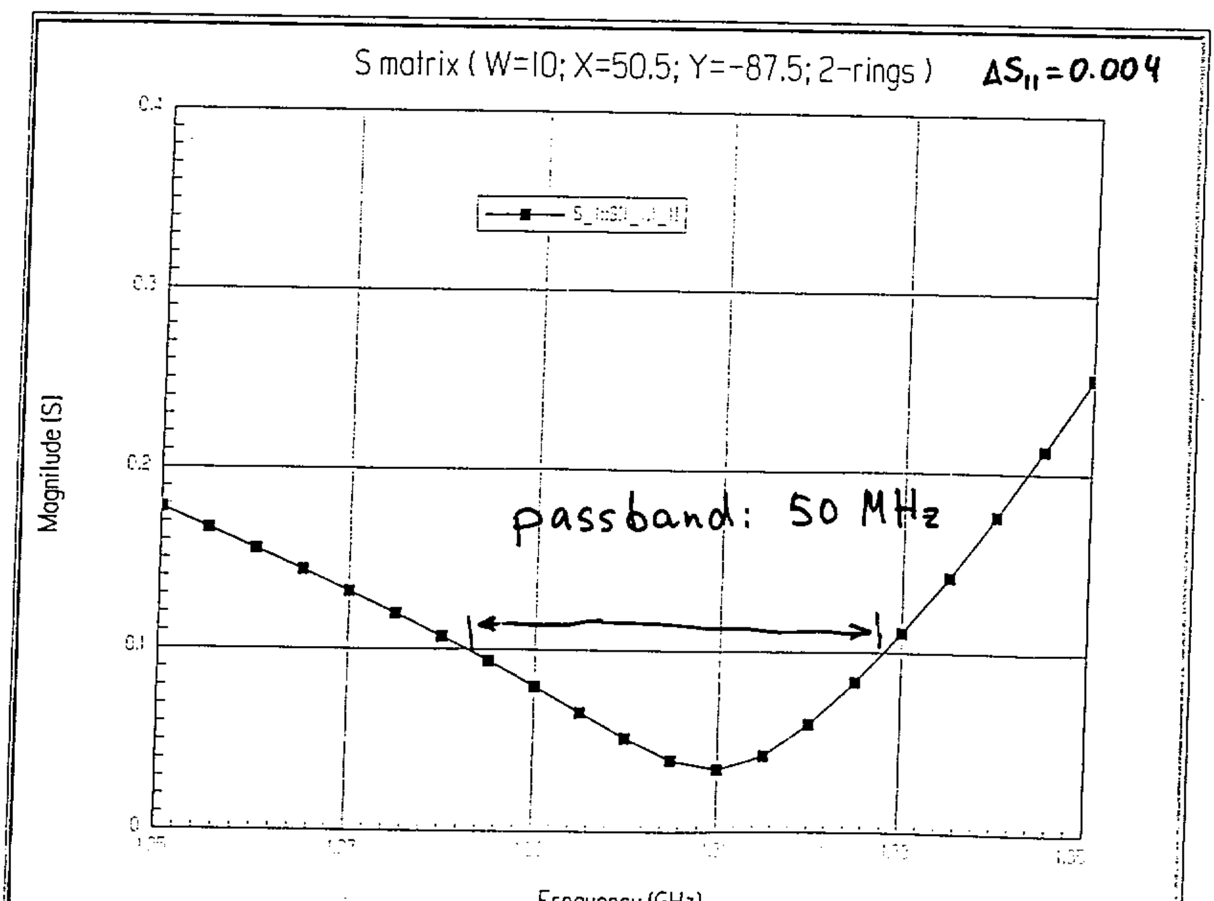

Sensitivity: $\frac{\Delta F_{min}}{\Delta h} = 14 \frac{MHz}{mm}$; **STUBS**: $\frac{\Delta F_{min}}{\Delta y} = 4 \frac{MHz}{mm}$; $\frac{\Delta S_{11}}{\Delta x} = 0.03/m$

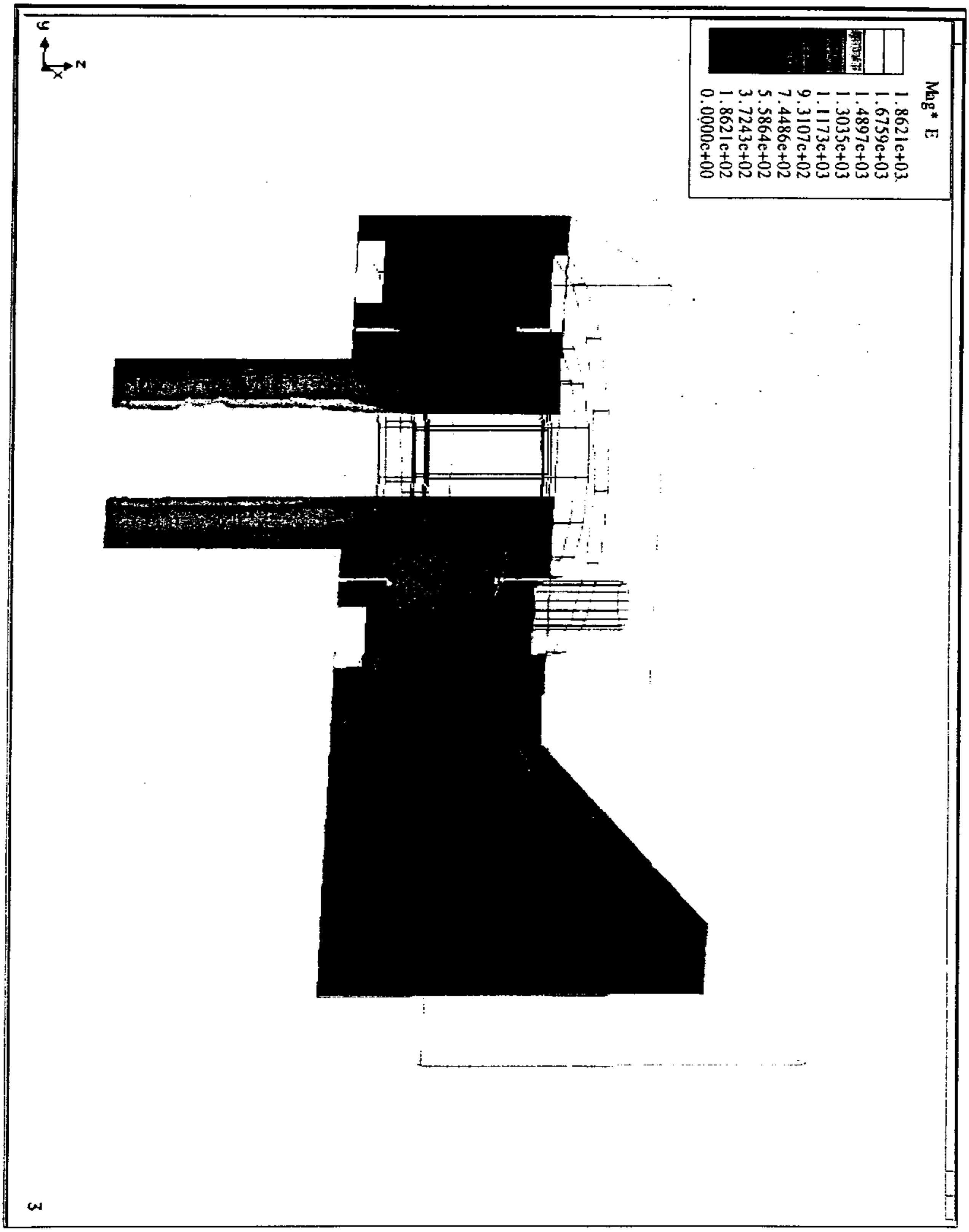
Mag* E
1.8621e+03
1.6759e+03
1.4897e+03
1.3035e+03
1.1173e+03
9.3107e+02
7.4486e+02
5.5864e+02
3.7243e+02
1.8621e+02
0.0000e+00
y
z
x
3

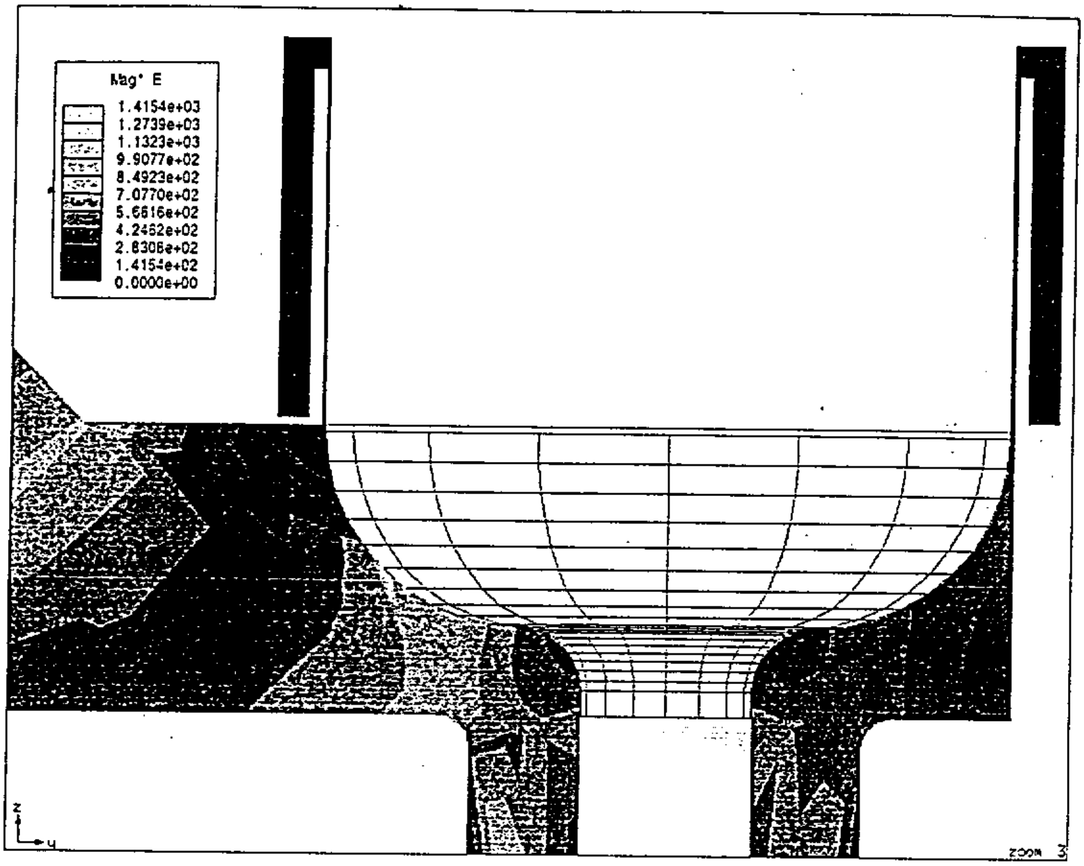
Mag' E
1.4154e+03
1.2739e+03
1.1323e+03
9.9077e+02
8.4923e+02
7.0770e+02
5.6616e+02
4.2462e+02
2.8306e+02
1.4154e+02
0.0000e+00
z
y
zoom 3

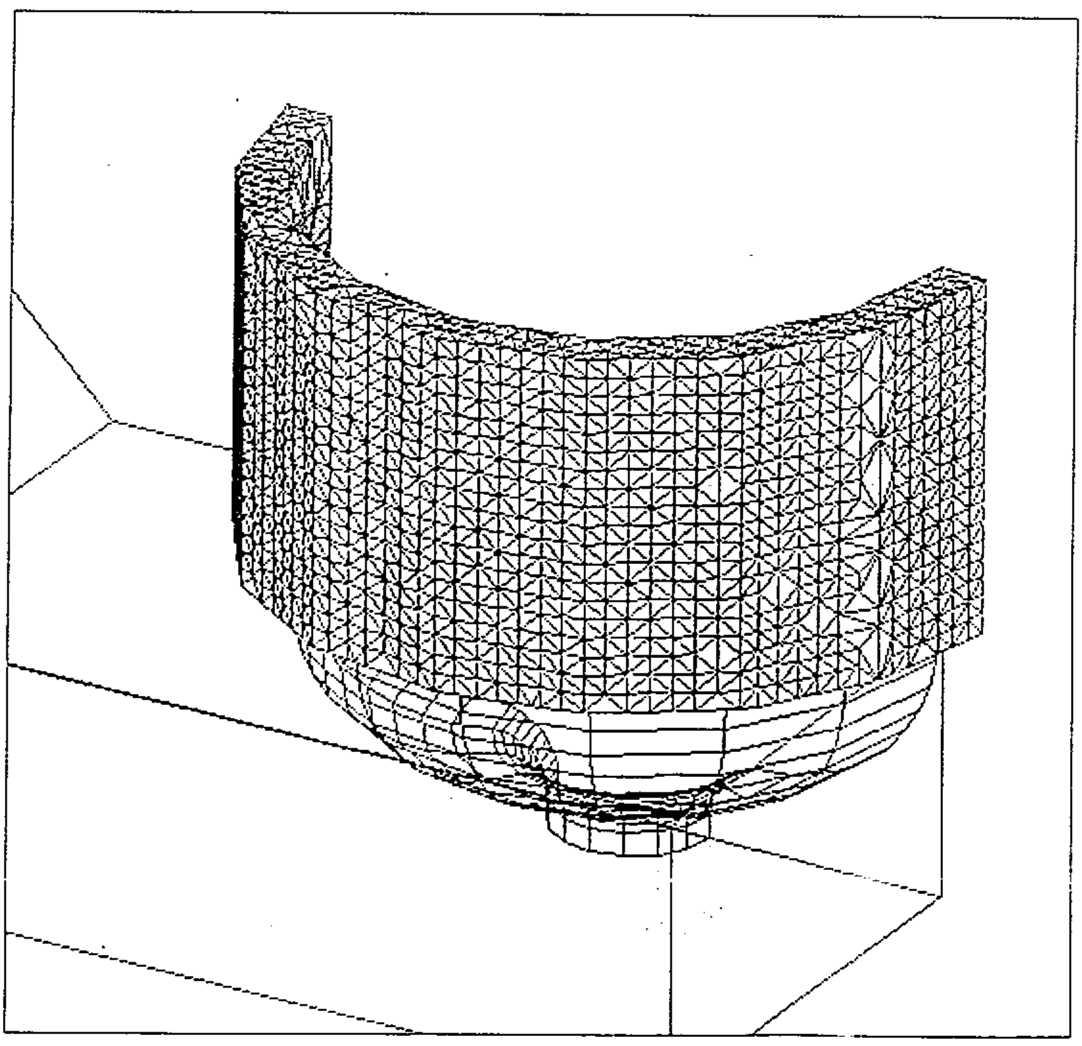

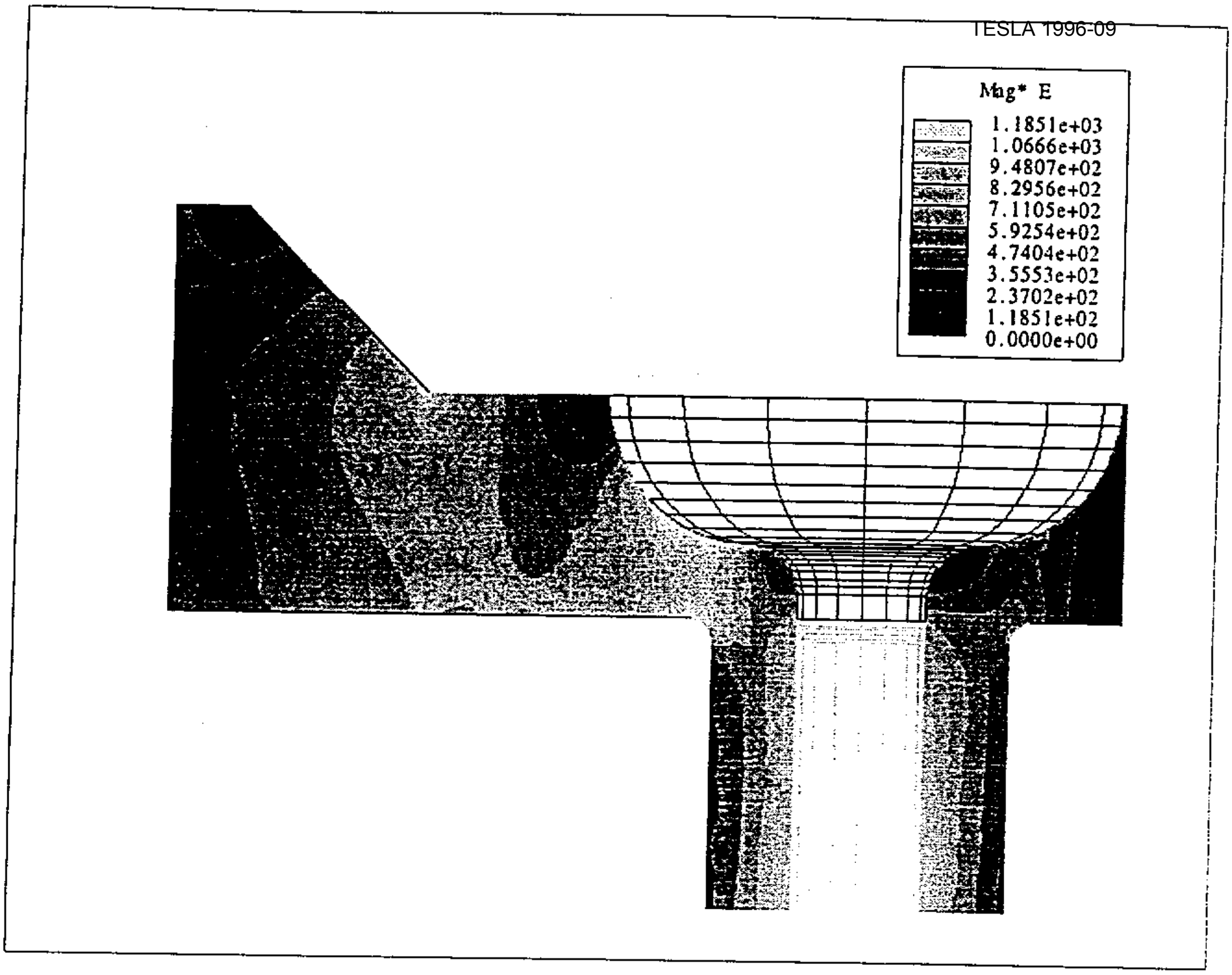

Figure 1: *WG-coax doorknob transition Ø62 mm.*

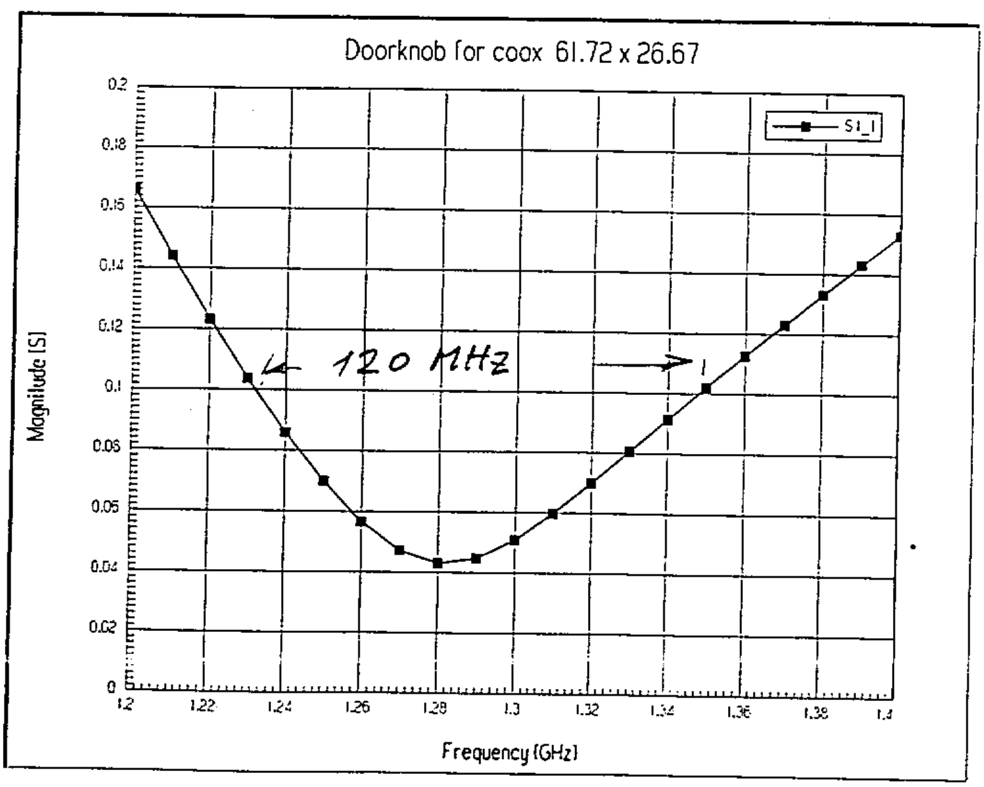

Figure 2: *Reflected power a-HFSS simulation, b - measured*

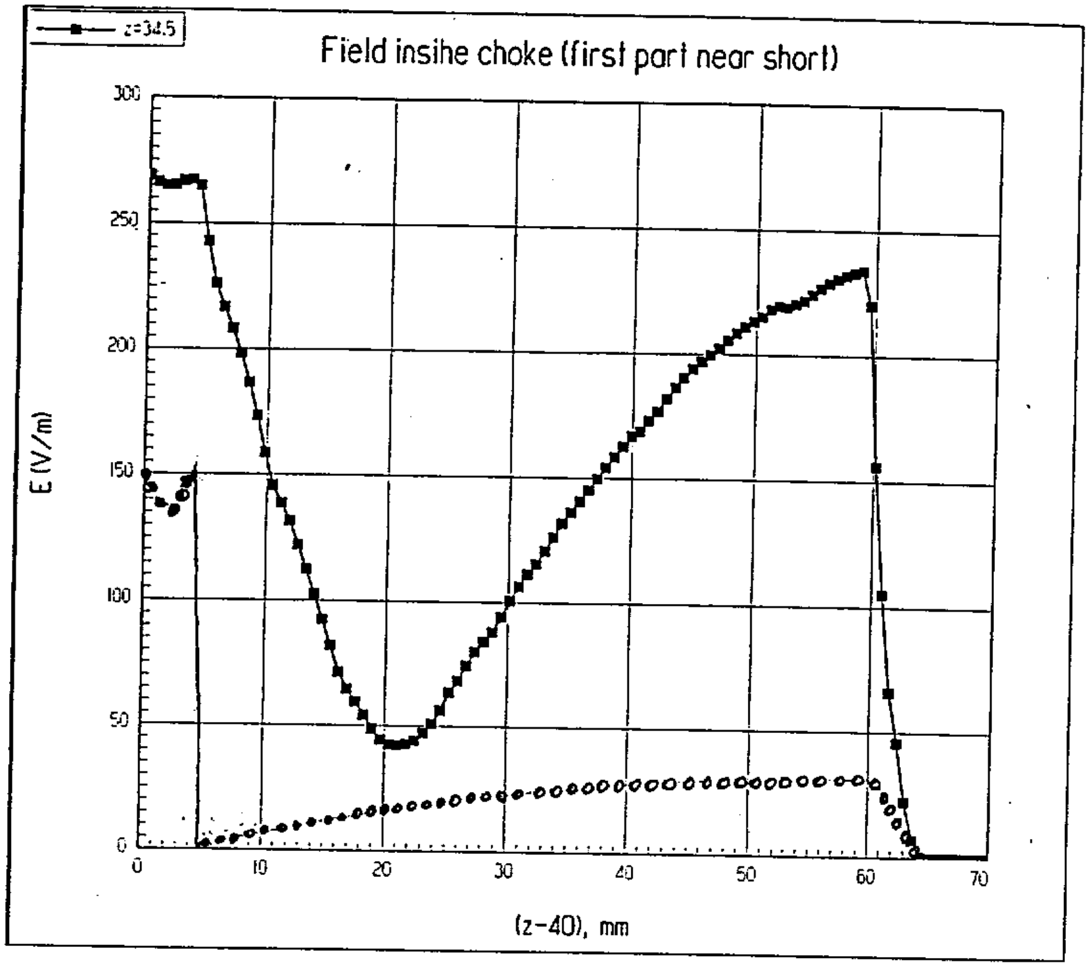
z=34.5
Field insihe choke (first part near short)
E (V/m)
(z-40), mm
0
50
100
150
200
250
300
10
20
30
40
50
60
70

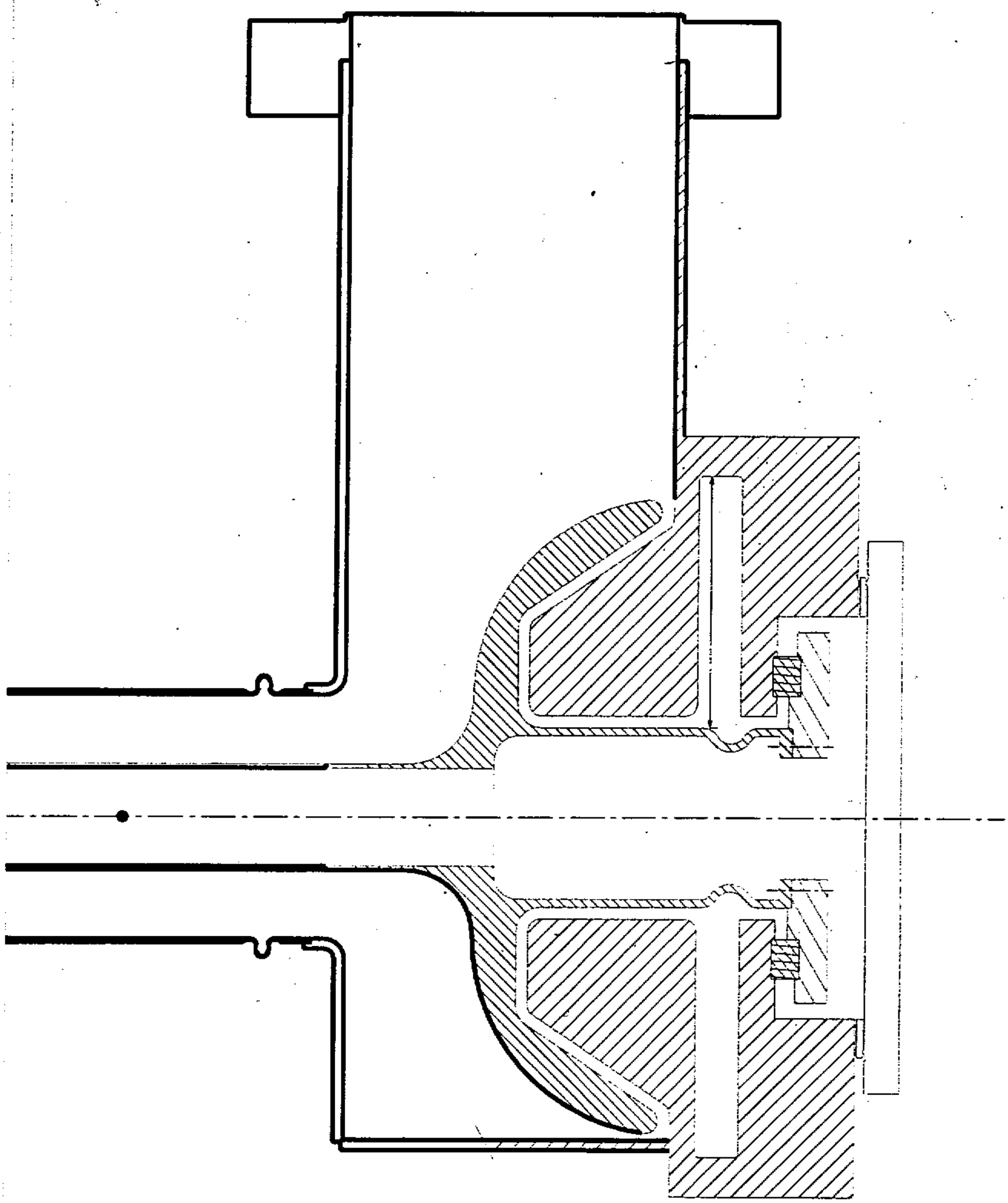

R/D Power Coupler
CEA Saclay & IN_2P_3 Orsay

1) WG-coaxial transition with polarization

2 types will be developed in parallel :

- High Voltage under air (CERN type)
  with cylindrical window
  small gap, isolation with Kapton

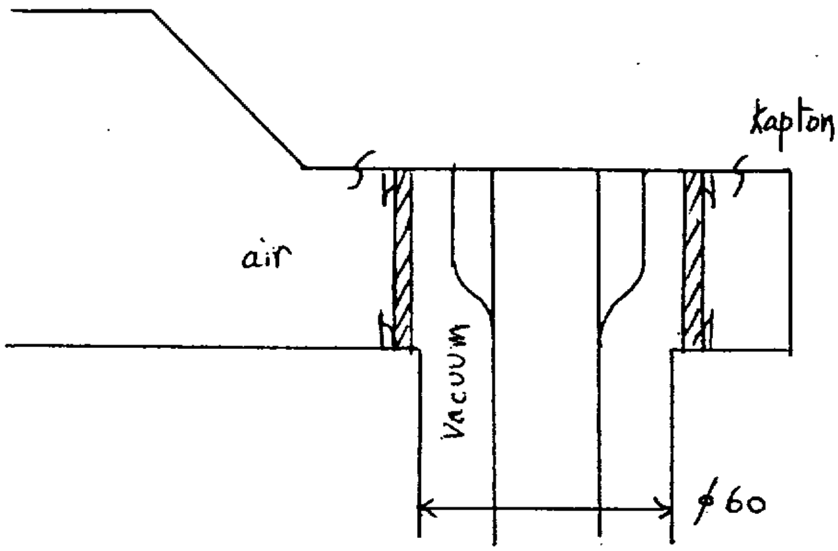

- High Voltage under vacuum
  without window
  large gap, isolation with ceramics + choke → N. Sdiak calculations

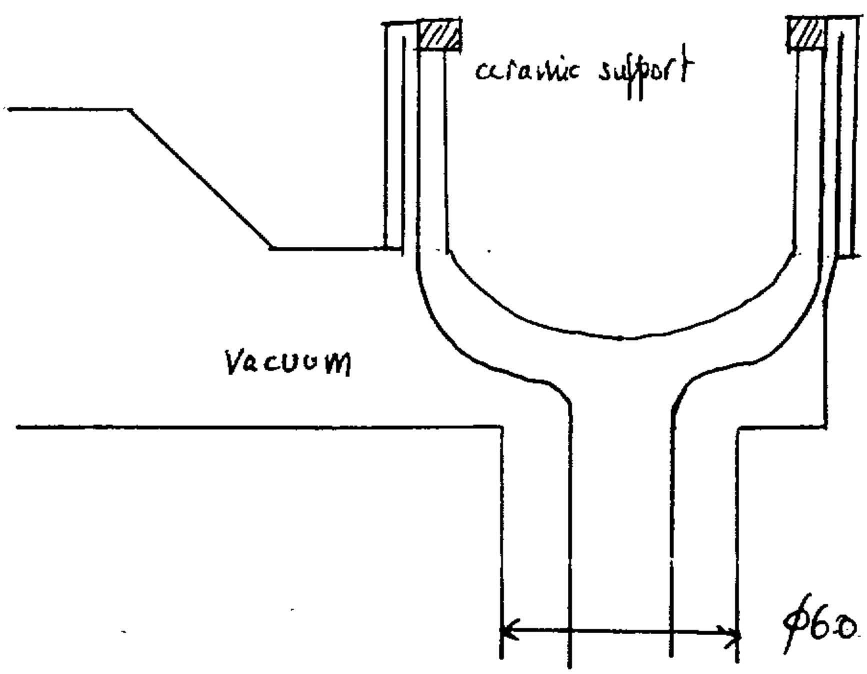

2) Study of windows

with multipacting calculations, test and comparison of 3 types

- conical window = Fermilab window

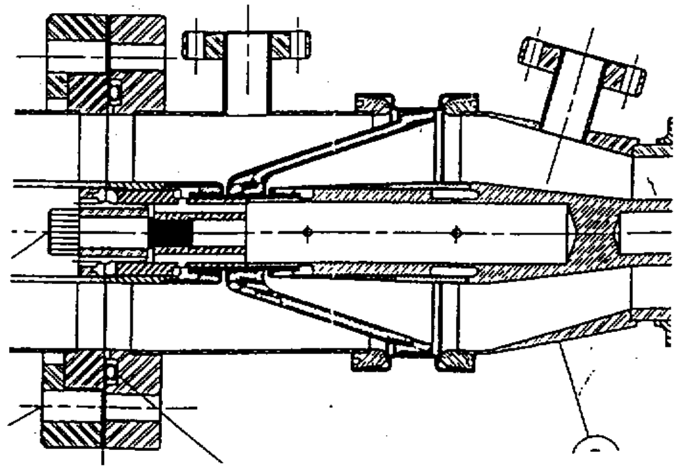

- cylindrical window = modified DESY window (ϕ = 60 mm)

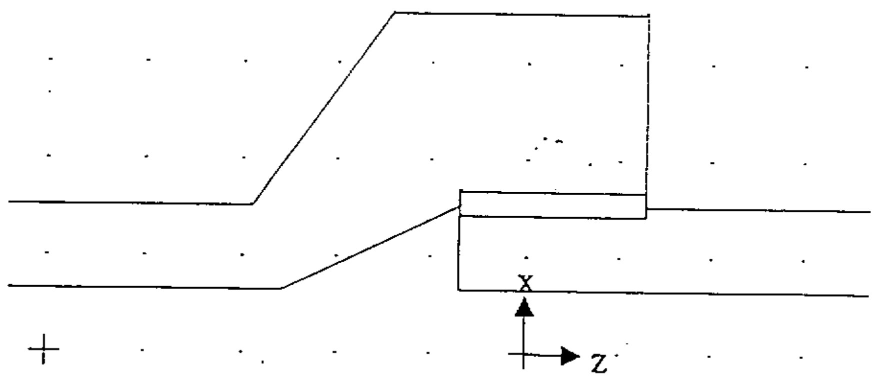

- TW disc window

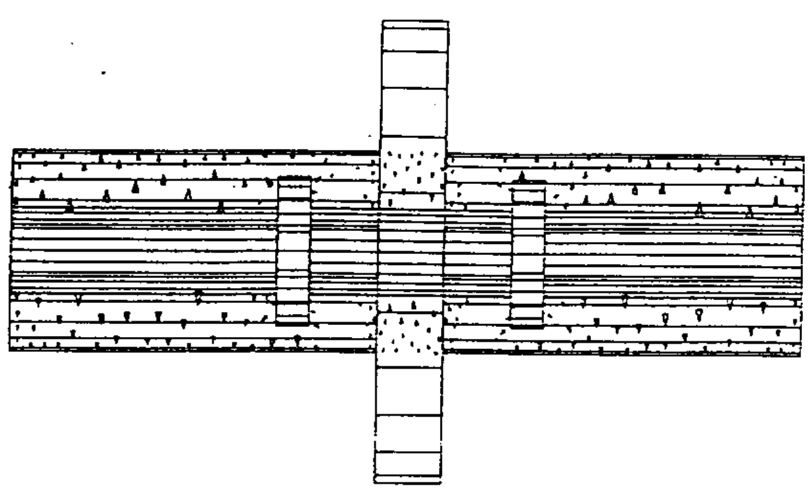

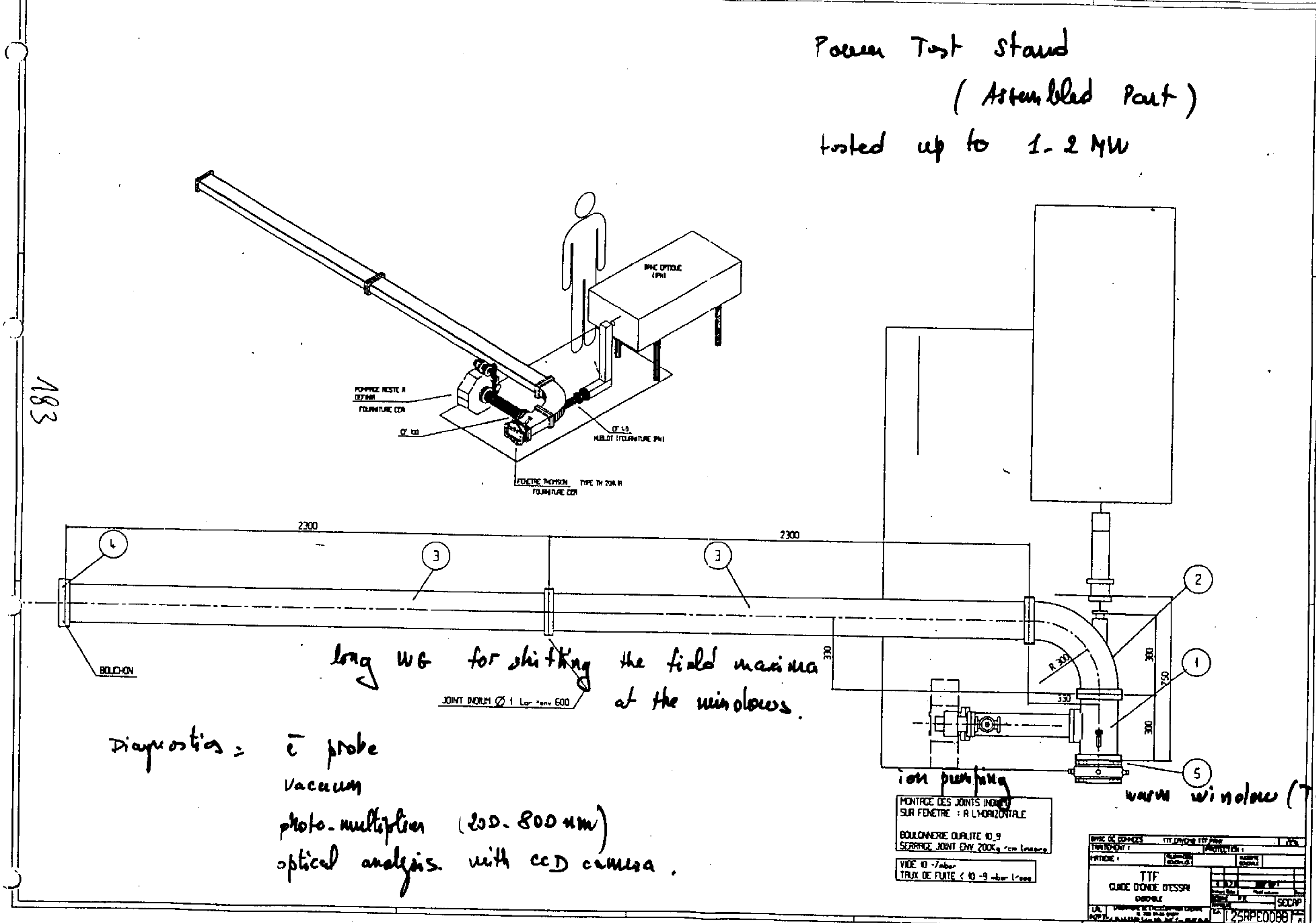
Power Test Stand
(Assembled Part)
tested up to 1-2 MW
BANC OPTIQUE (PH)
POMPAGE RESTE A DEFINIR
FOURNITURE CER
CF 100
CF 40
HUBLOT (FOURNITURE PH)
FENETRE THOMSON TYPE TH 20... R
FOURNITURE CER
2300
2300
BOUCHON
long WG for shifting the field maxima at the windows.
JOINT INDIUM Ø 1 Lor. env 600
R 300
330
330
300
300
750
ion pumping
warm window (Thomson
MONTAGE DES JOINTS INDIUM SUR FENETRE : A L'HORIZONTALE
BOULONNERIE QUALITE 10_9
SERRAGE JOINT ENV 200Kg /cm linéaire
VIDE 10 -7mbar
TAUX DE FUITE < 10 -9 mbar l/sec
Diagnostics : ē probe
vacuum
photo-multiplier (200-800 nm)
optical analysis with CCD camera.
TTF
GUIDE D'ONDE D'ESSAI
ENSEMBLE
SECAP
25RPE0088

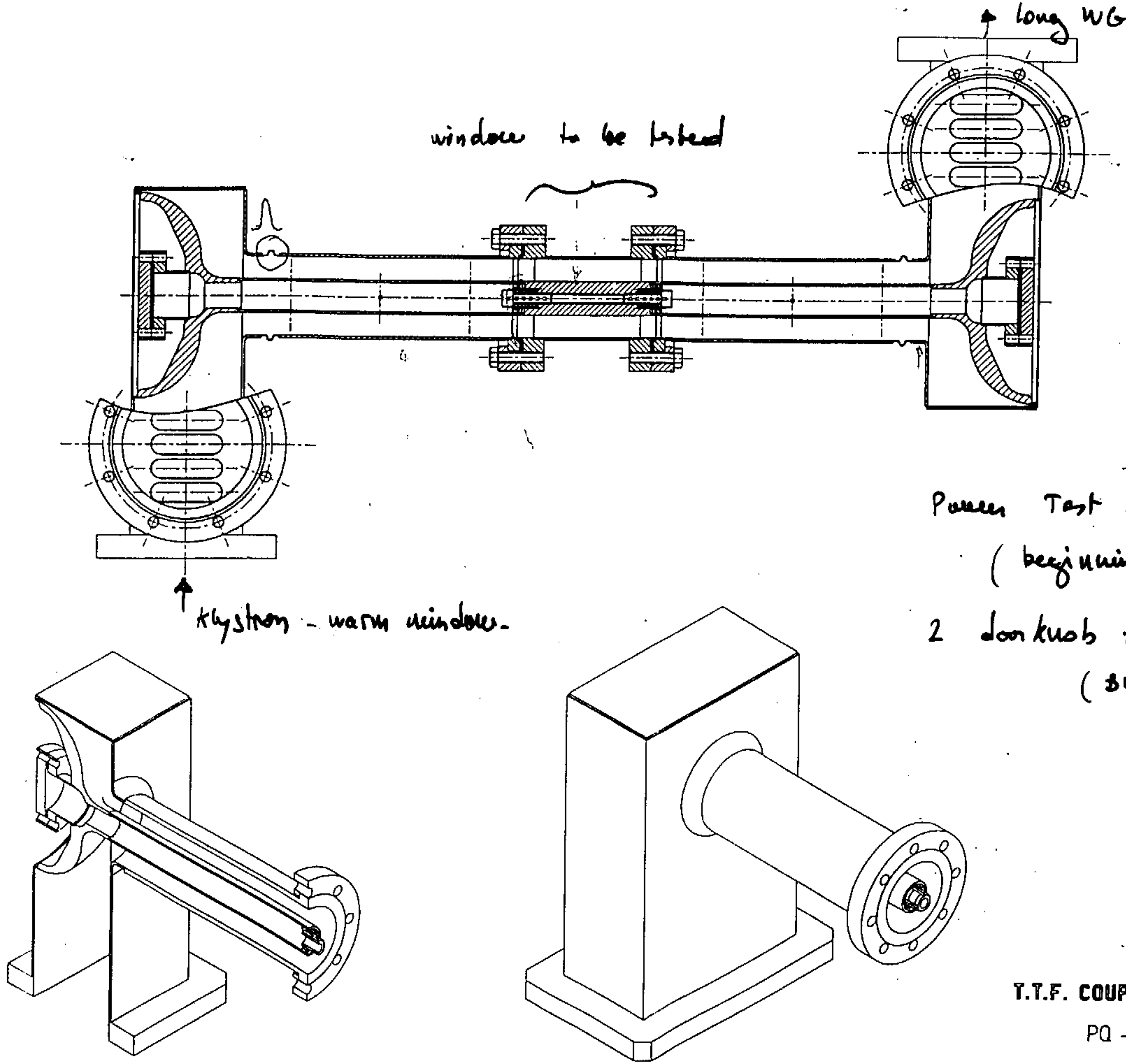

Power Test stand
(beginning of september)
2 doorknob transitions.
(BW = 140 MHz).

T.T.F. COUPLEUR de PUISSANCE

PQ - 230 000 A

26.01.96 Le Roux ech. 1

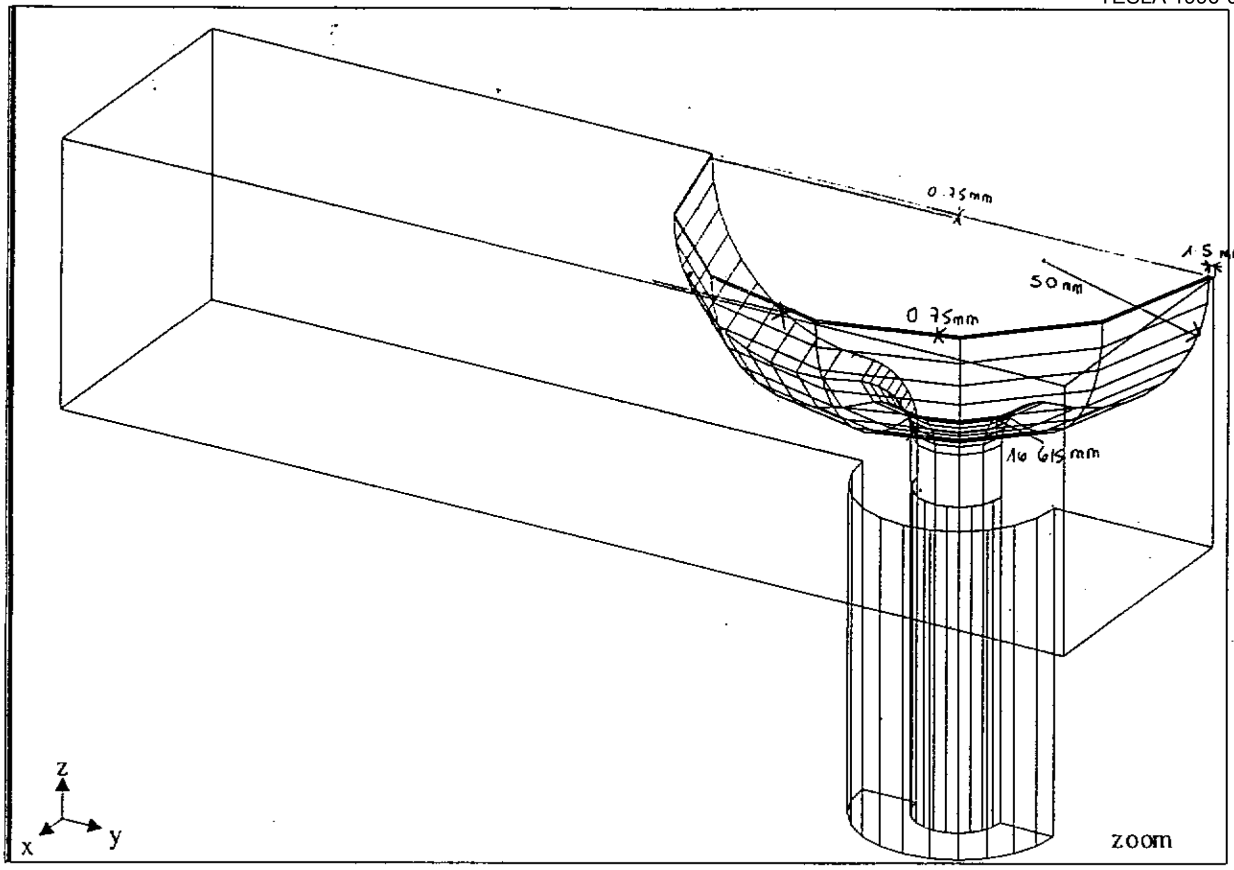
0.75mm
1.5 mm
50 mm
0.75mm
16.615mm
z
x
y
zoom

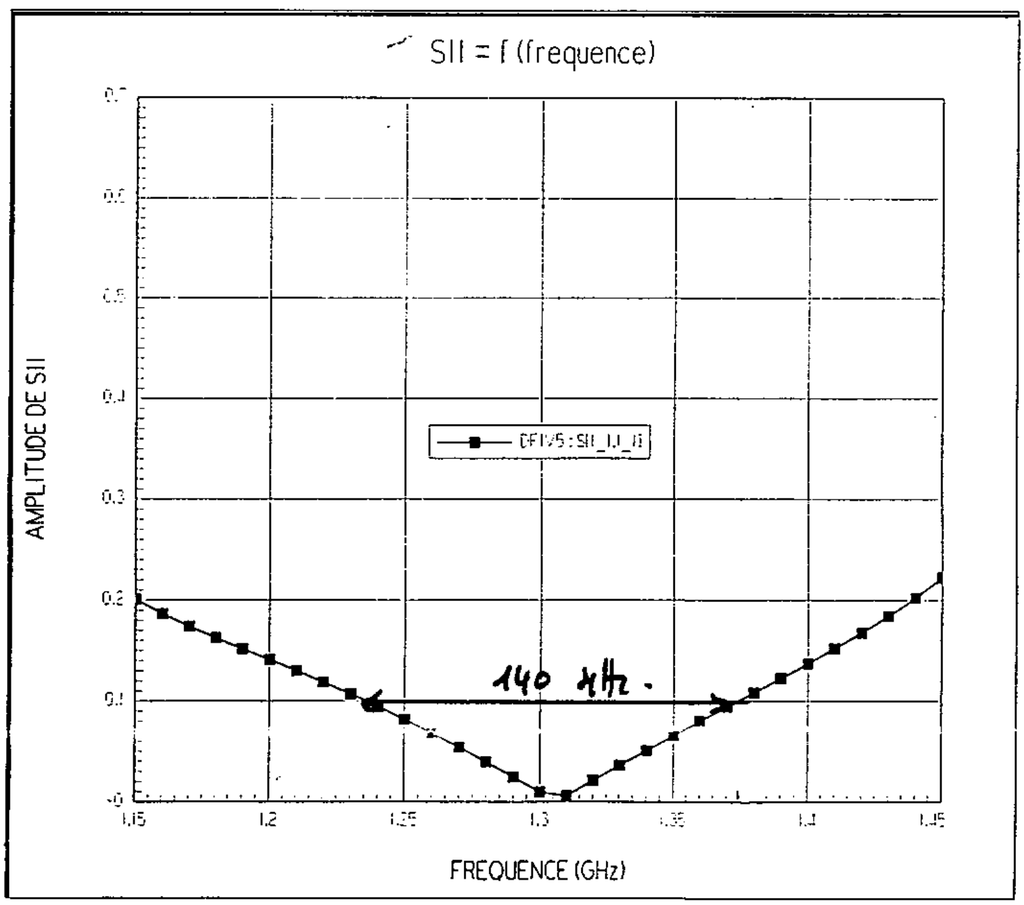
S11 = f (frequence)
AMPLITUDE DE S11
0.7
0.6
0.5
0.4
0.3
0.2
0.1
1.15
1.2
1.25
1.3
1.35
1.4
1.45
FREQUENCE (GHz)
140 kHz.

3) room temperature Power Test Stand

klystron 2 MW, long waveguide for "maximum voltage" shifting for testing

- warm windows + WG-coax transitions
- different cold windows → drawings.
- rf contacts of an alternate design

4) alternate design = telescopic coupler (LAL) → N. Solyak R. Panvier

could avoid the cold window

while keeping the cavity closure during assembly

5) Bellows with copper coatings → S. Chel.

dust. particles counting apparatus. during working groups.

galvanic deposition + magnetron sputtering have been tested

⚠ water rinsing → oxydation.

Experience with Input Couplers at CEBAF

presented by D. Proch

POSSIBLE CONTRIBUTIONS TO WINDOW PERFORMANCE

Losses:

- Ceramic
- Coating
- Indium Joints
- *Metallization*
- Nb - foil
- Geometry - Modeling - Multipacting

Arcing/Interlock Trips :

- Vacuum Bursts
- Waveguide Arcs/Warm Waveguide/Procedures
- *Charging of Ceramics*
  - Electrons
  - X - rays
  - Shielding

Cavity/Waveguide Interaction

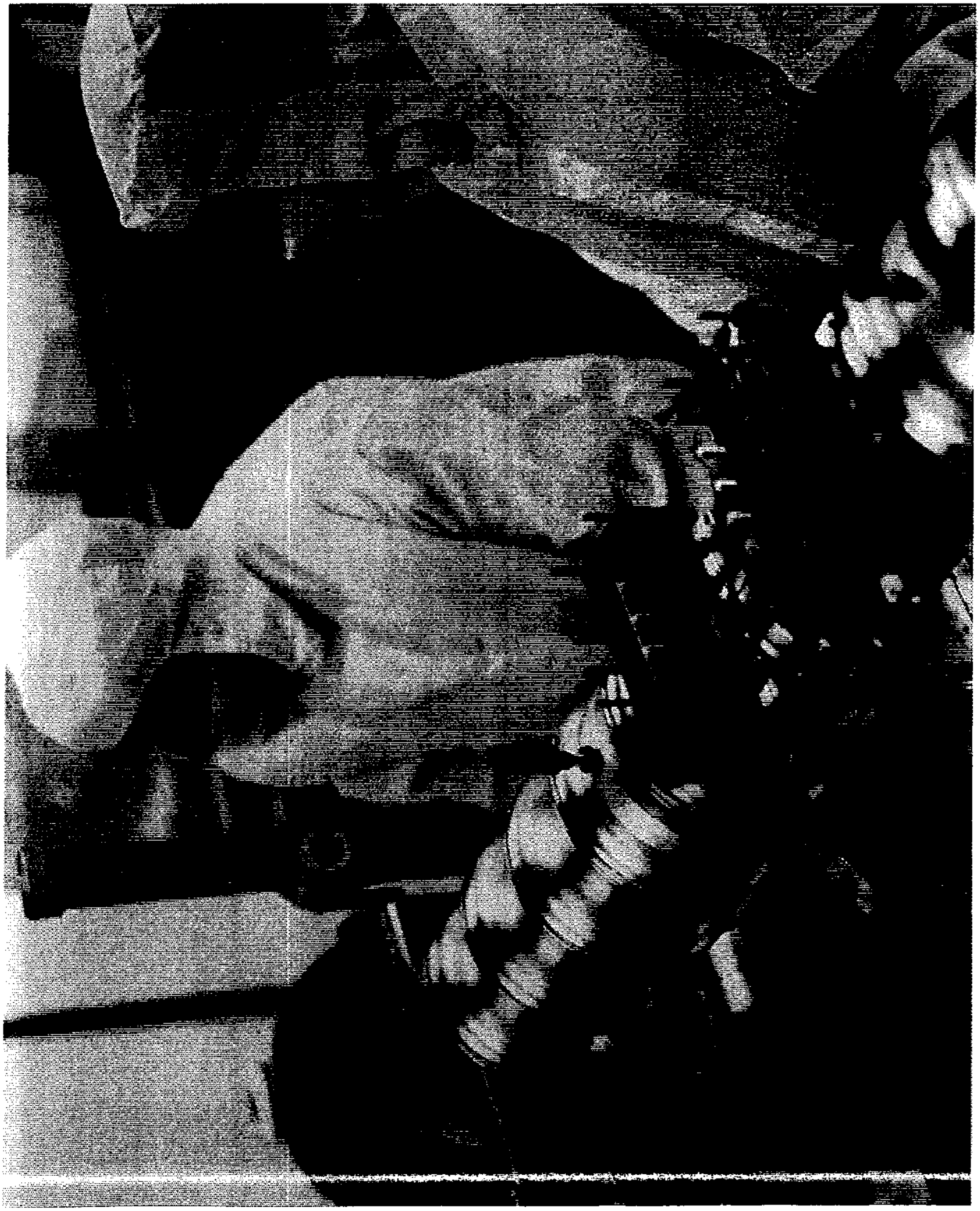

WINDOW DEVELOPMENT

ISSUES	INDICATIONS/ SUPPORTING EVIDENCE	EFFECT ON CAVITY/ACCEL. PERFORMANCE	AVENUES TO ATTACK PROBLEM
Losses	Measured ΔT at frame IR - pick-up Lowered Q-values Dependence of Q on Qext, location,metallization... λ/2- resonator tests	Lower Q Cryogenic losses = increased costs possible nc transition of Nb	Screen commercial metall. pick best, reproduce fabricate windows for FEL Develop sc metallization Understand all contributions to losses
"Arcing"	Observed arcs (diff.kinds) Temporal characteristics Optical spectra charging of windows, arc trails punctures	Interlock trips on RF unstable beam possible window damage, vacuum failure, performance degradation	a). Dog Leg coupler : avoid charging of ceramic by shielding e^- , X-rays b). Eliminate window c). Develop charge drainage
Cavity/ Window Interaction	Cavity performance depending on window/no window , on location , on orientation?	Q-degradation increased losses due to FE/MP?	a) verify with specialized experiments b).eliminate interaction if it exists

Superconducting Window Metallization

a). Sputtered Nb - metallization ,
brazing to eyelet with superconducting, low temperature brazing alloy (*in - house*)

b). Thick film NbTi metallization , brazing to eyelet with superconducting alloy (*outside*)

c). Active alloy lead metallization
a Ti-hydride layer on the Al_2O_3 bonds lead to Nb - eyelet after a thin copper film has been deposited (*in-house/outside*)

Sheet3

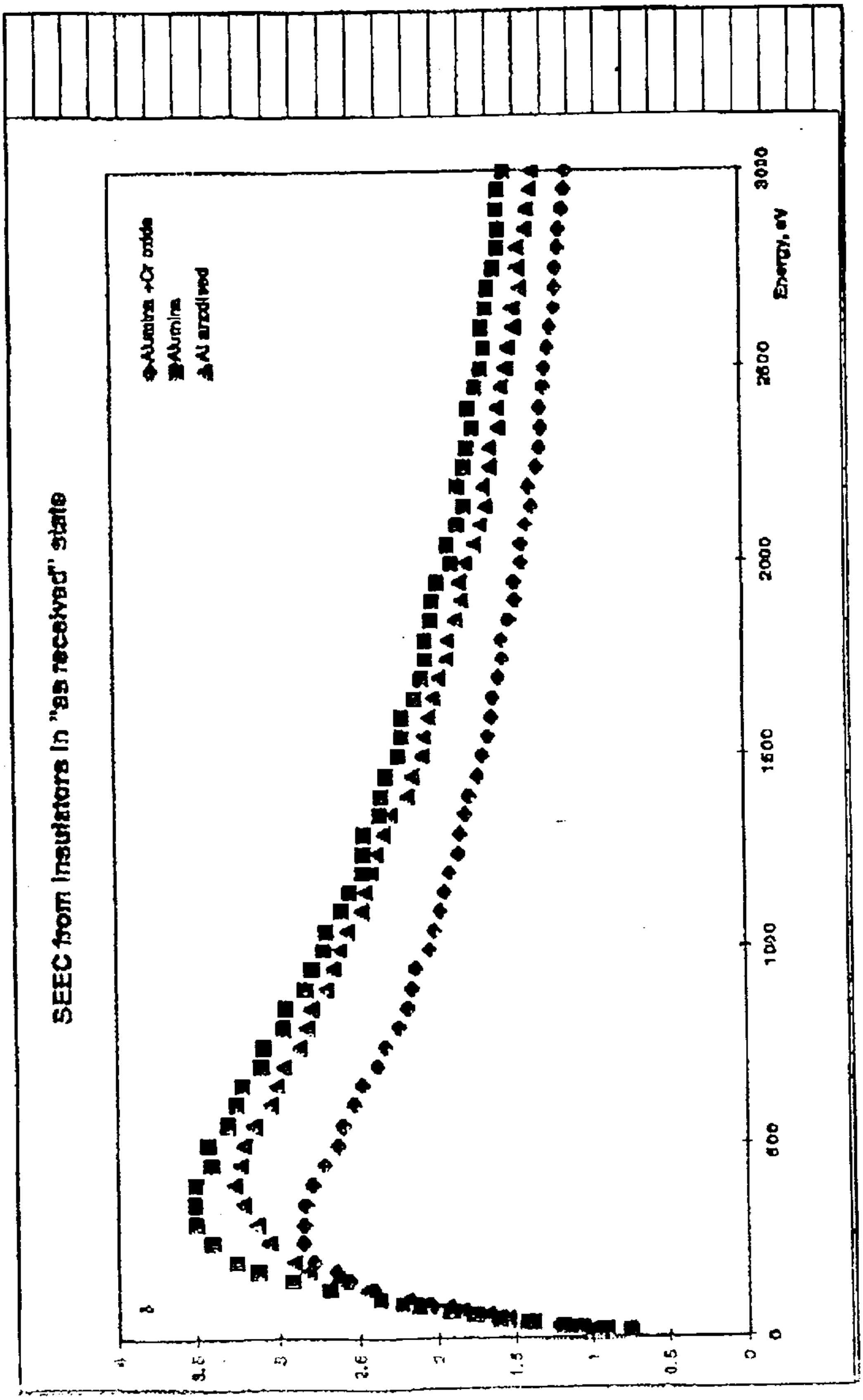

Page 1

192

CEBAF
The Continuous Electron Beam Accelerator Facility

IA355n 4/15/96

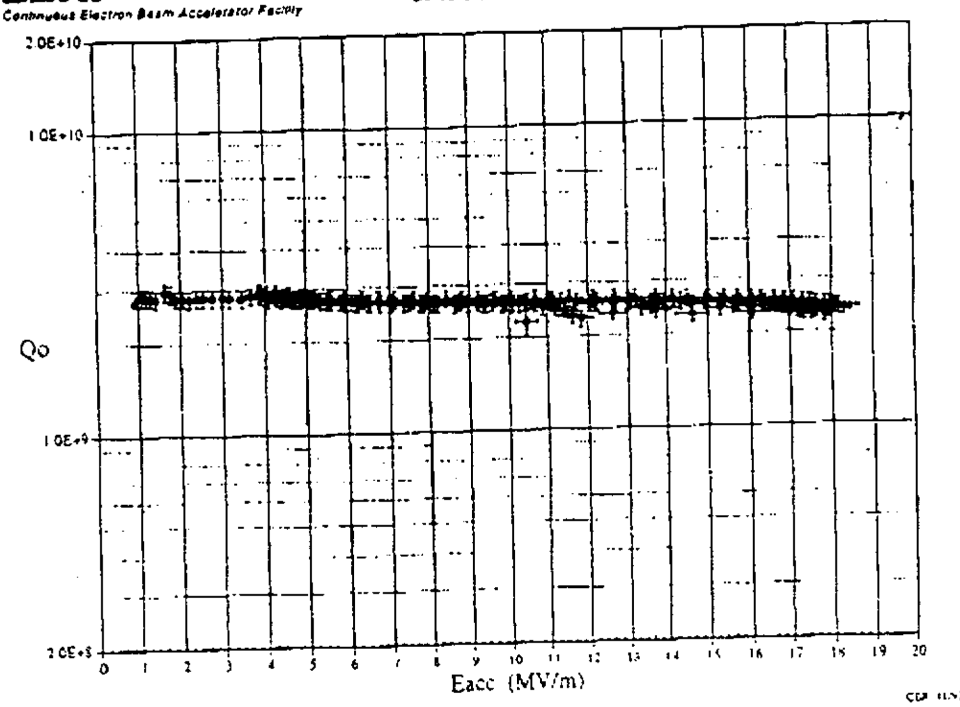

CEBAF
The Continuous Electron Beam Accelerator Facility

IA080c 4/15/96

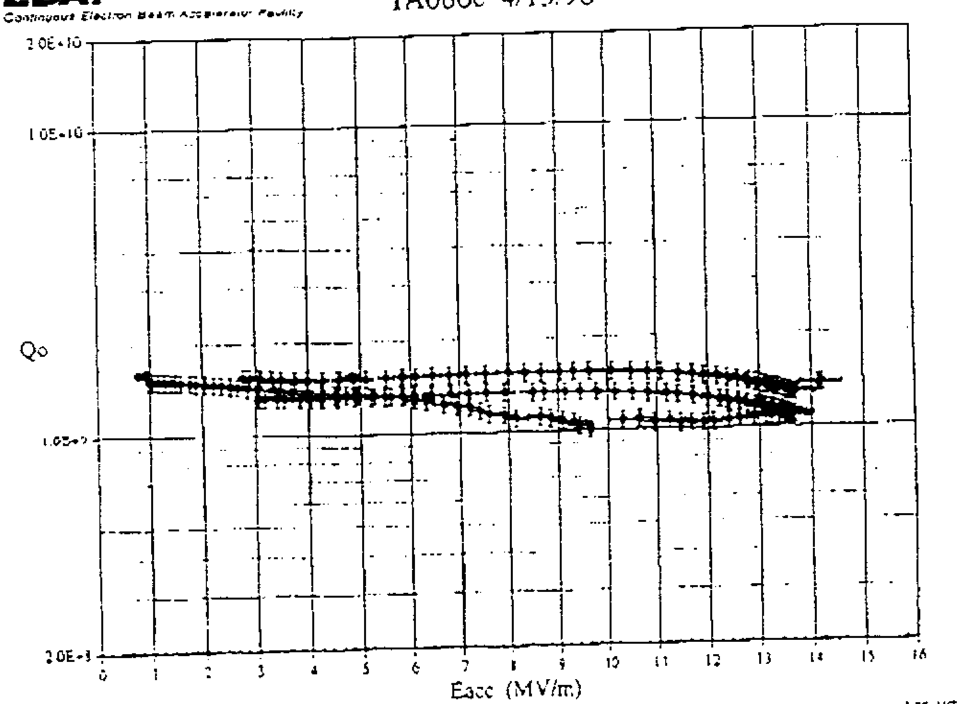

high gradient cavities, but not used for FEL linac
due to high losses in window area

FEL Cavity Pair
Bis jetzt nicht verwendet
wegen "Window-losses"

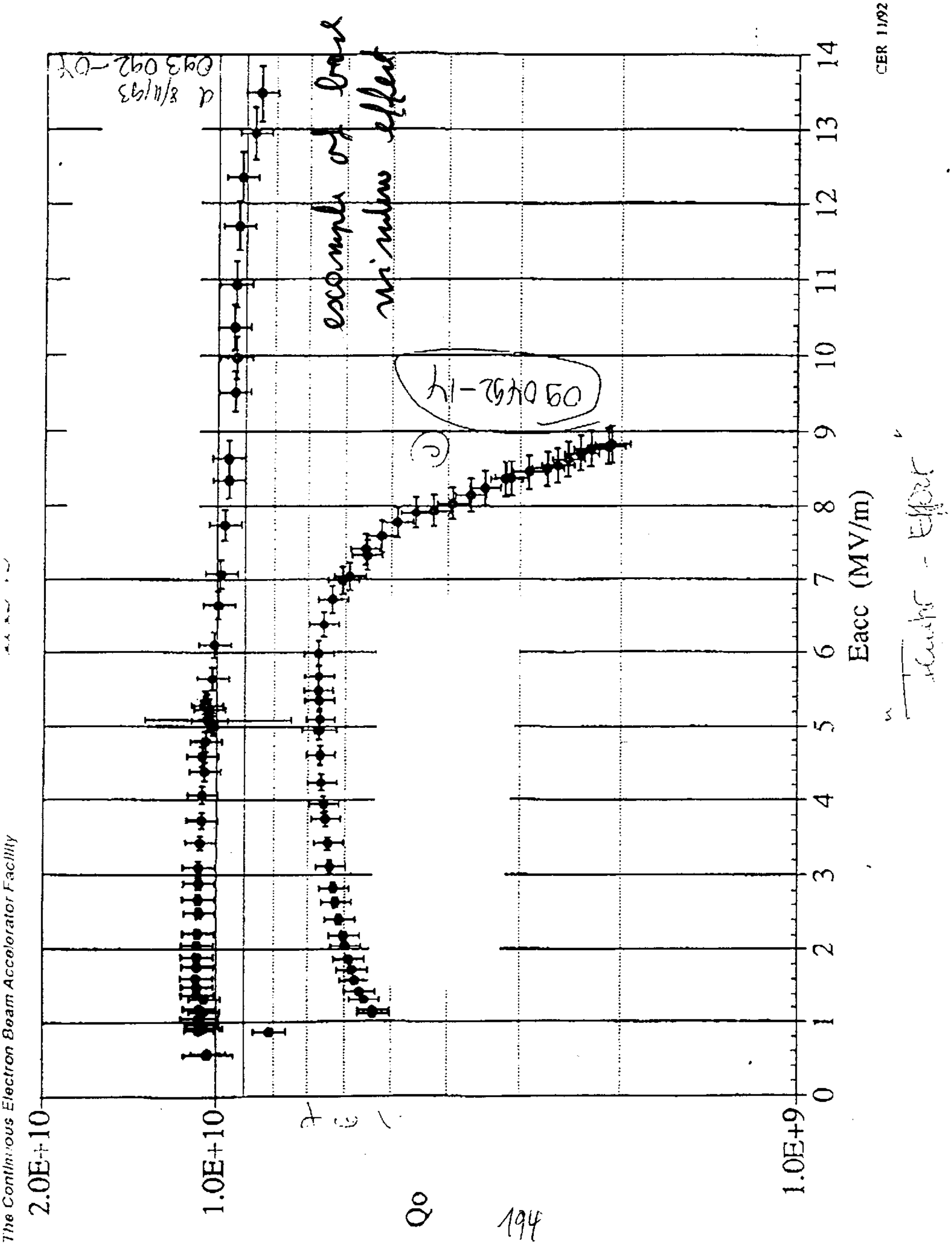
The Continuous Electron Beam Accelerator Facility
CER 11/92
Qo
2.0E+10
1.0E+10
1.0E+9
Eacc (MV/m)
0
1
2
3
4
5
6
7
8
9
10
11
12
13
14

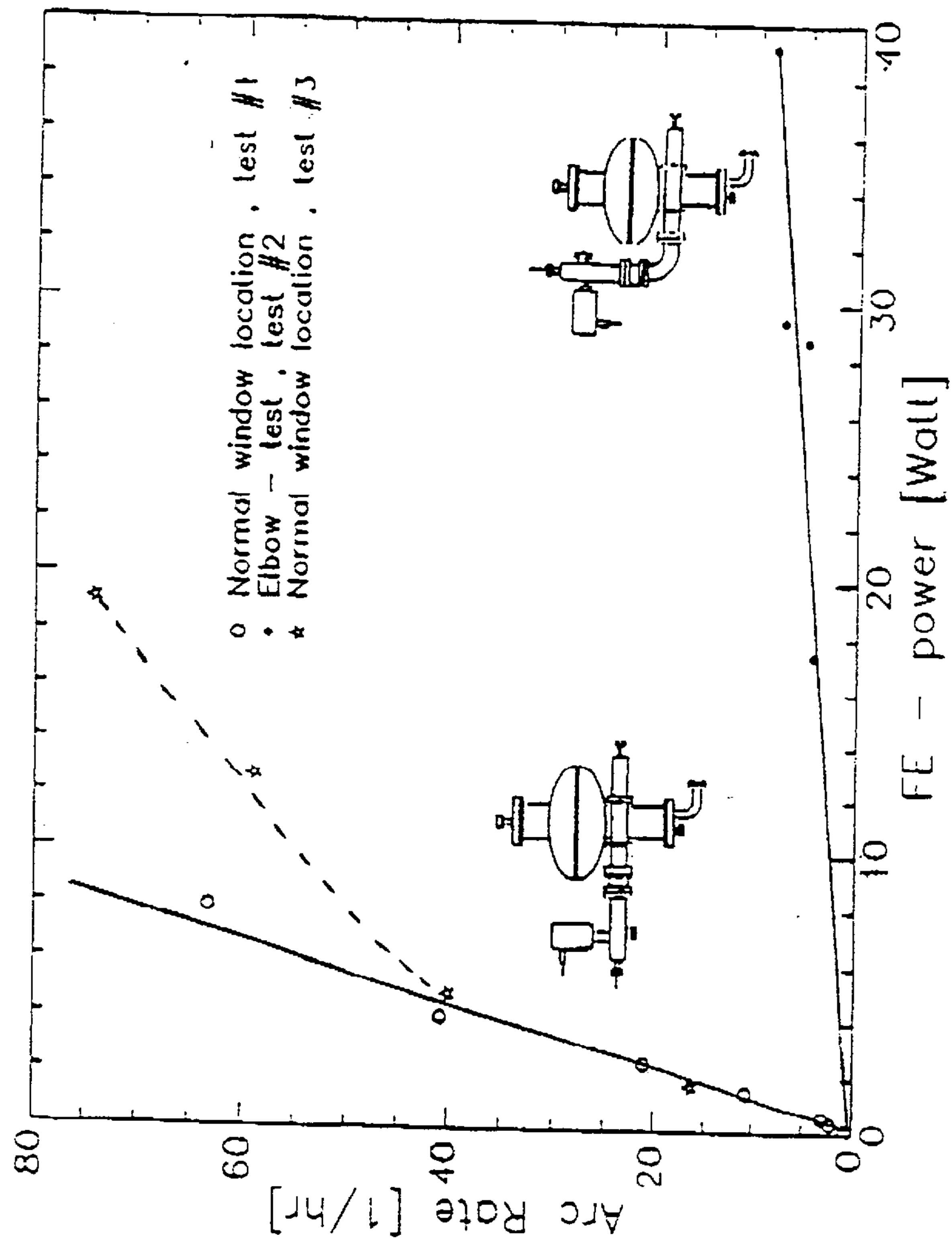

Fig. 1 : Arc rate as a function of power dissipated in field emission loading.